

THE UNIVERSITY OF MICHIGAN
COLLEGE OF ENGINEERING
Department of Mechanical Engineering
Heat Transfer Laboratory

Technical Report No. 2

TRANSIENT NATURAL CONVECTION FLOWS IN CLOSED CONTAINERS

Hussein Zaky Barakat
John A. Clark

ORA Project 04268

under contract with:

NATIONAL AERONAUTICS AND SPACE ADMINISTRATION
GEORGE C. MARSHALL SPACE FLIGHT CENTER
CONTRACT NO. NAS-8-825
HUNTSVILLE, ALABAMA

Administered through:

OFFICE OF RESEARCH ADMINISTRATION ANN ARBOR

August 1965

engn
UMR 0205

ACKNOWLEDGMENT

The authors wish to express their appreciation to Professors Vedat S. Arpaci, Robert C. F. Bartels and Wen-Jei Yang, for their interest and cooperation in serving as members of the doctoral thesis advisory committee.

This work was completed under the sponsorship of the George C. Marshall Space Flight Center, NASA, Huntsville, Alabama under Contract NAS-8-825. The authors gratefully acknowledge the assistance and support in this work of Messrs. H. G. Paul, G. K. Platt, and C. C. Wood.

TABLE OF CONTENTS

	Page
LIST OF ILLUSTRATIONS	vi
NOMENCLATURE	x
ABSTRACT	xiii
Chapter	
1. INTRODUCTION	1
2. REVIEW OF THE LITERATURE	9
3. STATEMENT AND PHYSICS OF THE PROBLEM	24
3.1 Introduction	24
3.2 Description of the First Model	25
3.3 Description of the Second Model	27
3.4 Generalized Formulation of the First Model	28
3.5 Simplified Formulation of the First Model	34
3.5.1 Rectangular Coordinates	34
3.5.2 Formulation of the Simplified Model, Cylindrical Coordinates	37
3.6 Formulation of the Second Model	40
3.6.1 Rectangular Coordinates	40
3.6.2 Formulation of the Second Model, Cylindrical Coordinates	42
4. TRANSFORMATION OF THE PARTIAL DIFFERENTIAL EQUATIONS	44
4.1 Rectangular Coordinates	44
4.2 Cylindrical Coordinates	46
4.3 Boundary Conditions	48
4.3.1 Rectangular Coordinates	48
4.3.2 Cylindrical Coordinates	50
4.4 Dimensionless Form of the Equations	51
4.4.1 Rectangular Coordinates	51
4.4.2 Cylindrical Coordinates	54
5. METHOD OF SOLUTION	57
5.1 Introduction	57
5.2 Approximation of Derivatives by Finite- Difference	57

TABLE OF CONTENTS (Continued)

	Page
5.3 Note on the Classification of Partial Differential Equations	60
5.4 Finite Difference Representation of the Energy and Vorticity Equations (Parabolic Type)	61
5.5 Vorticity-Stream Function Equation	70
5.6 Calculation of the Velocity Components	72
5.7 Treatment of Boundary Conditions	74
5.8 The Procedure of Calculations	76
5.8.1 Rectangular System	76
5.8.2 Cylindrical System	77
5.9 A Note on the Use of Unconditionally Stable Methods for the Solution of the Energy and Vorticity Equations	78
 6. STABILITY ANALYSIS	 81
6.1 Definitions	81
6.2 A Note on the Linearization of the Differential Equations	83
6.3 Methods of Stability Analysis	84
6.3.1 Stability of Positive Type Differential Equations	85
6.3.2 Electric Circuit Analogy	91
6.3.3 The Von Neumann Method of Stability Analysis	92
6.4 Stability of the Energy and Vorticity Equations	97
6.5 A More General Approach to the Stability of the Explicit Finite-Difference Equations	109
6.6 Summary of the Results of this Chapter	113
 7. EXPERIMENTAL WORK	 116
7.1 Description of the Rectangular Apparatus	116
7.2 Description of the Cylindrical Apparatus	123
7.3 Experimental Procedure	123
7.4 Procedure of Data Reduction	124
 8. RESULTS	 135
8.1 Introduction	135
8.2 Discussion of the Results for the Rec- tangular Cavity, Poets Problem	140

TABLE OF CONTENTS (Concluded)

	Page
8.3 Theoretical Results for the Natural Con- vection in Pressurized Containers, First Model	141
8.4 Experimental and Analytical Results, Second Model	152
8.4.1 Results of the Rectangular Container	152
8.4.2 Results of the Cylindrical Container	165
8.5 Effect of Grid Size	184
8.6 Summary of the Results	189
8.7 Recommendations for Future Work	193
 APPENDIX I. METHOD OF SOLUTION OF A SYSTEM OF LINEAR ALGEBRAIC EQUATIONS HAVING A THREE DIAGONAL MATRIX	 195
 APPENDIX II. THE STABILITY ANALYSIS OF FORMULATION (ii) USING VON NEUMANN METHOD	 196
 APPENDIX III. THE COMPUTER PROGRAM FOR THE CYLINDER	 200
 APPENDIX IV. TYPICAL PRINTED COMPUTER OUTPUT	 207
 REFERENCES	 214

LIST OF ILLUSTRATIONS

Table	Page
I. Properties of Liquid Nitrogen at 150°R	142
II. Properties of Water for the Conditions of Runs 2, 3 and 4, Cylindrical Container	184
III. Effect of the Grid Size on the Computed Results for Run No. 1, Rectangular Container	185
Figure	
1. Typical propellant feed system for flight vehicle.	3
2. Relationship between vehicle thrust and final oxygen tank pressurant mass-pressure ratio.	6
3. Comparison of the weights of the propellant feed systems of two flight vehicles.	7
4. Typical analytical model for liquid stratification analysis.	11
5. Container configuration and coordinate system.	29
6. Finite difference network.	59
7. Sketch of rectangular container.	117
8. Thermocouple locations in the rectangular container.	119
9. Test vessel assembly.	121
10. View of the experimental apparatus.	125
11. View of the experimental apparatus.	126
12. View of the experimental apparatus.	127
13. Typical wall temperature response, rectangular container.	129

LIST OF ILLUSTRATIONS (Continued)

Figure	Page
14. Wall temperature distribution, run 2, cylindrical container.	131
15. Wall temperature distribution, run 3, cylindrical container.	132
16. Wall temperature distribution, run 4, cylindrical container.	133
17. Results for the rectangular cavity problem using 31x31 grid.	136
18. Results for the rectangular cavity problem using 11x11 grid.	137
19. Isotherms and streamlines, rectangular container.	143
20. Isotherms and streamlines, rectangular container.	144
21. Streamlines for the case of cylindrical container.	145
22. Isotherms and streamlines for cylindrical container.	146
23. Isotherms and streamlines for cylindrical container.	147
24. Results of flow visualizations made by Eichorn.	149
25. Effect of gravity level on liquid and wall temperature, cylindrical container.	151
26. Measured axial temperature distribution in the rectangular container, run 1.	153
27. Calculated and measured liquid temperature response in the rectangular container, run 1.	154
28. Measured wall temperature in the rectangular container.	156
29. Isotherms and streamlines in the rectangular container, run 1.	157
30. Isotherms and streamlines in the rectangular container, run 1.	158

LIST OF ILLUSTRATIONS (Continued)

Figure	Page
31. Isotherms and streamlines in the rectangular container, run 1.	159
32. Isotherms in the rectangular container.	160
33. Streamlines in the rectangular container, run 1.	161
34. Isotherms and streamlines in the rectangular container, run 1.	162
35. Schlieren photographs for stratification without wall baffles.	164
36. Liquid temperature response in the cylindrical container, run 2.	166
37. Liquid temperature response in the cylindrical container, run 3.	167
38. Liquid temperature response in the cylindrical container, run 4.	168
39. Axial temperature distribution obtained for the cylindrical container.	169
40. Typical Visicorder output record.	170
41. Typical Visicorder output record.	171
42. Typical Visicorder output record.	172
43. Typical Visicorder output record.	173
44. Isotherms and streamlines in the cylindrical container, run 2.	174
45. Isotherms and streamlines in the cylindrical container, run 2.	175
46. Isotherms and streamlines in the cylindrical container, run 2.	176

LIST OF ILLUSTRATIONS (Concluded)

Figure	Page
47. Isotherms and streamlines in the cylindrical container, run 3.	177
48. Isotherms and streamlines in the cylindrical container, run 3.	178
49. Isotherms and streamlines in the cylindrical container, run 3.	179
50. Isotherms and streamlines in the cylindrical container, run 4.	180
51. Isotherms and streamlines in the cylindrical container, run 4.	181
52. Isotherms and streamlines in the cylindrical container, run 4.	182
53. Effect of the grid size on the calculated wall temperature.	186
54. Calculated velocity distribution at high values of time in the cylindrical container, run 2.	188
55. Calculated velocity distribution at low values of time in the cylindrical container, run 2.	190

NOMENCLATURE

a	half the width of the container
b	the initial height of the liquid
C_p	constant pressure specific heat, BTU/lbm ^o F
Gr	Grashof number = $g\beta(T_s - T_o)a^3/\nu^2$
Gr*	Modified Grashof number = $g\beta a^4(q/A)_w/(K\nu^2)$
g	the acceleration of gravity, ft/sec ²
h_{fg}	latent heat of evaporation or condensation BTU/lbm
K	thermal conductivity, BTU/hr ft ^o F
M	number of divisions in the axial direction
N	" " " " " transverse direction
p	pressure
r	radius, ft
R	dimensionless radius
Pr	Prandtl number = ν/α
Ra	Rayleigh number, (GrPr)
$(q/A)_w$	heat flux at the walls of the tank per unit area, BTU/hr-ft ²
T	temp R
t	time, sec.
u	x-component of the velocity, ft/sec
v	y-component of the velocity, ft/sec
U	dimensionless x-component of the velocity

NOMENCLATURE (Continued)

V	dimensionless y-component of the velocity
x	axial distance, ft
X	dimensionless x
y	transverse, or normal distance measured from center line, ft
Y	dimensionless y
w	$= \frac{a^2}{b^2} \frac{\partial^2 \psi}{\partial x^2} + \frac{\partial^2 \psi}{\partial y^2}, \text{ for rectangular coord.}$ $= \frac{1}{R} \left(\frac{a^2}{b^2} \frac{\partial^2 \psi}{\partial x^2} - \frac{1}{R} \frac{\partial \psi}{\partial R} + \frac{\partial^2 \psi}{\partial R^2} \right) \text{ for cylindrical coord.}$
α	thermal diffusivity, ft ² /sec
β	coefficient of thermal expansion,
γ	amplification factor, Equation (6.23)
$\mu(k_1, k_2)$	function of time governing the growth of the temperature, Equation (6.45)
$\xi(k_1, k_2)$	function of time governing the growth of the vorticity, Equation (6.44)
ΔX	grid size in the axial direction
ΔY	" " " " Y-direction
ΔR	" " " " R-direction
Δt	time increment
ρ	density, lbm/ft ³
μ	viscosity, lbm/ft-sec
ν	kinematic viscosity, ft ² /sec
ϕ	dissipation function for two dimensional incompressible flow is given by

NOMENCLATURE (Concluded)

$$\phi = 4 \left(\frac{\partial u}{\partial x} \right)^2 + \left(\frac{\partial v}{\partial x} + \frac{\partial u}{\partial y} \right)^2$$

τ	dimensionless time
θ	dimensionless temperature
ψ	stream function
λ	an eigen value

Subscripts

c	cold wall
g	vapor
h	hot wall
s	saturation or liquid surface
i,j	denotes position in the space grid
o	denotes initial conditions
w	wall

Superscript

n	denotes the time level
---	------------------------

ABSTRACT

An analytical and experimental study is reported of the transient, laminar natural convection heat and mass transfer in two-dimensional partially filled rectangular and cylindrical liquid containers. The container sidewalls undergo arbitrary time and space dependent wall temperature or heat flux. The liquid surface is either adiabatic or assumes a constant temperature. The latter of these conditions corresponds to the case of natural convection in pressurized cryogenic containers. The first is considered to approximate the liquid surface boundary condition when it is exposed to the ambient with appropriate measures to minimize the effect of evaporation and heat transfer to the atmosphere. The effect of the gravity level, heat flux, and the surface temperature on the nature of the transient is discussed. Analytical results, which show the effect of each of these parameters are given.

The two-dimensional momentum and continuity equations were cast into the form of a time-dependent vorticity equation and an elliptic type equation relating the stream function and the vorticity. These equations together with the energy equation, were solved numerically. An explicit finite-difference approximation technique, was developed for this purpose. Three other finite-difference formulations, two implicit and one explicit, are also discussed.

The problems of stability and convergence of the numerical solution are given special attention. Stability criteria are obtained based on the von Neumann method of stability analysis and the concept of "positive-type differences." It was found that in most cases both methods of stability analysis lead to the same criterion. It was also found that the application of von Neumann method of stability analysis to partial differential equations similar to those considered here may lead to erroneous conclusions. Accordingly, a different procedure to examine the stability of such equations is presented, which in most cases leads to the same stability criterion.

Experimental measurements of transient temperature distributions in water were obtained for four different heat fluxes of 500, 1000, 2000, and 4000 Btu/hr/ft² in a cylindrical container, 3-7/8 in. inner diameter and 9 in. high. These heat levels correspond to modified Grashof numbers of 4.75×10^8 , 9.5×10^8 , 1.9×10^9 , and 3.8×10^9 , respectively, based on the cylinder radius.

Theoretical results were obtained for the first three heat flux levels using the measured time and space dependent wall temperature as

input to the computer program. The theoretical and measured temperatures are in good agreement.

Analytical results are presented for the case of natural convection in a rectangular and a cylindrical container, whose walls are subjected to a constant heat flux, its bottom insulated and the liquid surface assumes a step change in temperature.

Theoretical solution obtained by the present method for the natural convection in a rectangular cavity, which has one side heated, the other cooled and a linear bottom and top temperature variation is also in good agreement with a known analytical solution.

The analytical results are presented in the form of a series of transient isotherms and streamline plots. The results show that in both the rectangular and the cylindrical containers a vortex is formed near the wall at the top of the containers at small time levels. At higher time levels, this vortex moves towards the bottom of the container. Calculations also showed that after some time following the introduction of the transient, another vortex is formed at the liquid surface near the centerline. The time level at which this vortex is formed as well as its nature depends upon the heat flux level and the liquid surface boundary condition.

Finally, it should be mentioned that the method of solution reported here can be utilized for the analysis of natural or forced convection flow problems in any two-dimensional geometry.

CHAPTER 1

INTRODUCTION

The phenomenon of natural convection in closed containers has been of considerable interest in engineering applications. It has been utilized for the cooling of gas turbine blades by hollowing the blade and connecting it to a reservoir of cooled fluid. The large centrifugal force caused by the turbine rotary motion and the existence of temperature gradients along the blade axis cause the cold fluid near the reservoir end to replace the hot fluid at the blade tip. The transfer of cold fluid to hot regions and vice-versa, and the resulting cooling of the blades allow the use of higher temperature gases than can be tolerated by uncooled blades. As a result, higher turbine efficiencies can be obtained.

Natural convection in closed vessels with internal heat sources has assumed increased importance in nuclear reactor cooling. Considerable research has been done on this problem.

In application to space flight, the phenomenon of natural convection heat and mass transfer within partially filled liquid containers has become of considerable interest in connection with liquid propellant tanks thermal stratification and associated processes. A great deal of research has been directed towards the study of the process of heat and mass transfer within such containers during the pressurized discharge of a liquid propellant in an effort to optimize the tank design and the determination of the pressurant requirements as well as the selection

of the operating parameters for large rocket vehicles. The pressurant requirement, the instantaneous mass flow rate, the burnout mass, which is the mass of the propellant remaining at the end of the discharge process, as well as the pressurization level are among the important parameters whose determination is of primary importance to the designer. The determination of these parameters and the design of the propellant tank feed systems require the understanding of several related processes, such as pressurization, liquid stratification and the transfer of mass and energy transfer at gas-liquid and gas-solid interfaces. A comprehensive discussion of these processes has been published (10).

Figure 1 shows a schematic propellant feed system in which these phenomena take place (49).* The liquid oxygen (LOX) tank is pressurized by a side stream of vaporized oxygen (GOX) from the LOX pumps. The pressurant mass flow rate is controlled by a heat exchanger and pressure regulating system. Heat is transferred between the high temperature pressurant (GOX) and the liquid propellant at the liquid-vapor interface. As a result, mass transfer i.e., evaporation or condensation, takes place there. In the same time, heat exchange occurs between the tank walls and both the liquid and gas phases. This latter mode of heat transfer to the tank walls is caused by heat leakage from the ambient, heating of the tank walls by solar radiation, by aerodynamic heating or a combination of them. These processes of heat and mass

*Numbers in parentheses indicate the references which are given at the end.

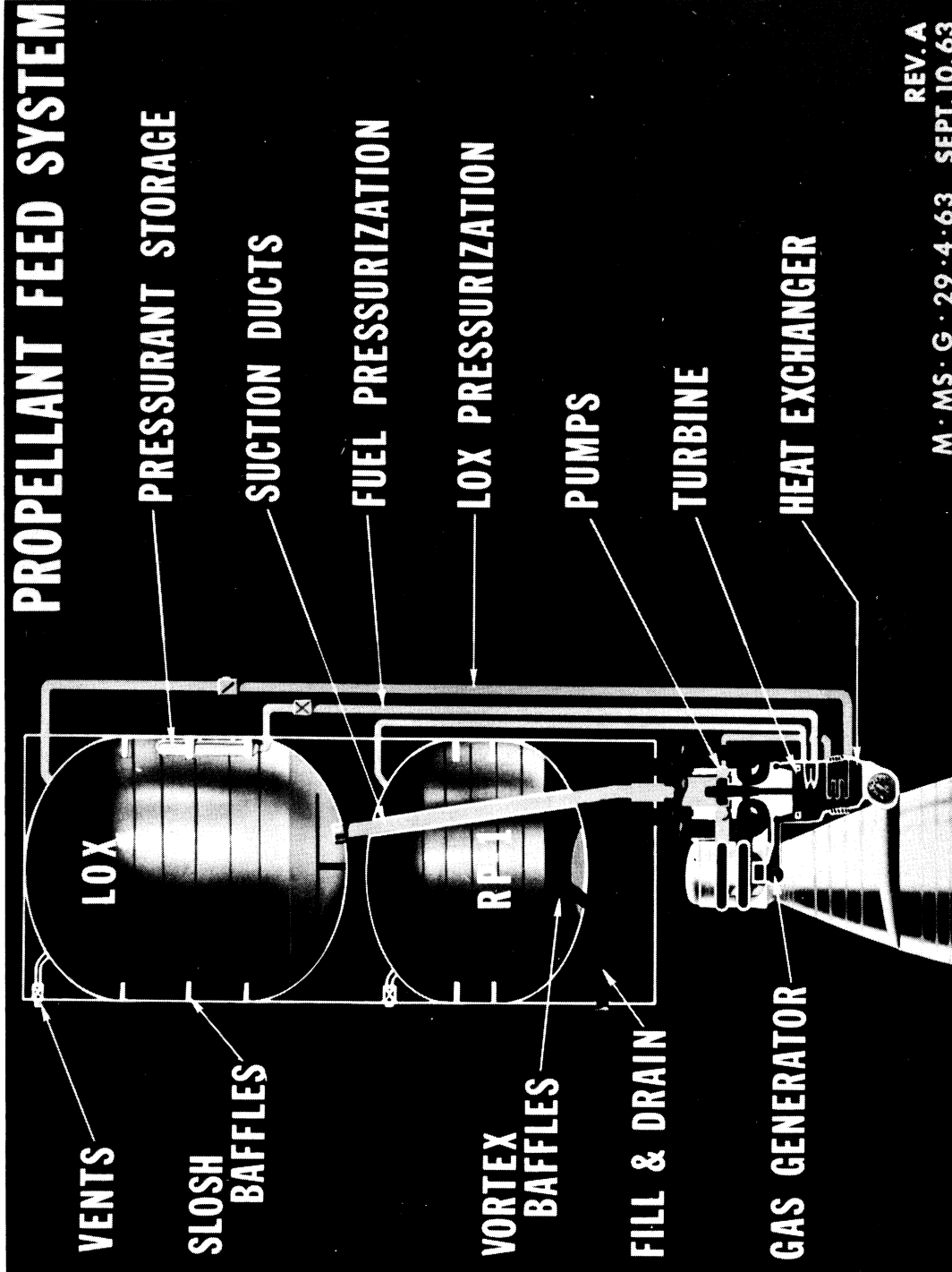


Fig. 1. Typical propellant feed system for flight vehicle.

transfer give rise to temperature and concentration gradients within both the gas and liquid. Natural convection flows are set up in both phases due to density variations caused by temperature gradients. Heated liquid near the tank wall is carried to the liquid-vapor interface, causing a hot layer of liquid, known as the stratified layer, to form at the liquid-vapor interface. The natural convection within the tank influences the temperature as well as the concentration gradients, which in turn control the process dynamics and the total pressurant consumption. The pressure level within the tank is dependent upon the pressure required to suppress pump cavitation at the engine pump inlet. The net positive suction head, NPSH, required to prevent pump cavitation is directly related to the temperature of the stratified layer at the end of the engine firing. Excessive temperature rise of the liquid would require higher pressures, which may cause structural weight penalties. For example, in the case of liquid hydrogen a 1°R increase in the liquid-vapor interface produces approximately a 3 psi increase in tank pressure. As a result of stratification, the pressure in cryogenic propellant containers has been found to be significantly greater than that corresponding to the vapor pressure at bulk (mixed) liquid temperature. The burn-out mass of pressurant is fixed by its mean temperature and pressure at the end of the discharge process. It is desired to keep this mass at a minimum.

The importance of the propellant feed system to the vehicle weight has been studied by Nein and Thompson (41). A summary of their findings

is given in Fig. 2, which shows the relationship between vehicle thrust and the mass-pressure ratio of the pressurant at the end of engine firing for some rocket systems. The result of this study reveals that should the tank pressure be increased, the burnout mass will be proportionately increased. Such an increase in tank pressure may be brought about by thermal stratification or by tank-layout considerations. Comparison between the weights of two similar vehicle designs which incorporate these considerations has been made by Platt et al., (49), and is given in Fig. 3.

A complete analysis of the mass and heat transfer interactions between the gas and liquid phases as well as between these phases and the container walls, which takes into consideration the effect of natural convection is presently unavailable.

In this work the analytical and experimental study of the two-dimensional, transient, laminar free convection in partially filled rectangular and cylindrical containers is undertaken. The geometry of the container, as well as the end effects invalidate the assumption of boundary layer flows. Therefore the boundary layer equations were not used. Instead, the full two-dimensional energy and Navier-Stokes equations are considered. These equations are not amenable to mathematical treatment using the classical methods. Furthermore, Ostromov (48) and Batchelor (8) found that neither the successive approximation nor the series expansion are suitable for handling such equations for

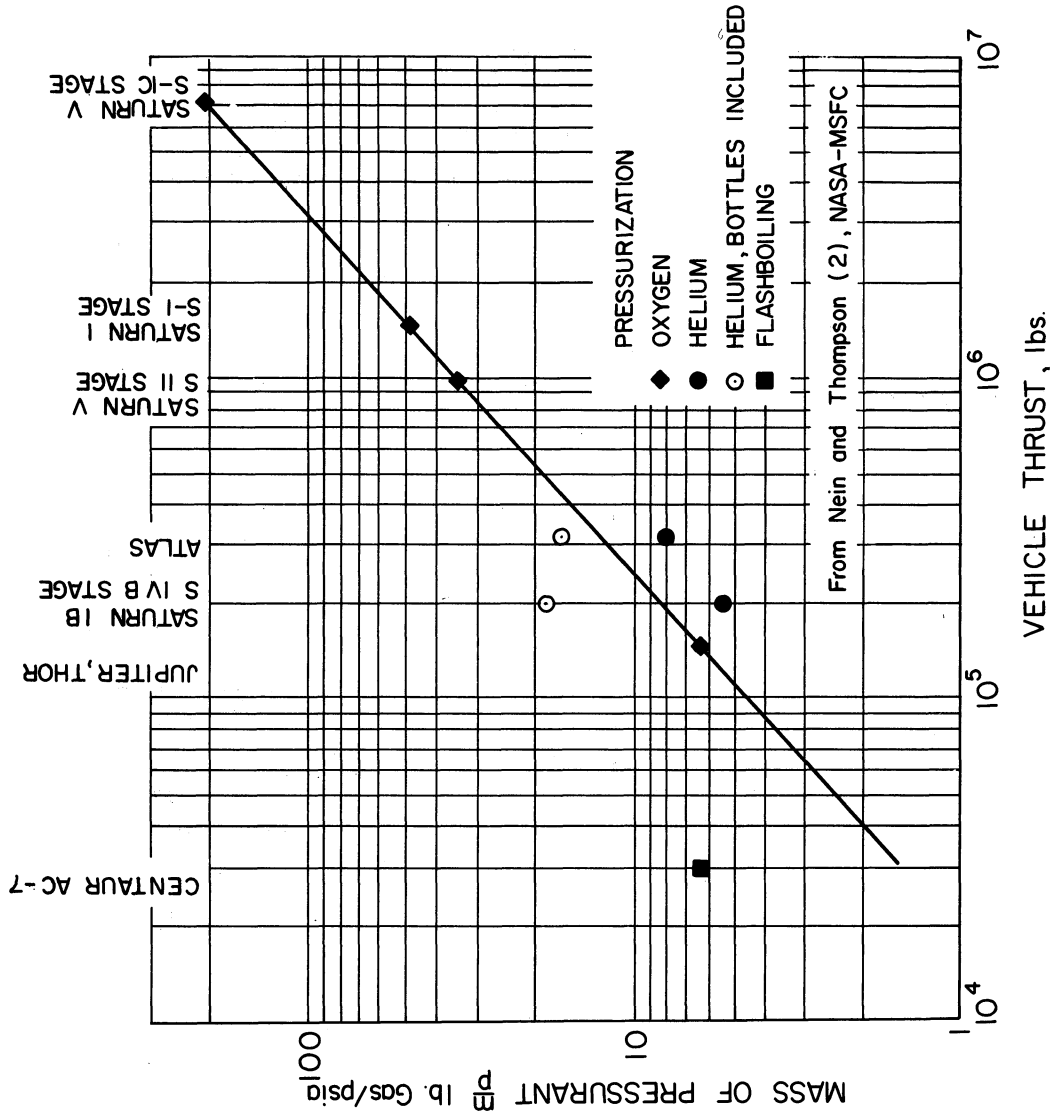


Fig. 2. Relationship between vehicle thrust and final oxygen tank pressurant mass-pressure ratio.

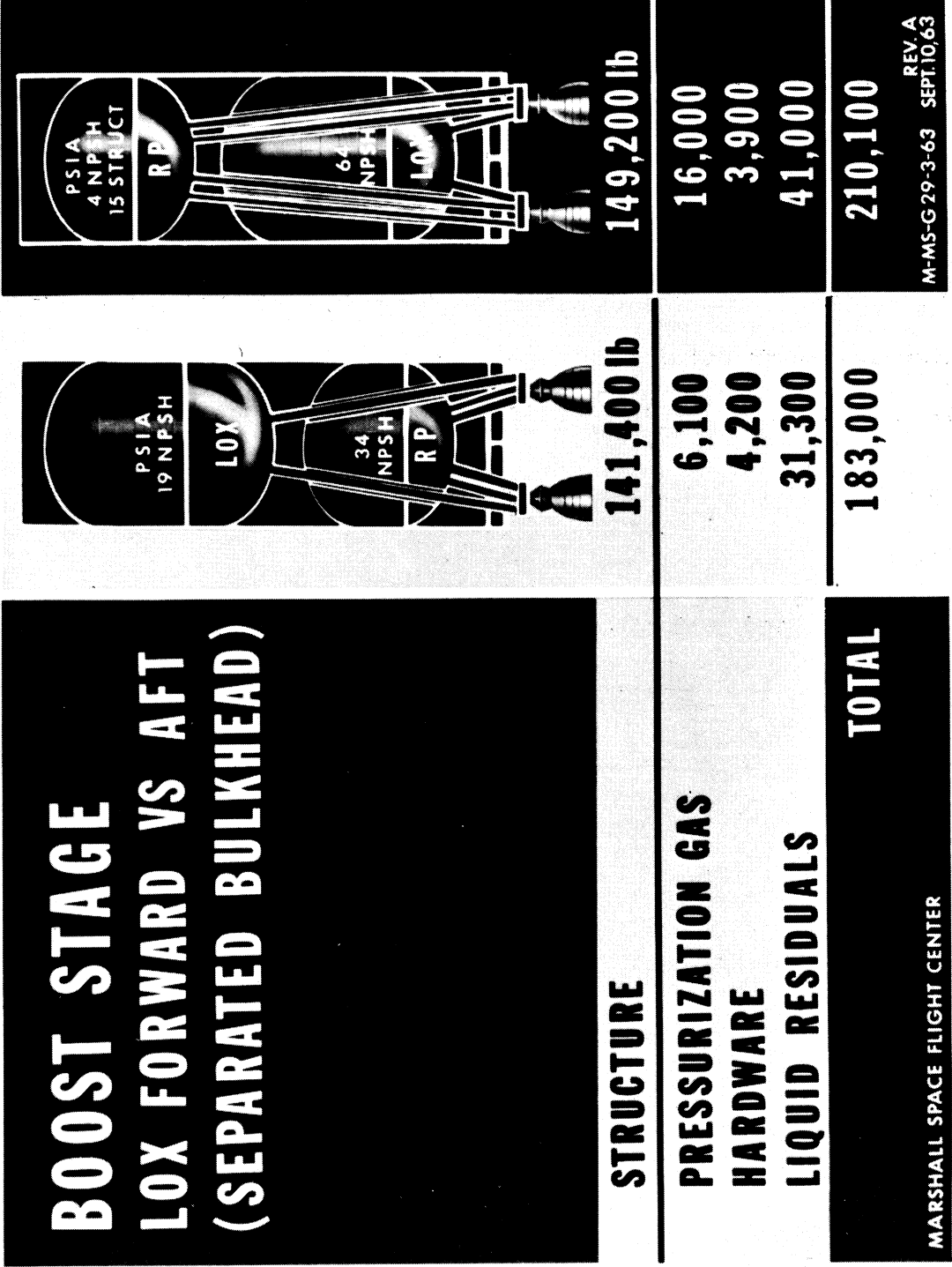


Fig. 3. Comparison of the weights of the propellant feed systems of two flight vehicles.

arbitrary Prandtl Number, Pr , and Grashof Number, Gr . Accordingly, it was decided to utilize a numerical procedure using the finite-difference approximation for the solution. The application of the finite-difference methods to the solution of such systems was not developed at the start of this work. Therefore in addition to the study of the phenomena of natural convection and thermal stratification, the study of the application of finite-difference techniques to such systems was undertaken. Considerable effort was given to the investigation of the stability problem, which is associated with the use of these methods.

The analytical results are compared with those obtained experimentally.

It is believed that the result of this research provides an improved understanding of the process mechanics of natural convection heat and mass transfer in closed containers. The results and conclusions reached concerning the use of the finite-difference method, for the solution of the governing differential equations will add some useful informations to the theory of numerical analysis. It is hoped that the method of solution developed here can be employed to study the natural convection in propellant tanks in both the gaseous and the liquid phases and to assist in the evaluation of associated processes such as interfacial mass and heat transfer.

CHAPTER 2

REVIEW OF THE LITERATURE

Considerable previous effort has been given to the study of natural convection heat and mass transfer. Many problems have been solved for different conditions of geometry and boundary conditions. These studies have been of analytical as well as of experimental nature. After the initiation of this work several analytical and experimental papers were published dealing with the natural convection in closed containers with free surfaces subject to side wall heating. The experimental results of Anderson and Kolar (1), showed that the stratification pattern is dependent upon whether the liquid heating is caused by side-wall heating, bottom heating, or by internal absorption of energy. The results obtained by Neff (39) and those obtained by Vliet and Brogan (73) support these conclusions. The experimental work of Barnett, et al., (7), which is made in a large cylindrical tank of the Saturn configuration, indicate that the gas pressure has an important effect on the liquid hydrogen stratification. They also presented a semi-empirical correlation for the axial temperature profile, which agrees with the test data. Schwind and Vliet (58) and Vliet and Brogan (73) have taken schlieren and shadowgraph pictures of the free convection with side-wall heating at various heat flux levels in rectangular containers with and without anti-slosh baffles. Other experimental work include that of Van Wylen, et al., (72), Fenster, et al., (19), Ordin, et al., (43), Scott, et al.,

(59), Swim (68) and Segel (60).

Based on the experimental observations of the nature of the flow a few models have been proposed for the analytical study of the stratification process. Most of these analytical approaches use the assumption of boundary layer flow along the wall. The model commonly used in these analyses is shown in Fig. 4. The heated liquid flows upward along the wall in a thin layer of thickness δ known as the boundary layer. The boundary layer is assumed to be zero at $x=0$, and grows in thickness with axial distance x . The heated liquid flows into the bottom of the stratified layer. The unmixed bulk liquid is at the initial temperature and is uniform. The liquid in the stratified layer is assumed to be either mixed or unmixed.

Publications which adopt the essential features of the model in Fig. 4 for unmixed stratified liquid, include Harper, et al. (25), Tellep and Harper (70), Schwind and Vliet (58), Ruder (55), Harper, et al. (24), Tatom, et al. (69), and Robbins and Rogers (53). Other studies treating the case of mixed (stratified) liquid include the work of Bailey and Fearn (3), Bailey, et al. (4,5), and Arnett and Millhiser (2).

The influence of liquid slosh and some of the factors governing it are reported by Coxe and Tatom (13), Eulitz (18) and Liu (37). An appraisal and evaluation of these works and others dealing with pressurization and interfacial phase changes has been given in Reference (10).

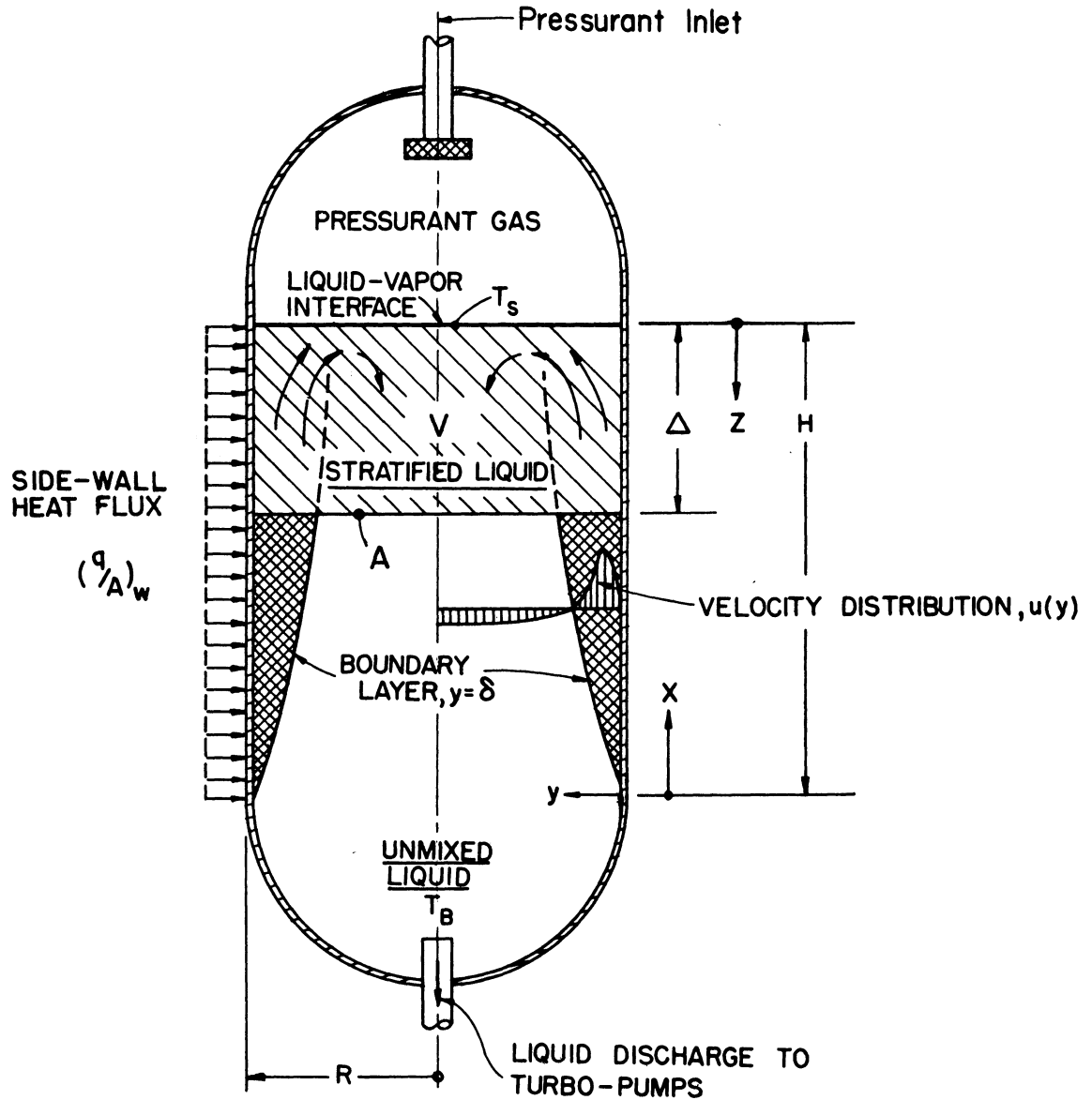


Fig. 4. Typical analytical model for liquid stratification analysis.

Therefore the details of such analyses will be omitted. However, it is important to review the assumptions introduced in constructing such models. These are listed as follows:

- (1) constant and uniform wall heat fluxes
- (2) no interfacial heat and mass transfer
- (3) constant axial acceleration
- (4) constant bulk temperature
- (5) A boundary layer flow along the wall, which is given by steady state, flat plate correlations.
- (6) The boundary layer thickness is time independent and is small compared to the container radius.

The complexity of the situation leads to the above simplifying assumptions. These assumptions ignore the influence of the time-transients on the boundary layer thickness as well as on the velocity distribution in the boundary layer. Furthermore the choice of the location of the axes, Fig. 4, is done arbitrary. In addition to that, these models ignore end effects, which may be important for vessel dimensions comparable to those used in flight vehicles i.e., length to radius ratios near unity.

The study of natural convection from plate surfaces and that in enclosed spaces has been studied by many investigators.

The case of a vertical element immersed in an infinite fluid initially at rest has received the most attention of many investigators. The time-steady laminar flow equations were first solved by Pohlhausen (50) for air. The experimental results of Schmidt and Beckman (51) are in good agreement with Pohlhausen's solution. Later, Ostrach (44) solved the same problem using numerical methods with high speed digital computer for different values of Prandtl number ranging from 0.01 to 1000.

The transient free-convection from vertical flat plates with and without appreciable thermal capacity and variable fluid properties has been studied by different investigators for different boundary conditions (21,28,56,61,65,66).

Leitzke (34) considered the steady state natural convection between two parallel infinite flat plates oriented in the direction of body force in which one plate is heated and the other is cooled uniformly. The measured temperature distribution across the fluid is in good agreement with the theory. A generalization to the same problem was carried on by Ostrach (44,45) in which the plates are maintained at constant temperatures not necessarily equal and the effect of heat sources and frictional heating was included. As anticipated heat sources and viscous heating increase the temperatures and the velocities between the plates. The transient free convection in a duct formed by two infinite parallel plates with arbitrary time variations in the wall temperature and the heat generation was studied by Zeiberg and Mueller (76).

The two dimensional steady-state convection in a long rectangle, of which the two long sides are vertical boundaries held at different temperature and the two horizontal boundaries either insulated or have linear temperature distribution, was considered by Batchelor (8). However, he did not solve for the velocity or temperature distribution. But he considered the determination of the rate of heat transfer between

the two vertical boundaries and the type of different flow regimes that occur for a given value of Rayleigh's number and aspect ratio. For Rayleigh's numbers less than 10^3 Batchelor uses a power series expansion in terms of Rayleigh's number Ra for the dimensionless temperature Θ and the stream function. On substitution of the power series in the governing differential equations and equating coefficients of the like powers of Ra , the problem is reduced to the solution of a series of linear partial differential equations. The Nusselt number defined as

$$NU = (q/A)_w / K(T_h - T_c)$$

is estimated to be of the order:

$$NU = l/d + 10^{-8} Ra^2$$

where: d is the distance between the plates and l the height of the duct. For the case of $l/d \rightarrow \infty$ he argues that for the regions not near the ends the temperature and the stream function take their asymptotic value which is given by the solution of two infinite parallel plates one heated and the other cooled. For infinite values of Ra , he postulates that an isothermal core exists having constant vorticity. He found that the governing equations for the general case could not be represented by a polynomial of small degree or could be handled by the Oseen Type of linearization.

Poots (51) solved the same problem handled by Batchelor. He obtained a numerical solution based on the use of orthogonal polynomials for the solution of the governing differential equations. Following

Batchelor the stream function and the nondimensional temperature were assumed to be represented by the complete double series of orthogonal functions

$$\Theta = \sum_{n=1}^{\infty} \sum_{m=1}^{\infty} A_{nm} \sin n\pi x \sin m\pi y$$

and

$$\Psi = \sum_{n=1}^{\infty} \sum_{m=1}^{\infty} B_{nm} X_n(x) Y_m(y)$$

where the A and B are constants which were evaluated numerically. The governing differential equations were reduced to two coupled algebraic equations to be solved simultaneously. The functions $X_n(x)$ were chosen to satisfy the fourth order Sturm-Liouville system and the orthogonality property. The method of solution is tedious and the calculations are practically impossible for Rayleigh's numbers greater than 10^4 and aspect ratios greater than 4.

Lighthill (36) examined natural convection flows generated by large centrifugal forces in a tube closed at one end and open at the other end to an infinite reservoir, where the tube walls are maintained at a constant temperature. Such a situation exists in cooling gas turbine blades. He predicted that one of the following three regimes may exist depending upon the product of Grashof number and the radius to length ratio of the tube. The assumed flow regimes are:

(1) Similarity flow: For small values of this product, i.e., for large values of length to radius ratio for a given Grashof number, the

boundary layer fills the tube. The velocity and temperature profiles are fully developed. He predicted that for this type of flow, the velocity and temperature distribution are similar at each section of the tube, only their scale is increasing as the orifice is approached. Assuming that the velocity and temperature vary linearly along the tube, he concluded that there exists an aspect ratio for which the temperature changes from its value at the orifice to the value at the bottom. Extending the tube beyond the length determined by the above ratio, the additional length is filled with fluid at rest at the walls temperature.

(2) Boundary layer type of flow: For high values of the product of Grashof number and radius to length ratio, i.e., for short tubes, the flow is of boundary layer type, the extreme case of it when the boundary layer fills a negligible portion of the tube area, the flow approximates the free convection flow up a flat plate.

(3) Non-Similarity regime: This is the type of flow predicted to exist for values of length to radius ratio which lie between the values corresponding to the first and the second case. The boundary layer fills a large portion of the tube section. He used the Squire technique to solve the first and the third case.

Hammitt (23) considered the case of a closed vertical cylinder with internal heat generation. He used the Lighthill technique modified to account for the heat sources. The agreement between the calculated and measured values of Nusselt's number is not good. This is probably

due to some of the inevitable assumptions, which are made. These assumptions are: (1) small inertia forces compared to buoyancy and shear (2) radial extent of the temperature and velocity boundary layers is the same (3) the boundary layer approximation apply. The first one is valid for large Prandtl numbers, while the second is valid for Prandtl numbers near unity. The disadvantage of this method of solution is that it is not capable of detailed examination of the end conditions. Smith (63) extended Hammit's analysis to two-dimensional rectangular containers.

Following Lighthill, Ostrach and Thornton (47) considered a geometrically similar case with a linear wall temperature. In Ostrach's paper as well as in Lighthill's paper, attention was given to the stagnation of natural convection flows at the closed end. The same problem considered by Lighthill was solved by Levy (35) using integral method. He assumes the upward flow consists of a layer of thickness δ , near the wall, the remaining of the tube being filled with cold fluid flowing down. He assumes three regimes of flow similar to those postulated by Lighthill. If the tube length is less than or equal to a length l , the stagnation region does not exist and the upflow convective layer increases with x . For axial distance $x > l_1$, δ reaches a constant value d and such a flow occurs for $l_1 < x < l_2$. For $x > l_2$, a stagnation region exists at the closed section of the tube.

Romonov (54) using also integral technique, solved the same problem considered by Lighthill and Levy. His calculations agree with those

of Lighthill for infinite Prandtl number, but it differs considerably for Prandtl numbers near unity. The measured and the calculated temperatures are in a good agreement for different wall temperatures.

A large number of experimental studies of flat plates, immersed in an infinite fluid at rest, either heated or cooled has been done. In general, there has been a good agreement between the theory and experiments. A considerable experimental work has been done in the field of natural convection in tubes and enclosures. These have been concerned with specialized applications and particular configurations. Most of these experimentations were done in connection with cooling gas turbine blades and nuclear reactors applications.

Probably the most comprehensive experimental studies of natural convection in thermosyphons are those conducted by Martin (38) in an attempt to check the theoretical work of Lighthill. His results agree qualitatively although the measured heat transfer coefficients are two folds larger than that predicted by Lighthill. From measurements of heat transfer rates, the three regimes predicted by Lighthill were identified. The heat transfer was greatest for large values of the product of Grashof number and the radius length ratio, being highest at the bottom of the tube which indicates that boundary layer type of flow exists. At small values of the product, the heat transfer varied linearly from the orifice to zero at the bottom of the tube, from which he concluded that the similarity regime exists. A region of instabilities

occurred between the above two steady regimes which is characterized by nonsinusoidal oscillatory flow.

The explorations of the air flow patterns in the space between two heated wide plates closed at the bottom, open at the top, and insulated at the sides done by Siegel and Norris (62) shed some light on the oscillatory flow mentioned by Martin. For spacing of 0.28 the plate height, the flow pattern was symmetric with upward flowing boundary layers near each plate surface and downflow in between. When the spacing was reduced to 0.21 the height, the flow pattern became asymmetric with half the cross section occupied by upward flow (near one plate) and the half near the other plate occupied by downward flow. For smaller spacings, the asymmetric pattern persisted with periodic nonsinusoidal reversal in flow direction and temperature fluctuations.

Curren and Zalbak (14) conducted an experimental investigation to determine the effect of length to diameter ratio of closed end coolant passages on natural convection water cooling of gas turbines. They reported no significant difference in the heat transfer for the different length to diameter ratios investigated ranging from 5:1 to 25.5:1. For the largest length to diameter ratio 25.5:1 the boundary layer fills 87% of the tube cross section.

The visual studies of Sparrow and Kaufman (67) of free convection of water in a narrow vertical enclosure, cooled at the top through a copper surface and open at the bottom to a heated reservoir revealed that the flow pattern is not steady. No region of the enclosure is

permanently a region of upflow or of downflow. The size of the various upflow and downflow regions varied along the length of the enclosure at a given time. The number and size of upflow and downflow regions also varied with time. However, end effects were observed and a continuous downflow took place in a $3/4$ " band adjacent to both walls. Generally, the dominating character of the flow was instability.

Hartnett, et al., (26,27,32) studied the free convection heat transfer for the geometry postulated by Lighthill but with a constant heat flux at the tube wall using water and mercury as working fluids. The effect of inclining the tube was also investigated. Temperature oscillations of the same nature as that reported by Martin and Siegel and Norris were observed. On the contrary of the results reported by Curren and Zalabak, the heat transfer was considerably influenced by length to radius ratio. A decrease in length to radius ratio from 22.5 to 15 results in approximately 100 per cent increase in the Nusselt numbers.

The natural convection flow pattern in viscous oil in rectangular tanks heated at the center by vertical coil heater studied by Skipper, et al., (63) consisted of a narrow chimney of hot oil rising vertically around the heater surface and above it and a horizontal layer of hot oil at the free surface separated from the remaining cold oil below by a sharp vertical gradient. The hot oil layer had a small vertical temperature gradient, with maximum temperature at the top. The hot oil

layer at the surface became thicker and thicker with continued heating. The hot oil was found to flow downward at the walls of the tank while there were suggestions of circulating currents at the side of the rising chimney. The flow pattern shown suggests that a vortex was formed at the free surface near the center line where the hot rising chimney is bifurcated and spread horizontally along the surface. Similar vortices were observed by Eichhorn (17). These vortices were formed at the free surface of water near the walls of a cylindrical tube 2 in. diameter and 5 in. long uniformly heated at the walls and open at the top.

It has been recognized that as of now the solution of complicated problems of fluid flow and heat transfer can be obtained by numerical methods only. Among these the finite-difference techniques seemed to require minimum simplifying assumptions and idealizations as compared to other numerical methods. Indeed, finite-differences have been used by many investigators for the solution of the momentum and energy equations. These problems and consequently the finite-difference procedures used, varied in complexity.

The finite-difference solution of the laminar boundary layer equations describing the natural convection process from isothermal vertical flat plates and that inside a horizontal cylinder is given by Hellums and Churchill (28). They employed an explicit finite-difference procedure similar to that adopted here, (Chapter 5). The results obtained for the flat plate are in good agreement with solution of Ostrach (44).

The discrepancy between the experimental and the theoretical results for the horizontal cylinder is within 30 to 50%.

Simultaneously with the initial phase of this research (11) two other independent theoretical studies treating similar problems were reported. These are by Fromm (21) and Wilkes (74). These studies are significant since they handle problems similar in nature and complexity to that considered here.

Fromm (21) investigated the unsteady wake behind a small rectangular obstacle placed normal to the flow caused by two moving parallel walls. The time-dependent vorticity equation was solved using a Dufort and Frankel type representation for the second order terms $\partial^2 w / \partial x^2$ and $\partial^2 w / \partial y^2$, while the nonlinear terms $u(\partial w / \partial x)$ and $v(\partial w / \partial y)$ were treated using central differences at time level n . Accordingly the values of the vorticity at the time level $(n+1)$ can be explicitly calculated. The equation relating the vorticity and stream function, defined here as the vorticity-stream function equation, (see Chapter 5), was solved using the Gauss-Seidel iterative method. Fromm did not give stability analysis for his finite-difference formulation. However, he considered the stability of the vorticity equation with either of the diffusion or the convective terms present. Furthermore, he resorted to mathematical experimentation to determine the size of the time increment which makes the solution stable, by observing the manner in which any introduced error may decay or amplify. In addition, a small time increment was used. Problems having Reynold numbers, based on the obstacle width

normal to the flow, as high as 1000 were handled.

The natural convection from a rectangular two-dimensional cavity considered by Poots (51) was solved by Wilkes (74) using finite-differences. An implicit alternating direction technique was used to advance the temperature and vorticity fields across any time step. According to the stability analysis made by him using the Von-Neumann method of stability analysis the method is unconditionally stable. However actual calculations showed that this formulation is suitable for low Grashof and Prandtl numbers only.

Both Fromm's and Wilkes' Formulations have the advantage of using central differences for approximating the convective terms $u(\partial w/\partial x)$, $v(\partial w/\partial y)$, ...etc. As will be explained in Chapter 5, this representation is preferable from the standpoint of the truncation error. However, as found in this present study there are restrictions to the use of central differences which may not be satisfied at large Reynolds or Grashof numbers. The nature of these restraints is discussed in Chapter 6.

CHAPTER 3

STATEMENT AND PHYSICS OF THE PROBLEM

3.1 INTRODUCTION

A two-dimensional, closed container, partially filled with liquid in unsteady, laminar flow is considered. Two different geometrical configurations are examined:

- (a) A two-dimensional rectangular tank, and
- (b) A two-dimensional cylindrical tank.

The governing partial differential equations as well as the boundary conditions for each configuration will be given in subsequent sections, each being considered separately. However, the following discussion regarding the physics and nature of the problem applies to both configurations.

The purpose of this work is the investigation of thermal stratification in partially filled, liquid propellant containers.

This was accomplished by an investigation of two theoretical models, each of which is outlined below. The first model is very general and includes the influence of pressurization and various types of wall effects. The second model was selected in order to provide physical base to which the theoretical analysis could be related. This model does not include the influence of pressurization, but introduces an interfacial boundary conditions compatible with an experiment which is simple, yet completely adequate to check the principal points of the theory. Theoretical

calculations are made, however, for both models. Neither models considers the process of discharge although this effect can readily be concluded. In addition a single component system is studied. Extension of the analysis to multi-component systems is within the capability of the formulation and method of solution, however.

3.2 DESCRIPTION OF THE FIRST MODEL

The first model was chosen to correspond to the physical situation in the propellant container. The container is assumed to be partially filled with a liquid. The initial conditions in the liquid and the vapor, are assumed to be known. From these initial conditions, the wall of the vessel is subjected to a change in temperature, or to be exposed to a heat flux, either of which may be an arbitrary function of tank height and time. Simultaneously the pressure in the vapor space is changed to P_s . The pressure P_s may be equal to or greater than the initial pressure P_0 , or may vary with time. The measurements of references 12 and 19 indicate that the interface rises very rapidly to the equilibrium temperature T_s corresponding to the pressure P_s in the vapor space. These perturbations in the boundary conditions lead to a series of non-equilibrium phenomena within the container. Natural convection currents are set up in the liquid and in the vapor space. At the same time the liquid-vapor system tends to adjust to the new non-equilibrium condition within the tank by transferring mass and energy across the interface by either evaporation or condensation.

The conditions of the liquid-vapor interface couple the simultaneous transport processes in the liquid and gas phases. The rate of mass transfer by evaporation or condensation across the liquid-vapor interface depends on the relative rates of heat transfer from each phase at the interface. Any imbalance of the heat transfer across the liquid-vapor interface is counterbalanced by a phase change at the interface. Should heat transfer from the vapor dominate that to the liquid, evaporation will occur; if the opposite is true, the vapor will condense; if the respective heat transfer rates are the same, neither evaporation nor condensation takes place.

Both the interfacial phase change and the convective action within both phases influence the growth of the stratified layer of liquid at the interface, which, in turn, affects both the interfacial and convective phenomena. Such interactions have not been completely formulated and apparently no solution is yet available which considers these interactions. This is a result of the complexity of the processes which makes it difficult to obtain a generalized solution to the problem. In this analysis, however, the problem can be formulated in its general form taking into consideration the interaction between the liquid and vapor phases. Later, in Section 3.5, a simplified model, which is sufficient for the purpose of this work, will be considered. However, it is worthwhile to mention that the method of solution developed here and applied to the simplified model, can be utilized to study the physical phenomena associated with the more generalized process. Such

a solution will be of value to engineers concerned with the design and development of propellant containers and associated systems.

3.3 DESCRIPTION OF THE SECOND MODEL

It was mentioned before that the basic objective of this work is the analytical prediction of thermal stratification in stored cryogenic liquids in partially filled containers. However, since the stratification phenomenon is encountered in all liquids, the experimental study of this phenomenon can, therefore, be carried in noncryogenic liquids, as well. The use of such liquids facilitates the experimental set-up considerably, and allows the evaluation of the theoretical results in the light of the experimentally obtained data. For these reasons, a series of experiments were carried on in a two, geometrically different, two-dimensional containers, one of which is rectangular and the other is cylindrical.

Both containers were partially filled with non-cryogenic liquid. The vapor-liquid interfacial boundary condition differs in this case from that described in the first model. The heat losses from the liquid to the vapor is assumed to be negligible. The interface is therefore considered adiabatic. This condition should be regarded as an approximation for the interfacial condition in an experiment carefully conducted to minimize the heat losses from the interface. This particular point will be discussed further in the formulation of the problem Section 3.6 as well as in discussing both the experimental procedure, Chapter 7, and

the experimental results, Chapter 8.

3.4 GENERALIZED FORMULATION OF THE FIRST MODEL

In this section the problem is formulated in its general form. The governing partial differential equations, as well as the boundary conditions, are given for the rectangular container. Although the same generalized formulation can be easily made for the cylindrical coordinates, its details will be omitted.

A rectangular two-dimensional container of width $2a$ and height h is partially filled with a liquid. The initial height of the liquid is b , and the depth of the vapor is c . The origin of the coordinate system is taken at the middle of the tank bottom with x -positive in the direction of the liquid as shown in Fig. 5. The g level is assumed sufficiently high so that the effect of surface tension can be neglected. The location of the liquid vapor interface at any one time is given by $x = X(t)$. The differential equations governing the transient velocity and temperature distribution in both the liquid and the vapor regions developed as follows.

The momentum equations

(i) The x -momentum equation:

$$\rho \left(\frac{\partial u}{\partial t} + u \frac{\partial u}{\partial x} + v \frac{\partial u}{\partial y} \right) = -\rho g - \frac{\partial p}{\partial x} + \frac{\partial}{\partial x} \left[\mu \left\{ 2 \frac{\partial u}{\partial x} - \frac{2}{3} \left(\frac{\partial u}{\partial x} + \frac{\partial v}{\partial y} \right) \right\} \right] + \frac{\partial}{\partial y} \left[\mu \left(\frac{\partial u}{\partial y} + \frac{\partial v}{\partial x} \right) \right] \quad (3.1)$$

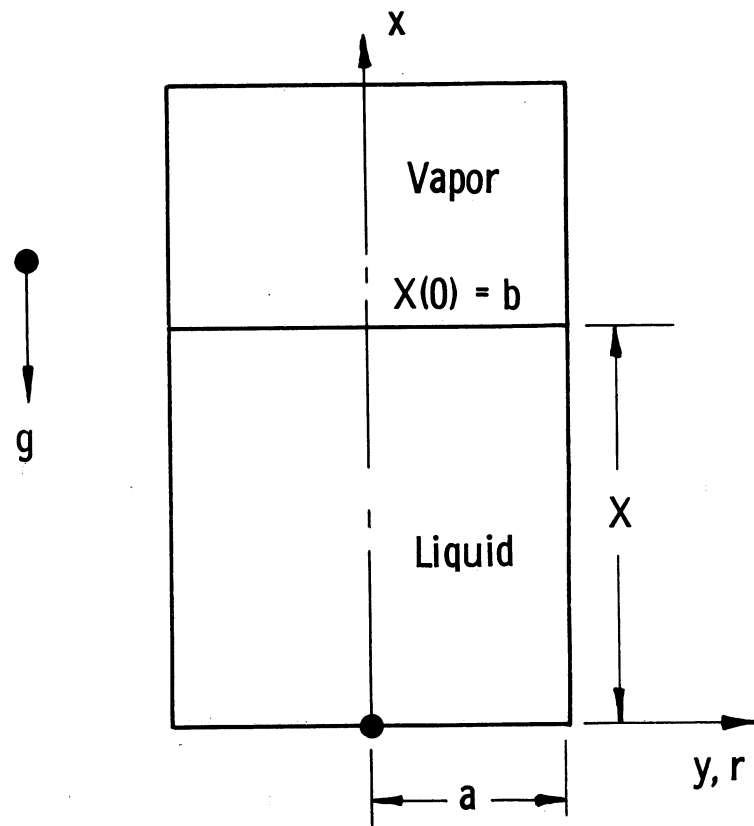


Fig. 5. Container configuration and coordinate system.

(ii) The y-momentum equation:

$$\rho \left(\frac{\partial v}{\partial t} + u \frac{\partial v}{\partial x} + v \frac{\partial v}{\partial y} \right) = - \frac{\partial p}{\partial y} + \frac{\partial}{\partial x} \left[\mu \left(\frac{\partial u}{\partial y} + \frac{\partial v}{\partial x} \right) \right] + \frac{\partial}{\partial y} \left[\mu \left\{ 2 \frac{\partial v}{\partial y} - \frac{2}{3} \left(\frac{\partial u}{\partial x} + \frac{\partial v}{\partial y} \right) \right\} \right] \quad (3.2)$$

The continuity equation

$$\frac{\partial \rho}{\partial t} + \frac{\partial(\rho u)}{\partial x} + \frac{\partial(\rho v)}{\partial y} = 0 \quad (3.3)$$

The energy equation

$$\rho C_p \left(\frac{\partial T}{\partial t} + u \frac{\partial T}{\partial x} + v \frac{\partial T}{\partial y} \right) = \frac{\partial p}{\partial t} + u \frac{\partial p}{\partial x} + v \frac{\partial p}{\partial y} + \frac{\partial}{\partial x} \left(K \frac{\partial T}{\partial x} \right) + \frac{\partial}{\partial y} \left(K \frac{\partial T}{\partial y} \right) + \mu \phi \quad (3.4)$$

where, ϕ is the dissipation function and is given by:

$$\phi = 2\mu \left[\left(\frac{\partial u}{\partial x} \right)^2 + \left(\frac{\partial v}{\partial y} \right)^2 \right] + \mu \left(\frac{\partial u}{\partial y} + \frac{\partial v}{\partial x} \right)^2 \quad (3.5)$$

The Initial Conditions

In this generalized formulation, arbitrary initial velocity and temperature distributions are considered. This generalization of the initial conditions does not impose any restrictions or difficulties, as far as the solution is concerned, because the method of solution used in this work permits such a generalization. It is required, of course, that the initial conditions be known from past velocity and temperature-time history. These initial conditions are given by:

$$(1) \quad T(x, y, 0) = T_0(x, y) \quad (3.6)$$

$$(2) \quad T_g(x, y, 0) = T_{g_0}(x, y) \quad (3.7)$$

$$(3) \quad u(x,y,0) = u_0(x,y) \quad (3.8)$$

$$(4) \quad u_g(x,y,0) = u_{g_0}(x,y) \quad (3.9)$$

$$(5) \quad v(x,y,0) = v_0(x,y) \quad (3.10)$$

$$(6) \quad v_g(x,y,0) = v_{g_0}(x,y) \quad (3.11)$$

The Boundary Conditions

Velocity Boundary Conditions

Assuming the no slip condition to prevail at the tank walls, the following boundary conditions are obtained:

$$(7) \quad u(0,y,t) = 0 \quad (3.12)$$

$$(8) \quad u(x,\pm a,t) = 0 \quad (3.13)$$

$$(9) \quad v(0,y,t) = 0 \quad (3.14)$$

$$(10) \quad v(x,\pm a,t) = 0 \quad (3.15)$$

$$(11) \quad u_g(x,\pm a,t) = 0 \quad (3.16)$$

$$(12) \quad v_g(x,\pm a,t) = 0 \quad (3.17)$$

The boundary conditions in the vapor space at the top of the container depend upon whether the tank is closed or vented and upon the pressurant inlet design. The choice of these boundary conditions, therefore, can be made only for a specific system. For these reasons these boundary conditions will not be given here.

The interfacial boundary conditions are of primary importance for the study of the interactions of the liquid and vapor phases. Assuming zero shear stress at the liquid-vapor interface, the following is obtained:

$$(13) \quad \frac{\partial v}{\partial x} (X,y,t) = 0 \quad (3.18)$$

$$(14) \quad \frac{\partial v_g}{\partial x} (X,y,t) = 0 \quad (3.19)$$

According to the assumption that the liquid surface will remain flat the velocity of the liquid-vapor interface is given by:

$$(15) \quad u (X,y,t) = u_g(X,y,t) = \frac{dX}{dt} . \quad (3.20)$$

The motion of the liquid-vapor interface may be due to discharge, interfacial phase change or both. When container draining is not considered, dX/dt will represent the interfacial velocity caused by phase changes.

From the geometric symmetry of the configuration with respect to the x-axis the y-component of the velocity is zero along the x axis of the container. Furthermore the x-component of the velocity is symmetric. Hence,

$$(16) \quad v(x,0,t) = 0 \quad (3.21)$$

$$(17) \quad \frac{\partial u}{\partial y} (x,0,t) = 0 \quad (3.22)$$

$$(18) \quad v_g(x,0,t) = 0 \quad (3.23)$$

$$(19) \quad \frac{\partial u_g}{\partial y} (x,0,t) = 0 \quad (3.24)$$

Thermal Boundary Conditions

The bottom of the container is assumed to be adiabatic. The walls of the container are either subjected to a space and time dependent heat flux, or they undergo any arbitrarily specified change in temperature. The boundary conditions at the top of the container will be determined,

as stated before, by the conditions at the vapor inlet. Consequently, the temperature boundary conditions in the vapor space at the container top will not be considered here. From the symmetry of the container, the temperature will be symmetric. From these considerations the following boundary conditions can be written:

$$\begin{aligned}
 (20) \quad & a-K \frac{\partial T}{\partial y}(x, \pm a, t) = f_1(x, t) \\
 & \text{or} \\
 & b-T(x, \pm a, t) = f_2(x, t)
 \end{aligned}
 \left. \vphantom{\begin{aligned} (20) \quad a-K \frac{\partial T}{\partial y}(x, \pm a, t) = f_1(x, t) \\ \text{or} \\ b-T(x, \pm a, t) = f_2(x, t) \end{aligned}} \right\} 0 \leq x \leq X \quad (3.25)$$

$$\begin{aligned}
 (21) \quad & a-(K \frac{\partial T}{\partial y}(x, \pm a, t))_g = f_3(x, t) \\
 & b-T_g(x, \pm a, t) = f_4(x, t)
 \end{aligned}
 \left. \vphantom{\begin{aligned} (21) \quad a-(K \frac{\partial T}{\partial y}(x, \pm a, t))_g = f_3(x, t) \\ b-T_g(x, \pm a, t) = f_4(x, t) \end{aligned}} \right\} X \leq x \leq h \quad (3.26)$$

$$(22) \quad \frac{\partial T}{\partial x}(0, y, t) = 0 \quad (3.27)$$

$$(23) \quad \frac{\partial T}{\partial y}(x, 0, t) = 0 \quad (3.28)$$

$$(24) \quad \frac{\partial T_g}{\partial y}(x, 0, t) = 0 \quad (3.29)$$

where f_1 , f_2 , f_3 and f_4 determine either the specified tank wall heat flux or tank wall temperature as indicated by Equations (3.25) and (3.26). The liquid-vapor interface is assumed to be at the equilibrium temperature, T_s , corresponding to the pressure P_s in the vapor space, i.e.

$$(25) \quad T(X, y, t) = T_g(X, y, t) = T_s \quad (3.30)$$

Conservation of energy at the interface determines its velocity as a function of the rate of heat transfer between the interface and the liquid and vapor phases. Hence,

$$\rho_{fg} \cdot \frac{dX}{dt} = K \frac{\partial T}{\partial x} (X,y,t) - K_g \frac{\partial T_g}{\partial x} (X,y,t) \quad * \quad (3.31)$$

It should be noted here that when the pressure in the vapor space is specified the interfacial temperature will be given by Equation (3.30). Such a situation may exist in vented tanks or in tanks fitted with pressure regulators to maintain the pressure in the tank at a pre-determined level. For cases in which the tank is not vented or if intermittent venting of the tank is provided, it would be necessary to consider the interactions between the vapor and liquid phases in order to determine the pressure-time history in the tank, as well as, the interfacial temperature-time history.

3.5 SIMPLIFIED FORMULATION OF THE FIRST MODEL

3.5.1 Rectangular Coordinates

The description of the physical phenomena for the situations in which the pressure within the tank is not prescribed is complex. For this reason a simplified model is adopted, without impairing the utility of its solution. In this model only the liquid region is considered.

*This equation does not include the effect of discharge. Should it be desirable to consider the process of liquid discharge Equation (3.31) would be written:

$$\rho_{fg} \left(\frac{dX}{dt} + \frac{\dot{m}}{2\rho a} \right) = K \frac{\partial T}{\partial x} (X,y,t) - K_g \frac{\partial T_g}{\partial x} (X,y,t) \quad (3.31a)$$

where

\dot{m} : discharge flow rate.

The assumptions made in simplifying the problem are:

- (1) Incompressible liquid.
- (2) The pressure in the ullage space, P_g , is either a known function of time, or is constant. Consequently, the interfacial temperature, T_g , will be specified.
- (3) The amount of evaporation or condensation is small. Therefore the interfacial displacement is neglected and the interface remains always at $x=b$.

Assumptions (2) and (3) permit the consideration of the liquid and vapor regions separately, since in this case each phase exchanges heat with both the interface and the container walls independently from the other.

*Boussinesq
assumptions*

- (4) The fluid properties are constant. Density variations are allowed in the body force term only in the x-momentum equation.
- (5) The pressure terms and the dissipation function in the energy equation are neglected.
- (6) The variations in pressure and density from their initial values caused by fluid motion and temperature gradients will be small. Therefore, density variations are caused by temperature changes. The density ρ can then be approximated by:

$$\rho = \rho_0(1 + \beta(T_0 - T)) \quad (3.32)$$

where ρ_0 and T_0 are reference values of the density and temperature respectively, for which, in this analysis, the initial values are taken. β is the coefficient of thermal expansion.

In this case the governing differential equations (3.1), (3.2), (3.3) and (3.4) reduce to:

The x-momentum

$$\rho \left(\frac{\partial u}{\partial t} + u \frac{\partial u}{\partial x} + v \frac{\partial u}{\partial y} \right) = -\rho g - \frac{\partial p}{\partial x} + \mu \left(\frac{\partial^2 u}{\partial x^2} + \frac{\partial^2 u}{\partial y^2} \right) \quad (3.33)$$

The y-momentum

$$\rho \left(\frac{\partial v}{\partial t} + u \frac{\partial v}{\partial x} + v \frac{\partial v}{\partial y} \right) = - \frac{\partial p}{\partial y} + \mu \left(\frac{\partial^2 v}{\partial x^2} + \frac{\partial^2 v}{\partial y^2} \right) \quad (3.34)$$

The continuity equation

$$\frac{\partial u}{\partial x} + \frac{\partial v}{\partial y} = 0 \quad (3.35)$$

The energy equation

$$\frac{\partial T}{\partial t} + u \frac{\partial T}{\partial x} + v \frac{\partial T}{\partial y} = \alpha \left(\frac{\partial^2 T}{\partial x^2} + \frac{\partial^2 T}{\partial y^2} \right) \quad (3.36)$$

The initial conditions

$$(26) \quad T(x,y,0) = T_0(x,y) \quad (3.37)$$

$$(27) \quad u(x,y,0) = u_0(x,y) \quad (3.38)$$

$$(28) \quad v(x,y,0) = v_0(x,y) \quad (3.39)$$

The Boundary ConditionsVelocity Boundary Conditions

$$(29) \quad u(b,y,t) = 0 \quad (3.40)$$

$$(30) \quad u(0,y,t) = 0 \quad (3.41)$$

$$(31) \quad u(x,\pm a,t) = 0 \quad (3.42)$$

$$(32) \quad \frac{\partial u}{\partial y} (x,0,t) = 0 \quad (3.43)$$

$$(33) \quad v(x,\pm a,t) = 0 \quad (3.44)$$

$$(34) \quad v(x,0,t) = 0 \quad (3.45)$$

$$(35) \quad v(0,y,t) = 0 \quad (3.46)$$

$$(36) \quad \frac{\partial v}{\partial x} (b,y,t) = 0 \quad (3.47)$$

Temperature Boundary Conditions

$$(37) : T(b,y,t) = T_s(t) \quad (3.48)$$

$$(38) : a-K \frac{\partial T}{\partial y}(x,\pm a,t) = \frac{q''}{A}(x,t)$$

$$\text{or} \quad (3.49)$$

$$b- T(x,\pm a,t) = T_w(x,t)$$

$$(39) \frac{\partial T}{\partial x}(0,y,t) = 0 \quad (3.50)$$

$$(40) \frac{\partial T}{\partial y}(x,0,t) = 0 \quad (3.51)$$

As mentioned earlier the method of solution allows the use of any arbitrary initial and boundary conditions. Therefore the general boundary and initial conditions written for the general model are retained here. Also it should be mentioned that the above boundary conditions were chosen to approximate the actual situation as much as possible. However any combination of these conditions, or others, can certainly be handled using the same method of analysis employed in this work.

3.5.2 Formulation of the Simplified Model, Cylindrical Coordinates

In this case a cylindrical container whose radius is a is partially filled with a liquid, Fig. 5.

The physical phenomena and the interactions between the liquid and vapor phases in the tank, which are described earlier during the formulation of the problem in rectangular coordinates, take place independent of the geometry of the container. Accordingly, the generalized formula-

tion given for the rectangular coordinates can be modified to suit cylindrical coordinates. In order to avoid unnecessary repetition, the generalized formulation will not be given for cylindrical coordinates, and only the simplified model will be considered. The same assumptions made earlier are retained here and for clarity, they are listed again:

- (1) incompressible fluid
- (2) constant pressure in the ullage space, P_g
- (3) negligible evaporation or condensation
- (4) constant fluid properties. Only density variations are allowed in the body force term. These variations are given by Equation (3.32).
- (5) The dissipation function and the pressure terms in the energy equations are neglected.

The governing partial differential equations are:

The x-momentum

$$\rho \left(\frac{\partial u}{\partial t} + u \frac{\partial u}{\partial x} + v \frac{\partial u}{\partial r} \right) = -\rho g - \frac{\partial p}{\partial x} + \mu \left(\frac{\partial^2 u}{\partial x^2} + \frac{1}{r} \frac{\partial u}{\partial r} + \frac{\partial^2 u}{\partial r^2} \right) \quad (3.52)$$

The Radial momentum

$$\rho \left(\frac{\partial v}{\partial t} + u \frac{\partial v}{\partial x} + v \frac{\partial v}{\partial r} \right) = - \frac{\partial p}{\partial r} + \mu \left(\frac{\partial^2 v}{\partial x^2} - \frac{v}{r^2} + \frac{1}{r} \frac{\partial v}{\partial r} + \frac{\partial^2 v}{\partial r^2} \right) \quad (3.53)$$

The Continuity

$$\frac{\partial u}{\partial x} + \frac{\partial v}{\partial r} + \frac{v}{r} = 0 \quad (3.54)$$

The energy equation

$$\frac{\partial T}{\partial t} + u \frac{\partial T}{\partial x} + v \frac{\partial T}{\partial r} = \alpha \left[\frac{\partial^2 T}{\partial x^2} + \frac{1}{r} \frac{\partial T}{\partial r} + \frac{\partial^2 T}{\partial r^2} \right] \quad (3.55)$$

The initial conditions

$$T(x, r, 0) = T_0(x, r) \quad (3.56)$$

$$u(x, r, 0) = u_0(x, r) \quad (3.57)$$

$$v(x, r, 0) = v_0(x, r) \quad (3.58)$$

The Boundary ConditionsVelocity Boundary Conditions

$$u(b, r, t) = 0 \quad (3.59)$$

$$u(0, r, t) = 0 \quad (3.60)$$

$$u(x, \pm a, t) = 0 \quad (3.61)$$

$$\frac{\partial u}{\partial r}(x, 0, t) = 0 \quad (3.62)$$

$$v(x, \pm a, t) = 0 \quad (3.63)$$

$$v(x, 0, t) = 0 \quad (3.64)$$

$$v(0, r, t) = 0 \quad (3.65)$$

$$\frac{\partial v}{\partial x}(b, r, t) = 0 \quad (3.66)$$

Thermal Boundary Conditions

$$T(b, r, t) = T_s \quad (3.67)$$

$$a - K \frac{\partial T}{\partial r}(x, \pm a, t) = \frac{q''}{A}(x, t) \quad (3.68)$$

$$b - T(x, \pm a, t) = T_w(x, t) \quad (3.69)$$

$$\frac{\partial T}{\partial x}(0, r, t) = 0 \quad (3.70)$$

$$\frac{\partial T}{\partial r}(x, 0, t) = 0 \quad (3.71)$$

3.6 FORMULATION OF THE SECOND MODEL

3.6.1 Rectangular Coordinates

The reason for the choice of this model, as well as, the basic difference between the two models are clear from the description of the two models, which is given earlier. The basic difference between the two models lies in the boundary condition at the free liquid surface. Otherwise, the rest of the boundary and initial conditions, as well as, the mechanisms of heat and mass transport are the same in both cases. For these reasons, the formulation of this problem will be made as briefly as possible. Reference to the formulation of the previous model will be made where it seems feasible.

The same rectangular two-dimensional tank, Fig. 1, is filled with a liquid. The tank is open at the top to the atmosphere. Beginning from some initial conditions, the tank walls exhibit a transient temperature change. The tank wall temperature is a prescribed function of time and axial location. The wall temperature-time history is obtained by measuring the wall temperature at different locations at various time levels, as will be described later in Chapter 7. The temperature and velocity-time history within the tank is sought.

The assumptions made in this problem do not differ basically from those made earlier. However, they will be repeated here for clarity, and are:

- (1) Incompressible fluid.

- (2) Constant fluid properties. Density variations are allowed in the body force term only in the x-momentum equation.
- (3) The dissipation function as well as the pressure terms in the energy equation are negligible.
- (4) Density variation is only a function of temperature, Equation (3.32).
- (5) No evaporation at the free surface.
- (6) Negligible heat transfer at the free surface.

According to the above assumptions, the governing differential equations will be the same as those obtained earlier for the first model, Equations (3.33) through (3.36). Also, the initial conditions will be given by Equations (3.37) through (3.39). The same is true for the velocity boundary conditions, Equations (3.40) to (3.47).

Temperature Boundary Conditions

The difference between the two models is in the temperature boundary conditions, which in this case are given by:

- (1) specified wall temperature,

$$T(x, \pm a, t) = T_w(x, t) \quad (3.72)$$

- (2) insulated bottom,

$$\frac{\partial T}{\partial x}(0, y, t) = 0 \quad (3.73)$$

- (3) symmetry with respect to the x-axis,

$$\frac{\partial T}{\partial y}(x, 0, t) = 0 \quad (3.74)$$

- (4) adiabatic free surface, according to assumptions 5 and 6,

$$\frac{\partial T}{\partial x}(b, y, t) = 0 \quad (3.75)$$

While evaporation can, by appropriate measures, be prevented, as will be discussed later, some heat losses by convection from the free

surface will certainly be encountered. Therefore condition 4, Equation (3.75) should be regarded as an approximation to the actual situation. This approximation will be good for small time and low heating rates. Perhaps the best representation to the actual heat transfer process at the free surface would be by accounting for the heat transferred between the liquid and the ambients through the use of a convective heat transfer coefficient. This latter alternative is not adopted here, however, and Equation (3.75) is used.

3.6.2 Formulation of the Second Model, Cylindrical Coordinates

In this case the same cylindrical container is partially filled with a liquid, Fig. 5. Similar to the case for rectangular coordinates, the container walls are subjected to a transient temperature perturbation. The governing differential equations are given by Equations (3.52) through (3.55). The initial conditions and the velocity boundary conditions are the same as those given for the first model, Equations (3.56) through (3.66). The temperature boundary conditions are similar to those considered for the rectangular model and they are:

- (1) specified wall temperature;

$$T(x, \pm a, t) = T_w(x, t) \quad (3.76)$$

- (2) insulated bottom,

$$\frac{\partial T}{\partial x}(0, r, t) = 0 \quad (3.77)$$

- (3) symmetry with respect to the x-axis;

$$\frac{\partial T}{\partial r}(x, 0, t) = 0 \quad (3.78)$$

(4) adiabatic free surface;

$$\frac{\partial \Pi}{\partial x}(b, r, t) = 0 \quad (3.79)$$

CHAPTER 4

TRANSFORMATION OF THE PARTIAL DIFFERENTIAL EQUATIONS

The governing partial differential equations in the form given are not suitable for finite-difference approximation for two reasons,

1. The four equations considering the effects of momentum, continuity and energy when replaced by finite-differences, will give rise to four linear algebraic equations in three unknowns at each nodal point in the grid. Hence these will be $4N$ equations, where N is the number of the nodal points in the domain considered. There will be $3N$ unknowns, namely, T_1, \dots, T_N , u_1, \dots, u_N and v_1, \dots, v_N corresponding to the $4N$ algebraic equations. It is clear that in order to solve the algebraic equations for the unknown functions, it is necessary to reduce the number of equations to equal the number of unknowns. This can be achieved by the use of the stream function and the introduction of the vorticity, which reduces the system to one of $3N$ equations in $3N$ unknowns.
2. The presence of the pressure terms in the momentum equations is undesirable.

Accordingly, the partial differential equations were transformed to an equivalent, but more convenient form as follows.

4.1 RECTANGULAR COORDINATES

It is assumed that the pressure p can be written as, Reference (31):

$$p = p_0 + p' \quad (4.1)$$

where p_0 is the hydrostatic pressure and p' is the change in pressure from the hydrostatic pressure, therefore;

$$\frac{\partial p}{\partial x} = -\rho_0 g + \frac{\partial p'}{\partial x} \quad (4.2)$$

$$\frac{\partial p}{\partial y} = \frac{\partial p'}{\partial y} \quad (4.3)$$

where ρ_0 is the density corresponding to p_0 . Upon differentiating the x-momentum equation with respect to y and the y-momentum equation with respect to x, subtracting the second from the first to eliminate the pressure terms, and using Equations (3.32), (3.35), (4.2) and (4.3), the two momentum Equations (3.33) and (3.34) are transformed into the following equation:

$$\begin{aligned} \frac{\partial}{\partial t} \left(\frac{\partial u}{\partial y} - \frac{\partial v}{\partial x} \right) + u \frac{\partial}{\partial x} \left(\frac{\partial u}{\partial y} - \frac{\partial v}{\partial x} \right) + v \frac{\partial}{\partial y} \left(\frac{\partial u}{\partial y} - \frac{\partial v}{\partial x} \right) = \\ g \beta \frac{\partial T}{\partial y} + \nu \left[\frac{\partial}{\partial x^2} \left(\frac{\partial u}{\partial y} - \frac{\partial v}{\partial x} \right) + \frac{\partial}{\partial y^2} \left(\frac{\partial u}{\partial y} - \frac{\partial v}{\partial x} \right) \right] \end{aligned} \quad (4.4)$$

This result can be simplified by the introduction of the vorticity defined as

$$w' = \frac{\partial u}{\partial y} - \frac{\partial v}{\partial x} \quad (4.5)$$

Then Equation (4.4) can be rewritten as

$$\frac{\partial w'}{\partial t} + u \frac{\partial w'}{\partial x} + v \frac{\partial w'}{\partial y} = g \beta \frac{\partial T}{\partial y} + \nu \left(\frac{\partial^2 w'}{\partial x^2} + \frac{\partial^2 w'}{\partial y^2} \right) \quad (4.6)$$

Equations (4.5) and (4.6) are equivalent to the two momentum equations, and the latter is known as the vorticity equation. The solution obtained from Equations (4.5) and (4.6) will satisfy both the x- and y-momentum equations. In order to satisfy the continuity equation, the stream function ψ' is introduced in Equation (4.5). The stream function ψ' is defined such that the continuity equation is satisfied if the u

and v velocities are written

$$u = \frac{\partial \psi'}{\partial y} \quad (4.7)$$

$$v = - \frac{\partial \psi'}{\partial x} \quad (4.8)$$

Using (4.7) and (4.8) in Equations (3.36), (4.5) and (4.6), the following equations are obtained

$$\frac{\partial T}{\partial t} + \frac{\partial \psi'}{\partial y} \cdot \frac{\partial T}{\partial x} - \frac{\partial \psi'}{\partial x} \cdot \frac{\partial T}{\partial y} = \alpha \left(\frac{\partial^2 T}{\partial x^2} + \frac{\partial^2 T}{\partial y^2} \right) \quad (4.9)$$

$$\frac{\partial w'}{\partial t} + \frac{\partial \psi'}{\partial y} \cdot \frac{\partial w'}{\partial x} - \frac{\partial \psi'}{\partial x} \cdot \frac{\partial w'}{\partial y} = g \beta \frac{\partial T}{\partial y} + \nu \left(\frac{\partial^2 w'}{\partial x^2} + \frac{\partial^2 w'}{\partial y^2} \right) \quad (4.10)$$

$$w' = \frac{\partial^2 \psi'}{\partial x^2} + \frac{\partial^2 \psi'}{\partial y^2} \quad (4.11)$$

The system of Equations (4.9), (4.10) and (4.11) are equivalent to the system of Equation (3.33) through (3.36). However the transformed equations are more suitable to handle by finite-difference techniques.

4.2 CYLINDRICAL COORDINATES

Differentiating the x -momentum with respect to r and the r -momentum with respect to x , and combining both equations to eliminate the pressure terms, the following equation is obtained:

$$\begin{aligned} & \frac{\partial}{\partial t} \left(\frac{\partial u}{\partial r} - \frac{\partial v}{\partial x} \right) + u \frac{\partial}{\partial x} \left(\frac{\partial u}{\partial r} - \frac{\partial v}{\partial x} \right) + v \frac{\partial}{\partial r} \left(\frac{\partial u}{\partial r} - \frac{\partial v}{\partial x} \right) + \\ & \left(\frac{\partial u}{\partial r} - \frac{\partial v}{\partial x} \right) \left(\frac{\partial u}{\partial x} + \frac{\partial v}{\partial r} \right) = g \beta \frac{\partial T}{\partial r} + \nu \left[\frac{\partial^2}{\partial x^2} \left(\frac{\partial u}{\partial r} - \frac{\partial v}{\partial x} \right) + \right. \end{aligned} \quad (4.12)$$

$$\frac{1}{r} \frac{\partial}{\partial r} \left(\frac{\partial u}{\partial r} - \frac{\partial v}{\partial x} \right) + \frac{\partial^2}{\partial r^2} \left(\frac{\partial u}{\partial r} - \frac{\partial v}{\partial x} \right) - \frac{1}{r^2} \left(\frac{\partial u}{\partial r} - \frac{\partial v}{\partial x} \right) \quad (4.12)$$

If as before the function w' is defined by:

$$w' = \frac{\partial u}{\partial r} - \frac{\partial v}{\partial x} \quad (4.13)$$

also from the continuity we have:

$$\frac{\partial u}{\partial x} + \frac{\partial v}{\partial r} = -\frac{v}{r} \quad (4.14)$$

Using Equations (4.13) and (4.14), Equation (4.12) can be rewritten as:

$$\frac{\partial w'}{\partial t} + u \frac{\partial w'}{\partial x} + v \frac{\partial w'}{\partial r} - \frac{vw'}{r} = g\beta \frac{\partial T}{\partial r} + v \left(\frac{\partial^2 w'}{\partial x^2} - \frac{w'}{r^2} + \frac{1}{r} \frac{\partial w'}{\partial r} + \frac{\partial^2 w'}{\partial r^2} \right) \quad (4.15)$$

Since the velocity component v changes sign in the two-dimensional domain considered, the presence of the term vw'/r in the vorticity Equation (4.15) is undesirable. This is because it may present a computational stability problem, in case the value of this term is taken at the same time level at all nodal points. This problem could be avoided by taking the value of vw'/r to be that at the advanced time level if v is negative and is evaluated at the present time level if v is positive. The disadvantage of this procedure is that this term is not evaluated at the same time level at all nodal points. Because of this a different approach is taken to handle this problem, by which this term is eliminated from Equation (4.15) in the following way:

let:

$$w'' = \frac{w'}{r} \quad (4.16)$$

$$u = \frac{1}{r} \frac{\partial \psi'}{\partial r} \quad (4.17)$$

$$v = - \frac{1}{r} \frac{\partial \psi'}{\partial x} \quad (4.18)$$

Upon substitution of Equations (4.16) through (4.18) in Equations (3.55), (4.15) and (4.13), the latter system of equations reduces to:

$$\frac{\partial T}{\partial t} + \frac{1}{r} \frac{\partial \psi'}{\partial r} \cdot \frac{\partial T}{\partial x} - \frac{1}{r} \frac{\partial \psi'}{\partial x} \cdot \frac{\partial T}{\partial r} = \alpha \left(\frac{\partial^2 T}{\partial x^2} + \frac{1}{r} \frac{\partial T}{\partial r} + \frac{\partial^2 T}{\partial r^2} \right) \quad (4.19)$$

$$\frac{\partial w''}{\partial t} + \frac{1}{r} \frac{\partial \psi'}{\partial r} \cdot \frac{\partial w''}{\partial x} - \frac{1}{r} \frac{\partial \psi'}{\partial x} \cdot \frac{\partial w''}{\partial r} = \frac{1}{r} g \beta \frac{\partial T}{\partial r} + \nu \left[\frac{\partial^2 w''}{\partial x^2} + \frac{3}{r} \frac{\partial w''}{\partial r} + \frac{\partial^2 w''}{\partial r^2} \right] \quad (4.20)$$

$$w'' = \frac{1}{r^2} \left(\frac{\partial^2 \psi'}{\partial x^2} - \frac{1}{r} \frac{\partial \psi'}{\partial r} + \frac{\partial^2 \psi'}{\partial r^2} \right) \quad (4.21)$$

Equations (4.19), (4.20) and (4.21) are sufficient to determine the temperature and velocity distribution in the cylinder.

4.3 BOUNDARY CONDITIONS

The transformation of the energy, momentum and continuity equations which have T , u and v as variables into an equivalent system of partial differential equations in the temperature, vorticity and stream function requires obtaining the necessary boundary and initial conditions for the latter two functions. These are derived from the velocity boundary conditions, and are given below.

4.3.1 Rectangular Coordinates

(i) Stream function boundary conditions

$$1. \quad \psi'(0, y, t) = 0 \quad (4.22)$$

$$2. \quad \frac{\partial \psi'}{\partial x}(0, y, t) = 0 \quad (4.23)$$

$$3. \quad \psi'(b,y,t) = 0 \quad (4.24)$$

$$4. \quad \frac{\partial^2 \psi'}{\partial x^2} (b,y,t) = 0 \quad (4.25)$$

$$5. \quad \psi'(x,0,t) = 0 \quad (4.26)$$

$$6. \quad \frac{\partial^2 \psi'}{\partial y^2} (x,0,t) = 0 \quad (4.27)$$

$$7. \quad \psi'(x,\pm a,t) = 0 \quad (4.28)$$

$$8. \quad \frac{\partial \psi'}{\partial y} (x,\pm a,t) = 0 \quad (4.29)$$

(ii) Vorticity boundary conditions

The vorticity boundary conditions are derived from these given for the stream function above, as well as, from the momentum equations.

Equations (4.24) to (4.27) give the following two boundary conditions,

$$(1) \quad w'(b,y,t) = 0 \quad (4.30)$$

$$(2) \quad w'(x,0,t) = 0 \quad (4.31)$$

Two more boundary conditions on the vorticity are required at the tank wall and bottom, which are obtained from the x and y momentum equations respectively and they are:

$$(3) \quad \frac{\partial w'}{\partial y} (x,\pm a,t) = \frac{1}{\mu} (\rho g + \frac{\partial p}{\partial x} (x,\pm a,t)) \quad (4.32)$$

$$(4) \quad \frac{\partial w'}{\partial x} (0,y,t) = \frac{-1}{\mu} \frac{\partial p}{\partial y} (0,y,t) \quad (4.33)$$

The use of the last two boundary conditions requires of course, the determination of the pressure distribution. The differential equation governing the pressure field is obtained by differentiating the x-momentum and the y-momentum equations with respect to x and y respectively and combining the resulting equations to yield,

$$\frac{\partial^2 p}{\partial x^2} + \frac{\partial^2 p}{\partial y^2} = -g \frac{\partial \rho}{\partial x} + 2\rho \left(\frac{\partial^2 \psi'}{\partial x^2} \cdot \frac{\partial^2 \psi'}{\partial y^2} - \left(\frac{\partial^2 \psi'}{\partial x \partial y} \right)^2 \right) \quad (4.34)$$

Equations (4.9) to (4.11) and (4.22) through (4.34) determine the entire temperature, flow and pressure fields. However, the non-linear boundary conditions (4.32) and (4.33) will be avoided, since their use together with Equation (4.34) does not offer any advantages from the standpoint of the amount of computation required.

4.3.2 Cylindrical Coordinates

(i) Stream function boundary conditions

$$1. \quad \psi'(0, r, t) = 0 \quad (4.35) \quad \checkmark$$

$$2. \quad \frac{\partial \psi'}{\partial x}(0, r, t) = 0 \quad (4.36) \quad \checkmark$$

$$3. \quad \psi'(b, r, t) = 0 \quad \text{JF} \quad (4.37)$$

$$4. \quad \frac{\partial^2 \psi'}{\partial x^2}(b, r, t) = 0 \quad \text{JF} \quad (4.38)$$

$$\checkmark 5. \quad \psi'(x, 0, t) = 0 \quad \frac{\partial \psi}{\partial x} = 0 \quad \psi = \text{indep. of } x \quad (4.39) \quad \checkmark$$

$$\frac{\partial u}{\partial r}(x, 0, t) \checkmark 6. \quad \frac{\partial}{\partial r} \left(\frac{1}{r} \frac{\partial \psi'}{\partial r}(x, 0, t) \right) = 0 \quad \frac{1}{r} \frac{\partial \psi}{\partial r} = \text{const} \quad \psi = \text{fun. of } r \text{ only} \quad (4.40) \quad \checkmark$$

(indep. of r)

$$7. \quad \psi'(x, \pm a, t) = 0 \quad \psi = \int^r r(\text{const}) dr \quad (4.41) \quad \checkmark$$

$$8. \quad (\partial \psi' / \partial r)(x, \pm a, t) = 0 \quad = \text{const} [r^2]_{r \rightarrow 0} = 0 \quad (4.42) \quad \checkmark$$

(ii) Vorticity boundary conditions

The same procedure used in the rectangular container leads to the following boundary conditions;

$$1. \quad w''(b, r, t) = 0 \quad (4.43)$$

$$2. \quad w''(x, 0, t) = 0 \quad (4.44)$$

$$3. \frac{1}{r} \frac{\partial(w''r)}{\partial r} \Big|_{r=a} = \frac{1}{\mu} \left(\frac{\partial p}{\partial x} + g\rho \right) \Big|_{r=a} \quad (4.45)$$

$$4. \frac{\partial w''}{\partial x} (0, r, t) = \frac{-1}{\mu} \cdot \frac{\partial p}{\partial r} (0, r, t) \quad (4.46)$$

For completeness the equation describing the pressure field is given below;

$$\frac{\partial^2 p}{\partial x^2} + \frac{1}{r} \frac{\partial p}{\partial r} + \frac{\partial^2 p}{\partial r^2} = -g \frac{\partial \rho}{\partial x} - \rho \left[\frac{v^2}{r^2} + 2 \frac{\partial u}{\partial r} \cdot \frac{\partial v}{\partial x} + \left(\frac{\partial u}{\partial x} \right)^2 + \left(\frac{\partial v}{\partial r} \right)^2 \right] \quad (4.47)$$

4.4 DIMENSIONLESS FORM OF THE EQUATIONS

The substitutions necessary to non-dimensionalize the differential equations are:

$$\left. \begin{aligned} u &= \frac{\alpha b}{a^2} U & , & & v &= \frac{\alpha}{a} V \\ T - T_0 &= \frac{\nu \alpha b}{\beta g a^4} \Theta & , & & t &= \frac{a^2}{\alpha} \tau \\ x &= bX & , & & y &= aY \\ r &= aR & , & & w' &= \frac{\alpha b}{a^3} w \\ w'' &= \frac{\alpha b}{a^4} w & & & \psi' &= \alpha b \psi \end{aligned} \right\} \quad (4.48)$$

The resulting dimensionless equations are given below.

4.4.1 Rectangular Coordinates

The energy equation

$$\frac{\partial \theta}{\partial \tau} + \frac{\partial \psi}{\partial Y} \cdot \frac{\partial \theta}{\partial X} - \frac{\partial \psi}{\partial X} \cdot \frac{\partial \theta}{\partial Y} = \frac{a^2}{b^2} \frac{\partial^2 \theta}{\partial X^2} + \frac{\partial^2 \theta}{\partial Y^2} \quad (4.49)$$

The Vorticity Equations

$$\frac{\partial w}{\partial \tau} + \frac{\partial \psi}{\partial Y} \cdot \frac{\partial w}{\partial X} - \frac{\partial \psi}{\partial X} \cdot \frac{\partial w}{\partial Y} = P_r \left[\frac{\partial \theta}{\partial Y} + \frac{a^2}{b} \frac{\partial^2 w}{\partial X^2} + \frac{\partial^2 w}{\partial Y^2} \right] \quad (4.50)$$

$$w = \frac{a^2}{b^2} \frac{\partial^2 \psi}{\partial X^2} + \frac{\partial^2 \psi}{\partial Y^2} \quad (4.51)$$

$$U = \frac{\partial \psi}{\partial Y} \quad (4.52)$$

$$V = - \frac{\partial \psi}{\partial X} \quad (4.53)$$

Boundary Conditions(i) Stream function

$$1. \quad \psi(0, Y, \tau) = 0 \quad (4.54)$$

$$2. \quad \frac{\partial \psi}{\partial X}(0, Y, \tau) = 0 \quad (4.55)$$

$$3. \quad \psi(1, Y, \tau) = 0 \quad (4.56)$$

$$4. \quad \frac{\partial^2 \psi}{\partial X^2}(1, Y, \tau) = 0 \quad (4.57)$$

$$5. \quad \psi(X, 0, \tau) = 0 \quad (4.58)$$

$$6. \quad \frac{\partial^2 \psi}{\partial Y^2}(X, 0, \tau) = 0 \quad (4.59)$$

$$7. \quad \psi(X, \pm 1, \tau) = 0 \quad (4.60)$$

$$8. \quad \frac{\partial \psi}{\partial Y}(X, \pm 1, \tau) = 0 \quad (4.61)$$

(ii) Vorticity

$$1. \quad w(1, Y, \tau) = 0 \quad (4.62)$$

$$2. \quad w(X, 0, \tau) = 0 \quad (4.63)$$

Boundary conditions (4.32) and (4.33) will be disregarded here.

(iii) Thermal boundary conditions(iii.1) First model

$$1. \theta(1, Y, \tau) = \frac{a}{b} \cdot Pr \cdot Gr_s(\tau) \quad (4.64)$$

$$2. a - \frac{\partial \theta}{\partial Y}(X, 1, \tau) = \frac{a}{b} \cdot Pr \cdot Gr^* \quad (4.65)$$

or

$$b - B(X, 1, \tau) = \frac{a}{b} \cdot Pr \cdot Gr_w(X, \tau) \quad (4.66)$$

$$3. \frac{\partial \theta}{\partial X}(0, Y, \tau) = 0 \quad (4.67)$$

$$4. \frac{\partial \theta}{\partial Y}(X, 0, \tau) = 0 \quad (4.68)$$

(iii.2) Second model

$$1. \frac{\partial \theta}{\partial X}(1, Y, \tau) = 0 \quad (4.69)$$

$$2. \theta(X, 1, \tau) = \frac{a}{b} \cdot Pr \cdot Gr_w(X, \tau) \quad (4.70)$$

$$3. \frac{\partial \theta}{\partial X}(0, Y, \tau) = 0 \quad (4.71)$$

$$4. \frac{\partial \theta}{\partial Y}(X, 0, \tau) = 0 \quad (4.72)$$

where Gr_s and Gr_w are the Grashof numbers based on the surface and the wall temperatures respectively, Pr is the Prandtl Number and Gr^* is a modified Grashof Number, which are given by:

$$Gr_s(\tau) = (T_s - T_o) \frac{g\beta a^3}{\nu^2} \quad (4.73)$$

$$Gr_w(\tau) = (T_w - T_o) \frac{g\beta a^3}{\nu^2} \quad (4.74)$$

$$Gr^* = g\beta a^4 (q|A) | (K\nu^2)$$

Initial Conditions

The same non-dimensionalizing procedure leads to the following initial conditions,

$$\psi(X, Y, 0) = \psi_0(X, Y) \quad (4.75)$$

$$w(X, Y, 0) = w_0(X, Y) \quad (4.76)$$

$$\theta(X, Y, 0) = \theta_0(X, Y) \quad (4.77)$$

4.4.2 Cylindrical Coordinates

The Energy Equation

$$\frac{\partial \theta}{\partial \tau} + \frac{1}{R} \frac{\partial \psi}{\partial R} \cdot \frac{\partial \theta}{\partial X} - \frac{1}{R} \frac{\partial \psi}{\partial X} \cdot \frac{\partial \theta}{\partial R} = \frac{a^2}{b^2} \cdot \frac{\partial^2 \theta}{\partial X^2} + \frac{1}{R} \frac{\partial \theta}{\partial R} + \frac{\partial^2 \theta}{\partial R^2} \quad (4.78)$$

The Vorticity Equations

$$\frac{\partial w}{\partial \tau} + \frac{1}{R} \frac{\partial \psi}{\partial R} \cdot \frac{\partial w}{\partial X} - \frac{1}{R} \frac{\partial \psi}{\partial X} \cdot \frac{\partial w}{\partial R} = \text{Pr} \left(\frac{1}{R} \frac{\partial \theta}{\partial R} + \frac{a^2}{b^2} \frac{\partial^2 w}{\partial X^2} + \frac{3}{R} \frac{\partial w}{\partial R} + \frac{\partial^2 w}{\partial R^2} \right) \quad (4.79)$$

$$w = \frac{1}{R^2} \left(\frac{a^2}{b^2} \cdot \frac{\partial^2 \psi}{\partial X^2} - \frac{1}{R} \frac{\partial \psi}{\partial R} + \frac{\partial^2 \psi}{\partial R^2} \right) \quad (4.80)$$

$$U = \frac{1}{R} \frac{\partial \psi}{\partial R} \quad (4.81)$$

$$V = - \frac{1}{R} \frac{\partial \psi}{\partial X} \quad (4.82)$$

Boundary Conditions(i) Stream function boundary conditions

$$1. \quad \psi(0, R, \tau) = 0 \quad (4.83)$$

$$2. \quad \frac{\partial \psi}{\partial X}(0, R, \tau) = 0 \quad (4.84)$$

$$3. \quad \psi(1, R, \tau) = 0 \quad (4.85)$$

$$4. \frac{\partial^2 \psi}{\partial X^2} (1, R, \tau) = 0 \quad (4.86)$$

$$\checkmark 5. \psi(X, 0, \tau) = 0 \quad (4.87)$$

$$\checkmark 6. \frac{\partial}{\partial R} \left(\frac{1}{R} \frac{\partial \psi}{\partial R} (X, 0, \tau) \right) = 0 \quad (4.88)$$

$$7. \psi(X, 1, \tau) = 0 \quad (4.89)$$

$$8. \frac{\partial \psi}{\partial R} (X, 1, \tau) = 0 \quad (4.90)$$

(ii) Vorticity boundary conditions

$$1. w(1, R, \tau) = 0 \quad (4.91)$$

$$2. w(X, 0, \tau) = 0 \quad (4.92)$$

Boundary conditions (4.45) and (4.46) will also be disregarded.

(iii) Thermal boundary conditions

$$1. \theta(X, \pm 1, \tau) = (a/b) \cdot Pr \cdot Gr_w \quad (4.93)$$

$$2. \frac{\partial \theta}{\partial X} (0, R, \tau) = 0 \quad (4.94)$$

$$3. \frac{\partial \theta}{\partial X} (1, R, \tau) = 0 \quad (4.95)$$

$$4. \frac{\partial \theta}{\partial R} (X, 0, \tau) = 0 \quad (4.96)$$

where Gr_w is given by Equation (4.74).

Initial Conditions

$$\theta(X, R, 0) = \theta_0(X, R) \quad (4.97)$$

$$\psi(X, R, 0) = \psi_0(X, R) \quad (4.98)$$

$$w(X, R, 0) = w_0(X, R) \quad (4.99)$$

From the above results, it is established that the temperature and flow fields are determined by the non-dimensional groups, (a/b) , Pr , Gr_s

and G_{T_w} or G_{T^*} , which are functions of the fluid properties, tank geometry and thermal boundary and initial conditions. It is frequently reported in the literature that the fluid in large vehicle containers is found to behave differently than in small test tanks. Whether the actual test conditions in the small tank corresponds to the actual conditions in the large tanks can be examined by comparing the above dimensionless groups in both cases. The use of small tanks in laboratory experiments is a matter of convenience and is usually desirable. However, in order that the experimental results obtained in the small tank correspond to those in the large tank, the above dimensionless groups should be the same in both cases. The initial conditions should, of course also be the same. This would insure that the dimensionless temperature and velocity would be the same. Also if the same fluid is used in both cases, then the designer can specify the tank geometry and the heat flux level so that the above conditions are satisfied.

CHAPTER 5

METHOD OF SOLUTION

5.1 INTRODUCTION

Finite-difference methods have been widely used for the study of linear partial differential equations, particularly for the solution of the heat conduction equation. However, the application of these methods to the solution of heat transfer in fluid flow problems, such as the study of natural convection, was until recently, very limited. This fact is due partly to the complicated form of the partial differential equations involved, and partly due to the difficulty in obtaining sound criterion for the stability problem, which is associated with the solution of such equations. The results of the analytical studies and mathematical experimentation made here and by others to study the stability problem will be given in the next chapter. In this chapter, the finite-difference equations for the energy and the vorticity equations will be developed and an outline for the solution will be made.

5.2 APPROXIMATION OF DERIVATIVES BY FINITE-DIFFERENCES

The use of finite-differences requires the establishment of a network or a system of grid points in the domain of interest. The choice of such a network is a matter of convenience and is generally affected by the coordinate system chosen, and the shape of the domain. In our case, this network is obtained by constructing a series of equally spaced

vertical and horizontal lines parallel to the X and the Y or R axes, Fig. 6. The subscripts i and j are used to refer to the position of the grid points in the two-dimensional domain, such that $X = (i-1) \Delta X$, $Y = (j-1) \Delta Y$ and $R = (j-1) \Delta R$. The origin of the coordinate axes is located at $(1,1)$. The superscript n refers to the level of time such that $\tau = n \cdot \Delta \tau$.

The basic idea in using the method of finite differences to solve partial differential equations, is the use of Taylor's series expansion to approximate the derivatives at a point in terms of the value of the function at the same point and/or at its neighboring points. This procedure assumes that a sufficient number of derivatives exists, which depends upon the order of the differential equation. In our case it is sufficient to assume that the function is analytic to the second derivative (20). Using a Taylor's series expansion, the following relations can be written;

$$f_{i+1,j} = f_{i,j} + \Delta x \frac{\partial f}{\partial x_{i,j}} + \frac{(\Delta x)^2}{2!} \frac{\partial^2 f}{\partial x^2_{i,j}} + \dots + \frac{(\Delta x)^{n-1}}{(n-1)!} \frac{\partial^{n-1} f}{\partial x^{n-1}_{i,j}} + R_n \quad (5.1)$$

$$f_{i-1,j} = f_{i,j} - \Delta x \frac{\partial f}{\partial x_{i,j}} + \frac{(\Delta x)^2}{2!} \frac{\partial^2 f}{\partial x^2_{i,j}} + \dots + \frac{(-\Delta x)^{n-1}}{(n-1)!} \frac{\partial^{n-1} f}{\partial x^{n-1}_{i,j}} + R_n \quad (5.2)$$

where R_n represents the remainder in Taylor's series expansion.

From Equations (5.1) and (5.2), the following different approximations to $\partial f / \partial x_{i,j}$ can be written,

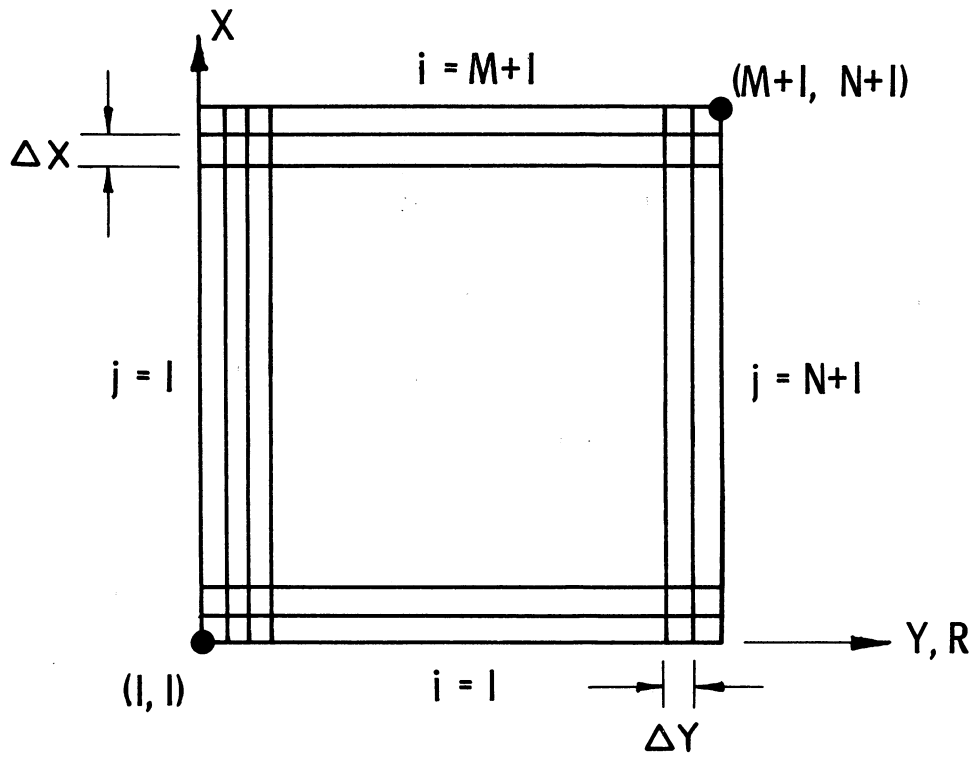


Fig. 6. Finite difference network.



$$\left(\frac{\partial f}{\partial x}\right)_{i,j} = \frac{f_{i+1,j} - f_{i,j}}{\Delta x} + O(\Delta x) \quad (5.3)$$

$$\left(\frac{\partial f}{\partial x}\right)_{i,j} = \frac{f_{i,j} - f_{i-1,j}}{\Delta x} + O(\Delta x) \quad (5.4)$$

$$\left(\frac{\partial f}{\partial x}\right)_{i,j} = \frac{f_{i+1,j} - f_{i-1,j}}{2(\Delta x)} + O(\Delta x)^2 \quad (5.5)$$

These differences are called forward, backward and central respectively. The last term in equations (5.3,5.4,5.5) indicates the order of the truncation error involved in replacing the derivatives by finite-differences. It is obvious that the central differences offer better approximation than the other representations. However, the choice of the type of difference approximation is also dictated by stability requirements as will be discussed later in Chapter 6.

Similarly, the second order derivative $\partial^2 f / \partial x^2_{i,j}$ can be approximated by,

$$\frac{\partial^2 f}{\partial x^2_{i,j}} = \frac{f_{i+1,j} - 2f_{i,j} + f_{i-1,j}}{(\Delta x)^2} + O(\Delta x)^2. \quad (5.6)$$

Likewise, expressions for $\partial f / \partial y$, $\partial f / \partial R$, $\partial^2 f / \partial y^2$ and $\partial^2 f / \partial R^2$ can be written.

5.3 NOTE ON THE CLASSIFICATION OF PARTIAL DIFFERENTIAL EQUATIONS

Partial differential equations are generally classified as elliptic, parabolic or hyperbolic. A complete discussion of this classification is given in Reference 78. The numerical procedure for the solution of any differential equation depends upon the classification of such equation. The energy and the vorticity equations, equations (4.49), (4.50),

(4.78) and (4.79), may be classified as parabolic partial differential equations, while the vorticity-stream function Equations (4.51) and (4.80) are regarded as elliptic equations. Therefore the procedure for obtaining the finite-difference solution of the energy and the vorticity equations will differ from that used for the vorticity-stream function equation. Accordingly, the method of solution of each type will be considered separately.

5.4 FINITE DIFFERENCE REPRESENTATION OF THE ENERGY AND VORTICITY EQUATIONS (Parabolic Type)

The finite-difference methods for solving the parabolic partial differential equations can be classified into two broad categories, as explicit or implicit. The time level, at which the spatial derivatives are differenced, generally determines whether the resulting scheme is explicit or implicit in nature. For example, if the values of the function at the present time level, where its values are known at all nodal points, are used in Equations (5.3) through (5.6), the resulting formulation is said to be explicit. Such a formulation enables the direct computation of the value of the function at all nodal points using a simple, marching-type procedure. The employment of the explicit methods, however, may require the use of small time increments, and consequently large machine time. To alleviate this problem, the implicit methods are usually suggested. Indeed, many of the authors who have investigated the use of finite-differences for the solution of

equations of the form (4.49), (4.50), (4.78) and (4.79) or similar systems, suggested that implicit methods, irrespective of their form, are unconditionally stable. By extensive study and experimentation it has been found hence, as outlined in Chapter 6, that this is true only if the coefficients of the resulting matrix satisfy a certain stability criterion.

The use of any of Equations (5.3), (5.9) and (5.5) together with Equation (5.6) would lead to different finite-difference approximations for the vorticity and energy equations. For brevity, only two different finite-difference representations will be given here. These are chosen primarily in order to discuss some of the problems associated with their use, namely the problem of stability. The discussions that follow in the rest of this chapter apply to other forms of finite-difference equations as well. Indicating by superscript $(n+1)$ the value of the function at the unknown time level and by n that at the present or the known time level, and substituting U for $\partial\psi/\partial Y$ and V for $-\partial\psi/\partial X$ in the energy and vorticity equations for convenience, the finite-difference approximations are written as follows,

I. Explicit difference representation:

A. Rectangular Coordinates

$$\frac{\theta_{i,j}^{n+1} - \theta_{i,j}^n}{\Delta\tau} + U \frac{\theta_{i,j}^n - \theta_{i-1,j}^n}{\Delta X} + V \frac{\theta_{i,j}^n - \theta_{i,j-1}^n}{\Delta Y} = \frac{a^2}{b^2} \frac{\theta_{i+1,j}^n - 2\theta_{i,j}^n + \theta_{i-1,j}^n}{(\Delta X)^2} + \frac{\theta_{i,j+1}^n - 2\theta_{i,j}^n + \theta_{i,j-1}^n}{(\Delta Y)^2} \quad (5.7)$$

$$\frac{w_{i,j}^{n+1} - w_{i,j}^n}{\Delta\tau} + U \frac{w_{i,j}^n - w_{i-1,j}^n}{\Delta X} + U \frac{w_{i,j}^n - w_{i,j-1}^n}{(\Delta Y)} = \text{Pr} \frac{\theta_{i,j+1}^{n+1} - \theta_{i,j-1}^{n+1}}{2(\Delta Y)} +$$

$$\text{Pr} \left[\frac{a^2}{b^2} \frac{w_{i+1,j}^n - 2w_{i,j}^n + w_{i-1,j}^n}{(\Delta X)^2} + \frac{w_{i,j+1}^n - 2w_{i,j}^n + w_{i,j-1}^n}{(\Delta Y)^2} \right] \quad (5.8)$$

(ii)

$$\frac{\theta_{i,j}^{n+1} - \theta_{i,j}^n}{\Delta\tau} + U \frac{\theta_{i+1,j}^n - \theta_{i-1,j}^n}{2(\Delta X)} + V \frac{\theta_{i,j+1}^n - \theta_{i,j-1}^n}{2(\Delta Y)} =$$

$$\frac{a^2}{b^2} \frac{\theta_{i+1,j}^n - 2\theta_{i,j}^n + \theta_{i-1,j}^n}{(\Delta X)^2} + \frac{\theta_{i,j+1}^n - 2\theta_{i,j}^n + \theta_{i,j-1}^n}{(\Delta Y)^2}$$

(5.9)

$$\frac{w_{i,j}^{n+1} - w_{i,j}^n}{\Delta\tau} + U \frac{w_{i+1,j}^n - w_{i-1,j}^n}{2(\Delta X)} + V \frac{w_{i,j+1}^n - w_{i,j-1}^n}{2\Delta Y} = \text{Pr} \frac{\theta_{i,j+1}^{n+1} - \theta_{i,j-1}^{n+1}}{2\Delta Y} +$$

$$\text{Pr} \left[\frac{a^2}{b^2} \frac{w_{i+1,j}^n - 2w_{i,j}^n + w_{i-1,j}^n}{(\Delta X)^2} + \frac{w_{i,j+1}^n - 2w_{i,j}^n + w_{i,j-1}^n}{(\Delta Y)^2} \right] \quad (5.10)$$

B. Cylindrical Coordinates

(i)

$$\frac{\theta_{i,j}^{n+1} - \theta_{i,j}^n}{\Delta\tau} + U \frac{\theta_{i,j}^n - \theta_{i-1,j}^n}{\Delta X} + V \frac{\theta_{i,j}^n - \theta_{i,j-1}^n}{\Delta R} = \frac{a^2}{b^2} \frac{\theta_{i+1,j}^n - 2\theta_{i,j}^n + \theta_{i-1,j}^n}{(\Delta X)^2} +$$

$$\frac{1}{R} \frac{\theta_{i,j+1}^n - \theta_{i,j-1}^n}{2\Delta R} + \frac{\theta_{i,j+1}^n - 2\theta_{i,j}^n + \theta_{i,j-1}^n}{(\Delta R)^2} \quad (5.11)$$

$$\frac{w_{i,j}^{n+1} - w_{i,j}^n}{\Delta\tau} + U \frac{w_{i,j}^n - w_{i-1,j}^n}{(\Delta X)} + V \frac{w_{i,j}^n - w_{i,j-1}^n}{\Delta R} = \frac{\text{Pr}}{R} \frac{\theta_{i,j+1}^{n+1} - \theta_{i,j-1}^{n+1}}{2\Delta R} +$$

$$\text{Pr} \left[\frac{a^2}{b^2} \frac{w_{i+1,j}^n - 2w_{i,j}^n + w_{i-1,j}^n}{(\Delta X)^2} + \frac{1}{R} \frac{w_{i,j+1}^n - w_{i,j-1}^n}{2(\Delta R)} + \frac{w_{i,j+1}^n - 2w_{i,j}^n + w_{i,j-1}^n}{(\Delta R)^2} \right] \quad (5.12)$$

(ii)

$$\begin{aligned} \frac{\theta_{i,j}^{n+1} - \theta_{i,j}^n}{\Delta \tau} + U \frac{\theta_{i+1,j}^n - \theta_{i-1,j}^n}{2(\Delta X)} + V \frac{\theta_{i,j+1}^n - \theta_{i,j-1}^n}{2(\Delta R)} &= \frac{a^2}{b^2} \frac{\theta_{i+1,j}^n - 2\theta_{i,j}^n + \theta_{i-1,j}^n}{(\Delta X)^2} \\ &+ \frac{1}{R} \cdot \frac{\theta_{i,j+1}^n - \theta_{i,j-1}^n}{2(\Delta R)} + \frac{\theta_{i,j+1}^n - 2\theta_{i,j}^n + \theta_{i,j-1}^n}{(\Delta R)^2} \end{aligned} \quad (5.13)$$

$$\frac{w_{i,j}^{n+1} - w_{i,j}^n}{\Delta \tau} + U \frac{w_{i+1,j}^n - w_{i-1,j}^n}{2 \Delta X} + V \frac{w_{i,j+1}^n - w_{i,j-1}^n}{2 \Delta R} = \frac{\text{Pr}}{R} \frac{\theta_{i,j+1}^{n+1} - \theta_{i,j-1}^{n+1}}{2 \Delta R} +$$

$$\text{Pr} \left[\frac{a^2}{b^2} \frac{w_{i+1,j}^n - 2w_{i,j}^n + w_{i-1,j}^n}{(\Delta X)^2} + \frac{3}{R} \frac{w_{i,j+1}^n - w_{i,j-1}^n}{2\Delta R} + \frac{w_{i,j+1}^n - 2w_{i,j}^n + w_{i,j-1}^n}{(\Delta R)^2} \right] \quad (5.14)$$

In the remainder of this chapter, most of the discussion will be directed to the rectangular system. The same discussion applies to the cylindrical case. In situations where the need arises to consider the cylindrical equations separately, sufficient discussion will be devoted for this purpose.

Versions (i) and (ii) given above are two different explicit finite-difference representations of the same partial differential equations. The difference between the two is in the approximation of the nonlinear terms $U \partial \theta / \partial X$, $V \partial \theta / \partial Y$, $U \partial w / \partial X$, ... etc. In the first backward differences were used, while central differences were used in the other. The use of the central differences i.e., formulation (ii), is preferred from the point of view of the truncation errors. However, from the standpoint of practical and computational procedures this formulation is useful only for cases where the Grashof or Rayleigh numbers

are low, i.e., for small velocities. Such cases are usually of less practical importance. This preference is attributed to stability requirements as will be shown in Chapter 6.

It will be demonstrated later that when U and V are positive, then formulation (i) is stable provided that the time increment $\Delta\tau$ is chosen to satisfy the stability criteria given by inequalities (6.37) and (6.38) for the rectangular coordinates and inequalities (6.41), (6.42) and (6.43) for the cylindrical case, as discussed in Sections 6.3 and 6.4.

Likewise it will be shown that formulation (ii) is stable provided that inequalities (6.61) and (6.62) are satisfied.

The difficulty in using the central differences is clear from these inequalities. For high Grashof numbers the dimensionless velocities U and V will be high. Therefore small grid sizes must be used in order to satisfy the above mentioned inequalities. For example, as described later the velocities U and V reach values as high as 1000 for run No. 1 where $a/b = 0.183$. A few arithmetic operations show that (5.17) and (5.18) require that $\Delta X \leq 6.7 \times 10^{-5}$, $\Delta Y \leq 0.002$. The use of such small grid sizes requires storage beyond the capacity of any present digital computing machine. Furthermore tremendous amount of machine time would be required to handle such cases.

II. Implicit finite-difference representation

The implicit forms corresponding to versions i and ii are coded iii and iv respectively and are given below.

A. Rectangular Coordinates

(iii)

$$\frac{\theta_{i,j}^{n+1} - \theta_{i,j}^n}{\Delta\tau} + U \frac{\theta_{i,j}^{n+1} - \theta_{i-1,j}^{n+1}}{(\Delta X)} + V \frac{\theta_{i,j}^{n+1} - \theta_{i,j-1}^{n+1}}{\Delta Y} = \frac{a^2}{b^2} \frac{\theta_{i+1,j}^{n+1} - 2\theta_{i,j}^{n+1} + \theta_{i-1,j}^{n+1}}{(\Delta X)^2} + \frac{\theta_{i,j+1}^{n+1} - 2\theta_{i,j}^{n+1} + \theta_{i,j-1}^{n+1}}{(\Delta Y)^2} \quad (5.15)$$

$$\frac{w_{i,j}^{n+1} - w_{i,j}^n}{\Delta\tau} + U \frac{w_{i,j}^{n+1} - w_{i-1,j}^{n+1}}{\Delta X} + V \frac{w_{i,j}^{n+1} - w_{i,j-1}^{n+1}}{\Delta Y} = \text{Pr} \frac{\theta_{i,j+1}^{n+1} - \theta_{i,j-1}^{n+1}}{2(\Delta Y)} + \text{Pr} \left[\frac{a^2}{b^2} \frac{w_{i+1,j}^{n+1} - 2w_{i,j}^{n+1} + w_{i-1,j}^{n+1}}{(\Delta X)^2} + \frac{w_{i,j+1}^{n+1} - 2w_{i,j}^{n+1} + w_{i,j-1}^{n+1}}{(\Delta Y)^2} \right] \quad (5.16)$$

(iv)

$$\frac{\theta_{i,j}^{n+1} - \theta_{i,j}^n}{\Delta\tau} + U \frac{\theta_{i+1,j}^{n+1} - \theta_{i-1,j}^{n+1}}{2(\Delta X)} + V \frac{\theta_{i,j+1}^{n+1} - \theta_{i,j-1}^{n+1}}{2(\Delta Y)} = \frac{a^2}{b^2} \frac{\theta_{i+1,j}^{n+1} - 2\theta_{i,j}^{n+1} + \theta_{i-1,j}^{n+1}}{(\Delta X)^2} + \frac{\theta_{i,j+1}^{n+1} - 2\theta_{i,j}^{n+1} + \theta_{i,j-1}^{n+1}}{(\Delta Y)^2} \quad (5.17)$$

$$\frac{w_{i,j}^{n+1} - w_{i,j}^n}{\Delta\tau} + U \frac{w_{i+1,j}^{n+1} - w_{i-1,j}^{n+1}}{2(\Delta X)} + V \frac{w_{i,j+1}^{n+1} - w_{i,j-1}^{n+1}}{2(\Delta Y)} = \text{Pr} \frac{\theta_{i,j+1}^{n+1} - \theta_{i,j-1}^{n+1}}{2(\Delta Y)} + \text{Pr} \left[\frac{a^2}{b^2} \frac{w_{i+1,j}^{n+1} - 2w_{i,j}^{n+1} + w_{i-1,j}^{n+1}}{(\Delta X)^2} + \frac{w_{i,j+1}^{n+1} - 2w_{i,j}^{n+1} + w_{i,j-1}^{n+1}}{(\Delta Y)^2} \right] \quad (5.18)$$

B. Cylindrical Coordinates

(iii)

$$\frac{\Theta_{i,j}^{n+1} - \Theta_{i,j}^n}{\Delta\tau} + U \frac{\Theta_{i,j}^{n+1} - \Theta_{i-1,j}^{n+1}}{\Delta X} + V \frac{\Theta_{i,j}^{n+1} - \Theta_{i,j-1}^{n+1}}{\Delta R} = \frac{a^2}{b^2} \frac{\Theta_{i+1,j}^{n+1} - 2\Theta_{i,j}^{n+1} + \Theta_{i-1,j}^{n+1}}{(\Delta X)^2} +$$

$$\frac{1}{R} \left[\frac{\Theta_{i,j+1}^{n+1} - \Theta_{i,j-1}^{n+1}}{2(\Delta R)} + \frac{\Theta_{i,j+1}^{n+1} - 2\Theta_{i,j}^{n+1} + \Theta_{i,j-1}^{n+1}}{(\Delta R)^2} \right] \quad (5.19)$$

$$\frac{w_{i,j}^{n+1} - w_{i,j}^n}{\Delta\tau} + U \frac{w_{i,j}^{n+1} - w_{i-1,j}^{n+1}}{\Delta X} + V \frac{w_{i,j}^{n+1} - w_{i,j+1}^{n+1}}{\Delta R} = \frac{\text{Pr}}{R} \frac{\Theta_{i,j+1}^{n+1} - \Theta_{i,j-1}^{n+1}}{2\Delta R} +$$

$$\text{Pr} \left[\frac{a^2}{b^2} \frac{w_{i+1,j}^{n+1} - 2w_{i,j}^{n+1} + w_{i-1,j}^{n+1}}{(\Delta X)^2} + \frac{1}{R} \frac{w_{i,j+1}^{n+1} - w_{i,j-1}^{n+1}}{2(\Delta R)} + \frac{w_{i,j+1}^{n+1} - 2w_{i,j}^{n+1} + w_{i,j-1}^{n+1}}{(\Delta R)^2} \right] \quad (5.20)$$

(iv)

$$\frac{\Theta_{i,j}^{n+1} - \Theta_{i,j}^n}{\Delta\tau} + U \frac{\Theta_{i+1,j}^{n+1} - \Theta_{i-1,j}^{n+1}}{2\Delta X} + V \frac{\Theta_{i,j+1}^{n+1} - \Theta_{i,j-1}^{n+1}}{2\Delta R} = \frac{a^2}{b^2} \frac{\Theta_{i+1,j}^{n+1} - 2\Theta_{i,j}^{n+1} + \Theta_{i-1,j}^{n+1}}{(\Delta X)^2} +$$

$$\frac{1}{R} \left[\frac{\Theta_{i,j+1}^{n+1} - \Theta_{i,j-1}^{n+1}}{2\Delta R} + \frac{\Theta_{i,j+1}^{n+1} - 2\Theta_{i,j}^{n+1} + \Theta_{i,j-1}^{n+1}}{(\Delta R)^2} \right] \quad (5.21)$$

$$\frac{w_{i,j}^{n+1} - w_{i,j}^n}{\Delta\tau} + U \frac{w_{i+1,j}^{n+1} - w_{i-1,j}^{n+1}}{2(\Delta X)} + V \frac{w_{i,j+1}^{n+1} - w_{i,j-1}^{n+1}}{2\Delta R} = \frac{\text{Pr}}{R} \frac{\Theta_{i,j+1}^{n+1} - \Theta_{i,j-1}^{n+1}}{2(\Delta R)} +$$

$$\text{Pr} \left[\frac{a^2}{b^2} \frac{w_{i+1,j}^{n+1} - 2w_{i,j}^{n+1} + w_{i-1,j}^{n+1}}{(\Delta X)^2} + \frac{1}{R} \frac{w_{i,j+1}^{n+1} - w_{i,j-1}^{n+1}}{2(\Delta R)} + \frac{w_{i,j+1}^{n+1} - 2w_{i,j}^{n+1} + w_{i,j-1}^{n+1}}{(\Delta R)^2} \right] \quad (5.22)$$

Apart from stability requirements, formulations (ii) and (iv) require the solution of a five diagonal matrix, which is usually obtained by iterative methods. The most suitable method for the present equations is the Gauss-Seidel iterative method. This method requires that the coefficients in every equation satisfy a certain criterion, namely, that the sum of the absolute values of the coefficients of the variables at the nodal points $(i+1,j)$, $(i-1,j)$, $(i,j+1)$ and $(i,j-1)$ must not exceed the absolute value of the coefficient of the function at (i,j) .

It is not difficult to see that for $U \geq 0$ and $V \geq 0$, formulation (iii) satisfies this requirement. This will also be true if either U or V or both are negative and implicit forward differences were used in the corresponding nonlinear terms. In addition, it will be shown in Section 6.4 that this formulation is unconditionally stable.

The application of the same criterion to formulation (iv), Equations (5.17) and (5.18), shows that Gauss-Seidel method can be employed for the solution of these equations. The conditions necessary in order that this method converges can be established as follows:

Case 1

$$|U| \leq 2 \frac{a^2}{b^2} \frac{1}{\Delta X} ; |U| \leq 2 \text{Pr} \frac{a^2}{b^2} \frac{1}{\Delta X} \quad (5.23)$$

$$|V| \leq \frac{2}{\Delta Y} ; |V| \leq \frac{2\text{Pr}}{\Delta Y} \quad (5.24)$$

If inequalities (5.23) and (5.24) are satisfied, the Gauss-Seidel iterative method converges. In addition the resulting difference equations will be unconditionally stable. No restrictions on the size of the time increment are imposed neither by stability nor by the method chosen for numerical reduction of the equations.

Case 2

$$|U| \geq \frac{2a^2}{b^2} \cdot \frac{1}{\Delta X} \quad ; \quad |U| \geq 2 \text{Pr} \frac{a^2}{b^2} \cdot \frac{1}{\Delta X} \quad (5.25)$$

$$|V| \geq \frac{2}{\Delta Y} \quad ; \quad |V| \geq \frac{2\text{Pr}}{\Delta Y} \quad (5.26)$$

In this case the Gauss-Seidel method requires that the time increment should satisfy the following inequalities:

$$\Delta\tau \leq \frac{1}{\frac{|U|}{\Delta X} - \frac{2a^2}{b^2} \frac{1}{\Delta X^2} + \frac{|V|}{\Delta Y} - \frac{2}{(\Delta Y)^2}} \quad (5.27)$$

$$\Delta\tau \leq \left(\frac{|U|}{\Delta X} - \text{Pr} \frac{2a^2}{b^2} \cdot \frac{1}{(\Delta X)^2} + \frac{|V|}{\Delta Y} - \frac{2\text{Pr}}{(\Delta Y)^2} \right) \quad (5.28)$$

Inequalities (5.27) and (5.28) are imposed by the method used for the reduction of the set of algebraic Equations (5.17) and (5.18) under conditions (5.25) and (5.26), and are not imposed by stability requirement.

As a matter of fact formulation (iv), Equations (5.17) and (5.18) behaves in a way similar to formulation (ii), i.e., if (5.25) and (5.26) are satisfied, then the finite difference Equations (5.17) and (5.18) are unstable.

From the above discussion it appears that the use of central differences in the terms $U \partial\theta/\partial X$, $V \partial\theta/\partial Y, \dots$, etc., is impractical irrespective of whether implicit or explicit methods are used. On the other hand it seems that the one-sided differences, i.e., forward or backward differences, are the most suitable form for the approximation of these terms.

From the analysis cited above it is clear that one has no choice except to use either formulation (i) which is explicit or formulation (iii) which is implicit. It was decided to use formulation (i) in preference to formulation (iii). A full account of the background of this choice is given in Section 5.8..

5.5 VORTICITY-STREAM FUNCTION EQUATION

The vorticity-stream function Equations (4.51) and (4.80) are replaced by:

A. Rectangular Coordinates

$$w_{i,j} = \frac{a^2}{b^2} \cdot \frac{\psi_{i+1,j} - 2\psi_{i,j} + \psi_{i-1,j}}{(\Delta X)^2} + \frac{\psi_{i,j+1} - 2\psi_{i,j} + \psi_{i,j-1}}{(\Delta Y)^2} \quad (5.29)$$

B. Cylindrical Coordinates

$$w_{i,j} = \frac{1}{R^2} \left[\frac{a^2}{b^2} \frac{\psi_{i+1,j} - 2\psi_{i,j} + \psi_{i-1,j}}{(\Delta X)^2} - \frac{1}{R} \frac{\psi_{i,j+1} - \psi_{i,j-1}}{2(\Delta R)} + \frac{\psi_{i,j+1} - 2\psi_{i,j} + \psi_{i,j-1}}{(\Delta R)^2} \right] \quad (5.30)$$

As mentioned earlier, the method of solving the vorticity-stream function Equations (5.29) and (5.30) may differ from that used in solving

the energy and vorticity equations. While the energy and the vorticity equations can be solved either using an explicit marching type procedure or by using the Gauss-Seidel iterative method, as it is the case if implicit methods are chosen, the vorticity-stream function equation is usually solved by iterative methods. A wider class of iterative methods can be employed for this purpose. Among these methods are the Gauss-Seidel method, which was used by Fromm (21), the successive overrelaxation by points, used by Wilkes (74), and the block successive overrelaxation methods. The point successive overrelaxation method converges faster than the Gauss-Seidel method, while the block successive overrelaxation methods are superior to both of them. Among the block iterative methods are the successive row iteration, the simultaneous row iteration and the successive line overrelaxation. The reader is referred to Reference (71) for a comprehensive study of all these methods. Here an account will be given only of the method employed for solving the vorticity-stream function equations. The method used is essentially a modified form of the line successive iteration, in which row iteration was followed by column iteration. It is found that this procedure gives faster convergence than in cases when only row or column successive iteration methods are used. The iterative formulae for this method applied to Equation (5.29) are:

Successive row iteration

$$\psi_{i,j}^{p+1/2} = \frac{1}{2\left(1 + \left(\frac{a\Delta Y}{b\Delta X}\right)^2\right)} \left[\psi_{i,j+1}^{p+1/2} + \psi_{i,j-1}^{p+1/2} + \frac{a^2(\Delta Y)^2}{b^2(\Delta X)^2} \left(\psi_{i+1,j}^p + \psi_{i-1,j}^p \right) - (\Delta Y)^2 w_{i,j} \right] \quad (5.31)$$

Successive column iterations

$$\psi_{i,j}^{p+1} = \frac{1}{2\left(1 + \left(\frac{b\Delta X}{a\Delta Y}\right)^2\right)} \left[\psi_{i+1,j}^{p+1} + \psi_{i-1,j}^{p+1} + \left(\frac{b\Delta X}{a\Delta Y}\right)^2 \left(\psi_{i,j+1}^{p+1/2} + \psi_{i,j-1}^{p+1} \right) - \frac{b^2}{a^2} \Delta X^2 w_{i,j} \right] \quad (5.32)$$

where the superscript p refers to the number of iterations. Similar formulas can be written for the cylindrical coordinates, Equation (5.30). The use of (5.31) and (5.32) requires the solution of a tridiagonal matrix which can be done very easily using a simple algorithm derived from the Gaussian elimination method. This algorithm was used first by Bruce, Peaceman, Rachford and Rice (9). The description of this procedure is given in Appendix I.

The number of iterations required by this iterative method in order that the maximum change in the magnitude of the stream function at any nodal point does not exceed 0.3% using 31x31 grid did not exceed one iteration in most cases. This is largely due to the fast convergence of the method of iteration and also to the small size of the time increment used.

5.6 CALCULATION OF THE VELOCITY COMPONENTS

Any of Equations (5.3), (5.4) or (5.5) can be used to calculate the velocity components U and V . Actually finite-differences similar to Equation (5.3) were used in Reference (11). However, it was reported later by Wilkes (74), that formulae which have higher order truncation errors gave better results for the case of natural convection

between two infinite parallel plates. Accordingly, the same formulas used by Wilkes were adopted here and are:

A. Rectangular

(i) For nodal points not adjacent to the boundary

$$U_{i,j} = \frac{\partial \psi}{\partial Y_{i,j}} = \frac{\psi_{i,j-2} - 8\psi_{i,j-1} + 8\psi_{i,j+1} - \psi_{i,j+2}}{12 \Delta Y} \quad (5.33)$$

$$V_{i,j} = -\frac{\partial \psi}{\partial X_{i,j}} = \frac{-\psi_{i-2,j} + 8\psi_{i-1,j} - 8\psi_{i+1,j} + \psi_{i+2,j}}{12 \Delta X} \quad (5.34)$$

(ii) For nodal points adjacent to the boundary

$$\checkmark U_{i,1} = \frac{2\psi_{i,2}}{\Delta Y} \quad (5.35)$$

$$U_{i,2} = \frac{6\psi_{i,3} - 3\psi_{i,2} - \psi_{i,4}}{6\Delta Y} \quad (5.36)$$

$$U_{i,N} = \frac{3\psi_{i,N} - 6\psi_{i,N-1} + \psi_{i,N-2}}{6\Delta Y} \quad (5.37)$$

$$\text{Sign } \checkmark V_{2,j} = \frac{\psi_{4,j} - 6\psi_{3,j} + 3\psi_{2,j}}{6\Delta X} \quad (5.38)$$

$$\text{Sign } \checkmark V_{M,j} = (6\psi_{M-1,j} - 3\psi_{M,j} - \psi_{M-2,j}) / 6\Delta X \quad (5.39)$$

$$\checkmark V_{M+1,j} = (8\psi_{M,j} - \psi_{M-1,j}) / 6\Delta X \quad (5.40)$$

B. Cylindrical

(i) For nodal points not adjacent to the boundary

$$U_{i,j} = \frac{1}{R} \frac{\partial \psi}{\partial R} = \frac{1}{R} \left[\frac{\psi_{i,j-2} - 8\psi_{i,j-1} + 8\psi_{i,j+1} - \psi_{i,j+2}}{12 \Delta R} \right] \quad (5.41)$$

$$V_{i,j} = -\frac{1}{R} \frac{\partial \psi}{\partial X} = \frac{1}{R} \left[\frac{-\psi_{i-2,j} + 8\psi_{i-1,j} - 8\psi_{i+1,j} + \psi_{i+2,j}}{12 \Delta X} \right] \quad (5.42)$$

(ii) At the center line,

The velocity component $U_{i,1}$ is calculated according to;

$$\lim_{R \rightarrow 0} \frac{1}{R} \frac{\partial U}{\partial R} = \left(\frac{\partial^2 U}{\partial R^2} \right)_{R=0}$$

therefore the following formula for $U_{i,1}$ was used,

$$U_{i,1} = \frac{2\psi(I,2)}{(\Delta R)^2} \quad (5.43)$$

(iii) Points adjacent to the boundary

$$U_{i,2} = \left[\frac{6\psi_{i,3} - 3\psi_{i,2} - \psi_{i,4}}{(\Delta R)^2} \right] \quad (5.44)$$

$$U_{i,N} = \frac{1}{R(N)} \left[\frac{3\psi_{i,N} - 6\psi_{i,N-1} + \psi_{i,N-2}}{6 \Delta R} \right] \quad (5.45)$$

$$V_{2,j} = \frac{1}{R} \left[\frac{\psi_{4,j} - 6\psi_{3,j} + 3\psi_{2,j}}{6 \Delta X} \right] \quad (5.46)$$

$$V_{M,j} = \frac{1}{R} \left[\frac{6\psi_{M-1,j} - 3\psi_{M,j} - \psi_{M-2,j}}{6 (\Delta X)} \right] \quad (5.47)$$

$$V_{M+1,j} = \frac{1}{R} \left[\frac{8\psi_{M,j} - \psi_{M-1,j}}{6 \Delta X} \right] \quad (5.48)$$

5.7 TREATMENT OF BOUNDARY CONDITIONS

In this section the treatment of the temperature and the vorticity boundary conditions will be discussed. No difficulties are encountered at the boundaries, where the value of these functions are specified. Cases in which a derivative of the function is specified require some attention.

The following approximation for the case of specified wall heat flux is used,

$$\left(\frac{\partial^2 \theta}{\partial Y^2}\right)_{i,N+1} = 2\left(\theta_{i,N} - \theta_{i,N+1} + \Delta Y \cdot \left(\frac{\partial \theta}{\partial Y}\right)_{\text{wall}}\right) / (\Delta Y)^2 + O(\Delta Y) \quad (5.49)$$

and

$$\left(\frac{\partial^2 \theta}{\partial R^2}\right)_{i,N+1} = 2\left(\theta_{i,N} - \theta_{i,N+1} + \Delta R \left(\frac{\partial \theta}{\partial R}\right)_{\text{wall}}\right) / \Delta R^2 + O(\Delta R) \quad (5.50)$$

$$\left(\frac{\partial^2 \theta}{\partial X^2}\right)_{1,j} = 2(\theta_{2,j} - \theta_{1,j}) / (\Delta X)^2 \quad (5.51)$$

$$\left(\frac{\partial^2 \theta}{\partial X^2}\right)_{M+1,j} = 2(\theta_{M,j} - \theta_{M+1,j}) / (\Delta X)^2. \quad (5.52)$$

The vorticity boundary conditions at the wall and bottom given by Equations (4.32, 4.33) and (4.45, 4.46) are difficult to use. Therefore, an alternative method was used to handle these boundary conditions. The step-by-step explicit computation procedure allows progressing from one vorticity distribution to the next a short time later at all nodal points except those on the boundary, using the values of the vorticities at earlier time. The new values of vorticity are used to determine the stream function distribution. The stream function is then used to compute the values of the vorticity at the solid boundaries. Using Taylor's series expansion together with boundary conditions (4.54) through (4.61) and (4.83) through (4.90), the following expressions can be easily obtained for the vorticity at the solid boundaries;

A. Rectangular System

$$w_{i,N+1} = (8 \psi_{i,N} - \psi_{i,N-1})/2(\Delta Y)^2 \quad (5.53)$$

$$w_{1,j} = \frac{a^2}{b^2} (8 \psi_{2,j} - \psi_{3,j})/2(\Delta X)^2 \quad (5.54)$$

B. Cylindrical Coordinates

$$w_{i,N+1} = (8 \psi_{i,N} - \psi_{i,N-1})/2(\Delta R)^2 \quad (5.55)$$

$$w_{1,j} = \frac{a^2}{b^2} \cdot \frac{1}{R^2} (8 \psi_{2,j} - \psi_{3,j})/2(\Delta X)^2 \quad (5.56)$$

5.8 THE PROCEDURE OF CALCULATIONS

In this chapter the application of finite-difference methods to the solution of the two-dimensional, laminar, natural convection in rectangular and cylindrical coordinates was discussed. It is worthwhile now to summarize the procedure used to obtain the solution. The step-by-step numerical technique followed in this work to compute the new values of the dependent variables across any time step is as follows:

5.8.1 Rectangular System

1. A suitable time increment is chosen. The stability criterion given by inequalities (6.37) and (6.38) is tested. The time step may be altered as necessary to maintain stability.
2. The new temperature distribution is computed from Equation (5.7).
3. The results obtained for the temperature distribution are used in Equation (5.8) to calculate the vorticity at all interior nodal points.

4. Equation (5.29) is used to find the stream function at all the interior nodal points. The method described in Section 5.5, is used for the solution of this equation.
5. The vorticities at the solid boundaries i.e., at the wall and the bottom of the container, are calculated using Equations (5.53) and (5.54) respectively.
6. The velocity components U and V are calculated using the appropriate one of Equations (5.33) through (5.40).

5.8.2 Cylindrical System

The same procedure mentioned above applies to the cylindrical case. The equations pertaining to cylindrical coordinates are used, of course. The only difference lies in calculating the temperature at the center line. Since both R and $\partial\theta/\partial R$ approach zero as R approaches zero, the term $1/R \partial\theta/\partial R$ in the energy equation is replaced at the center line by its limit as the radius becomes zero i.e.,

$$\lim_{R \rightarrow 0} \frac{1}{R} \frac{\partial\theta}{\partial R} = \left(\frac{\partial^2\theta}{\partial R^2} \right)_{R=0} \quad (5.57)$$

accordingly the following equation is used to calculate the center-line temperature, assuming that $U \geq 0$;

$$\frac{\theta_{i,1}^{n+1} - \theta_{i,1}^n}{\Delta\tau} + U \frac{\theta_{i,1}^n - \theta_{i-1,1}^n}{\Delta X} = \frac{a^2}{b^2} \frac{\theta_{i+1,1}^n - 2\theta_{i,1}^n + \theta_{i-1,1}^n}{(\Delta X)^2} + 4 \frac{\theta_{i,2}^n - \theta_{i,1}^n}{(\Delta R)^2} \quad (5.58)$$

For negative velocity U, forward differences should be used for $U \partial\theta/\partial X$.

5.9 A NOTE ON THE USE OF UNCONDITIONALLY STABLE METHODS FOR THE SOLUTION OF THE ENERGY AND VORTICITY EQUATIONS

It was shown in Section 5.4 that two of the discussed methods, namely formulations (i) and (iii) are suitable for handling the energy and the vorticity equations. Formulation (i) is explicit and simple to use, while formulation (iii) is implicit. The explicit method demands that the time increment be small in order to satisfy stability requirement, inequalities (6.37) and (6.38). As a result, the amount of machine time required to obtain the solution may become large particularly for high Grashof numbers.

To avoid the restrictions on the time increment, implicit methods are usually suggested. Iterative methods are usually employed for the solution of the resulting algebraic equations. Since the velocities U and V are functions of space and time, it appears that the Gauss-Seidel iterative method is the most suitable one for this purpose. This may require a large number of iterations per time step. Furthermore increasing the size of the time step would increase the number of iterations required to achieve any reasonable degree of numerical accuracy. The advantages of these methods from the standpoint of savings in machine time then are of doubtful value.

The use of unconditionally stable explicit methods becomes therefore very attractive, since it eliminates the difficulties outlined above, i.e., allows the use of large time increments, and the employment of the marching type solution without resort to iterative methods.

Such a method was not available, until the method of Reference (6) was developed, in which multi-level formulae were used to obtain an explicit unconditionally stable method for solving the heat conduction equation. The same authors were able through the use of multi-level finite-difference approximation for the first order derivatives $\partial T/\partial x$, ...,etc., to extend the same procedure for the solution of equations having convective terms such as the energy and the vorticity equations.

The unconditionally stable methods described above can be successfully employed to handle the energy equation. The use of these methods for the solution of the vorticity equation may have limited advantages over the explicit method used in this work, formulation (i). This is due to the lack of explicit, linear boundary conditions for the vorticity at the solid boundaries. Such a situation does not exist in the case of the energy equation. The vorticity nonlinear boundary conditions (4.32), (4.33), (4.45) and (4.46) were in fact disregarded. Instead these boundary conditions were treated in the manner described in Section 5.7 by Equations (5.53) through (5.56). In the case of implicit methods, or any method that require the use of the vorticity at the boundary taken at the $n+1$ time level in order to advance the values of the vorticity at the interior nodal points from the n th to the $(n+1)$ time level, the value of the wall vorticity at the n th level has to be used to approximate that at the $(n+1)$ time level, because the latter is not known. Such a linearization of the boundary conditions requires the use of small time increments so that w_{wall}^n be a good

approximation for w_{wall}^{n+1} . That such is the case has been demonstrated by using the Gauss-Seidel iterative method to solve the system of Equations (5.7) and (5.8), for the same initial and boundary conditions for run 1. When the vorticity at the wall was treated in the manner outlined in Section 5.8, accumulator overflow took place, although the method is unconditionally stable. The time and spatial increments were 0.01 and 0.1 respectively. To prove the point further an artificial boundary condition on the vorticity $w_{\text{wall}}=0$ was assumed. No accumulator overflow was encountered even for larger time increments. Wilkes (74), also reported that instability took place for the simple case of natural convection between two parallel plates, although the method which he used for this case is unconditionally stable. All these facts support the view that the vorticity nonlinear boundary conditions at the wall are barriers against the use of large time increments and consequently do not allow the use of unconditionally stable methods to solve the vorticity equation. It was found by experimentation that the stability criterion given by Equation (6.38) gives a qualitative estimate of the size of the time increment that should be used in the vorticity equation. It is of course possible to use unconditionally stable methods to solve the energy equation and the explicit method, Equation (5.8) to solve the vorticity equation. A smaller time step $\Delta\tau$ is used in the vorticity equation, while larger time step, $m \Delta\tau$, can be used in the energy equation, where m is an integer. Then each cycle of the temperature calculation is accompanied by m cycles of the vorticity calculation.

CHAPTER 6

STABILITY ANALYSIS

In Chapter 5 the finite-difference representations of the governing partial differential equations was presented. In this chapter, the stability and convergence of these finite-difference equations will be examined and criteria defined.

6.1 DEFINITIONS

The stability of the difference equations has been a subject for many investigators. Nevertheless, one rarely meets precise definition of the concepts of stability and convergence of finite-difference equations. Some of these definitions will be quoted here.

O'Brien, Hyman and Kaplan (42) defined the stability and convergence in the following way. Let E represent the exact solution of the partial differential equation, D the exact solution of the finite-difference equations, and N the numerical solution of the difference equations. The value of $(E-D)$ is called the truncation error. To find the conditions under which $D \rightarrow E$ is the problem of CONVERGENCE. The quantity $(D-N)$ is called the numerical error. It may be due to round-off errors or any other kind of error. To find the conditions under which $(D-N)$ is small throughout the entire region of integration is the problem of STABILITY.

In principle, the numerical error can be kept under control even for some unstable cases, (see Reference (42)), by carrying out the calculations with sufficient precision. This, of course, is attainable only with computing machines that carry an infinite number of digits. Therefore, it is natural to look for criteria of stability that involve bounds on the numerical error. Forsythe and Wasow (20) have adopted the following definition. If the error introduced at every step due to round-off errors is $\epsilon(x,y,t)$ such that $|\epsilon| \leq \delta$, then a finite-difference procedure is called stable if the numerical error tends to zero with δ and does not grow faster than $(\Delta s)^{-1}$ where Δs is the mesh size.

Lax and Richtmyer (32) consider that, for an initial value problem, the solution of the difference equation $F(x,t)$ is said to converge to the solution of the differential problem $G(x,t)$ if

$$\lim_{\Delta s \rightarrow 0} |F(x,t) - G(x,t)| = 0,$$

for a general initial function $f(x)$.

A finite-difference equation is called stable by Lax and Richtmyer (32) if the solution $F(x,t)$ corresponding to a general initial function $f(x)$ satisfies a boundedness relation of the form

$$\|F(x,t)\| \leq \varphi(t) \|f(x)\| \text{ for } 0 \leq t \leq t_1 \quad (6.1)$$

where $\varphi(t)$ is independent of Δs . This condition is more restrictive than that adopted by Forsythe and Wasow (20), since they allow for the bound to grow like a power of Δs^{-1} .

A third concept, which is usually associated with finite-differences is the consistency. A finite-difference equation is considered to be consistent with the given differential equation if the truncation error involved in replacing the derivatives by finite-differences vanishes as the spatial and time increments approaches zero. It is sometimes said that such a difference equation is a formal representation of the differential equation. Lax (33) proved that for linear partial differential equations if the consistency condition is satisfied, then stability and convergence are equivalent and stability implies convergence.

6.2 A NOTE ON THE LINEARIZATION OF THE DIFFERENTIAL EQUATIONS

In the present problem, the governing partial differential equations are linearized by assuming that the velocity components U and V appearing in the nonlinear terms $U (\partial\theta/\partial X)$, $V (\partial\theta/\partial Y)$, $U (\partial w/\partial X)$, ... etc., are known and are taken to be equal to their values at the time level $n\Delta\tau$. The time step $\Delta\tau$ should, of course, be taken small enough so that U^n be a good approximation to U^{n+1} . The order of the error involved by carrying out this linearization can be obtained by using Taylor's series expansion as follows:

If U_0 and U are the values of the velocity component U at time levels τ_0 and $\tau = \tau_0 + \Delta\tau$ respectively, then

$$U = U_0 + \Delta\tau \left(\frac{\partial U}{\partial \tau} \right)_\beta, \quad (6.2)$$

where $0 \leq \beta \leq \Delta\tau$

Then

$$U \frac{\partial \theta}{\partial x} = U_0 \cdot \frac{\partial \theta}{\partial x} + \Delta\tau \left(\frac{\partial U}{\partial \tau} \right)_\beta \frac{\partial \theta}{\partial x} \quad (6.3)$$

The approximation involved in replacing the nonlinear terms $U (\partial\theta/\partial x)$, $V (\partial\theta/\partial y)$, ...etc., in Equations (4.49), (4.50), (4.78) and (4.79) by their counterparts in the finite-difference Equations (5.7) through (5.14) and (5.16) through (5.22), as shown in Equation (6.3) is of order $O(\Delta\tau)$. This linearization error goes to zero as the time increment goes to zero. Indeed, all the errors induced by any of the various finite-difference methods given in Chapter 5, namely truncation and linearization errors, go to zero as both the spatial and the time increments go to zero, and all of the above mentioned finite-difference methods satisfy the consistency condition.

The linearization of the partial differential equation in the manner previously described allows the use of Lax's equivalence theorem mentioned above to prove the convergence of the finite-difference method adopted here. As a matter of fact, the same procedure can be used to prove the convergence of any stable, formal finite-difference representation of the governing partial differential equations.

6.3 METHODS OF STABILITY ANALYSIS

The subject of stability of finite-difference equations has been widely discussed in the literature. Various methods were developed for

testing the stability of the difference equations. Most of these methods are valid for linear differential equations with constant coefficients and few are applicable to linear differential equations with variable coefficients. A survey of these methods is beyond the scope of this work. However, three methods of stability analysis, which can be applied to partial differential equations with variable coefficients will be briefly discussed. Comparison between the stability criteria obtained by these different methods will be made.

6.3.1 Stability of Positive Type Difference Equations

We are concerned here with differential equations of the form

$$\frac{\partial f}{\partial t} = a_0 \frac{\partial^2 f}{\partial x^2} + a_1 \frac{\partial^2 f}{\partial y^2} + a_2 \frac{\partial f}{\partial x} + a_3 \frac{\partial f}{\partial y} \quad (6.4)$$

Where a_0, a_1, a_2, a_3 and a_4 are functions of x, y and t , and a_0 and a_1 are non-negative.

Using Taylor's series expansion Equation (6.3) can be formally approximated by a two-level explicit finite-difference equation, which can be written as

$$\begin{aligned} F_{i,j}^{n+1} = & a_{i,j} F_{i,j}^n + a_{i+1,j} F_{i+1,j}^n + a_{i-1,j} F_{i-1,j}^n + a_{i,j+1} F_{i,j+1}^n \\ & + a_{i,j-1} F_{i,j-1}^n \end{aligned} \quad (6.5)$$

where the coefficients $a_{i,j}, \dots$ etc., are functions of x, y and t .

The finite-difference Equation (6.4) is called of positive type if the coefficients $a_{i,j}, a_{i+1,j}, \dots$ etc., are non-negative, i.e.

$$a_{i,j} \geq 0, \text{ for all } i, j \quad (6.6)$$

Explicit positive type-difference equations can be obtained for partial differential equations of the form (6.4) by using one sided derivatives i.e., forward or backward derivatives according to the sign of the coefficients a_2 and a_3 . If $a_2 < 0$, backward differences, Equation (5.4), should be used for approximating the derivative $\partial f / \partial x$, otherwise forward differences, Equation (5.3), should be employed. The same procedure should be followed in approximating $\partial f / \partial y$. The resulting finite-difference equations will be of the positive type provided that the following inequality is satisfied at all (i,j) ,

$$1 \geq \left(\frac{2a_0}{\Delta x^2} + \frac{2a_1}{\Delta y^2} + \frac{|a_2|}{\Delta x} + \frac{|a_3|}{\Delta y} \right) \cdot \Delta t \quad (6.7)$$

It will be shown below that inequality (6.7) is sufficient to ensure the stability of the explicit finite-difference scheme (6.5). It is not difficult to verify that the coefficients of Equation (6.5) have sum equal to unity i.e.,

$$a_{i,j} + a_{i-1,j} + a_{i+1,j} + a_{i,j+1} + a_{i,j-1} = 1 \quad (6.8)$$

Conditions (6.6) and (6.8) imply that,

$$\begin{aligned} \text{Max}_{i,j} |F_{i,j}^{n+1}| &\leq \text{Max}_{(i,j)} |F_{i,j}^n| \leq \text{Max}_{(i,j)} |F_{i,j}^{n-1}| \\ &\leq \dots \leq \text{Max}_{(i,j)} |f_{i,j}^0| \end{aligned} \quad (6.9)$$

where $f_{i,j}^0$ is the initial condition at (i,j) . Inequality (6.9) shows that stability, in the sense of inequality (6.1), is satisfied. If consistency is satisfied, then according to Lax's theorem the solution of the finite-

difference equations converges to that of the partial differential equations as the increments Δx , Δy and Δt go to zero.

Inequality (6.7) is the stability criterion for this formulation.

The stability and boundedness of implicit finite-difference methods of positive type has been proved by Forsythe and Wasow (20). The use of one sided derivatives in the manner outlined above yields an implicit positive type finite-difference form for the differential Equation (6.4), which is

$$F_{i,j}^{n+1} = b_{i,j} F_{i,j}^{n+1} + b_{i+1,j} F_{i+1,j}^{n+1} + b_{i-1,j} F_{i-1,j}^{n+1} + b_{i,j+1} F_{i,j+1}^{n+1} + b_{i,j-1} F_{i,j-1}^{n+1} \quad (6.10)$$

The coefficients in Equation (6.10) are always positive, irrespective of the magnitudes of Δt , Δx and Δy . These coefficients will be given by:

$$\left. \begin{aligned} b_{i,j} &= 1/b \\ b_{i+1,j} &= \left(\frac{a_0}{(\Delta x)^2} + \frac{a_2}{\Delta x} \right) \Delta t/b, & a_2 > 0 \\ &= a_0 \Delta t/b (\Delta x)^2, & a_2 < 0 \\ b_{i-1,j} &= a_0 \Delta t/b (\Delta x)^2, & a_2 > 0 \\ &= \left(\frac{a_0}{(\Delta x)^2} - \frac{a_2}{\Delta x} \right) \Delta t/b, & a_2 < 0 \\ b_{i,j+1} &= \left(\frac{a_1}{(\Delta y)^2} + \frac{a_3}{\Delta y} \right) \Delta t/b, & a_3 > 0 \\ &= a_1 \Delta t/b (\Delta y)^2, & a_3 < 0 \\ b_{i,j-1} &= a_1 \Delta t/b (\Delta y)^2, & a_3 > 0 \\ &= \left(\frac{a_1}{(\Delta y)^2} - \frac{a_3}{\Delta y} \right) \Delta t/b, & a_3 < 0 \end{aligned} \right\} \quad (6.11)$$

$$b = 1 + \left(\frac{2a_0}{(\Delta x)^2} + \frac{2a_1}{(\Delta y)^2} + \frac{|a_2|}{\Delta x} + \frac{|a_3|}{\Delta y} \right) \Delta t$$

Accordingly Equation (6.10) is unconditionally stable.

Thus far the one-sided derivative has been employed to obtain positive type finite-difference representation of Equation (6.4) and sufficient conditions for stability have been derived. It is also possible to employ central differences, Equation (5.5), to approximate the first order derivatives $\partial f/\partial x$ and $\partial f/\partial y$ of Equation (6.4). The conditions under which the finite-difference method becomes of positive type can be established. In this case, Equations (5.5) and (5.6) may be used to obtain the following explicit finite-difference equation for the differential Equation (6.4),

$$F_{i,j}^{n+1} = C_{i,j} F_{i,j}^n + C_{i+1,j} F_{i+1,j}^n + C_{i-1,j} F_{i-1,j}^n + C_{i,j+1} F_{i,j+1}^n + C_{i,j-1} F_{i,j-1}^n \quad (6.12)$$

where:

$$\left. \begin{aligned} C_{i,j} &= 1 - 2a_0 \Delta t / (\Delta x)^2 - 2a_1 \Delta t / (\Delta y)^2 \\ C_{i+1,j} &= (a_0 / (\Delta x)^2 + a_2 / \Delta x) \cdot \Delta t \\ C_{i-1,j} &= (a_0 / (\Delta x)^2 - a_2 / \Delta x) \cdot \Delta t \\ C_{i,j+1} &= (a_1 / (\Delta y)^2 + a_3 / \Delta y) \cdot \Delta t \\ C_{i,j-1} &= (a_1 / (\Delta y)^2 - a_3 / \Delta y) \cdot \Delta t \end{aligned} \right\} \quad (6.13)$$

Therefore the conditions necessary for making (6.12) of positive type are,

$$\Delta x \leq |a_0 / a_2| \quad (6.14)$$

$$\Delta y \leq |a_1/a_3| \quad (6.15)$$

$$\Delta t \leq \frac{1}{[2a_0|(\Delta x)^2 + 2a_1|(\Delta y)^2]} \quad (6.16)$$

At this point it is necessary to emphasize the fact that subject to conditions (6.14) through (6.16), central differences, can be employed to obtain stable explicit finite-difference formulations for the solution of Equation (6.5). Furthermore it is not difficult to see that any of Equations (5.3) to (5.5) can be used to approximate the first order derivatives and sufficient conditions to ensure stability of the resulting two level difference equations can be derived. These conditions may be given by one or more of inequalities (6.7), (6.14), (6.15) or (6.16). This is in contradiction with the arguments made by some authors that only the use of one-sided derivatives would yield stable finite-difference forms.

It is also clear that the use of central differences would yield implicit positive type finite-difference approximations for Equation (6.4), assuming that conditions (6.14) and (6.15) are satisfied. The resulting implicit finite-difference equation can be written as;

$$F_{i,j}^{n+1} = d_{i,j} F_{i,j}^n + d_{i+1,j} F_{i+1,j}^{n+1} + d_{i-1,j} F_{i-1,j}^{n+1} + d_{i,j+1} F_{i,j+1}^{n+1} + d_{i,j-1} F_{i,j-1}^{n+1} \quad (6.17)$$

where,

$$\begin{aligned}
 d_{i,j} &= 1/C \\
 d_{i+1,j} &= (a_0/(\Delta x)^2 + a_2/\Delta x)\Delta t/C \\
 d_{i-1,j} &= (a_0/(\Delta x)^2 - a_2/\Delta x)\Delta t/C \\
 d_{i,j+1} &= (a_1/\Delta y^2 + a_3/\Delta y)\Delta t/C \\
 d_{i,j-1} &= (a_1/\Delta y^2 - a_3/\Delta y)\Delta t/C \\
 C &= 1 + 2[a_0/(\Delta x)^2 + a_1/(\Delta y)^2]\Delta t
 \end{aligned} \tag{6.18}$$

The conclusion made in the above paragraph regarding the possibility of using forward, backward or central differences to approximate Equation (6.4) by stable finite-difference forms of positive type is general and mathematically sound. It is based on the definition and properties of positive type difference equations. The use of central differences is the most desirable because it offers the least truncation error. However, conditions (6.14) and (6.15), which are imposed by stability of such a formulation should be satisfied.

From the practical point of view, (6.14) and (6.15) can be satisfied for values of $|(a_0/a_2)|$ and $|a_1/a_3|$, which lead to a reasonable number of grid points. For cases where $|a_0| \ll |a_2|$ and/or $|a_1| \ll |a_3|$, the use of central differences will be impractical. Indeed, for problems of practical interest, such as natural convection problems with high Grashof numbers and/or small a/b ratios, $a_0 \ll |a_2|$ and $a_1 \ll |a_3|$. For such problems the use of one-sided differences for approximating the first order derivatives in the nonlinear terms offers the best choice of two undesirable alternatives.

Finally, it should be mentioned that the stability criteria imposed by the positive type finite-differences are regarded to be conservative. Nevertheless, the use of this procedure yielded sufficient stability criteria for the finite-difference form given by Equation (6.17), while other methods for stability analysis failed to predict its behavior. This point will be discussed further in discussing the Von Neumann method of stability analysis, as well as, in investigating the stability of formulations (i) through (iv) given in Chapter 5.

6.3.2 Electric Circuit Analogy

The concept of circuit theory dealing with electrical instability was applied to study the stability of finite-difference equations by Karplus (30). Two criteria for the stability of finite-difference equations, which have the same form as the equilibrium equations of the electric network were given. This method can be applied to examine the stability of any finite-difference approximations of Equation (6.4) as follows;

Assuming that the difference equations can be written in the following form;

$$C_0(F_{i+1,j}^n - F_{i,j}^n) + C_1(F_{i-1,j}^n - F_{i,j}^n) + C_2(F_{i,j+1}^n - F_{i,j}^n) + C_3(F_{i,j-1}^n - F_{i,j}^n) +$$
(6.19)

$$C_4(F_{i,j}^{n+1} - F_{i,j}^n) = 0$$

where $C_0 > 0$.

Then the finite difference Equation (6.19) is stable under any of the two following conditions:

- (1) If all the coefficients C_0, C_1, C_2, C_3 and C_4 are positive
- (2) If some of these coefficients are negative, a sufficient condition for the stability is that the algebraic sum of the coefficients be negative.

The stability criteria obtained by this method lead in most cases to finite-difference equations of positive type. However the second condition seems to be more promising for the study of cases where the finite-difference equations are not of positive type. The application of this method to the two-level finite difference versions of the differential Equation (6.4) will yield the same conclusions reached above using the concept of "positive type difference-equations."

Upon examination of the stability of most of the known finite-difference methods for the solution of the heat conduction equation, it was found that if condition (2) given by Karplus is modified to read as follows: "If some of the coefficients are negative, a sufficient condition for the stability is that the algebraic sum of the coefficients should not be greater than zero," then the behavior of a wider class of explicit finite-difference methods such as those of Dufort and Frankel (15), and Barakat and Clark (6), whose stability cannot be predicted by the conditions given originally by Karplus, can be determined by this method.

6.3.3 The von Neumann Method of Stability Analysis

This method was first described by O'Brien, Hyman and Kaplan (42). It is regarded by most authors to be more general than the previous ones. According to this method, it is assumed that the solution of the

finite-difference equations can be represented by a Fourier expansion written as a product of three independent functions each depending on only one of the independent variables. This solution is then substituted in the finite-difference equations and the conditions necessary in order that the general term in the Fourier expansion remains bounded are established. Theoretically this method applies to a small class of linear equations with constant coefficients, while the coefficients of the governing equations vary in magnitude and sign with time and location. According to Von Neumann, this difficulty can be circumvented by applying the method to a sequence of overlapping small regions, each region being so small that the coefficients may be considered constant. In the present case, the criterion obtained for the stability of the finite-difference equations will be tested at each nodal point and the time step is altered accordingly.

The basic idea of this method of stability analysis can be outlined as follows;

The general explicit finite-difference equation corresponding to Equation (6.4) can be written in the form

$$F_{i,j}^{n+1} = \sum_{r=-1}^{r=1} (C_{i+r,j} F_{i+r,j}^n + C_{i,j+r} F_{i,j+r}^n) \quad (6.20)$$

The solution of the initial value problem is expressed as a Fourier series,

$$F(x,y,t) = \sum_{k_1} \sum_{k_2} \xi(k_1, k_2, t) e^{i(k_1 x + k_2 y)} \quad (6.21)$$

where k_1 and k_2 are integers.

Substituting the Fourier series (6.21) in the finite-difference Equation (6.20), the following relationship is obtained

$$\xi^{(n+1)} = \left[\sum_{r=-1}^1 (C_{1+r,j} e^{ik_1 r \Delta x} + C_{1,j+r} e^{ik_2 r \Delta y}) \right] \xi^{(n)} \quad (6.22)$$

denoting the quantity between brackets in (6.22) by $\gamma^{(n)}$, Equation (6.22) can be rewritten as

$$\xi^{(n+1)} = \gamma^{(n)} \xi^{(n)}. \quad (6.23)$$

The factor γ is usually called the amplification factor.

From (6.23), it is clear that $\xi^{(n+1)}$ can be written as a function of $\xi^{(0)}$,

$$\xi^{(n+1)} = \gamma^{(0)} \gamma^{(1)} \dots \gamma^{(n-1)} \gamma^{(n)} \xi^{(0)} \quad (6.24)$$

If γ is time independent, then

$$\xi^{(n+1)} = (\gamma)^n \xi^{(0)} \quad (6.25)$$

It is clear that the solution will be bounded as $\Delta t \rightarrow 0$ and $n \rightarrow \infty$, if $\xi^{(n+1)}$ is bounded, which requires that;

$$\text{MAX}_{(k_1, k_2)} |\gamma| \leq 1 \quad (6.26)$$

Richtmeyer (52) relaxes this condition for linear differential equations with constant coefficients and expresses the stability condition as:

$$\text{MAX}_{(k_1, k_2)} |\gamma| \leq 1 + O(\Delta t) \quad (6.27)$$

He points out that in some problems it is possible for the component of the exact solution to grow exponentially with increasing time and the condition (6.26) will not permit such a growth and cannot be satisfied without violating the consistency condition. It appears that the use of stability condition (6.27) should be exercised with care since in some cases condition (6.27) will be misleading as discussed in Section 6.5.

In the case of time-dependent coefficients, a sufficient and necessary condition for stability is that the product $[\gamma^{(0)}\gamma^{(1)}\dots\gamma^{(n-1)}\gamma^{(n)}]$ be bounded. Accordingly, the following condition will be sufficient to ensure stability;

$$\text{Max}_{k_1, k_2} |\gamma^{(n)}| \leq 1 \quad (6.28)$$

The same method can be adopted to study the stability of a system of linear equations as follows.

Let \vec{F} be a vector of p components, which represents the functions to be determined. The finite-difference expression in this case can be written as

$$\vec{F}^{(n+1)} = A \vec{F}^{(n)} \quad (6.29)$$

where A is a $p \times p$ matrix.

The general term of the Fourier series expansion of \vec{F} can be written as,

$$\vec{\xi}(k_1, k_2, t) \cdot e^{i(k_1 x + k_2 y)} \quad (6.30)$$

where $\vec{\xi}$ is also a p -component vector.

The substitution of the Fourier series expansion (6.30) in the finite-difference Equation (6.29) give the relation between the values of the vectors $\vec{\xi}^{(n+1)}$ and $\vec{\xi}^{(n)}$, such a relationship will have the form,

$$\vec{\xi}^{(n+1)} = B \vec{\xi}^{(n)} \quad (6.31)$$

where B is a p x p matrix, called the amplification matrix.

For system of differential equations with constant coefficients, Equation (6.31) gives the following relationship,

$$\vec{\xi}^{(n+1)} = B^{(n+1)} \vec{\xi}^{(0)} \quad (6.32)$$

It is not difficult to show that in order that $\xi^{(n+1)}$ be bounded, the eigenvalues $\lambda_1, \dots, \lambda_p$ of the amplification matrix should satisfy the following inequality

$$\text{Max}_{(k_1, k_2)} |\lambda_i| \leq 1 \quad (6.33)$$

For problems with time-dependent coefficients, the coefficients of the amplification matrix changes with time and at each time step a new matrix is generated. Accordingly, (6.31) can be rewritten as,

$$\left. \begin{aligned} \vec{\xi}^{(1)} &= B^{(1)} \vec{\xi}^{(0)} \\ \vec{\xi}^{(2)} &= B^{(2)} \vec{\xi}^{(1)} \\ &\vdots \\ \vec{\xi}^{(n+1)} &= B^{(n+1)} \vec{\xi}^{(n)} \end{aligned} \right\} \quad (6.34)$$

It is assumed in this case that the stability of the finite-difference equations is satisfied if the eigenvalues of the amplification matrices $B^{(1)}, \dots, B^{(n+1)}$ satisfy inequality (6.33). Although this latter assumption is considered heuristic, the method has worked for a

wide class of problems. However, the failure of this method to predict the behavior i.e., stability or unstability of some of the most desirable finite-difference method, namely formulation (iv) of section 5.4, will be discussed in the next section, where the procedure for its numerical application will be given.

6.4 STABILITY OF THE ENERGY AND VORTICITY EQUATIONS

By applying any of the methods of stability analysis discussed earlier, sufficient criteria can be obtained for the stability of any finite-difference method that can be obtained by using any of the formulas (5.3), (5.4), (5.5) and (5.6) to approximate the partial derivatives in Equations (4.49), (4.50), (4.78) and (4.79). In this section, the stability of each of formulations (i) through (iv) given in Chapter 5 will be analyzed. The conditions under which each of these formulations becomes of the positive-type will be obtained. These conditions, which are sufficient for the stability of the finite-difference equations, will be compared with those obtained by using the Fourier series method.

(I) Stability of the Explicit-Difference Equations, Formulation (i)

(a) Rewriting each of Equations (5.7), (5.8), (5.11) and (5.12)

in the same form as Equation (6.5), the following is obtained;

$$\begin{aligned}
 & \text{A. Rectangular } (U \geq 0, V \geq 0) \\
 & \theta_{i,j}^{n+1} = \left[1 - \left(\frac{U_{i,j}}{\Delta X} + \frac{V_{i,j}}{\Delta Y} + \frac{2a^2}{b^2(\Delta X)^2} + \frac{2}{\Delta Y^2} \right) \Delta \tau \right] \theta_{i,j+\Delta \tau}^n \left(\frac{U_{i,j}}{\Delta X} + \frac{a^2}{b^2(\Delta X)^2} \right) \theta_{i-1,j}^n + \quad (6.35)
 \end{aligned}$$

$$\frac{a^2}{b^2} \frac{\Delta\tau}{(\Delta X)^2} \Theta_{i+1,j}^n + \Delta\tau \left(\frac{V_{i,j}}{\Delta Y} + \frac{1}{\Delta Y^2} \right) \Theta_{i,j-1}^n + \frac{\Delta\tau}{\Delta Y^2} \Theta_{i,j+1}^n \quad (6.35)$$

$$w_{i,j}^{n+1} = \left[1 - \Delta\tau \left(\frac{U_{i,j}}{\Delta X} + \frac{V_{i,j}}{\Delta Y} + \frac{2a^2}{b^2} \frac{\text{Pr}}{(\Delta X)^2} + \frac{2}{\Delta Y^2} \text{Pr} \right) \right] w_{i,j}^n + \Delta\tau \left(\frac{U_{i,j}}{\Delta X} + \frac{a^2}{b^2} \frac{\text{Pr}}{(\Delta X)^2} \right) w_{i-1,j}^n + \frac{a^2}{b^2} \frac{\text{Pr}}{(\Delta X)^2} \Delta\tau w_{i+1,j}^n + \left(\frac{V_{i,j}}{\Delta Y} + \frac{\text{Pr}}{(\Delta Y)^2} \right) \Delta\tau w_{i,j-1}^n + \frac{\Delta\tau \text{Pr}}{(\Delta Y)^2} w_{i+1,j}^n + \frac{\text{Pr} \Delta\tau}{2\Delta Y} \left[\Theta_{i,j+1}^{n+1} - \Theta_{i,j-1}^{n+1} \right] \quad (6.36)$$

$$\left(\frac{V_{i,j}}{\Delta Y} + \frac{\text{Pr}}{(\Delta Y)^2} \right) \Delta\tau w_{i,j-1}^n + \frac{\Delta\tau \text{Pr}}{(\Delta Y)^2} w_{i+1,j}^n + \frac{\text{Pr} \Delta\tau}{2\Delta Y} \left[\Theta_{i,j+1}^{n+1} - \Theta_{i,j-1}^{n+1} \right]$$

It is clear that Equations (6.35) and (6.36) will be of positive type if the following inequalities are satisfied;

$$\Delta\tau \left(\frac{|U_{i,j}|}{\Delta X} + \frac{|V_{i,j}|}{\Delta Y} + \frac{2a^2}{b^2} \frac{1}{(\Delta X)^2} + \frac{2}{(\Delta Y)^2} \right) \leq 1 \quad (6.37)$$

and

$$\Delta\tau \left(\frac{|U_{i,j}|}{\Delta X} + \frac{|V_{i,j}|}{\Delta Y} + \frac{2a^2}{b^2} \frac{\text{Pr}}{(\Delta X)^2} + \frac{2}{(\Delta Y)^2} \text{Pr} \right) \leq 1 \quad (6.38)$$

inequality (6.37) is obtained from the energy equation (6.35), while (6.38) is required by the vorticity equation (6.36).

It should be noted that the coefficient of $\Theta_{i,j-1}^{n+1}$ in Equation (6.36) is always negative. However since $\Theta_{i,j}$ will be bounded, then the last term in (6.36) will be bounded for any finite-value of $\Delta\tau$ and ΔY . This term remains bounded as either of $\Delta\tau$ or ΔY or both go to zero. The argument is clear for the case when $\Delta\tau$ goes to zero and ΔY remains finite. For the other case, inequality (6.37) requires that

$\Delta\tau$ goes faster to zero than (ΔY) , which will ensure the boundedness of this term as ΔY approaches zero.

Inequalities (6.37) and (6.38) could have been obtained directly by applying inequality (6.7) to the differential Equations (4.49) and (4.50).

The same stability criteria applies for the case in which any of the velocity coefficients U or V or both are negative provided that forward differences, Equation (5.3), are used in the corresponding nonlinear terms.

It may be of interest to examine the case of negative velocity components in Equations (6.35) and (6.36). In this case the coefficients of the finite-difference Equations (6.35) and (6.36) will be positive if,

$$|U|_{i,j} \leq \frac{a^2}{b^2} \frac{1}{\Delta X} ; |V|_{i,j} \leq \frac{1}{\Delta Y} ; \Delta\tau \left(\frac{a^2}{b^2} \frac{2}{(\Delta X)^2} + \frac{2}{(\Delta Y)^2} - \frac{|U|_{i,j}}{\Delta X} - \frac{|V|_{i,j}}{\Delta Y} \right) \leq 1 \quad (6.39)$$

$$|U|_{i,j} \leq \frac{a^2}{b^2} \frac{Pr}{\Delta X} ; |V|_{i,j} \leq \frac{Pr}{\Delta Y} ; \Delta\tau \left(\frac{a^2}{b^2} \frac{2Pr}{(\Delta X)^2} + \frac{2Pr}{(\Delta Y)^2} - \frac{|U|_{i,j}}{\Delta X} - \frac{|V|_{i,j}}{\Delta Y} \right) \leq 1 \quad (6.40)$$

A method similar to the latter case was used by Wu (7.5) for solving the laminar boundary layer equations. His stability criteria are similar to those given by Equations (6.39) and (6.40).

In the remainder of this section, the discussion will be limited to the rectangular coordinates. The same conclusions hold for the cylindrical case. Whenever it seems necessary, the stability criteria for the

cylindrical coordinates will be given without giving the details of their derivation.

B. Cylindrical Coordinates

Following the same procedure used in the rectangular case, it can be shown that the finite-difference Equations (5.11), (5.12) and (5.66) are of positive type provided the following inequalities are true;

$$\Delta\tau \left(\frac{|U|_{i,j}}{(\Delta X)} + \frac{|V|_{i,j}}{\Delta R} + \frac{a^2}{b^2} \frac{2}{(\Delta X)^2} + \frac{2}{(\Delta R)^2} \right) \leq 1 \quad (6.41)$$

$$\Delta\tau \left(\frac{|U|_{i,j}}{\Delta X} + \frac{|V|_{i,j}}{\Delta R} + \frac{2a^2}{b^2} \frac{\text{Pr}}{(\Delta X)^2} + \frac{2 \text{Pr}}{(\Delta Y)^2} \right) \leq 1 \quad (6.42)$$

$$\Delta\tau \left(\frac{|U|_{i,1}}{\Delta X} + \frac{2a^2}{b^2} \frac{1}{\Delta X^2} + \frac{4}{(\Delta R)^2} \right) \leq 1 \quad (6.43)$$

(b) The application of Fourier series method to formulation (i).

The solution of the difference equations can be written as a Fourier series, the form of which is as follows (27)

$$w_{i,j}^{(n)} = \sum_{k_1} \sum_{k_2} \xi^{(n)} e^{i(k_1 X + k_2 Y)} \quad (6.44)$$

$$\theta_{i,j}^{(n)} = \sum_{k_1} \sum_{k_2} \mu^{(n)} e^{i(k_1 X + k_2 Y)} \quad (6.45)$$

where k_1 and k_2 are intergers, n is a superscript denoting the n^{th} time period and ξ and μ are functions of k_1 and k_2 . Substituting the system of Equations (6.44) and (6.45) into Equations (6.35) and (6.36) the following equations are obtained after some algebraic manipulations:

wide class of problems. However, the failure of this method to predict the behavior i.e., stability or unstability of some of the most desirable finite-difference method, namely formulation (iv) of section 5.4, will be discussed in the next section, where the procedure for its numerical application will be given.

6.4 STABILITY OF THE ENERGY AND VORTICITY EQUATIONS

By applying any of the methods of stability analysis discussed earlier, sufficient criteria can be obtained for the stability of any finite-difference method that can be obtained by using any of the formulas (5.3), (5.4), (5.5) and (5.6) to approximate the partial derivatives in Equations (4.49), (4.50), (4.78) and (4.79). In this section, the stability of each of formulations (i) through (iv) given in Chapter 5 will be analyzed. The conditions under which each of these formulations becomes of the positive-type will be obtained. These conditions, which are sufficient for the stability of the finite-difference equations, will be compared with those obtained by using the Fourier series method.

(I) Stability of the Explicit-Difference Equations, Formulation (i)

(a) Rewriting each of Equations (5.7), (5.8), (5.11) and (5.12)

in the same form as Equation (6.5), the following is obtained;

$$A. \text{ Rectangular } (U \geq 0, V \geq 0) \quad (6.35)$$

$$\Theta_{i,j}^{n+1} = \left[1 - \left(\frac{U_{i,j}}{\Delta X} + \frac{V_{i,j}}{\Delta Y} + \frac{2a^2}{b^2(\Delta X)^2} + \frac{2}{\Delta Y^2} \right) \Delta \tau \right] \Theta_{i,j+\Delta \tau}^n \left(\frac{U_{i,j}}{\Delta X} + \frac{a^2}{b^2(\Delta X)^2} \right) \Theta_{i-1,j}^n +$$

$$\frac{a^2}{b^2} \frac{\Delta\tau}{(\Delta X)^2} \Theta_{i+1,j}^n + \Delta\tau \left(\frac{V_{i,j}}{\Delta Y} + \frac{1}{\Delta Y^2} \right) \Theta_{i,j-1}^n + \frac{\Delta\tau}{\Delta Y^2} \Theta_{i,j+1}^n \quad (6.35)$$

$$w_{i,j}^{n+1} = \left[1 - \Delta\tau \left(\frac{U_{i,j}}{\Delta X} + \frac{V_{i,j}}{\Delta Y} + \frac{2a^2}{b^2} \frac{\text{Pr}}{(\Delta X)^2} + \frac{2}{\Delta Y^2} \text{Pr} \right) \right] w_{i,j}^n + \Delta\tau \left(\frac{U_{i,j}}{\Delta X} + \frac{a^2}{b^2} \frac{\text{Pr}}{(\Delta X)^2} \right) w_{i-1,j}^n + \frac{a^2}{b^2} \frac{\text{Pr}}{(\Delta X)^2} \Delta\tau w_{i+1,j}^n + \quad (6.36)$$

$$\left(\frac{V_{i,j}}{\Delta Y} + \frac{\text{Pr}}{(\Delta Y)^2} \right) \Delta\tau w_{i,j-1}^n + \frac{\Delta\tau \text{Pr}}{(\Delta Y)^2} w_{i+1,j}^n + \frac{\text{Pr} \Delta\tau}{2\Delta Y} \left[\Theta_{i,j+1}^{n+1} - \Theta_{i,j-1}^{n+1} \right]$$

It is clear that Equations (6.35) and (6.36) will be of positive type if the following inequalities are satisfied;

$$\Delta\tau \left(\frac{|U_{i,j}|}{\Delta X} + \frac{|V_{i,j}|}{\Delta Y} + \frac{2a^2}{b^2} \frac{1}{(\Delta X)^2} + \frac{2}{(\Delta Y)^2} \right) \leq 1 \quad (6.37)$$

and

$$\Delta\tau \left(\frac{|U_{i,j}|}{\Delta X} + \frac{|V_{i,j}|}{\Delta Y} + \frac{2a^2}{b^2} \frac{\text{Pr}}{(\Delta X)^2} + \frac{2}{(\Delta Y)^2} \text{Pr} \right) \leq 1 \quad (6.38)$$

inequality (6.37) is obtained from the energy equation (6.35), while (6.38) is required by the vorticity equation (6.36).

It should be noted that the coefficient of $\Theta_{i,j-1}^{n+1}$ in Equation (6.36) is always negative. However since $\Theta_{i,j}$ will be bounded, then the last term in (6.36) will be bounded for any finite-value of $\Delta\tau$ and ΔY . This term remains bounded as either of $\Delta\tau$ or ΔY or both go to zero. The argument is clear for the case when $\Delta\tau$ goes to zero and ΔY remains finite. For the other case, inequality (6.37) requires that

$\Delta\tau$ goes faster to zero than (ΔY) , which will ensure the boundedness of this term as ΔY approaches zero.

Inequalities (6.37) and (6.38) could have been obtained directly by applying inequality (6.7) to the differential Equations (4.49) and (4.50).

The same stability criteria applies for the case in which any of the velocity coefficients U or V or both are negative provided that forward differences, Equation (5.3), are used in the corresponding nonlinear terms.

It may be of interest to examine the case of negative velocity components in Equations (6.35) and (6.36). In this case the coefficients of the finite-difference Equations (6.35) and (6.36) will be positive if,

$$|U|_{i,j} \leq \frac{a^2}{b^2} \frac{1}{\Delta X} ; |V|_{i,j} \leq \frac{1}{\Delta Y} ; \Delta\tau \left(\frac{a^2}{b^2} \frac{2}{\Delta X^2} + \frac{2}{(\Delta Y)^2} - \frac{|U|_{i,j}}{\Delta X} - \frac{|V|_{i,j}}{\Delta Y} \right) \leq 1 \quad (6.39)$$

$$|U|_{i,j} \leq \frac{a^2}{b^2} \frac{Pr}{\Delta X} ; |V|_{i,j} \leq \frac{Pr}{\Delta Y} ; \Delta\tau \left(\frac{a^2}{b^2} \frac{2Pr}{(\Delta X)^2} + \frac{2Pr}{(\Delta Y)^2} - \frac{|U|_{i,j}}{\Delta X} - \frac{|V|_{i,j}}{\Delta Y} \right) \leq 1 \quad (6.40)$$

A method similar to the latter case was used by Wu(75) for solving the laminar boundary layer equations. His stability criteria are similar to those given by Equations (6.39) and (6.40).

In the remainder of this section, the discussion will be limited to the rectangular coordinates. The same conclusions hold for the cylindrical case. Whenever it seems necessary, the stability criteria for the

cylindrical coordinates will be given without giving the details of their derivation.

B. Cylindrical Coordinates

Following the same procedure used in the rectangular case, it can be shown that the finite-difference Equations (5.11), (5.12) and (5.66) are of positive type provided the following inequalities are true;

$$\Delta\tau \left(\frac{|U|_{i,j}}{(\Delta X)} + \frac{|V|_{i,j}}{\Delta R} + \frac{a^2}{b^2} \frac{2}{(\Delta X)^2} + \frac{2}{(\Delta R)^2} \right) \leq 1 \quad (6.41)$$

$$\Delta\tau \left(\frac{|U|_{i,j}}{\Delta X} + \frac{|V|_{i,j}}{\Delta R} + \frac{2a^2}{b^2} \frac{Pr}{(\Delta X)^2} + \frac{2 Pr}{(\Delta Y)^2} \right) \leq 1 \quad (6.42)$$

$$\Delta\tau \left(\frac{|U|_{i,1}}{\Delta X} + \frac{2a^2}{b^2} \frac{1}{\Delta X^2} + \frac{4}{(\Delta R)^2} \right) \leq 1 \quad (6.43)$$

(b) The application of Fourier series method to formulation (i).

The solution of the difference equations can be written as a Fourier series, the form of which is as follows (27)

$$w_{i,j}^{(n)} = \sum_{k_1} \sum_{k_2} \xi^{(n)} e^{i(k_1 X + k_2 Y)} \quad (6.44)$$

$$\theta_{i,j}^{(n)} = \sum_{k_1} \sum_{k_2} \mu^{(n)} e^{i(k_1 X + k_2 Y)} \quad (6.45)$$

where k_1 and k_2 are intergers, n is a superscript denoting the n^{th} time period and ξ and μ are functions of k_1 and k_2 . Substituting the system of Equations (6.44) and (6.45) into Equations (6.35) and (6.36) the following equations are obtained after some algebraic manipulations:

$$\sum_{k_1} \sum_{k_2} \left\{ \xi^{(n+1)} - \xi^{(n)} (\alpha_1 + \alpha_2 e^{-ik_1 \Delta X} + \alpha_3 e^{-ik_2 \Delta Y} + \alpha_4 e^{ik_1 \Delta X} + \alpha_5 e^{ik_2 \Delta Y}) + \alpha_6 \mu^{(n+1)} \right\} e^{i(k_1 X + k_2 Y)} = 0$$

$$\sum_{k_1} \sum_{k_2} \left\{ \mu^{(n+1)} - \mu^{(n)} (C_1 + C_2 e^{-k_1 \Delta X} + C_3 e^{-ik_2 \Delta Y} + C_4 e^{ik_1 \Delta X} + C_5 e^{ik_2 \Delta Y}) \right\} e^{i(k_1 X + k_2 Y)} = 0$$

From the above equations it is concluded that the difference equations are satisfied if

$$\xi^{(n+1)} = \xi^{(n)} (\alpha_1 + \alpha_2 e^{-ik_1 \Delta X} + \alpha_3 e^{-ik_2 \Delta Y} + \alpha_4 e^{ik_1 \Delta X} + \alpha_5 e^{ik_2 \Delta Y}) + \alpha_6 \mu^{n+1} \quad (6.46)$$

and

$$\mu^{(n+1)} = \mu^{(n)} (\beta_1 + \beta_2 e^{-ik_1 \Delta X} + \beta_3 e^{-ik_2 \Delta Y} + \beta_4 e^{ik_1 \Delta X} + \beta_5 e^{ik_2 \Delta Y}) \quad (6.47)$$

where:

$$\alpha_1 = 1 - \left(2 \frac{a^2}{b^2} \frac{\text{Pr}}{(\Delta X)^2} + \frac{2 \text{Pr}}{(\Delta Y)^2} + \frac{U_{i,j}}{\Delta X} + \frac{V_{i,j}}{\Delta Y} \right) \Delta \tau$$

$$\alpha_2 = \left(\frac{a^2}{b^2} \frac{\text{Pr}}{(\Delta X)^2} + \frac{U_{i,j}}{\Delta X} \right) \Delta \tau$$

$$\alpha_3 = \left(\frac{\text{Pr}}{(\Delta Y)^2} + \frac{V_{i,j}}{\Delta Y} \right) \Delta \tau$$

$$\alpha_4 = \frac{a^2}{b^2} \frac{\text{Pr}}{(\Delta X)^2} \Delta \tau$$

$$\alpha_5 = \text{Pr} \Delta \tau / (\Delta Y)^2$$

$$\beta_1 = 1 - \left(2 \frac{a^2}{b^2} \frac{1}{(\Delta X)^2} + 2/(\Delta Y)^2 + U_{i,j}/\Delta X + V_{i,j}/\Delta Y \right) \Delta \tau$$

$$\beta_2 = (a^2/(b\Delta X)^2 + U_{i,j}/\Delta X) \Delta \tau$$

$$\beta_3 = (1/(\Delta Y)^2 + V_{i,j}/\Delta Y) \Delta \tau$$

$$\beta_4 = (a/(b\Delta X))^2 \Delta \tau$$

$$\beta_5 = \Delta \tau / (\Delta Y)^2$$

No definition has been given to α_8 since it has no effect on this analysis.

The system of Equations (6.46) and (6.47) are of the form:

$$\xi^{(n+1)} = a_{11}\xi^{(n)}(k_1, k_2) + a_{12}\mu^{(n)}(k_1, k_2) \quad (6.48)$$

$$\mu^{(n+1)} = a_{21}\xi^{(n)}(k_1, k_2) + a_{22}\mu^{(n)}(k_1, k_2) \quad (6.49)$$

In a matrix notation the above equalities can be written as

$$\begin{bmatrix} \xi^{(n+1)} \\ \mu^{(n+1)} \end{bmatrix} = \begin{bmatrix} a_{11} & a_{12} \\ a_{21} & a_{22} \end{bmatrix} \begin{bmatrix} \xi^{(n)} \\ \mu^{(n)} \end{bmatrix} \quad (6.50)$$

The quantity between the first brackets on the right hand side of (6.50) is the amplification matrix. The von Neumann condition necessary for stability is that: $|\lambda_{\max}| \leq 1$ where λ_{\max} is the largest eigenvalue of the amplification matrix. The eigenvalues are given by:

$$\begin{vmatrix} a_{11}-\lambda & a_{12} \\ a_{21} & a_{22}-\lambda \end{vmatrix} = 0 \quad (6.51)$$

Substituting the values of a_{11} , a_{12} , ... etc., in the above determinant and solving for λ we get:

$$\lambda_1 = \alpha_1 + \alpha_2 e^{-ik_1 \Delta X} + \alpha_3 e^{-ik_2 \Delta Y} + \alpha_4 e^{ik_1 \Delta X} + \alpha_5 e^{ik_2 \Delta Y} \quad (6.52)$$

$$\lambda_2 = \beta_1 + \beta_2 e^{-ik_1 \Delta X} + \beta_3 e^{-ik_2 \Delta Y} + \beta_4 e^{ik_1 \Delta X} + \beta_5 e^{ik_2 \Delta Y} \quad (6.53)$$

The coefficients $\alpha_1, \alpha_2, \dots, \beta_1, \beta_2, \dots$ etc., are all positive except α_1 and β_1 which may be positive or negative. The largest absolute values of λ_1 and λ_2 occur when all the terms in Equations (6.52) and (6.53) are real, i.e., when $k_1 \Delta X = k_2 \Delta Y = 2\pi$ then,

$$\lambda_{1\max} = \alpha_1 + \alpha_2 + \alpha_3 + \alpha_4 + \alpha_5 \quad (6.54)$$

$$\lambda_{2\max} = \beta_1 + \beta_2 + \beta_3 + \beta_4 + \beta_5 \quad (6.55)$$

Substituting the values of $\alpha_1, \alpha_2, \dots, \beta_1, \dots, \beta_5$ in λ_{\max}

$$\lambda_{1\max} = \lambda_{2\max} = 1 \quad (6.56)$$

Therefore, we can conclude that λ_{\max} will not exceed unity and it will not impose any stability restrictions. If there may be any restrictions, it will be to prevent the minimum value of λ from becoming less than -1.

The minimum of the eigenvalues occur when $k_1 \Delta X = k_2 \Delta Y = \pi$ and are given by

$$\lambda_{1\min} = \alpha_1 - \alpha_2 - \alpha_3 - \alpha_4 - \alpha_5$$

$$\lambda_{2\min} = \beta_1 - \beta_2 - \beta_3 - \beta_4 - \beta_5$$

or

$$\lambda_{1\min} = 1 - 2\Delta\tau(2Pr(a/b\Delta X)^2 + 2Pr/(\Delta Y)^2 + |U_{i,j}|/\Delta X + |V_{i,j}|/\Delta Y)$$

$$\lambda_{2\min} = 1 - 2\Delta\tau(2(a/b\Delta X)^2 + 2/(\Delta Y)^2 + |U_{i,j}|/\Delta X + |V_{i,j}|/\Delta Y)$$

Therefore for $|\lambda| \leq 1$ the following inequalities should be satisfied:

$$\Delta\tau \left(\frac{2a^2}{b^2(\Delta X)^2} + \frac{2}{(\Delta Y)^2} + |U_{i,j}|/\Delta X + |V_{i,j}|/\Delta Y \right) \leq 1 \quad (6.57)$$

$$\Delta\tau(2Pr(a/b\Delta X)^2 + 2Pr/(\Delta Y)^2 + |U_{i,j}|/\Delta X + |V_{i,j}|/\Delta Y) \leq 1 \quad (6.58)$$

Equations (6.57) and (6.58) are the necessary requirement for stability. For values of Prandtl number less than unity, inequality (6.57) is more restrictive and therefore should be used. For higher values of Prandtl number inequality (6.58) must be used.

The same stability criteria will be obtained if any of the velocity components U and V or both are negative and forward differences are used in the corresponding nonlinear terms.

It is quite clear that for this method the von Neumann method of stability analysis requires that the finite-difference equations be of positive type. As a matter of fact, all the conclusions reached above for this method using the concept of positive-type differences will be obtained using the von Neumann method.

(II) Stability of the Explicit Formulation (ii), Equations (5.9) and (5.10)

Equations (5.9) and (5.10) are rewritten in the form

$$\begin{aligned} \Theta_{i,j}^{n+1} = & \left(1 - \frac{2a^2}{b^2} \frac{\Delta\tau}{(\Delta X)^2} - \frac{2\Delta\tau}{(\Delta Y)^2} \right) \Theta_{i,j+\Delta\tau}^n \left(\frac{a^2}{b^2(\Delta X)^2} + \frac{U_{i,j}}{2\Delta X} \right) \Theta_{i-1,j}^n \\ & + \Delta\tau \left(\frac{a^2}{b^2} \frac{1}{(\Delta X)^2} - \frac{U_{i,j}}{2\Delta X} \right) \Theta_{i+1,j}^n \\ & + \Delta\tau \left(\frac{1}{(\Delta Y)^2} + \frac{V_{i,j}}{2\Delta Y} \right) \Theta_{i,j-1}^n + \Delta\tau \left(\frac{1}{(\Delta Y)^2} - \frac{V_{i,j}}{2\Delta Y} \right) \Theta_{i,j+1}^n \end{aligned} \quad (6.59)$$

$$\begin{aligned} w_{i,j}^{n+1} = & \left(1 - \frac{2a^2}{b^2} \frac{\text{Pr} \Delta\tau}{(\Delta X)^2} - \frac{2\text{Pr}\Delta\tau}{(\Delta Y)^2} \right) w_{i,j}^n + \Delta\tau \left(\frac{a^2}{b^2} \frac{\text{Pr}}{(\Delta X)^2} + \frac{U_{i,j}}{2\Delta X} \right) w_{i+1,j}^n + \\ & \Delta\tau \left(\frac{a^2}{b^2} \frac{\text{Pr}}{(\Delta X)^2} - \frac{U_{i,j}}{2\Delta X} \right) w_{i+1,j+\Delta\tau}^n \left(\frac{\text{Pr}}{(\Delta Y)^2} + \frac{V_{i,j}}{2\Delta Y} \right) w_{i,j-1}^n + \Delta\tau \left(\frac{\text{Pr}}{(\Delta Y)^2} - \frac{V_{i,j}}{2\Delta Y} \right) \\ & w_{i,j+1}^n + \frac{\Delta\tau \text{Pr}}{2\Delta Y} (\Theta_{i,j+1}^{n+1} - \Theta_{i,j-1}^{n+1}) \end{aligned} \quad (6.60)$$

The finite-difference Equation (6.59) is of positive-type i.e., stable provided that,

$$\Delta\tau \left(\frac{2a^2}{b^2} \frac{1}{(\Delta X)^2} + \frac{2}{(\Delta Y)^2} \right) \leq 1; \quad U \leq \frac{2a^2}{b^2} \frac{1}{\Delta X}; \quad V \leq \frac{2}{\Delta Y} \quad (6.61)$$

Likewise Equation (6.60) will be of positive type if;

$$\Delta\tau \left(\frac{2a^2}{b^2} \frac{\text{Pr}}{(\Delta X)^2} + \frac{2\text{Pr}}{(\Delta Y)^2} \right) \leq 1, \quad U \leq \frac{2a^2}{b^2} \frac{\text{Pr}}{\Delta X}; \quad V \leq \frac{2\text{Pr}}{\Delta Y} \quad (6.62)$$

Accordingly formulation (ii) is stable under conditions (6.61) and (6.62).

Application of the Fourier series method to formulation (ii) leads to the same stability criteria given by inequalities (6.61) and (6.62).

Substitution of the series (6.44) and (6.45) in Equations (6.59) and (6.60), following the same procedure used in the previous case, it will not be difficult to show that the eigenvalues of the amplification matrix are given by:

$$|\lambda_1|^2 = \left[1 - \frac{2a^2}{b^2} \frac{\text{Pr}}{(\Delta X)^2} \Delta\tau(1-\cos k_1 \Delta X) - \frac{2\text{Pr}}{(\Delta Y)^2} \Delta\tau(1-\cos k_2 \Delta Y) \right]^2 + i[(U\Delta\tau/\Delta X)\text{sink}_1 \Delta X + (V\Delta\tau/\Delta Y)\text{sink}_2 \Delta Y]^2 \quad (6.63)$$

$$|\lambda_2|^2 = \left[1 - \frac{2a^2}{b^2} \frac{\Delta\tau}{(\Delta X)^2} (1-\cos k_1 \Delta X) - \frac{\Delta\tau}{(\Delta Y)^2} (1-\cos k_2 \Delta Y) \right]^2 + [(U\Delta\tau/\Delta X)\text{sink}_1 \Delta X + (V\Delta\tau/\Delta Y)\text{sink}_2 \Delta Y]^2 \quad (6.64)$$

the conditions under which $|\lambda_1|$ and $|\lambda_2|$ become less than unity can be established by differentiating Equations (6.63) and (6.64) with respect to $(k_1 \Delta X)$ and $(k_2 \Delta Y)$ to obtain the maximum of λ_1 and λ_2 . The work involved is tedious. The details of the analysis are given in Appendix II. The results of Appendix II show that if inequalities (6.61) and (6.62) are violated, this method will be unstable.

(III) Stability of the Implicit Difference Equations, Scheme III

The implicit finite-difference Equations (5.15) and (5.16) in which implicit backward differences are used with positive velocity components U and V , and forward differences are used otherwise are unconditionally stable. This can be established by using any of the previously mentioned methods of stability analysis. Inspection of the coefficients of these difference equations shows that they are

of positive-type, regardless of the value of the time or the spatial, increments. The same conclusion will be reached by using the von Neumann method. The application of the latter method to this case is as simple as its application to formulation (i), and therefore it will be omitted.

The advantages and shortcomings of such methods, as well as the limitations on their use to solve the energy and vorticity equations, are discussed at length in Section 5.9, which should be consulted before using any unconditionally stable finite-differences to solve the vorticity equation.

(IV) Stability of the Implicit Difference Equations, Formulation (iv)

The study of the stability of this method deserves some special considerations for reasons that will be clear from the context of the following discussions. It is usually believed that implicit differences are unconditionally stable, as is the case for the heat diffusion equation. However, it will be seen that this is not true for differential equations containing first order derivatives.

The use of the von Neumann method shows that it is unconditionally stable. This can be demonstrated by substituting Equations (6.44) and (6.45) in Equations (5.25) and (5.26) to obtain the following relationship

$$\begin{aligned}\mu^{n+1} &= C_{11} \mu^n \\ \xi^{n+1} &= C_{21} \mu^n + C_{22} \xi^n\end{aligned}$$

where:

$$C_{11} = 1 / \left[1 + \frac{2a^2\Delta\tau}{b^2(\Delta X)^2} (1 - \text{cosk}_1\Delta X) + \frac{2\Delta\tau}{(\Delta Y)^2} (1 - \text{cosk}_2\Delta Y) + i \left(\frac{U\Delta\tau}{\Delta X} \text{sink}_1\Delta X + \frac{V\Delta\tau}{\Delta Y} \text{sink}_2\Delta Y \right) \right]$$

$$C_{21} = \frac{\text{Pr} \Delta\tau}{\Delta Y} i \text{sink}_2\Delta Y / C_{22}$$

$$C_{22} = 1 / \left[1 + \frac{2a^2\text{Pr}\Delta\tau}{b^2(\Delta X)^2} (1 - \text{cosk}_1\Delta X) + \frac{2\text{Pr}\Delta\tau}{(\Delta Y)^2} (1 - \text{cosk}_2\Delta Y) + i \left(\frac{U\Delta\tau}{\Delta X} \text{sink}_1\Delta X + \frac{V\Delta\tau}{\Delta Y} \text{sink}_2\Delta Y \right) \right]$$

The amplification matrix $B(t)$ is given by

$$B(t) = \begin{bmatrix} C_{11} & 0 \\ C_{21} & C_{22} \end{bmatrix}$$

The eigenvalues of the amplification matrix λ_1 and λ_2 are:

$$\lambda_1 = C_{11} \quad ; \quad \lambda_2 = C_{22}$$

The maximum of the absolute magnitude of λ_1 and λ_2 occurs when $\text{cosk}_1\Delta X = \text{cosk}_2\Delta Y = 1$ and

$$|\lambda_1|_{\max} = |\lambda_2|_{\max} = 1$$

Therefore, according to this method of stability analysis, this formulation should be unconditionally stable.

Actual calculations have shown that the above conclusion is erroneous. For the conditions of run 1, accumulator overflow took place after few time steps using 11x11 grid. The conditions required to make this of the positive-type i.e., stable, are:

$$U_{i,j} \leq \frac{2a^2}{b^2} \frac{1}{\Delta X} ; V_{i,j} \leq \frac{2}{\Delta Y} \quad (\text{From Energy Eq.}) \quad (6.65)$$

and

$$U_{i,j} \leq \frac{2a^2 Pr}{b^2 \Delta X} ; V_{i,j} \leq \frac{2Pr}{\Delta Y} \quad (\text{From Vort. Eq.}) \quad (6.66)$$

The calculations carried out for the conditions of run 1, using 11x11 grid and taking $(a/b) = 1$ and $g = 0.0322$ in order that (6.65) and (6.66) were satisfied, showed no signs of instability. Furthermore, the calculations show that even for the case of constant coefficients this method becomes unstable if inequalities (6.65) and (6.66) are violated.

6.5 A MORE GENERAL APPROACH TO THE STABILITY OF THE EXPLICIT FINITE-DIFFERENCE EQUATIONS

The stability of the various finite-difference formulations has been examined using different methods of stability analysis, namely the von Neumann method and the concept of positive-type differences. The application of the first method to difference equations with variable coefficients is considered heuristic. The second method, although mathematically sound, has failed to predict the stability of some useful finite-difference formulations.

In this section a more general approach to the study of the stability of the explicit finite-difference equations will be presented.

The explicit finite-difference Equation (6.5), whose stability criterion is required, is written in the following form which is the same as that of Equation (6.29).

$$\vec{F}^{(n+1)} = A^{(n+1)} \vec{F}^{(n)} \quad (6.67)$$

where $\vec{F}^{(n+1)}$ is a p-component column vectors $[F_{i,j}^{n+1}]$ and $A^{(n)}$ is a five-diagonal pxp matrix. The entries on any row of this matrix will be given by the coefficients $a_{i,j}$, $a_{i+1,j}$, $a_{i-1,j}$, $a_{i,j+1}$ and $a_{i,j-1}$.

From Equation (6.67), the following recurrence formulae can be written:

$$\begin{aligned} \vec{F}^{(1)} &= A^{(1)} \vec{F}^{(0)} \\ \vec{F}^{(2)} &= A^{(2)} \vec{F}^{(1)} = A^{(2)} A^{(1)} \vec{F}^{(0)} \\ &\vdots \\ \vec{F}^{(n+1)} &= A^{(n+1)} A^{(n)} \dots A^{(1)} \vec{F}^{(0)}. \end{aligned}$$

where $\vec{F}^{(0)}$ is the initial values of the vector \vec{F} . The norm of the vector $\vec{F}^{(n+1)}$, which is denoted by $\|\vec{F}^{(n+1)}\|$, satisfies the following inequality:

$$\begin{aligned} \|\vec{F}^{(n+1)}\| &\leq \|A^{(n+1)} A^{(n)} \dots A^{(1)}\| \cdot \|\vec{F}^{(0)}\| \\ &\leq \|A^{(n+1)}\| \cdot \|A^{(n)}\| \dots \|A^{(1)}\| \cdot \|\vec{F}^{(0)}\| \quad (6.69) \end{aligned}$$

From Equation (6.69) it is clear that for any initial vector $\vec{F}^{(0)}$, the vector $\vec{F}^{(n+1)}$ will be bounded if the product of the norms of the matrices $A^{(n+1)}, A^{(n)}, \dots, A^{(1)}$ is bounded. A sufficient condition for the boundedness of the vector $\vec{F}^{(n+1)}$ can therefore be written as:

$$\|A^{(n)}\| \leq 1 \quad (6.70)$$

Upon substitution of Equation (6.70) in inequality (6.68), the following inequality is obtained:

$$\|F^{(n+1)}\| \leq \|F^{(0)}\|, \quad (6.71)$$

which indicates that Equation (6.67) is stable assuming, of course, that (6.70) is satisfied.

The choice of the norm of the matrices $A^{(n)}$ is a matter of convenience. The most appropriate norm for use in connection with inequality (6.70) is the row norm which is defined by:

$$\|A^{(n)}\|_I = \max_j \sum_i |a_{i,j}|$$

Therefore, inequality (6.70) can be rewritten as:

$$\max_j \sum_i |a_{i,j}| \leq 1 \quad (6.72)$$

Inequality (6.72) is sufficient for the stability of the explicit finite-difference Equations (6.5).

Sometimes the criteria known to be sufficient are regarded as conservative. In order to evaluate the stability criteria given by inequality (6.72), it will be applied to the explicit finite-difference formulation of the energy equation given by Equation (5.7). It is not difficult to show that for this formulation, inequality (6.72) requires that

$$\left[2 \frac{a^2}{b^2} \frac{1}{(\Delta X)^2} + \frac{2}{\Delta Y^2} + \frac{|U_{i,j}|}{\Delta X} + \frac{|V_{i,j}|}{\Delta Y} \right] \Delta \tau \leq 1$$

which is the same criterion obtained previously. Furthermore, it is noticed that the resulting difference equations are of positive type.

As another example of the application of this method, the following one-dimensional diffusion equation, is considered.

$$\frac{\partial \theta}{\partial t} = \frac{\partial^2 \theta}{\partial X^2} \quad (6.73)$$

$$\frac{\theta_i^{n+1} - \theta_i^n}{\Delta t} = \frac{\theta_{i+1}^n + 2\theta_i^n + \theta_{i-1}^n}{(\Delta X)^2} \quad (6.74)$$

The stability condition (6.72) requires that:

$$\Delta t \leq \frac{(\Delta X)^2}{2} \quad (6.75)$$

Inequality (6.75) is precisely the established necessary stability criterion of formulation (6.74). The treatment of boundary conditions is accomplished by the application of the same criterion i.e., inequality (6.71).

The above results indicate that the method of stability analysis presented in this section seems to be promising, as far as the stability analysis of explicit finite-difference equations with variable coefficients are concerned.

It should be mentioned that the application of this method to all the explicit finite-difference formulations mentioned in earlier sections leads to the same conclusions concerning their stability.

It was also found that the application of the stability criterion given by inequality (6.72) to implicit finite-difference equations leads to the same conclusions obtained by other methods of stability

analysis. However, mathematical investigation of this case similar to that made for explicit formulations has not been worked yet.

6.6 SUMMARY OF THE RESULTS OF THIS CHAPTER

From the discussions presented in this chapter, the following conclusions can be drawn:

(1) Any finite-difference representation of the energy and vorticity equations or any partial differential equation which has the form of Equation (6.4) is stable if it is of positive type.

(2) For positive velocity components U and V , the use of backward differences, Equation (5.4) for approximating the first order derivatives in the nonlinear terms together with Equation (5.6) to approximate the second order derivatives, permits the construction of positive type difference equations, for which sufficient and practical stability criteria can be derived. The same is true should forward differences be used to approximate the nonlinear terms whose velocity coefficients are negative. At the present time, this method seems to be the most practical one to use, since the spatial increments can be chosen as desired, while the time increment is determined by stability considerations.

(3) The use of the central differences in the nonlinear terms, which is preferable from the point of view of the truncation error, is possible only for cases in which the resulting difference equations are of positive type. This requires that inequalities similar to

(6.61), (6.62) or (6.64) and (6.65) should be satisfied. For high velocities, i.e., high Rayleigh numbers, this would mean the use of very small spatial increments, which may require storage capacity beyond that of existing machines, and possibly a prohibitive amount of machine time. This applies to implicit, as well as, explicit methods, regardless whether the coefficients are constant or variable.

The necessity of satisfying the above mentioned inequalities was demonstrated by considering the following simple one-dimensional equation with constant coefficients.

$$\frac{\partial f}{\partial t} = a_0 \frac{\partial^2 f}{\partial x^2} + a_1 \frac{\partial f}{\partial x}; \quad f(0,t)=1, \quad f(1,t)=0, \quad f(x,0)=0$$

Accordingly the use of central differences to approximate $\partial f/\partial x$ requires that Δx be chosen such that:

$$\frac{2a_0}{\Delta x} \geq |a_1| \quad (6.76)$$

when $|a_1|$ was taken 5% larger than that required by the equality sign in Equation (6.76) unstable results were obtained.

The above conclusions are in contradiction with some published literature (52), which holds that for linear equations with constant coefficients stability is unaffected by the first order terms. These erroneous conclusions are based on the use of the stability criterion (6.27).

(4) The stability criteria obtained by the method of von Neumann are also those required to make the difference equations of positive-

type.

(5) The method of von Neumann leads to incorrect results when applied to implicit methods corresponding to differential equations of the form (6.4), whose difference equations are not of the positive-type. This was demonstrated by applying it to formulation (iv), as well as to other formulations, which are not reported here.

All the above conclusions were substantiated by mathematical experimentation using an IBM 7090 digital computer.

CHAPTER 7

EXPERIMENTAL WORK

An experimental program was carried to study the phenomenon of thermal stratification in liquid containers. The experiments were conducted in a cylindrical as well as a rectangular container. The results obtained from these experiments are compared to those of the theoretical analysis in Chapter 8.

7.1 DESCRIPTION OF THE RECTANGULAR APPARATUS

The apparatus consists of three parallel compartments separated by two, $1/16$ " thick copper walls. The middle compartment is used as a test section, while the outer two are used to intercept the steam used for heating, Fig. 7. The two outer containers, which are 3" wide, 9" high and 20" long are formed from $1/16$ " thick copper metal sheets. These two containers are placed parallel to each other, but 3" apart, over a flat plate of transite $1/4$ " thick, 9" wide and 20" long. The third compartment is formed between the two containers by using two end plates, 3" wide and 9" high to complete its sides. One of these end plates is from plexiglass and the other is made from transite. Rubber gaskets are used, where any two sides are screwed together, to prevent leakage. The middle compartment is filled with the test fluid, i.e., water to a height $8-1/4$ ". Heating of the walls of the middle container is accomplished by impinging steam on the

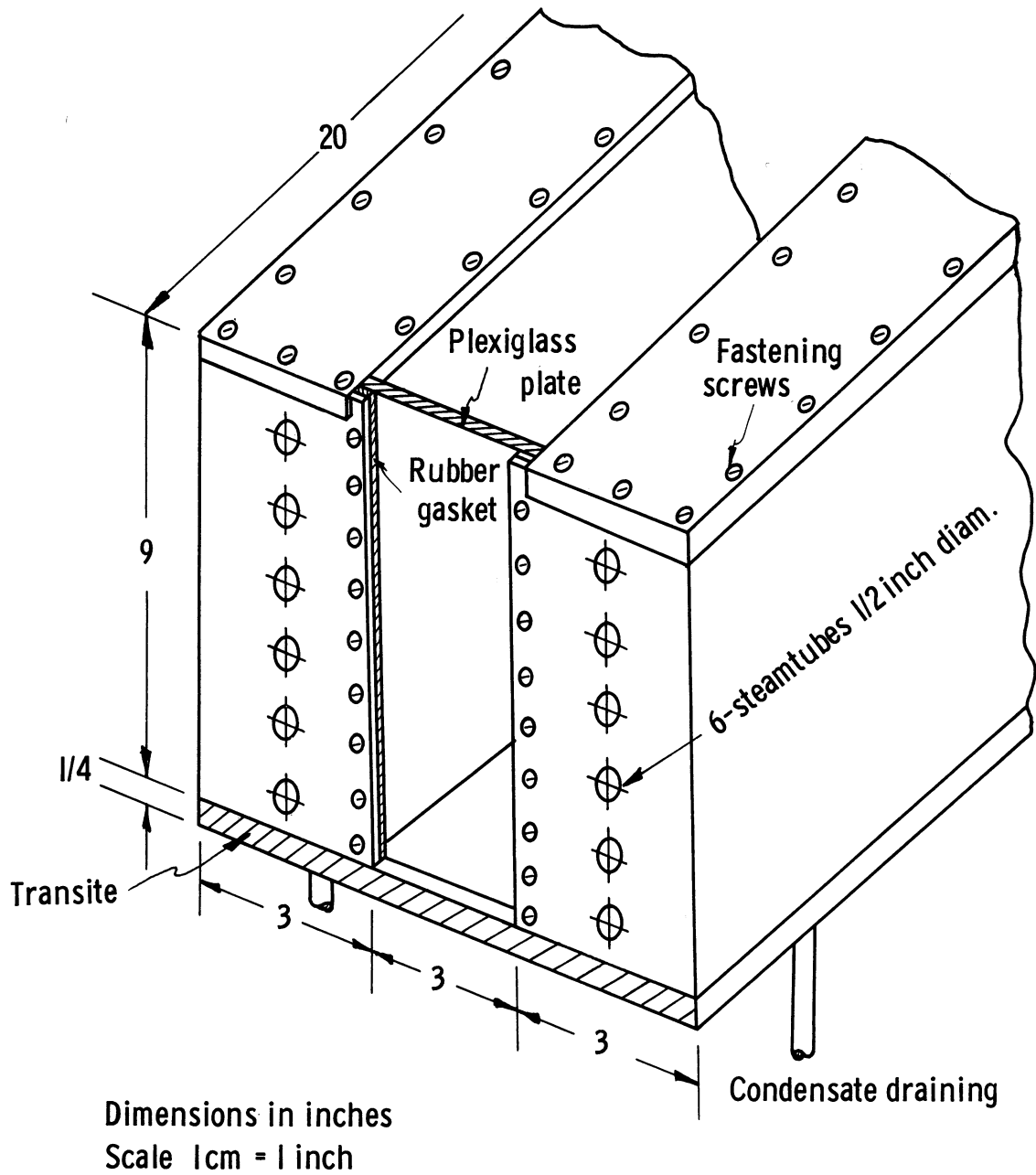


Fig. 7. Sketch of rectangular container.

walls separating the outer containers from the middle one. The steam issues from a number of fine holes drilled in copper tubes running through both containers. Six of these tubes are mounted horizontally, parallel to the walls in each outer container. The tubes of each bank are closed at one end, while steam is fed to the other end through a common header. Thus two steam headers are used. The condensate is drained from each outer container through a draining pipe $1/2$ " diameter. The steam supply systems for both tube banks are arranged in such a way to provide as much symmetry with tank center line, as possible.

Six thermocouples, number 13 through 18, are soldered to one of the container walls at heights $1-3/8$, $3-3/8$, $5-5/16$, $6-3/16$, $6-15/16$ and $7-1/2$ " from the bottom respectively. These thermocouples are located above each other at half the length of the container. Two additional thermocouples numbers 19 and 20 were added later to the same wall of the container at height $5-5/16$ " and are 5 and 15" from the container end. Also at the same time two thermocouples numbers 21 and 22 were soldered to the other wall at $5-5/16$ " height and at 5 and 10" from the same end. These four thermocouples were added to the wall in order to examine the spanwise variation of the wall temperature and the symmetry, Fig. 13, page 129.

Twelve thermocouples numbers 1 through 12 are used to measure the liquid temperature. The locations of these thermocouples as well as the others are shown in Fig. 8.

Locations of Thermocouples

Chromel vs. Constantan No. 30 duplex

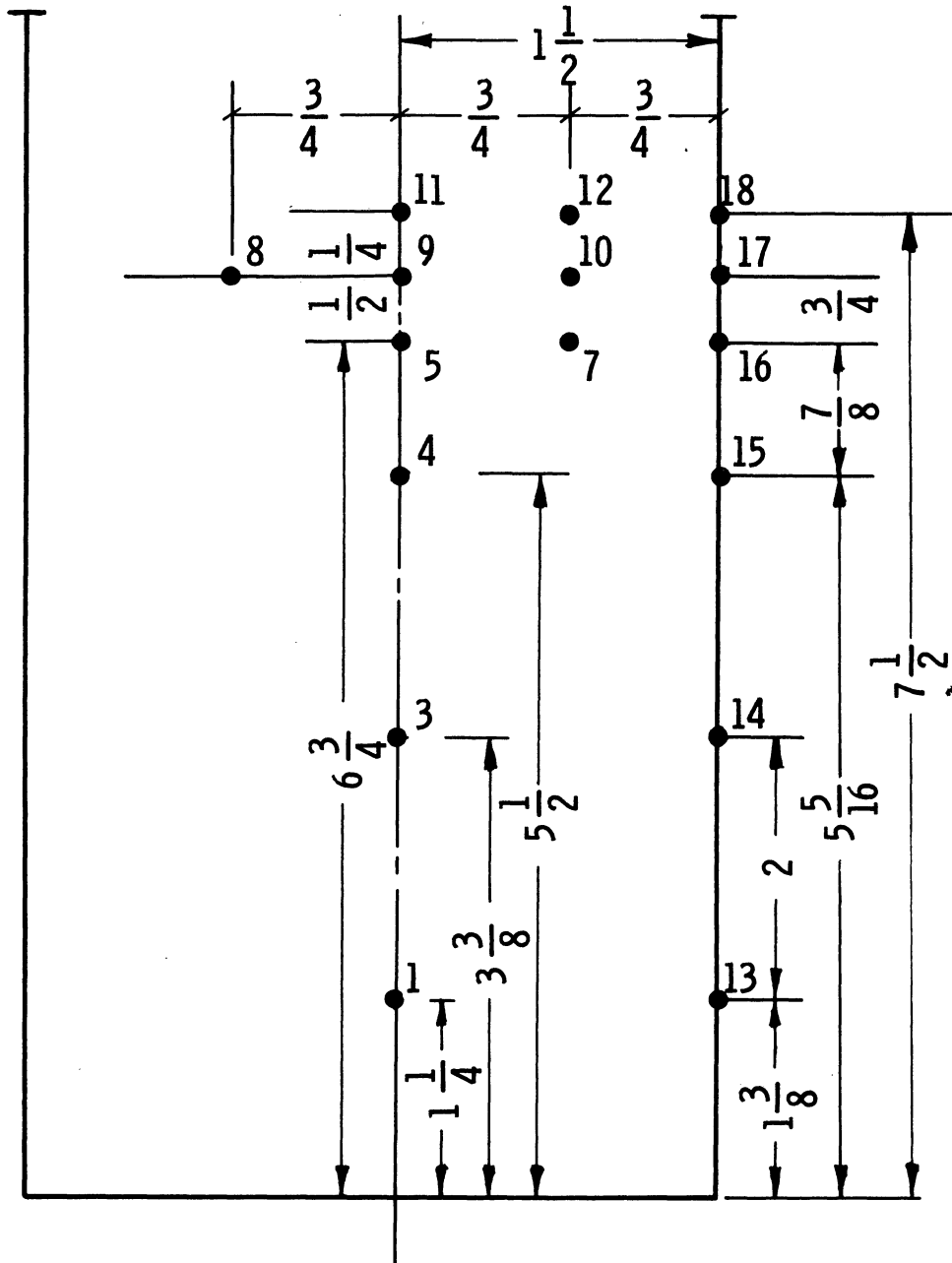


Fig. 8. Thermocouple locations in the rectangular container.

A 36-channel Honeywell visicorder model 1012 was used to record the temperature of these thermocouples. Chromel-constantan duplex gauge 30 wire is used for the thermocouples. An ice bath is used for the reference junctions. Each thermocouple circuit, consisting of the thermocouple itself, the visicorder channel to which it is connected and the necessary wiring, was calibrated individually.

7.2 DESCRIPTION OF THE CYLINDRICAL APPARATUS

The cylindrical apparatus consists of a bronze tube 4" outer diameter having 1/8" thick walls and 1 foot long. The details of the construction of the cylinder is shown in Fig. 9. The cylinder was closed at the bottom by pressing a bronze disc inside the cylinder to a depth of 5/16". Two other discs made of transite and styrofoam are glued together and inserted in the cylinder. They are fastened to bottom disc by 4 screws. A thin disc of teflon is cemented to the upper face of the styrofoam. The use of styrofoam reduces the heat losses through the cylinder bottom. Sealing of the bottom is accomplished by putting a thin layer of styrofoam cement over the teflon disc at the cylinder walls only. The cylinder walls are recessed to 1/32" thickness from both ends as shown in Fig. 9 to reduce the heat losses by conduction through the ends.

The cylinder is heated electrically using 1/2" wide and 0.0035" thick nichrome heating ribbon, which was wound helically around the cylinder. The pitch of the helix is equal to 5/8". The heating

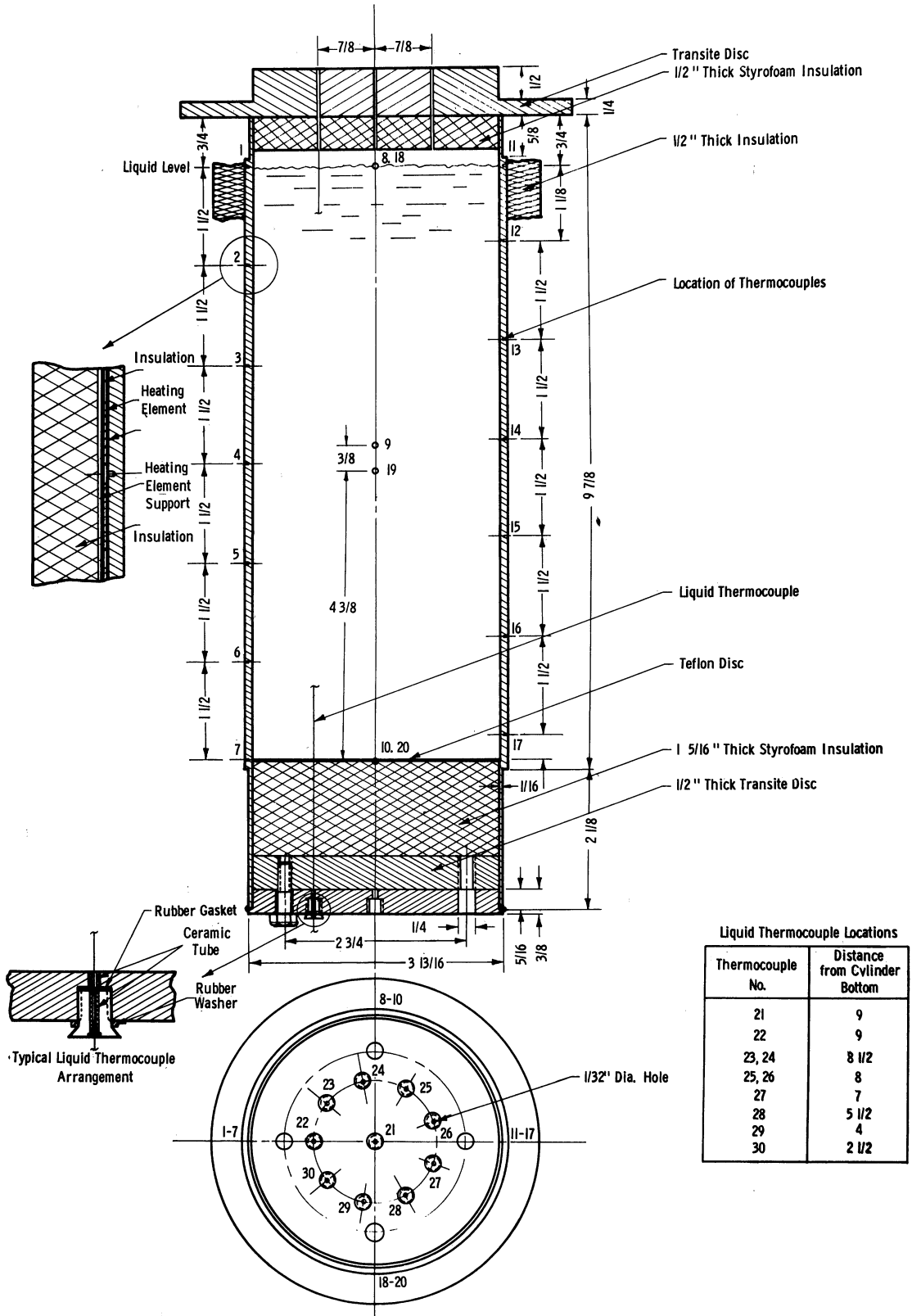


Fig. 9. Test vessel assembly.

ribbon was insulated from the cylinder by a layer of scotch electric tape No. 69, that withstands temperatures as high as 356°F. Two other layers of the same tape were wrapped over the heater ribbon in order to hold it in contact with the cylinder wall.

Twenty copper-constantan thermocouples number 1 through 20 are embedded in the cylinder wall. The locations of the thermocouples are shown in Fig. 9. These locations are chosen to enable the examination of the nature of the wall temperature distribution in the azimuthal direction. Therefore, enough information can be obtained to access the assumption of two-dimensional flow. Also, better evaluation of the axial wall temperature distribution can be made.

The liquid temperature is measured at ten locations using 30 gauge copper-constantan thermocouples. Four of these thermocouples are arranged in order to observe the symmetry with respect to the cylinder axis. Twenty galvanometers are available for use in the visicorder. Ten of the wall thermocouples are connected to the same channels measuring the liquid thermocouples through ten double-throw knife switches. Of course, either the liquid or wall temperature, which are connected to the same channel, can be recorded at a time.

The electric power was obtained by using a set of 12 volt batteries, which are arranged to give the desired voltage. This procedure was followed to eliminate the A.C. interference with the galvanometer signals. The voltage and current were measured using Weston D.C. voltmeter and ammeter models 1 and 901, respectively.

7.3 EXPERIMENTAL PROCEDURE

The containers are filled to the desired level with degassed water. Enough time was allowed before conducting the experiments in order to insure uniform initial temperature. In most of the cases the water was kept in the container overnight before conducting the experiment. This procedure helps to eliminate any initial natural convection currents that may exist in the container before beginning the experiment. During the initial stages of the experimental program, it was suspected, and later substantiated by actual measurements, that evaporation from the liquid surface would cause the free surface to deviate considerably from the adiabatic condition, which is assumed in the analytical solution. For this reason a thin film of oil of thickness $1/2$ mm was put over the surface of the water. It was verified that the oil film is effective in reducing the evaporation from the free surface. This was demonstrated by filling two identical pyrex glass beakers with water to the same height, one of which had a thin film of oil. Both were heated simultaneously until the water in both boiled and then heat was turned off. The beaker without the oil film cooled much faster than that with the oil film. Furthermore, it was found that the fluid temperature at the surface was about 12°F lower than that near the bottom in the beaker without the oil film. Such a temperature drop, which is due to evaporation, was not found in the beaker which had the oil film. The same phenomena were observed in similar tests using the rectangular container. Therefore, the oil

film was used in all the tests. In addition to that, the open ends of the containers were covered by styrofoam caps leaving an airspace about 1/4" thick between the liquid surface and the cover.

In the test using the rectangular tank, the condensate in the steam line, including that in the two banks of tubes in the heating compartments, was drained before conducting the experiments to prevent the condensate from impinging against the walls, causing them to vibrate and upset the zero velocity initial conditions as well as blunting the temperature transient. The zero-time level was taken to be that at which any of the wall thermocouples showed temperature rise for the case of the rectangular container. The instant at which the electric power was switched on, is considered the zero-time level for the cylindrical containers. The photographs given in Figs. 10, 11 and 12 show some of the equipment used.

7.4 PROCEDURE OF DATA REDUCTION

In the case of the rectangular container, it was postulated that due to the high thermal conductivity of the copper, the spanwise variation of the wall temperature will be negligible. It was also anticipated that since the heating arrangement is symmetrical with respect to the container centerline, the departure of the conditions of the experiment from those of a two-dimensional model will be small. Accordingly the readings of thermocouples 13 through 18 was considered to describe the wall temperature-time history. However, it was later found that

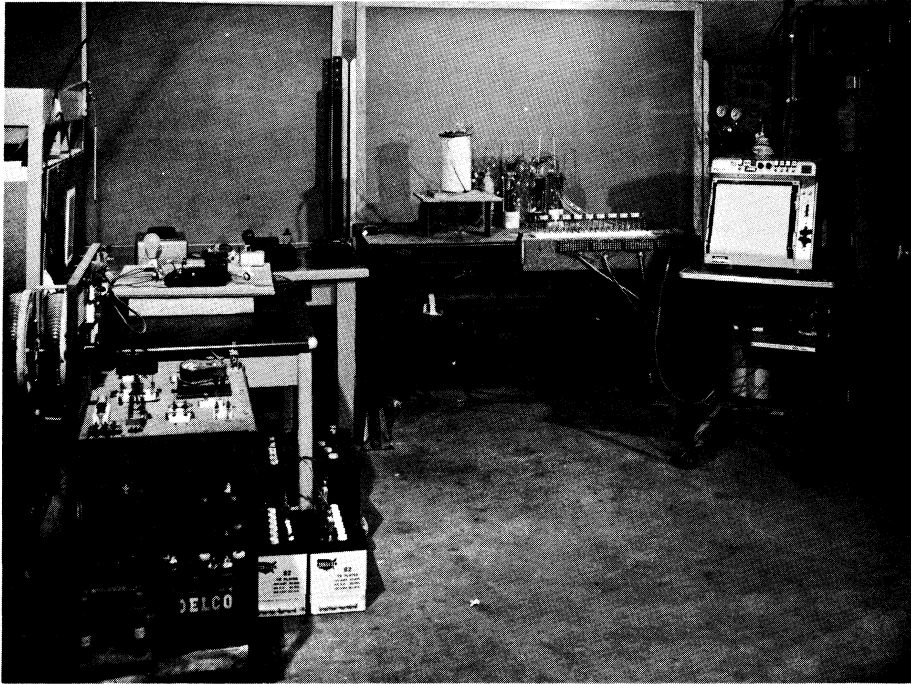


Fig. 10. View of the experimental apparatus.

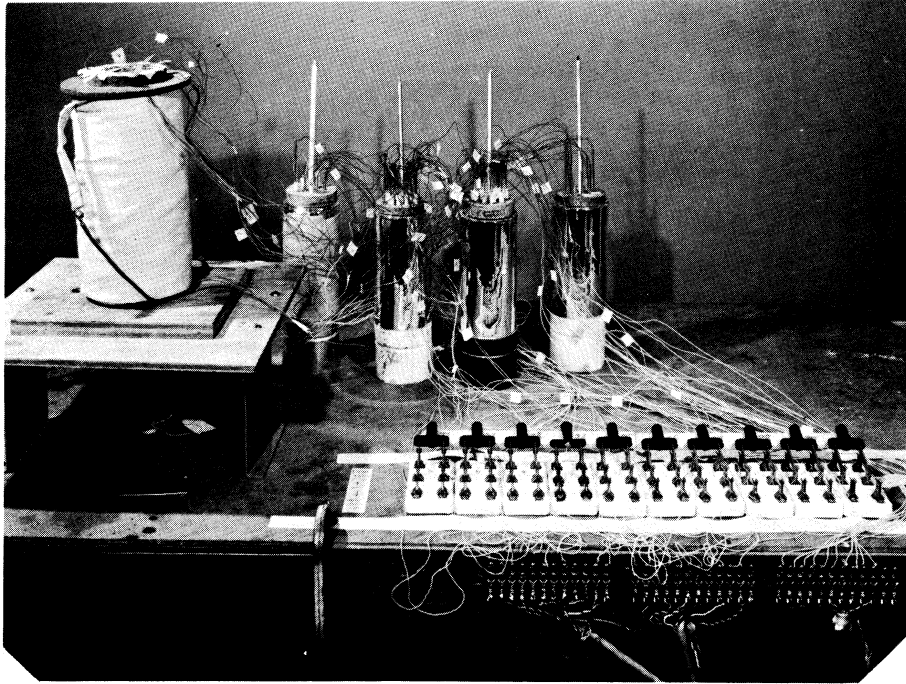


Fig. 11. View of the experimental apparatus.

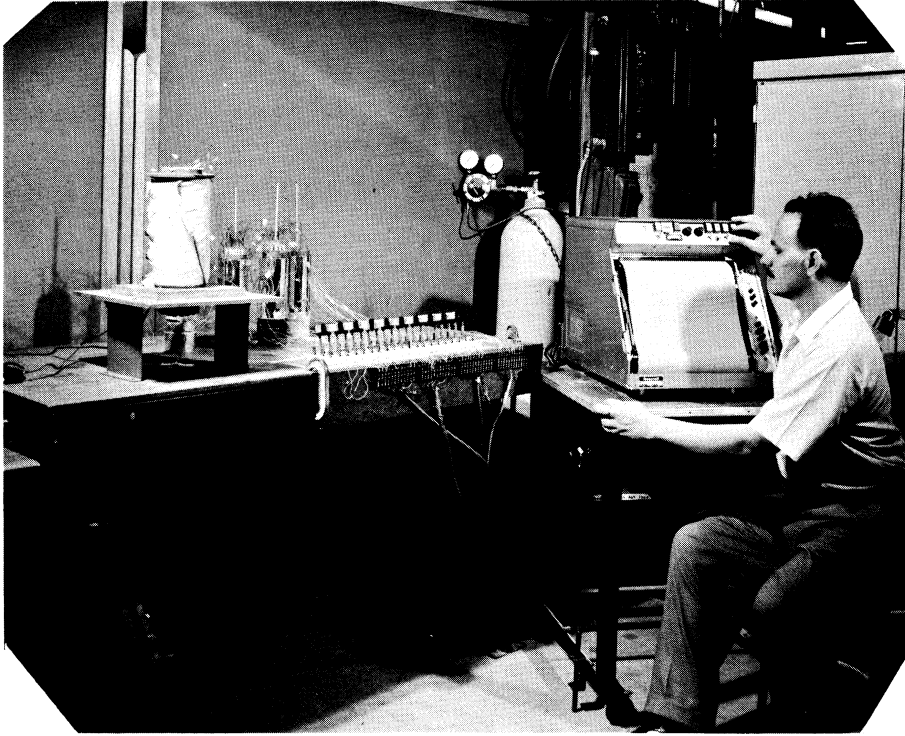


Fig. 12. View of the experimental apparatus.

the two-dimensional and symmetry conditions assumed are not actually met in the experiment. In order to check this point thermocouples number 19, 20, 21 and 22 were added to the wall, as discussed in Section 7.1. The reading of these thermocouples indicated that the conditions of the experiment do not correspond to those assumed in the analytical model. A typical temperature-time history for that of the wall at locations 15, 19, 20, 21 and 22 is shown in Fig. 13. In a two-dimensional model, which is symmetric with respect to the container axis, all of these temperatures should be the same. The deviation of the model from symmetry can be accounted for in the theoretical analysis for two dimensional cases. However, the departure from the two-dimensional case is considerable and therefore the results obtained from the two-dimensional analysis will not sufficiently represent the actual flow in this case. For the latter reason only few experiments were carried on in the rectangular container. The results obtained from the rectangular container served an important purpose. Beside showing the stratification phenomenon and the nature of the temperature-time transients, it also gave guidance to the choice of the wall thermocouple locations in the cylindrical container, so that a better representation of the wall temperature can be made. The location of the wall thermocouples in the cylindrical container are shown in Fig. 9. The temperatures measured at these locations when plotted versus their axial locations would indicate the deviation

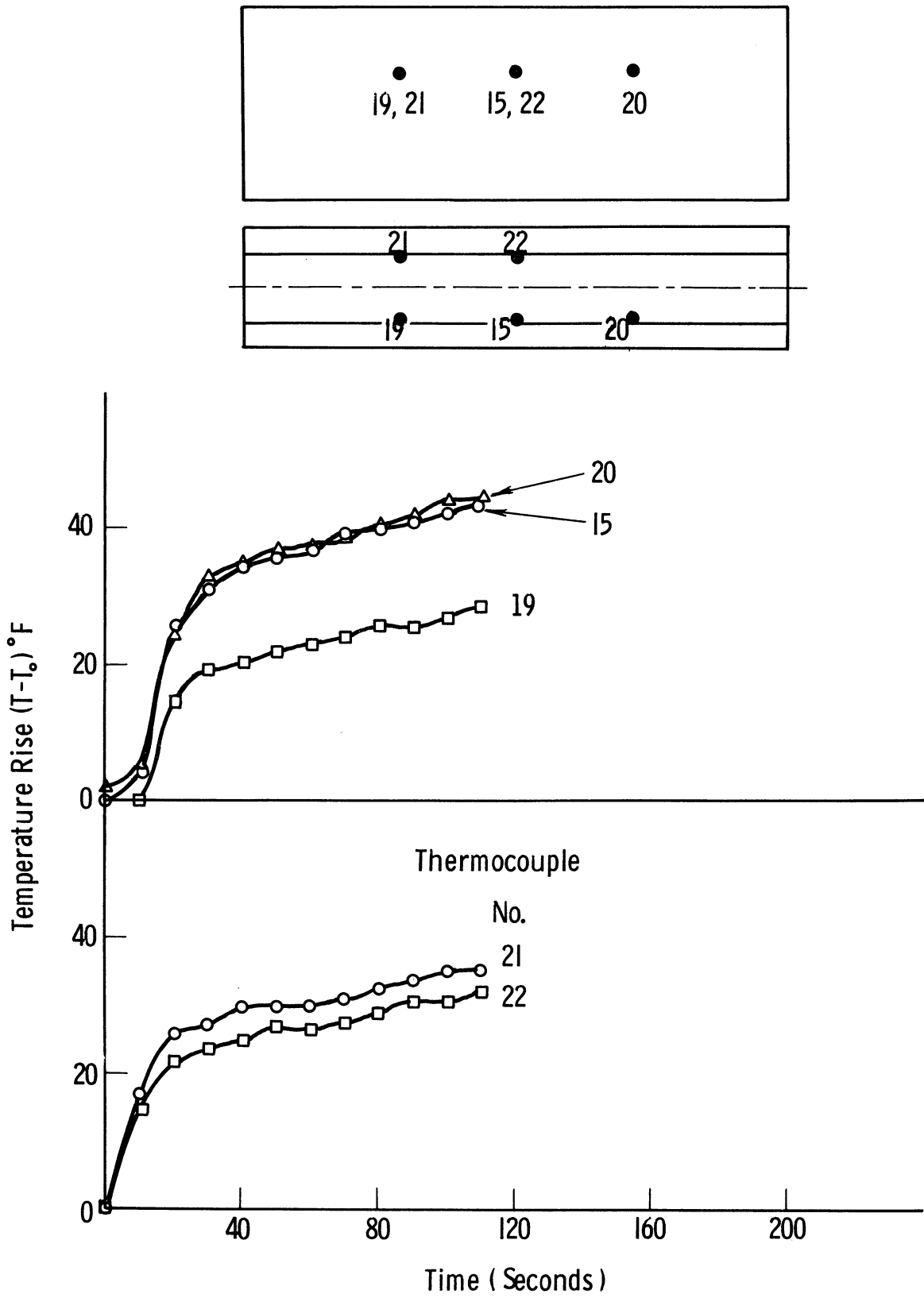


Fig. 13. Typical wall temperature response, rectangular container.

of the experiment from the condition of symmetry with respect to its axis. A total of 16 experiments were carried in the cylindrical container using four-different heat flux levels of 500, 1000, 2000 and 4000 Btu/hr ft². These experiments involved sufficient repeat runs in order to check the following:

1. Reproducibility of the results;
2. The conformity of the experiment with the two-dimensional model assumed in the theoretical calculations.

From these experiments it was found that the results are reproducible. In order to check the second condition, all the wall temperatures (thermocouples 1 through 20) in some of these were measured during most of the experiment. This procedure was repeated for all heat flux levels. The results were then plotted versus axial distance at various time levels. Figures 14, 15 and 16 show such a temperature distribution. The results obtained from the cylindrical container reveal that a true two-dimensional model was not completely achieved. This may be due to the manner in which the heating ribbon was wound around the cylinder, or may be due to separation of the heating ribbon from the cylinder walls because of thermal expansion. However, the deviation from two-dimensionality is not as serious as it is for the rectangular container, except for the highest heat flux level, for which comparison with the analytical solution was disregarded. The solid lines in Figs. 14, 15 and 16 are considered to represent the axial wall temperature distribution, which is used in the computer

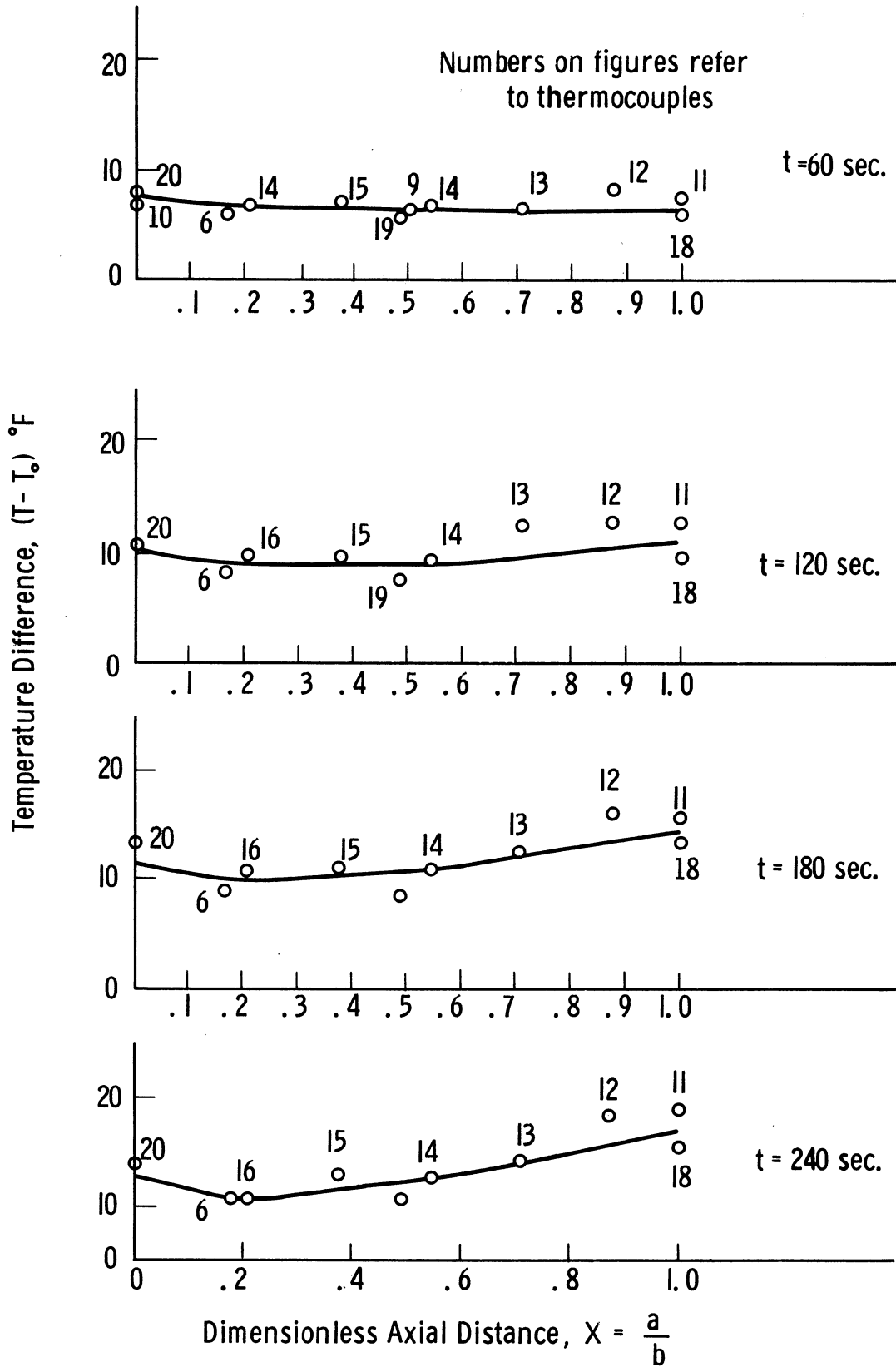


Fig. 14. Wall temperature distribution, run 2, cylindrical container. $(q/A)_w = 500 \text{ Btu/hr ft}^2$.

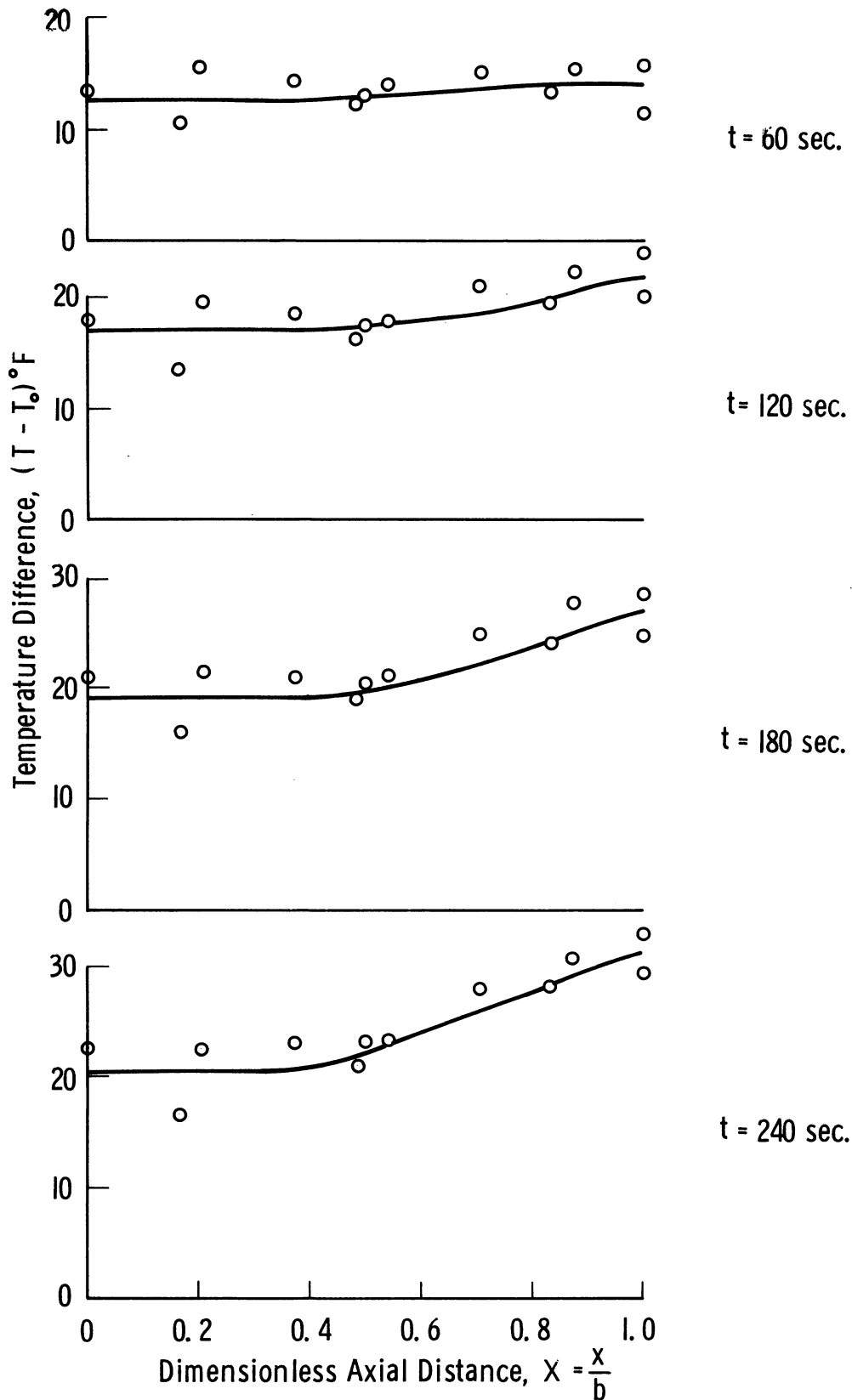


Fig. 15. Wall temperature distribution, run 3, cylindrical container. $(q/A)_w = 1000$ Btu/hr ft².

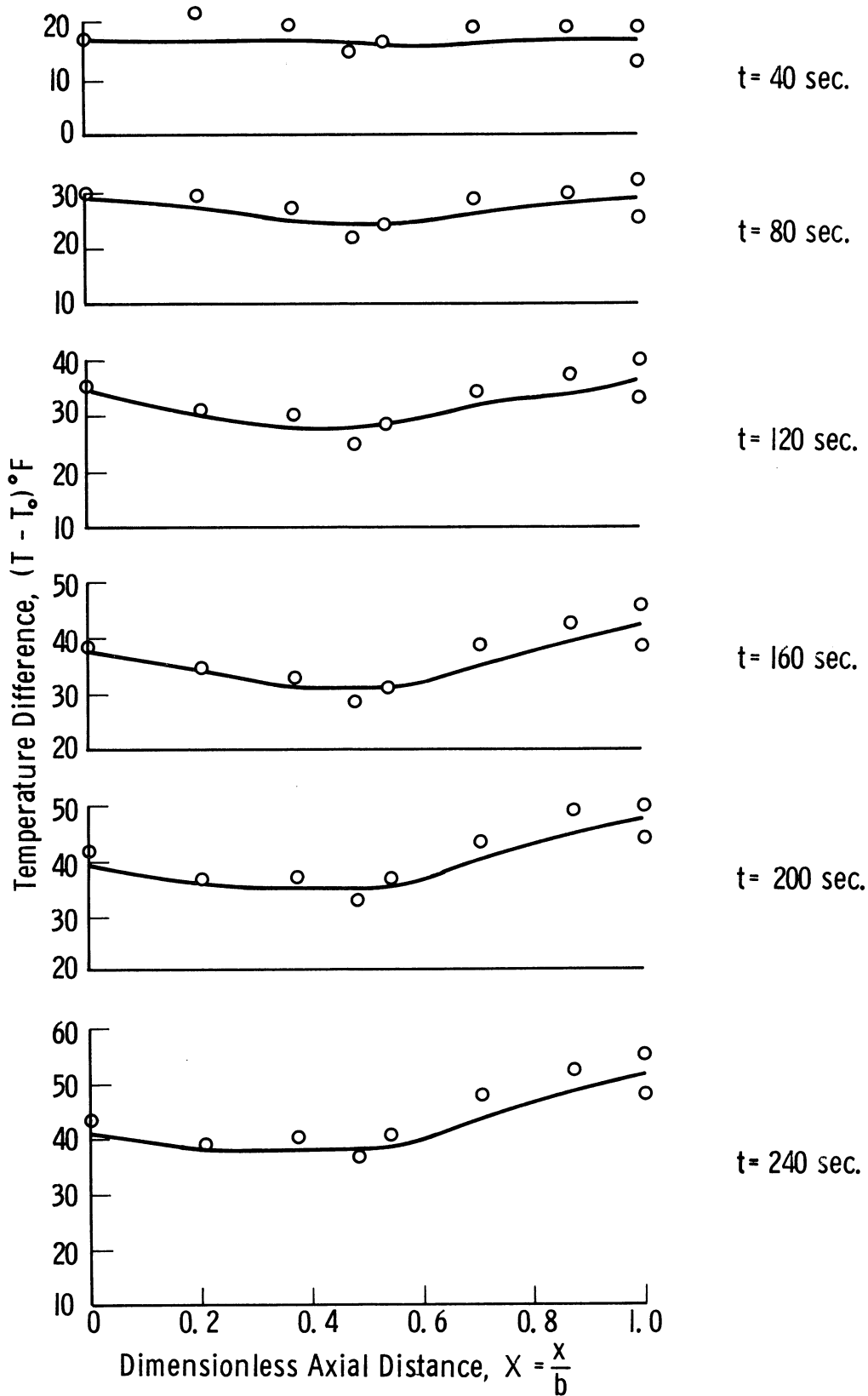


Fig. 16. Wall temperature distribution, run 4, cylindrical container. $(q/A)_w = 2000 \text{ Btu/hr ft}^2$.

program. The maximum deviation occurs near the container ends, as shown in these figures. The magnitude of this deviation is within $\pm 10\%$ for runs number 3 and 4 and is higher for run number 2.

CHAPTER 8

RESULTS

8.1 INTRODUCTION

In this chapter, the results of this study will be discussed.

These results fall into three categories.

(a) Analytical results for which no experimental counterpart is given. These represent the results obtained for the first model, which is described in Chapter 3. Calculations have been carried for the case of a constant wall heat flux and a constant free surface temperature for both the rectangular and the cylindrical containers. The boundary and initial conditions for these cases, as well as the fluid properties used are given in Table I, page 142. The results of the calculations using other boundary conditions have been reported elsewhere⁽¹¹⁾ and will not be repeated here.

(b) Analytical solution for the case of natural convection in a rectangular cavity which has been solved by Poots (51). Although the boundary conditions are different from those outlined earlier in Chapters 3 and 4, the same numerical procedure described in Chapter 5 is used for this case. The validity of the results obtained for other cases can be judged on the basis of the nature of the agreement between the finite-difference results and that of Poots. These results are given in Figs. 17 and 18.

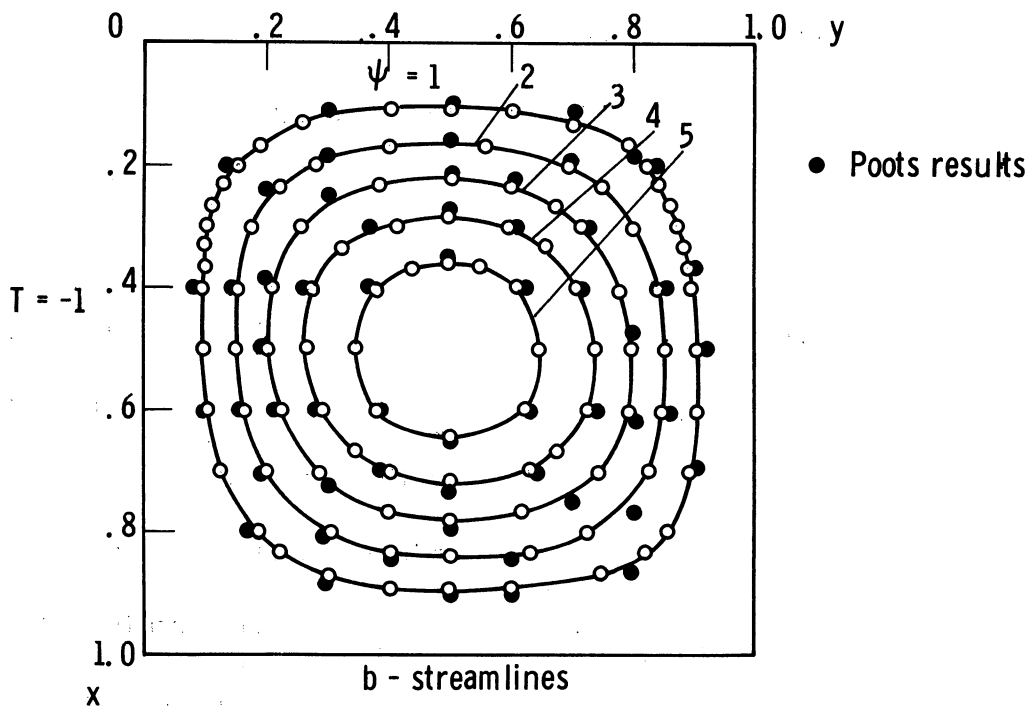
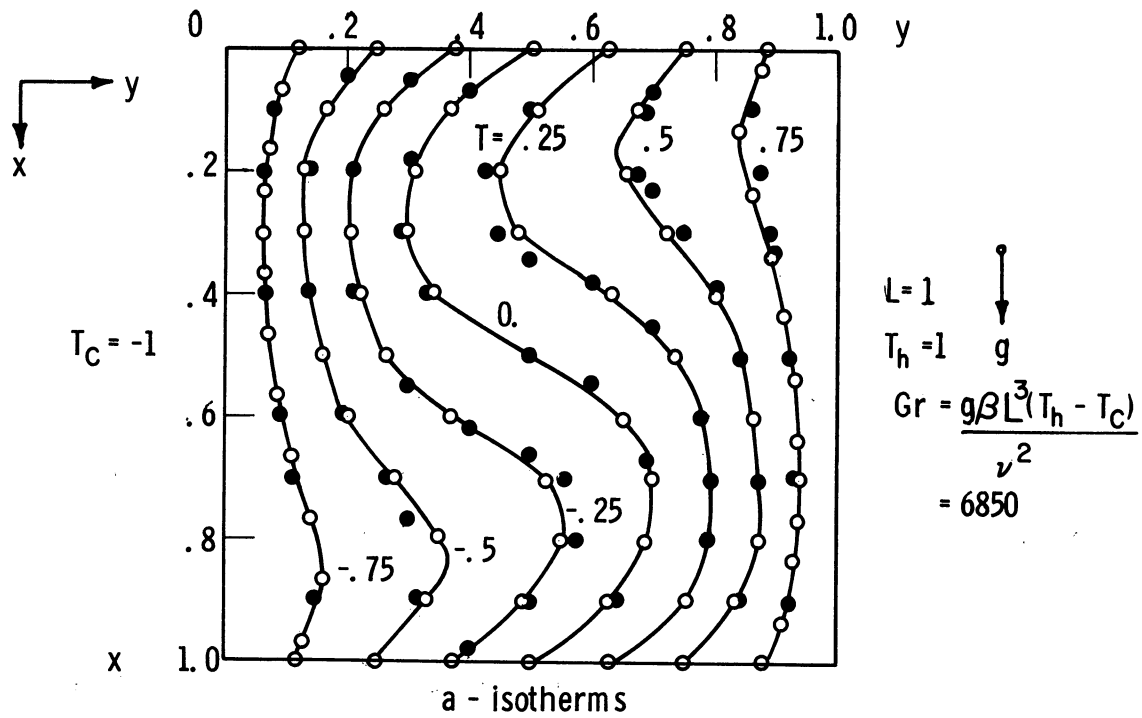
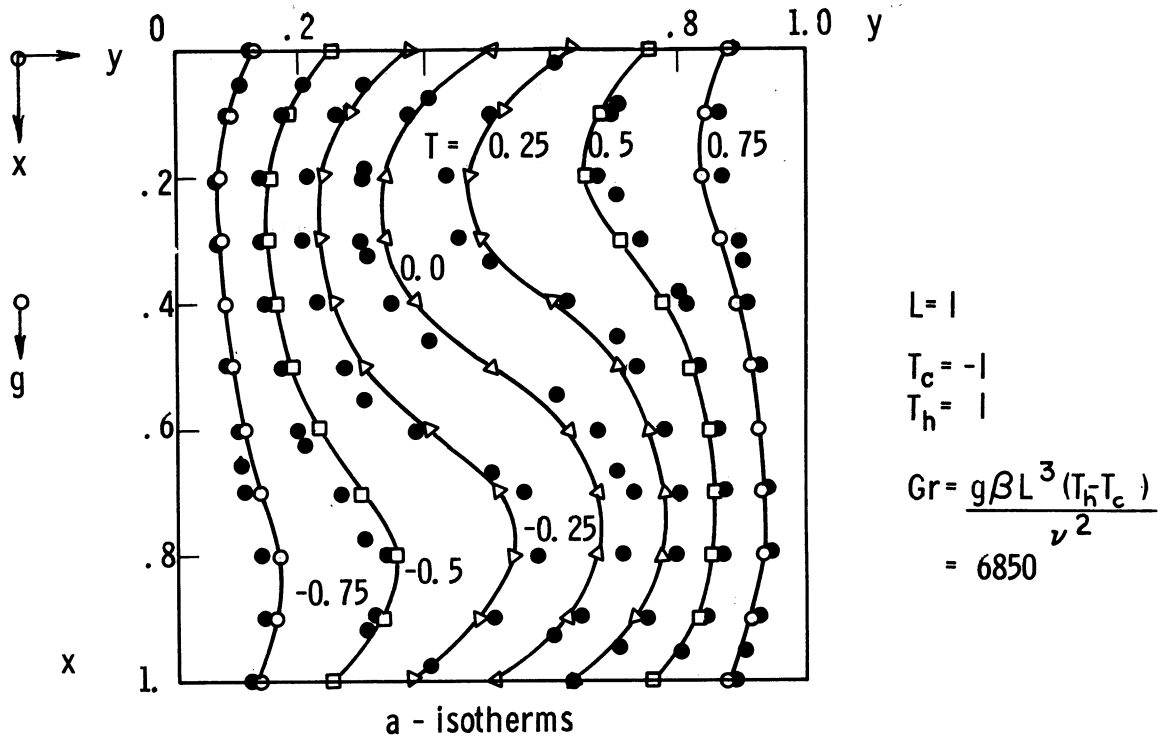


Fig. 17. Results for the rectangular cavity problem using 31×31 grid.



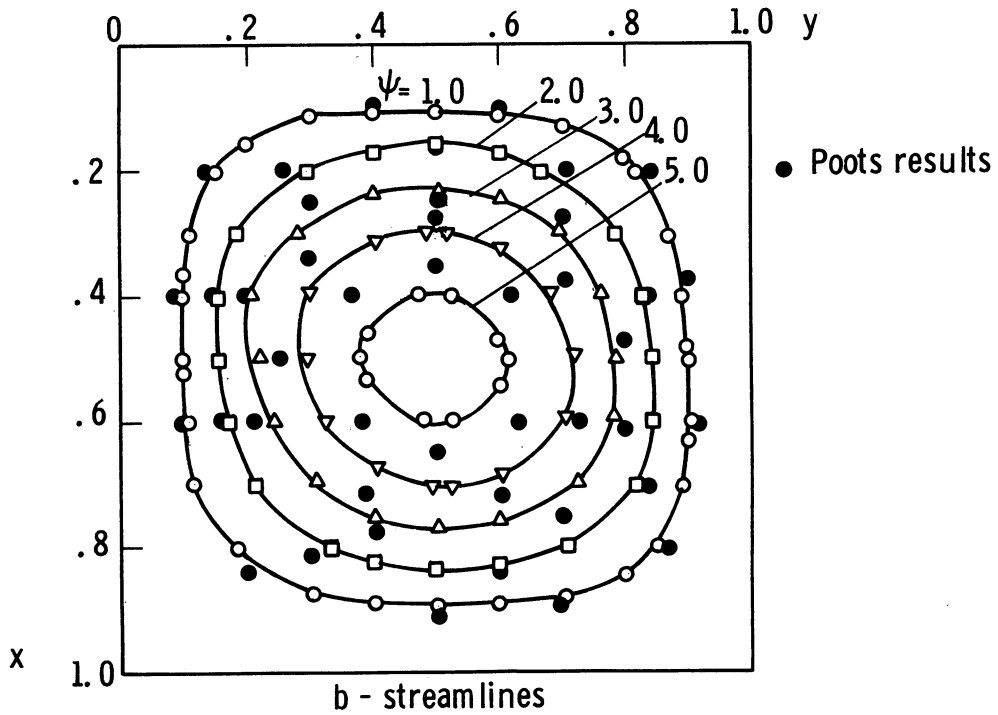
$$L = 1$$

$$T_c = -1$$

$$T_h = 1$$

$$Gr = \frac{g\beta L^3 (T_h - T_c)}{\nu^2}$$

$$= 6850$$



● Poots results

Fig. 18. Results for the rectangular cavity problem using 11x11 grid.

(c) Analytical solutions for the natural convection in rectangular and cylindrical containers for which experimental data are obtained. The theoretical model adopted in these calculations correspond to the second model described in Chapter 3. As was mentioned in Chapter 7, the wall temperatures of both containers at different axial locations were recorded as a continuous function of time. The value of the temperature at these locations at different time levels, which are separated by finite-time intervals, are used in the computer program to describe the wall temperature-time history. These values are punched on IBM cards and read in by the machine as input data. The desired values of the wall temperature at any axial location and at any time level are obtained from those programmed using linear interpolation in both space and time directions. The length of the time interval separating the programmed temperatures depends upon the nature of the wall temperature transients. For low heat flux, the temperature is almost a linear function of time. Therefore the time interval for such cases was taken as high as 60 sec. For higher heat flux, the time increment is taken smaller. This procedure is followed in order to avoid the uncertainties in calculating the wall heat flux level. Furthermore, the measurements of the wall temperature provide a basis, upon which the compliance of the experiment to the conditions of the theoretical model i.e., symmetry and two-dimensionality, can be judged. The validity of the theoretical results can be best evaluated by comparing the measured fluid temperatures with those analytically predicted,

assuming that the above mentioned conditions are fulfilled.

In solving the stream function-vorticity equation using the method of successive-line and column relaxation outlined in Chapter 5, it was found that the direction in which the domain was swept during the calculations influences the number of iterations required. If the row relaxation process was done advancing from the row $i=2$, which is next to the bottom of the container, in a direction of increasing i , to the row $i=M$, which is next to the container surface, and if in the same time the column relaxation process was done in an order of increasing j beginning at $j=2$ which is next to the centerline, the number of iterations required in this case were much higher than if the domain was swept in the opposite direction. In the latter procedure, the row relaxation is conducted beginning at the row $i=M$ in a decreasing order until the row $i=2$ is reached. Similarly, the column relaxation is carried in a direction of decreasing j beginning at the column $j=N$. Accordingly this procedure was followed in all the calculations. The number of iterations required to make the maximum relative change in the magnitude of the stream function across any one iteration to be less than 0.3% was in most cases equal to one. Other iterative methods exhibited the same phenomenon too. This is due to the fact that the rate of change of the vorticity, and consequently the rate of change of the stream function, across any one time step is higher near the side walls and the liquid surface. For this reason the change in the value of the stream function across any one iteration

will be higher if the calculations proceeded from $i=M$ and $j=N$, than if it is carried on beginning near the centerline at $i=2$ and $j=2$, where the rate of change of the vorticity is smaller.

The computations were carried on the IBM 7090 digital computer at the computing center of The University of Michigan. The machine time required to complete the calculation of U, V, θ, w and ψ is 5.7 sec. per time step for the 31×31 grid. The results were printed every 10 sec. Up to 600 time steps were encountered in each run, which means that 57 min. of machine time were used in each run. The velocities U and V were updated each two cycles of calculations of the temperature and vorticity fields in runs 3 and 4. This procedure enabled saving of more than 30% of the machine time for both runs. The time increment used in the calculations was 80% of that required by stability.

8.2 DISCUSSION OF THE RESULTS FOR THE RECTANGULAR CAVITY, POOTS PROBLEM

The steady state streamlines and isothermals obtained for the case of a rectangular cavity which has been solved by Poots is shown in Fig. 17. A 31×31 grid is used in this case. The agreement between the finite-difference solution and that given by Poots is good. These results are also in good agreement with those obtained by Wilkes (74). This agreement indicates the validity of both solutions. In addition to that, the investigation of this case helped to determine the grid size that should be used in subsequent cases, as will be discussed in Section 8.5.

As mentioned earlier, the geometry considered makes the assumption of boundary layer flow invalid. Therefore the concept of boundary layer flow and boundary layer thickness as applied to solutions obtained from the boundary layer equations cannot be used here. However, the concept of "boundary layer" will be used here in reference to the fluid region in the wall vicinity. Also the term "boundary layer thickness" is utilized to identify the distance from the container walls at which the velocity component parallel to the wall is equal to zero. Accordingly, it is clear from Fig. 17 that the boundary layer for the cavity problem is equal to half the width of the cavity.

8.3 THEORETICAL RESULTS FOR THE NATURAL CONVECTION IN PRESSURIZED CONTAINERS, FIRST MODEL

Calculations have been carried out for the case of a container with an insulated bottom whose walls are subjected to a uniform heat flux and the liquid surface is maintained at the equilibrium temperature corresponding to the ullage pressure. A heat flux level of 200 Btu/hr ft² is used in these calculations. The fluid properties chosen are those of liquid nitrogen initially at atmospheric pressure. The initial liquid temperature is 140°R. The liquid surface temperature undergoes a step change to 160°R, which corresponds to pressurization at 50 psia. The fluid properties, which are taken from Reference (77), are evaluated at a temperature equal to the average of the initial and liquid surface temperatures. These are given in Table I

below. The height of the liquid b is 1 ft and the width of the container and the container diameter $2a$ is 1/2 ft.

TABLE I

PROPERTIES OF LIQUID NITROGEN EVALUATED AT 150°R

Thermal diffusivity α , ft ² /sec	8.62x10 ⁻⁷
Thermal conductivity k , Btu/hr-ft-°R	0.0775
Kinematic viscosity ν , ft ² /sec	1.68x10 ⁻⁶
Coefficient of thermal expansion β , °R ⁻¹	1.33x10 ⁻³
Prandtl Number, Pr	1.91

The results for the rectangular container are shown in Figs. 19 and 20, while those for the cylindrical container are given in Figs. 21, 22 and 23 as a series of stream lines and isotherms at different time levels. Examination of the stream line plots shows that the flow pattern is essentially the same for both types of containers. The heated fluid in the boundary layer rises upward owing to buoyancy effects. Upon approaching the liquid surface, the flow changes its direction from upward to downward motion. The downward moving particles near the rising boundary layer reverse direction and join the upward flow, giving rise to a vortex near the wall. This vortex is formed near the liquid surface at small times and moves downward as the stratified layer grows. The fluid away from the edge of the boundary layer flows downward nearly to the bottom of the container, where it joins the fluid in the boundary layer.

Another interesting phenomenon is shown by the streamline plots. After sometime following the introduction of the transients, the stream

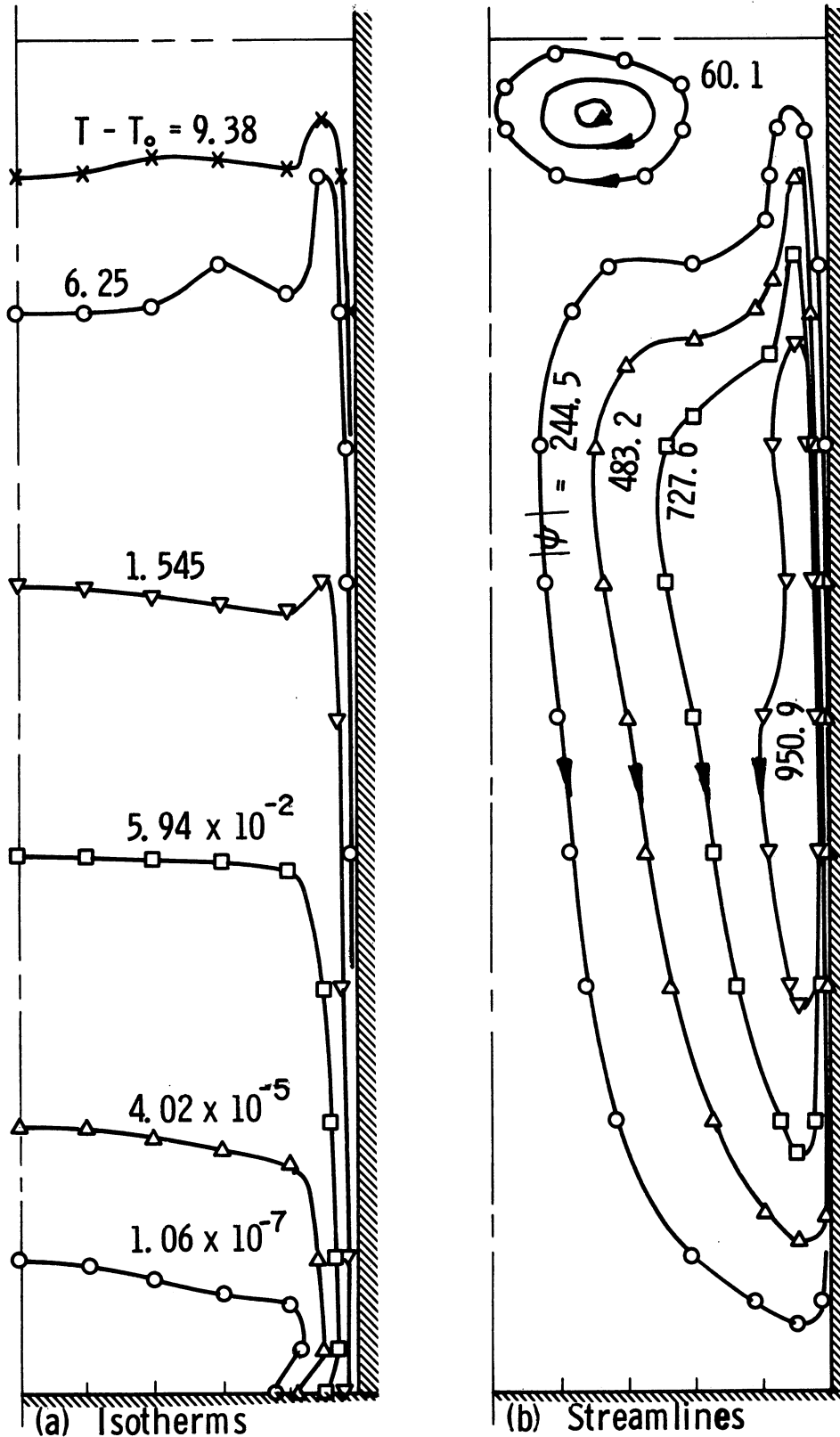


Fig. 19. Isotherms and streamlines, rectangular container. $(q/A)_w = 200 \text{ Btu/hr ft}^2$, $T_{\text{surf}} = T_{\text{sat}}$, time = 30 sec.

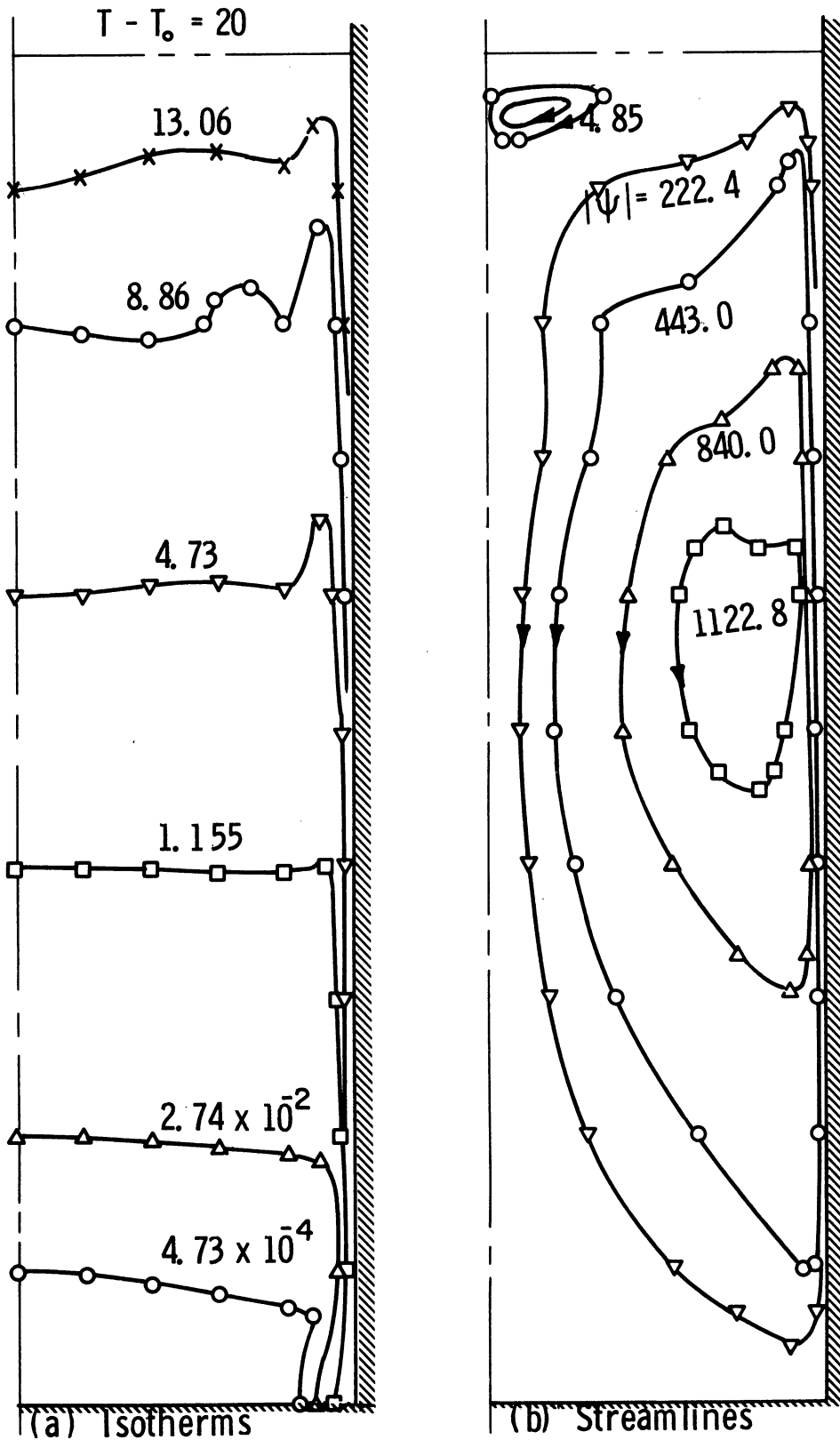


Fig. 20. Isotherms and streamlines, rectangular container. $(q/A)_w = 200 \text{ Btu/hr ft}^2$, $T_{\text{surf}} = T_{\text{sat}}$, time = 40 sec.

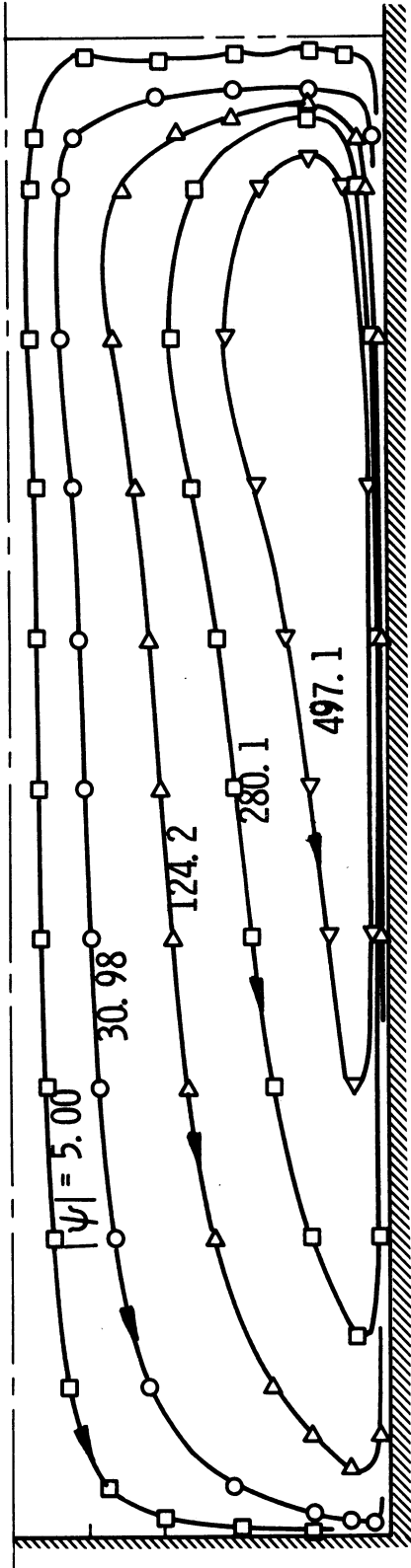


Fig. 21. Streamlines for the case of cylindrical container.
 $(q/A)_w = 200 \text{ Btu/hr ft}^2$, $T_{\text{surf}} = T_{\text{sat}}$, time = 10 sec.

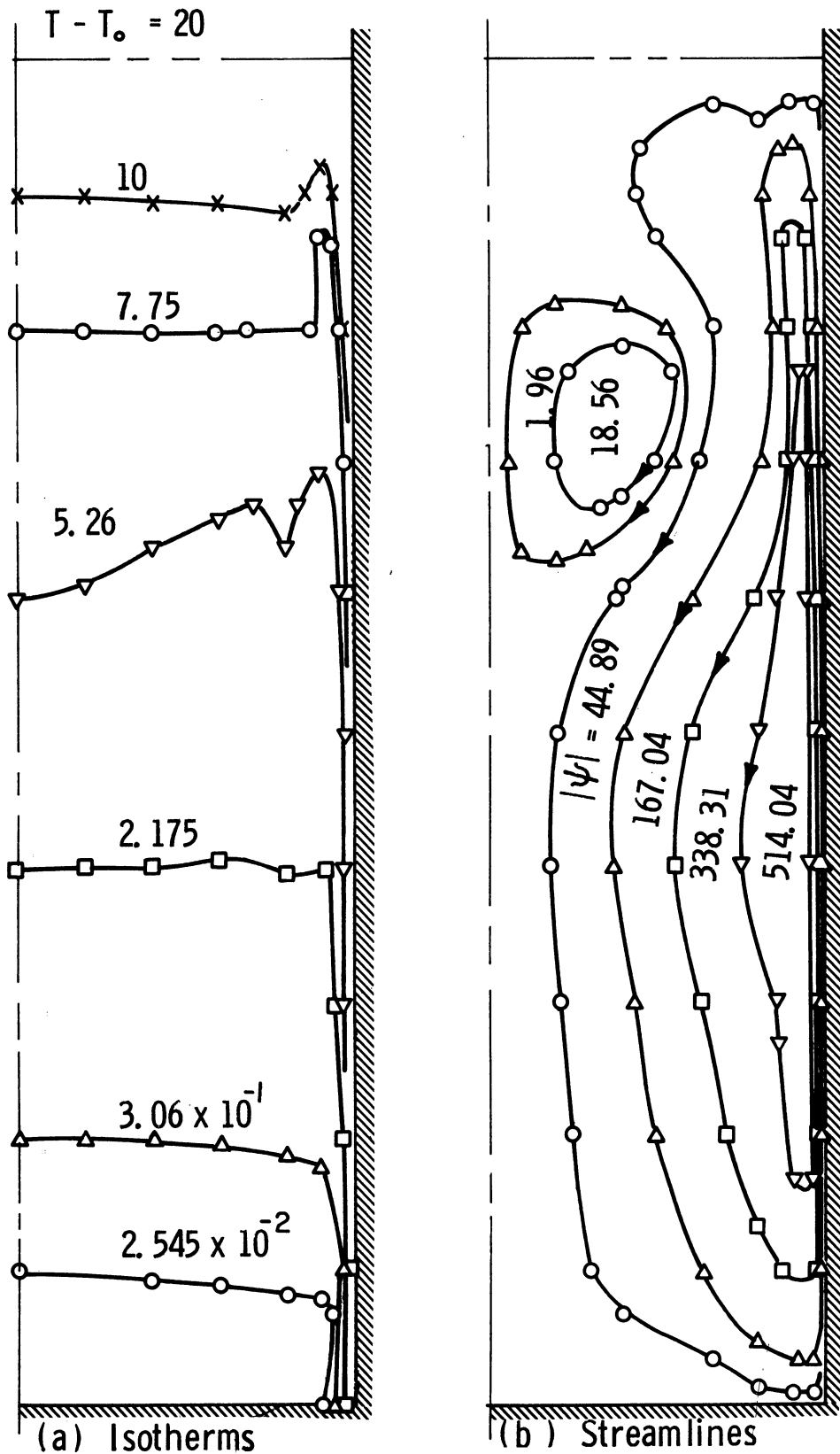


Fig. 22. Isotherms and streamlines for cylindrical container. $(q/A)_w = 200 \text{ Btu/hr ft}^2$, $T_{\text{surf}} = T_{\text{sat}}$, time = 30 sec.

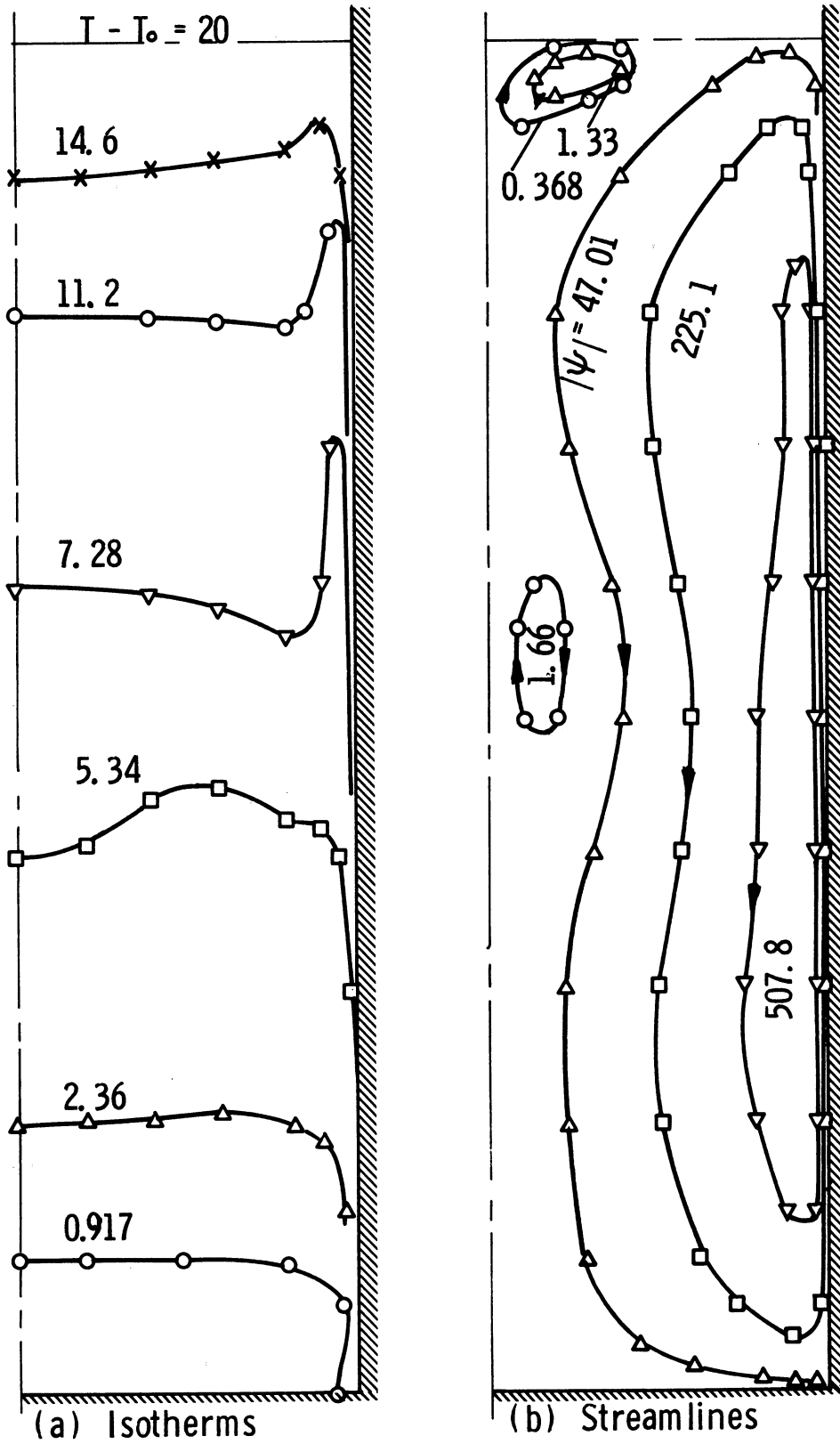


Fig. 23. Isotherms and streamlines for cylindrical container. $(q/A)_w = 200 \text{ Btu/hr ft}^2$, $T_{\text{surf}} = T_{\text{sat}}$, time = 40 sec.

lines show the presence of flow oscillations near the free surface, Fig. 21. At higher values of time these oscillations give rise to a vortex near the centerline. This vortex oscillates in magnitude and in location. First it forms near the liquid surface, grows in size and simultaneously shifts below the surface, after which it breaks away and the same cycle is repeated again. The formation of such vortices was reported by Eichorn (17). He conducted visual studies of the natural convection laminar flow of water using an electrically heated cylinder 2" diameter and 5" long. His results are given in Fig. 24. The magnitude of the heat flux was not given. From the discussion it is concluded that the results represent the unsteady state. Figures 24a and 24b show the flow pattern observed at high heating rate; Fig. 24c shows that obtained at low heating rates. At low heating rates, the streamlines assume a damped-wave shape; at high heating rates annular vortices repeatedly form near the free surface, roll up until a certain size is reached, where upon they move away from the cylinder and another vortex begins to form. His observations agree with the results presented here.

The isotherms show that the axial temperature gradient is negligible in the region below the stratified layer, while it is appreciable in the stratified layer. The temperature changes from that of the fluid bulk at the bottom of the stratified layer to the saturation temperature at the surface. Except in the boundary layer, the radial temperature gradient is generally negligible, as indicated by the isotherms in

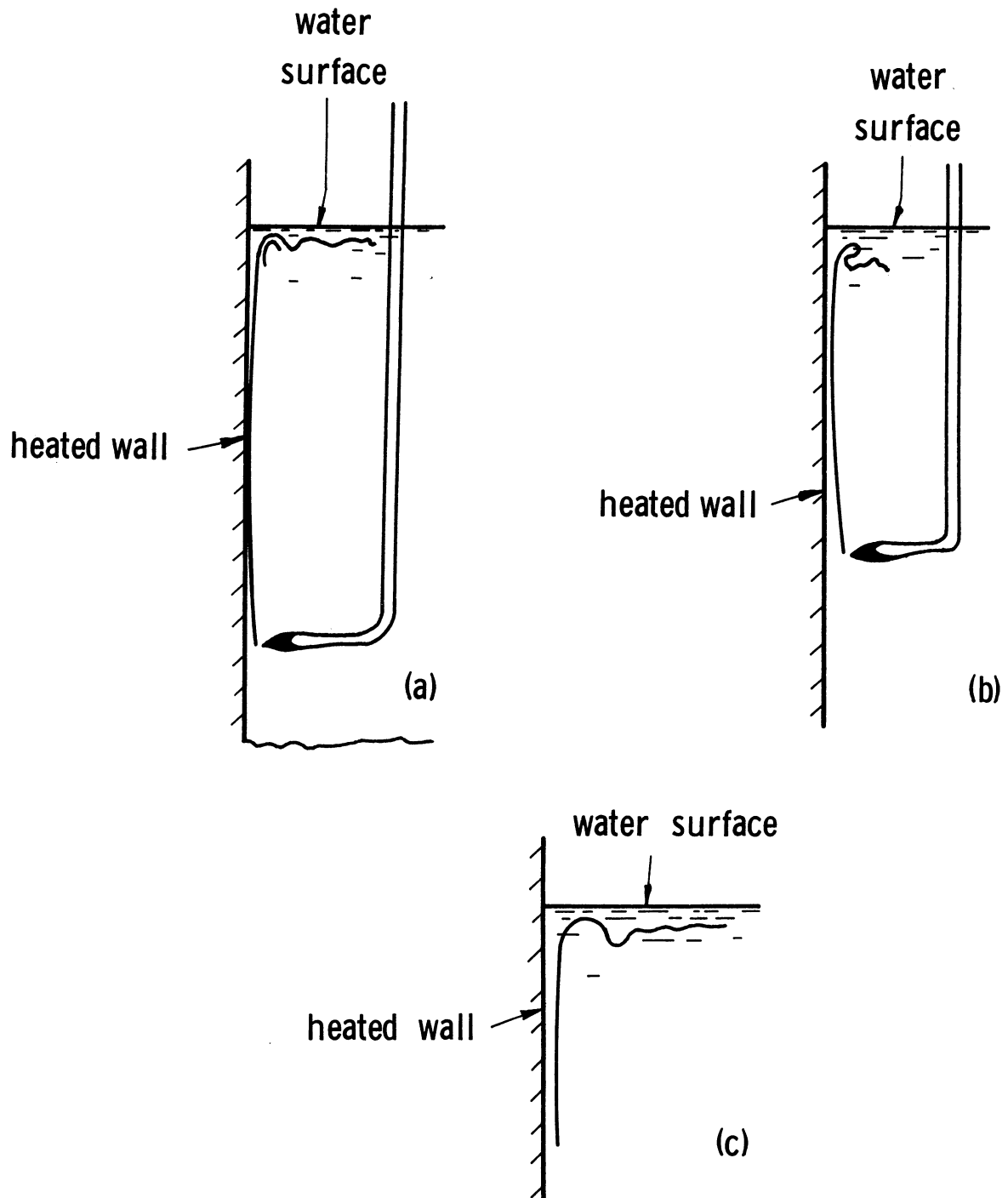


Fig. 24. Results of flow visualizations made by Eichorn.

Figs. 19, 20, 22 and 23. This phenomena can be explained as follows: for small times the fluid near the container walls flows upward in a thin layer. This heated fluid is discharged at and just below the free surface, where its transverse velocity is highest. To satisfy continuity, the heated fluid which is discharged at the free surface causes the colder fluid to move downward thus producing a series of isotherms. With time these isotherms penetrate further below the free surface. The transverse temperature gradient is higher near the wall and negligible in the remainder of the container. In the stratified region, the transverse temperature gradient in the boundary layer is smaller than near the bottom of the container.

Calculations also were carried to investigate the effect of the gravity level on the liquid surface temperature. These were done for the same cylindrical geometry using the same heat flux. Two different gravity levels were used in these calculations. These correspond to a normal and a reduced axial gravity levels of magnitudes 32.2 and 0.0322 ft/sec^2 respectively. The calculated wall temperature at $X=1$ and that of the liquid surface at the centerline are shown in Fig. 25. The wall and the liquid transients near the surface are higher for higher gravity levels. On the otherhand the wall temperature at the bottom is lower for higher gravities. The high rate of the flow, which means that more cold fluid is pumped into the boundary layer, increases the rate of heat removal from the wall near the bottom to the upper

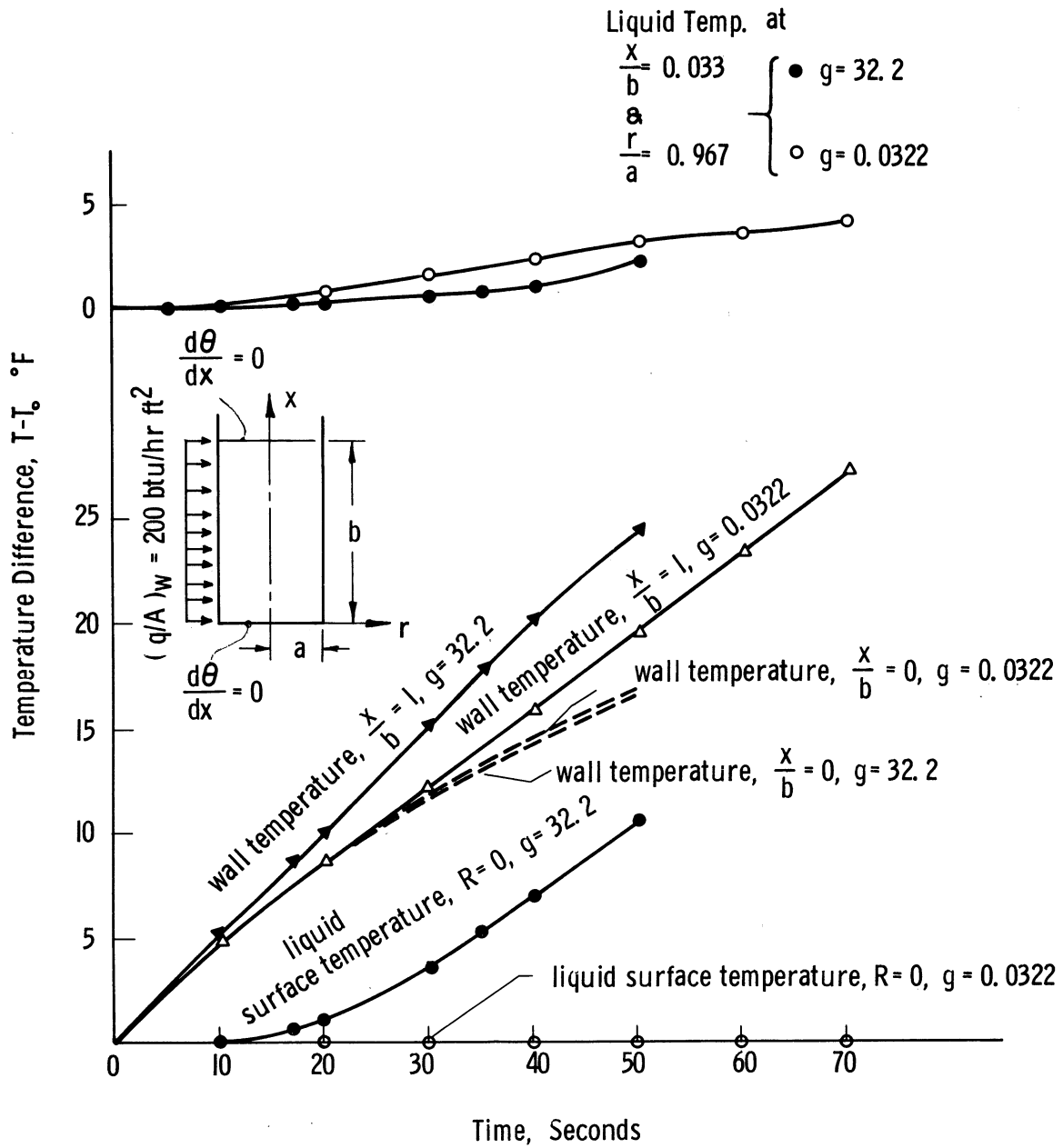


Fig. 25. Effect of gravity level on liquid and wall temperature, cylindrical container. $(q/A)_w = 200 \text{ Btu/hr ft}^2$, adiabatic upper and lower surfaces.

regions of the container. Accordingly more energy will be transferred from the wall at the lower regions to the upper regions of the container per unit time. As a result the fluid temperature near the bottom in the boundary layer will be lower for the high gravity as shown in Fig. 25. Therefore, at reduced gravity conditions the liquid will exhibit a lesser degree of stratification. A limiting case of course, will be that at zero gravity, which, for adiabatic upper and lower surfaces, will give zero axial temperature gradient i.e., no axial stratification, although radial variations in temperature will exist. These results are in contrast with the conclusions made in Reference (79), which were based on the results obtained by an integral method.

8.4 EXPERIMENTAL AND ANALYTICAL RESULTS, SECOND MODEL

8.4.1 Results of the Rectangular Container

The measured and calculated temperature-time history for a typical run obtained in the rectangular container is shown in Figs. 26 and 27. The results given in Fig. 26, which show the formation of a stratified layer at the liquid surface, indicate that in general, the heated fluid near the wall rises to the liquid surface even with nonuniform, nonsymmetric heating. Symmetry of the model can be examined by comparing the measurements from thermocouple number 15 with 22, and 19 with 21 given in Fig. 13. It can be seen here that symmetry is not achieved. Also the readings of 15, 19 and 20 indicate that three-

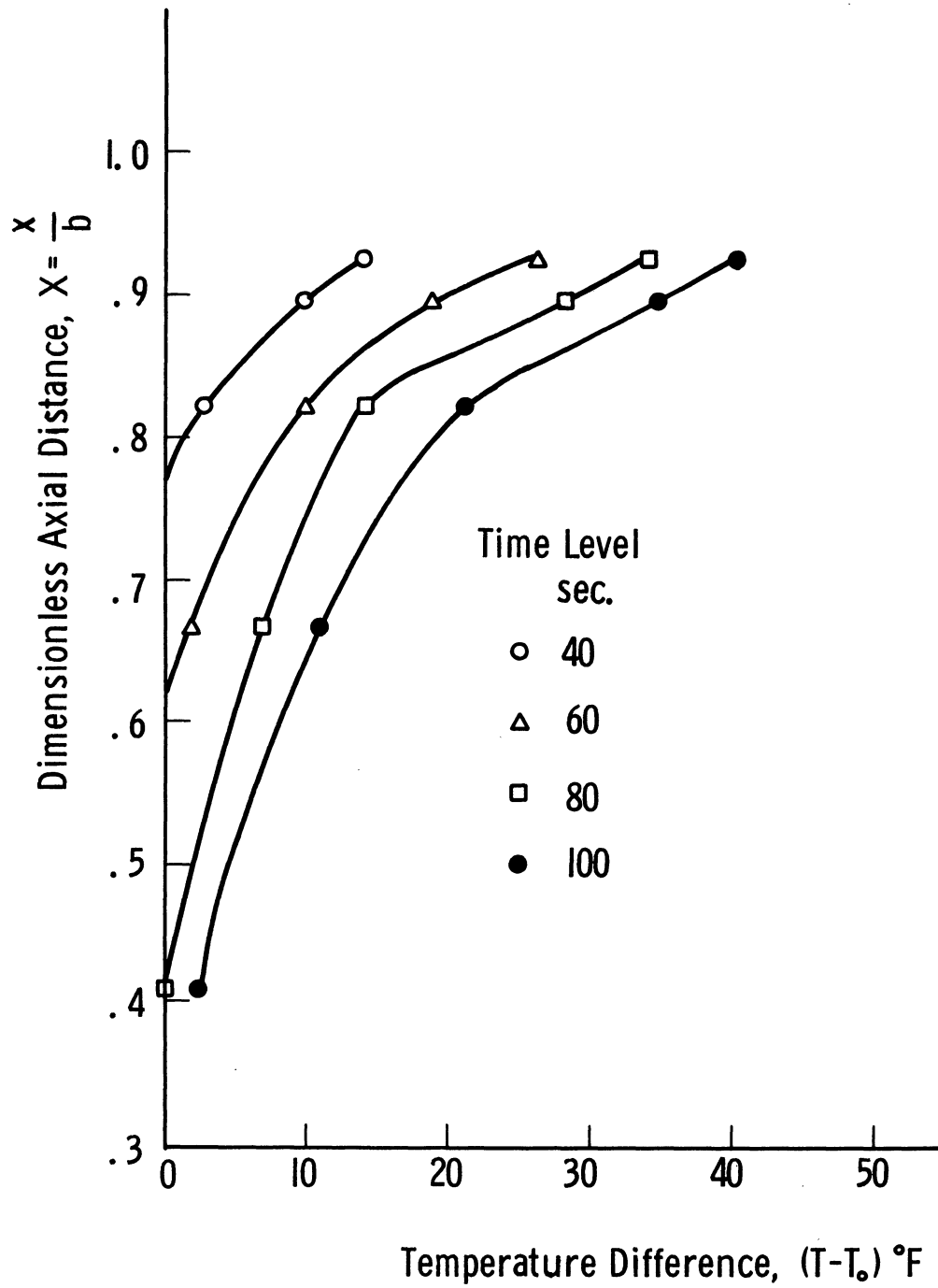


Fig. 26. Measured axial temperature distribution in the rectangular container, run 1.

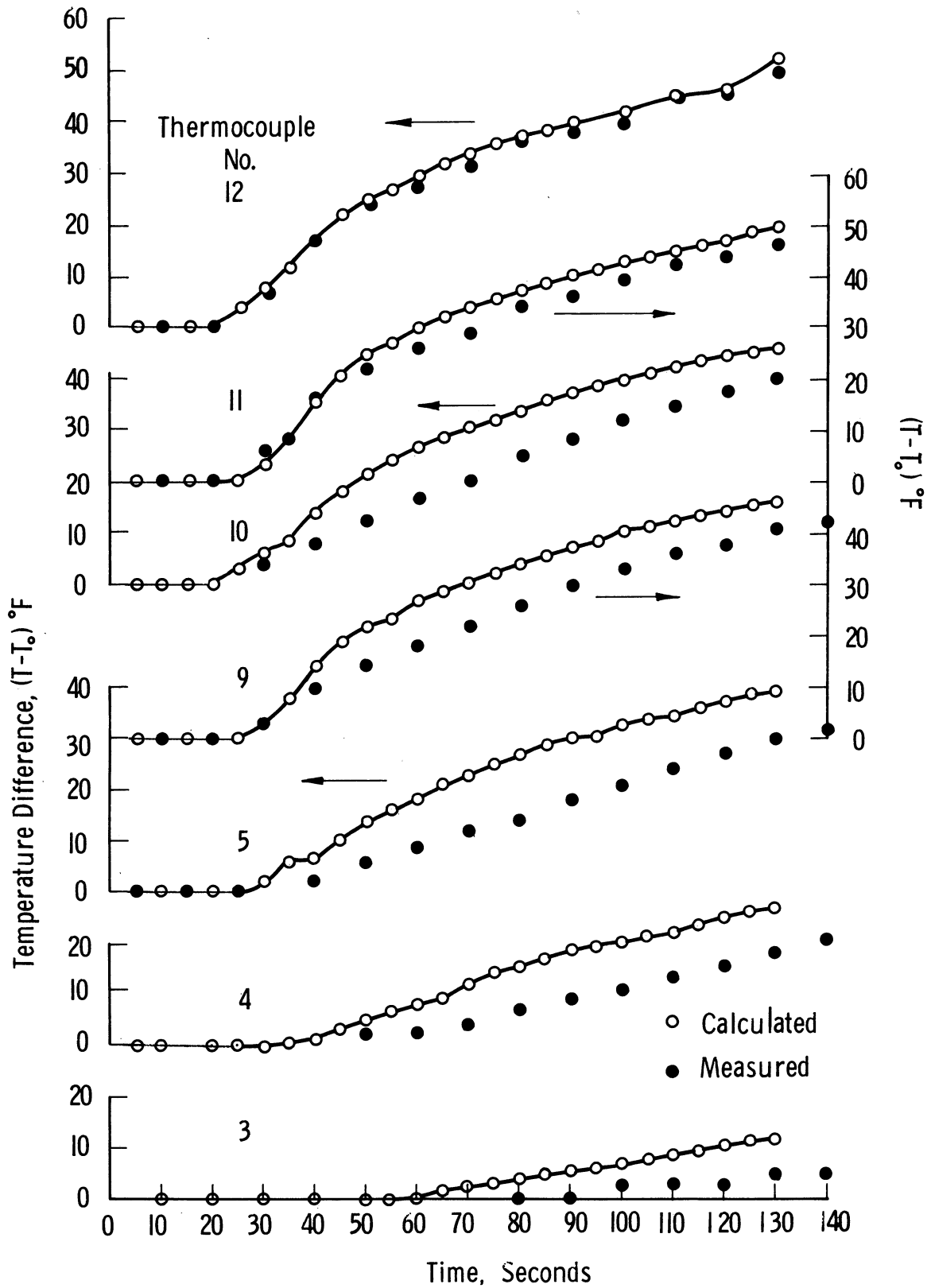


Fig. 27. Calculated and measured liquid temperature response in the rectangular container, run 1.

dimensional effects cannot be disregarded for the rectangular container. The wall temperature, which is used in the computer program, is measured at the middle of the container span. These are given in Fig. 28. As shown in Fig. 13, the temperature at this location as represented by number 15 is the highest wall temperature. The difference between the theoretical and the experimental results in the rectangular geometry is attributed to these factors. The calculated temperature are higher than the measured temperature, as it would be expected. Good agreement between the calculated and the measured temperature is obtained near the free surface, thermocouples 11 and 12, because the fluid near the wall, which rises along it and is discharged on the surface, is affected mostly by the wall temperature. Furthermore the calculated and the measured time at which temperature begins to change are in good agreement.

A series of isotherms and streamlines, which are calculated for this case is given in Figs. 29 through 34 for different time levels. These results, of course, correspond to a two-dimensional case, whose wall temperature is given by thermocouples 13 to 18. These results show that the heated fluid in the vicinity of the wall rises along the container walls. Upon approaching the liquid surface the rising fluid smoothly changes its direction from upward to downward flow. The downward moving particles near the rising boundary layer reverses direction and join the upward flow, thus causing the vortex near the wall. Examination of the flow pattern shows that this vortex is formed

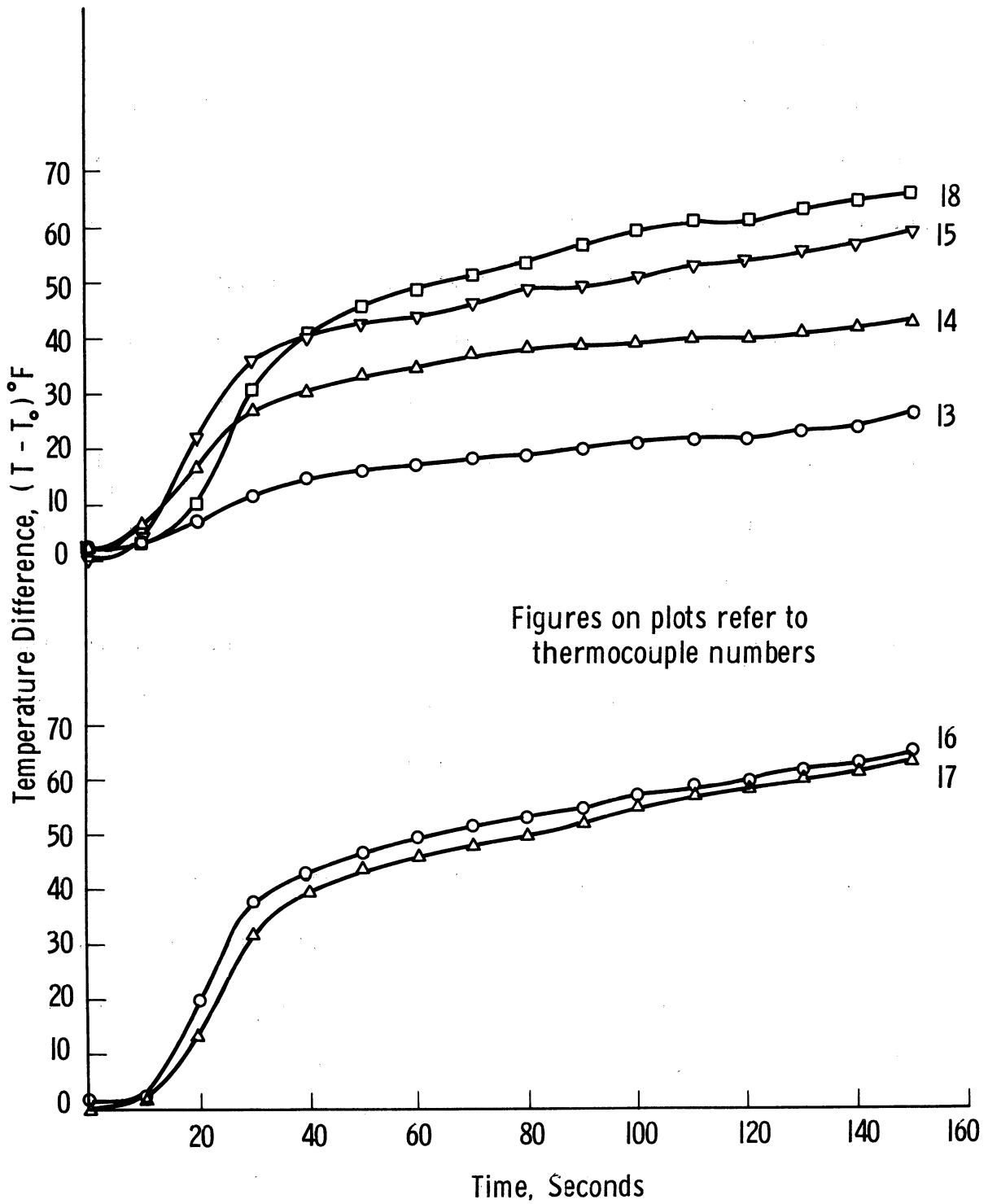


Fig. 28. Measured wall temperature in the rectangular container.

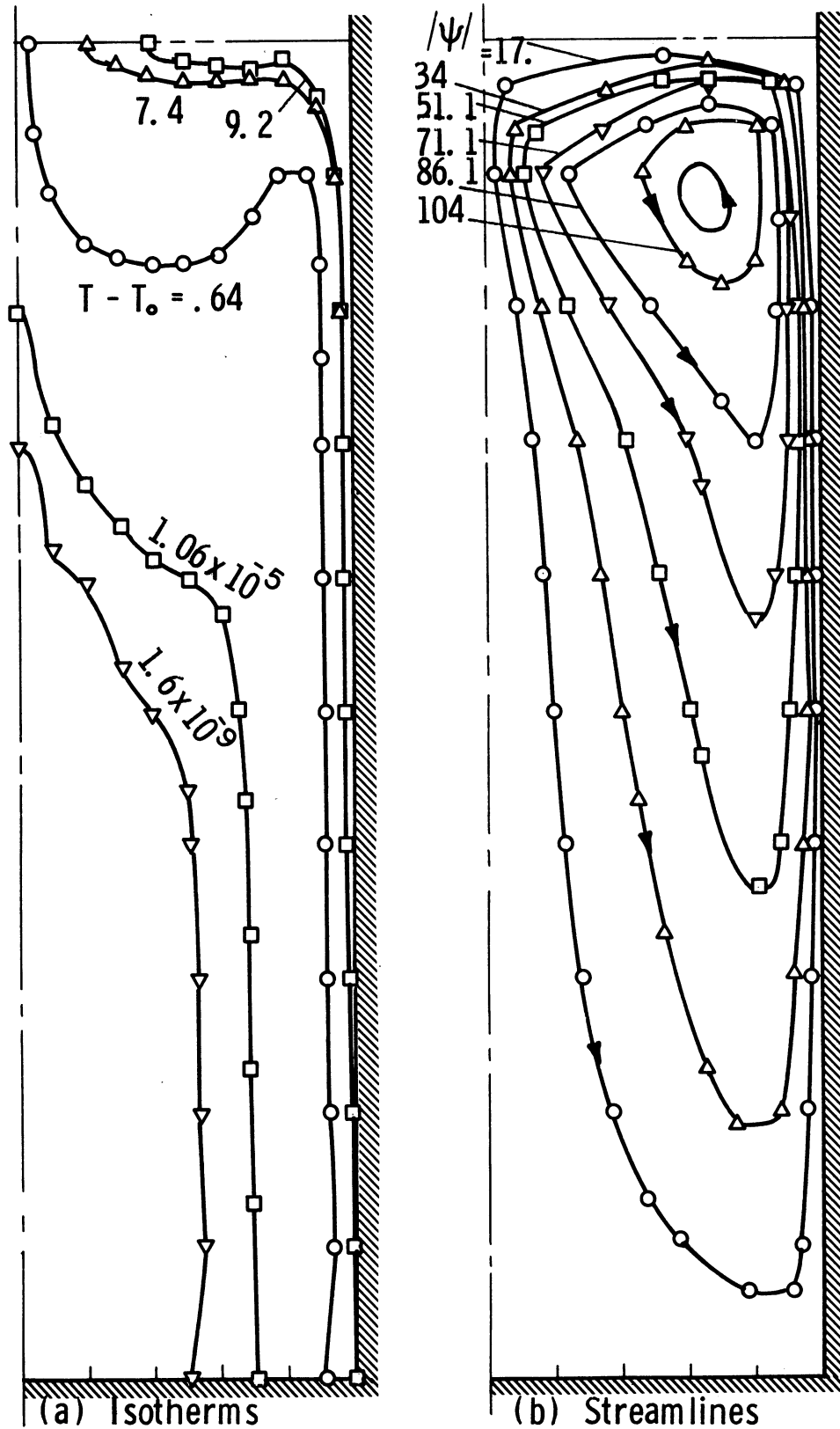


Fig. 29. Isotherms and streamlines in the rectangular container, run 1. Time = 25 sec.

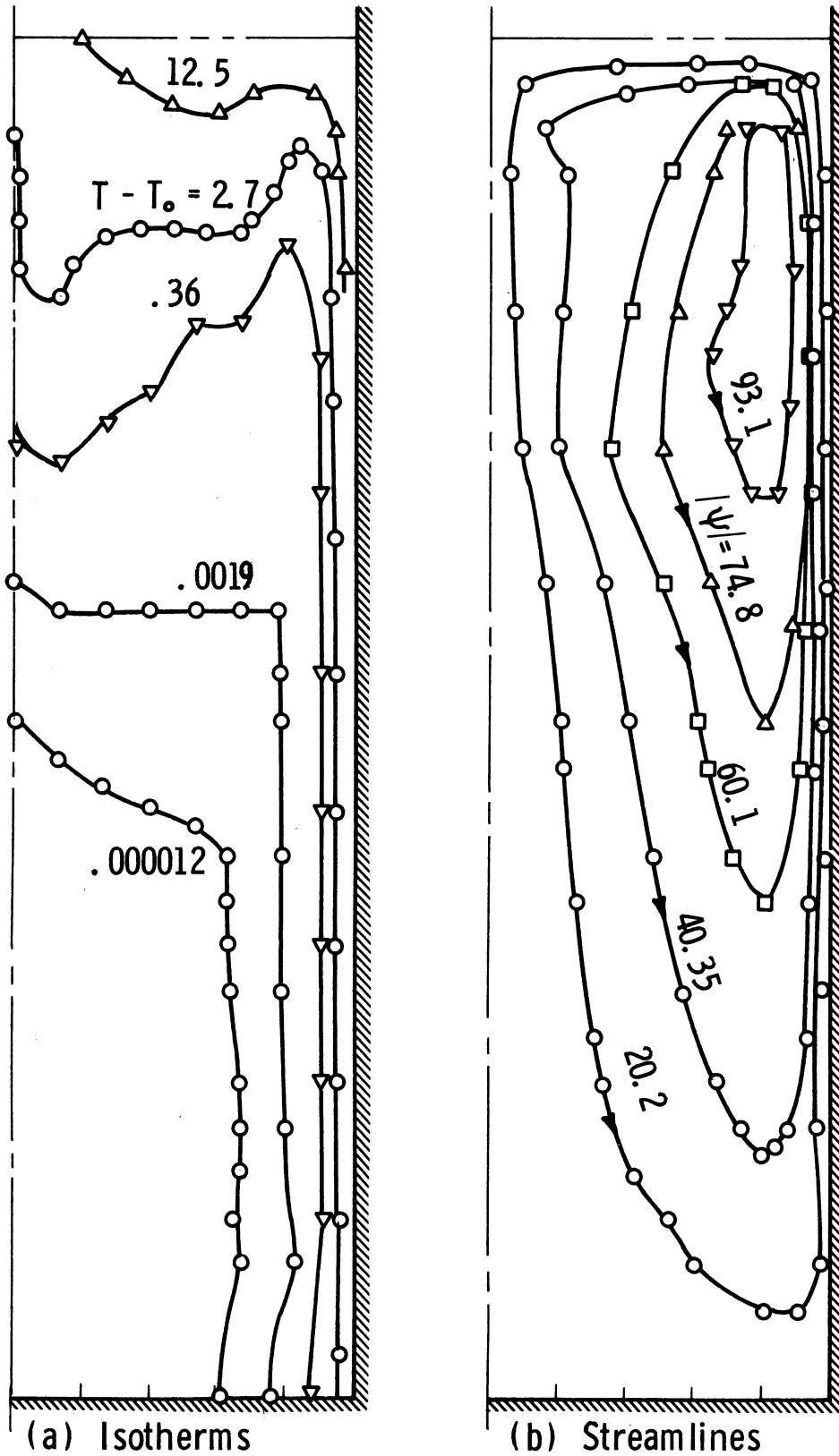


Fig. 30. Isotherms and streamlines in the rectangular container, run 1. Time = 40 sec.

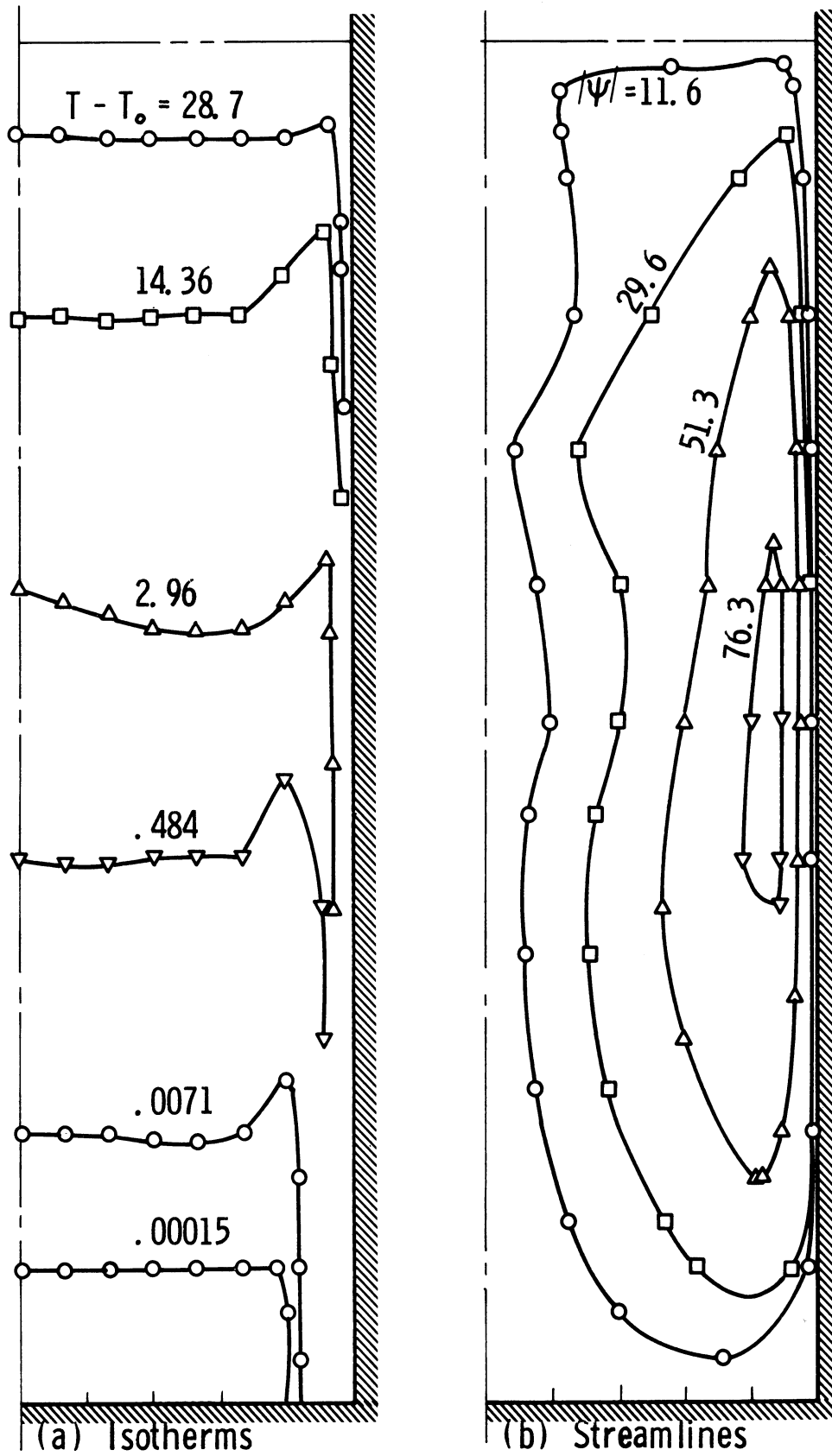


Fig. 31. Isotherms and streamlines in the rectangular container, run 1. Time = 55 sec.

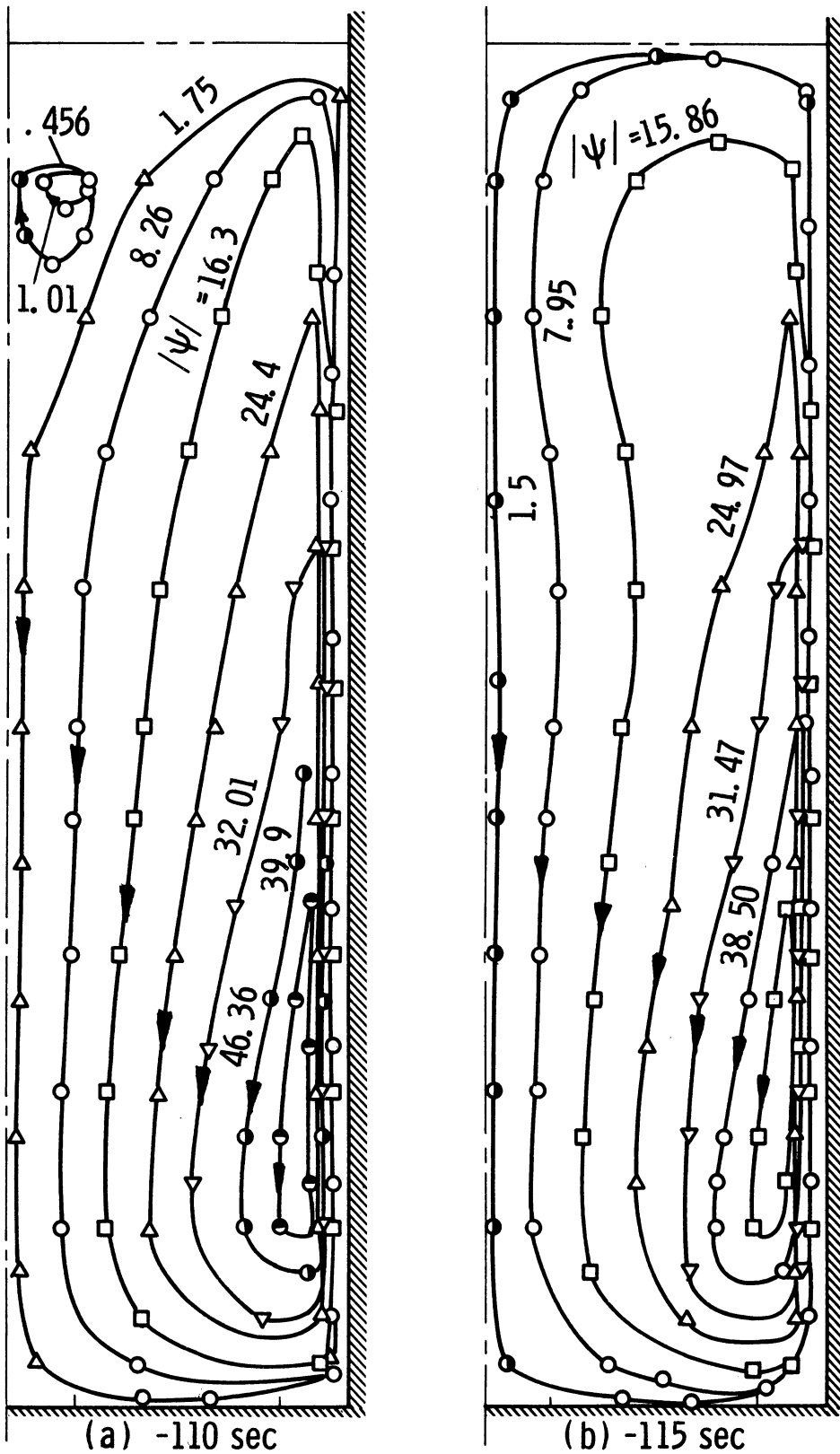


Fig. 32. Isotherms in the rectangular container, run 1. Time = 110 sec.

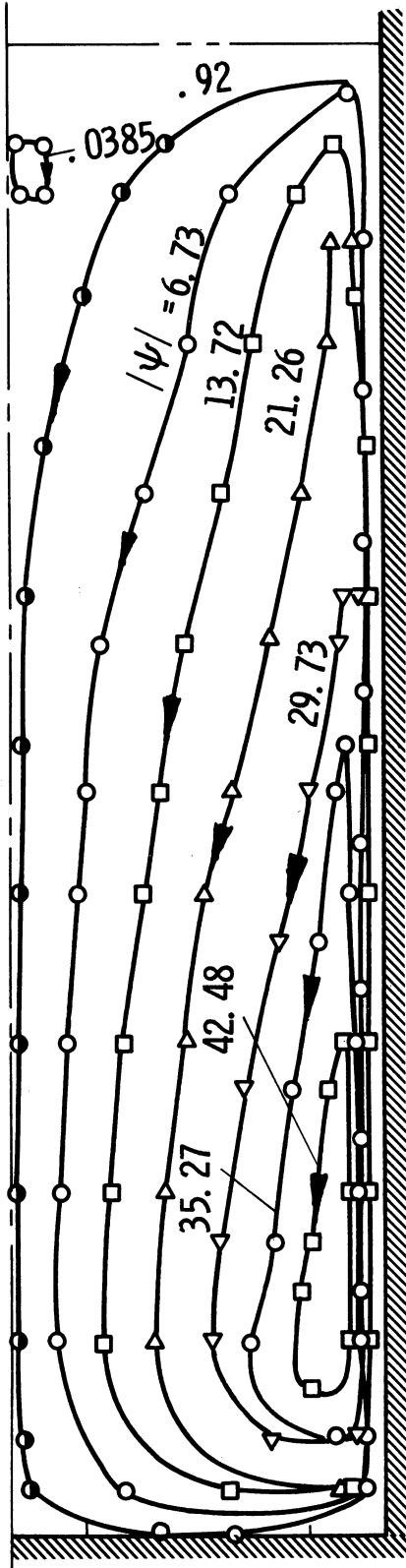


Fig. 33. Streamlines in the rectangular container, run 1. Time = 120 sec.

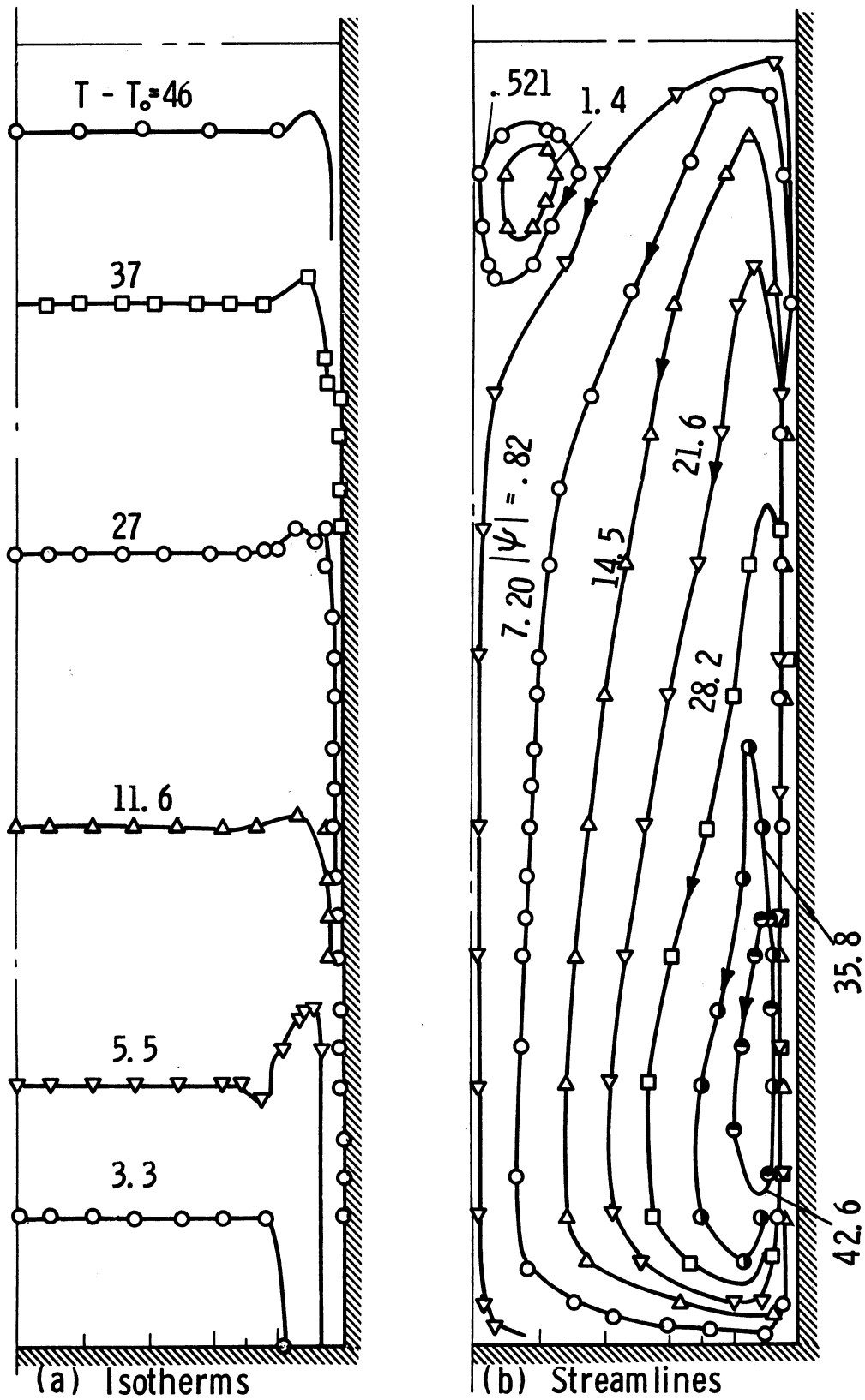


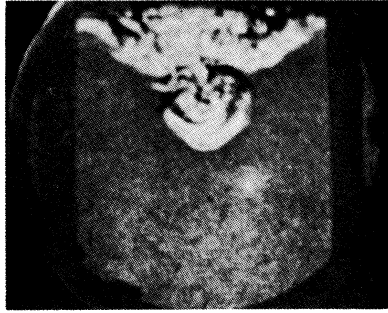
Fig. 34. Isotherms and streamlines in the rectangular container, run 1. Time = 126 sec.

near the liquid surface at small time levels, moves downward with time until it reaches the container bottom. This process is shown in Figs. 29 through 34. It is also clear from these figures that at small time levels the hot fluid, which is flowing upward, is dispersed into a thin layer near the fluid surface. As a result a stratified liquid layer is formed at the free surface. Some of this fluid moves along the fluid surface towards the centerline. The two fluid streams flowing towards the centerline from the right and the left hand sides meet at the centerline and is deflected downward there. As a result, the front of the stratified layer advances to larger depths in the centerline vicinity than near the wall, as indicated by the shape of the isotherms in Figs. 29 and 30. At higher values of time, the stratified layer front moves down at a uniform rate as shown by the shape of the streamlines of Figs. 31 and 34. Schlieren photographs shown in Fig. 35 taken by Vliet and Brogan (73) for the natural convection in a rectangular container whose dimensions are comparable to those used in this analysis indicate that the front of the stratified layer moves in the manner described above.

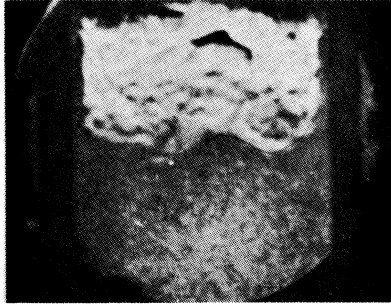
Another vortex is formed at the centerline near the free surface, which rolls until it grows to a certain size, then vanishes and a new vortex begins to form, Figs. 32, 33 and 34. The formation of the early discussed vortices were experimentally observed by Neff (39) and Eichorn (17).



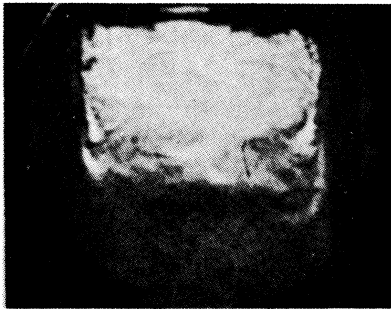
(a) 20 sec



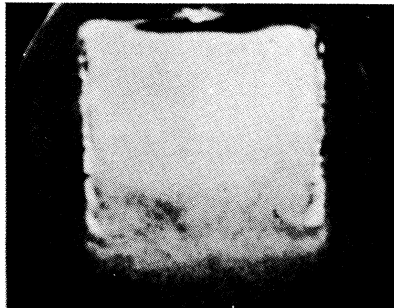
(b) 27 sec



(c) 40 sec



(d) 1 min



(e) 1-1/2 min

Fig. 35. Schlieren photographs for stratification without wall baffles. $q_w'' \approx 1.0 \text{ Btu/ft}^2 \text{ sec}$.

8.4.2 Results of the Cylindrical Container

The results obtained experimentally for the cylindrical container are given in Figs. 36 through 39. These figures show the effect of the heat flux level on the stratification phenomenon as well as on the nature of the temperature transients. These results indicate that the surface temperature rise is larger for higher heat fluxes. Figures 40 through 43, which are typical visicorder output show that the temperature near the liquid surface exhibits an oscillatory transients at small times, which later are damped. The temperature near the bottom of the tank shows a smaller degree of oscillations, which takes place at larger time. The magnitude of these oscillations varies with the heat flux level, the higher the heat flux level the larger the amplitude of these oscillations.

The theoretical results obtained for runs 2, 3 and 4 using a 31×31 grid are also given in Figs. 36, 37, 38 and 39. A series of isotherms and streamlines, which are obtained theoretically are given for each case at different values of time levels in Figs. 44 through 52. These isotherms and streamlines describe the temperature-time history, as well as the development of the flow pattern for each case. The flow development in these cases is similar to that in the rectangular containers which is discussed above, Section 8.4.1. At small values of time the stratified layer front near the centerline progresses at a rate higher than near the wall. Also a vortex is formed in the wall

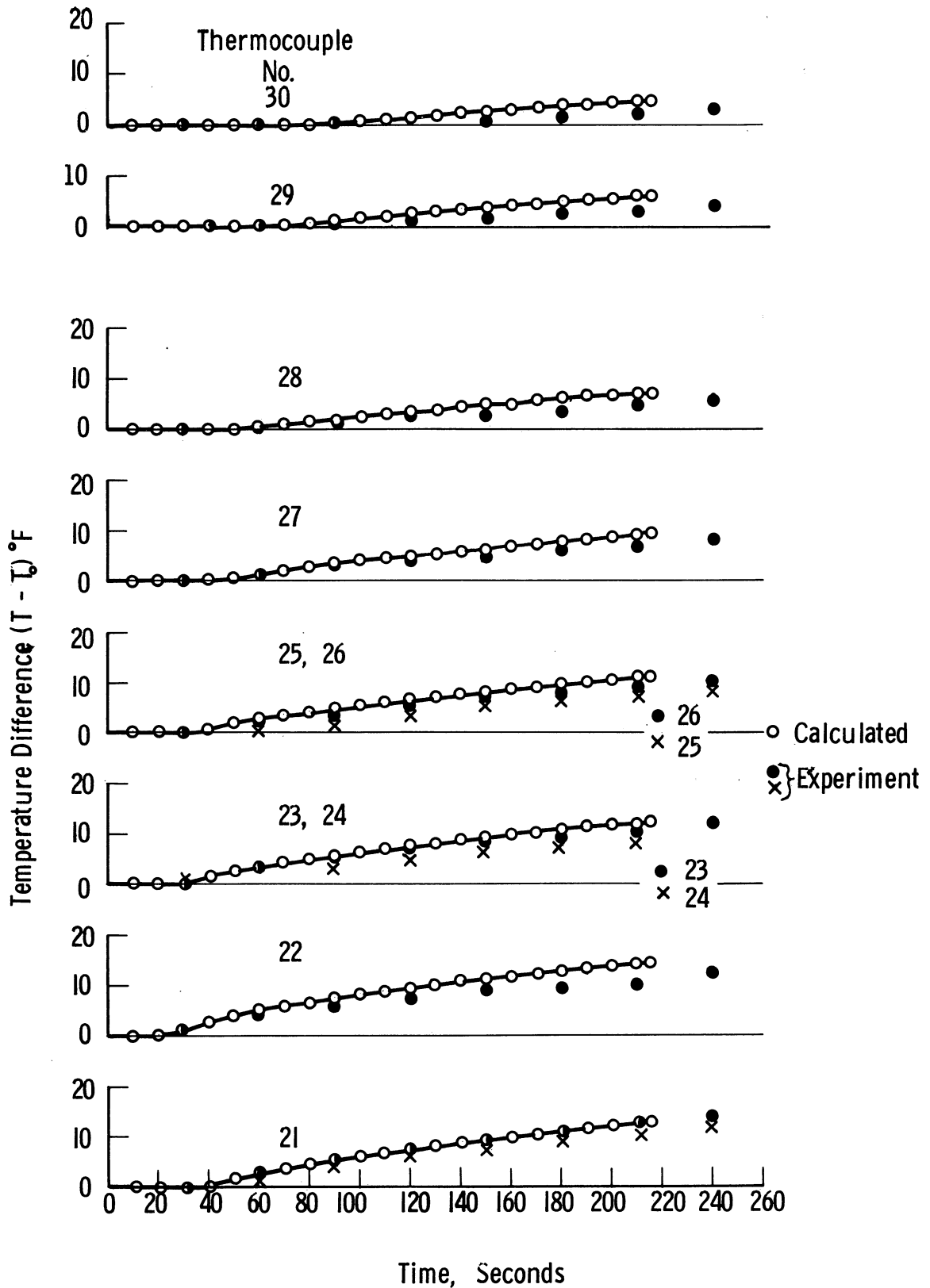


Fig. 36. Liquid temperature response in the cylindrical container, run 2. $(q/A)_w = 500 \text{ Btu/hr ft}^2$, $T_0 = 76^{\circ}\text{F}$.

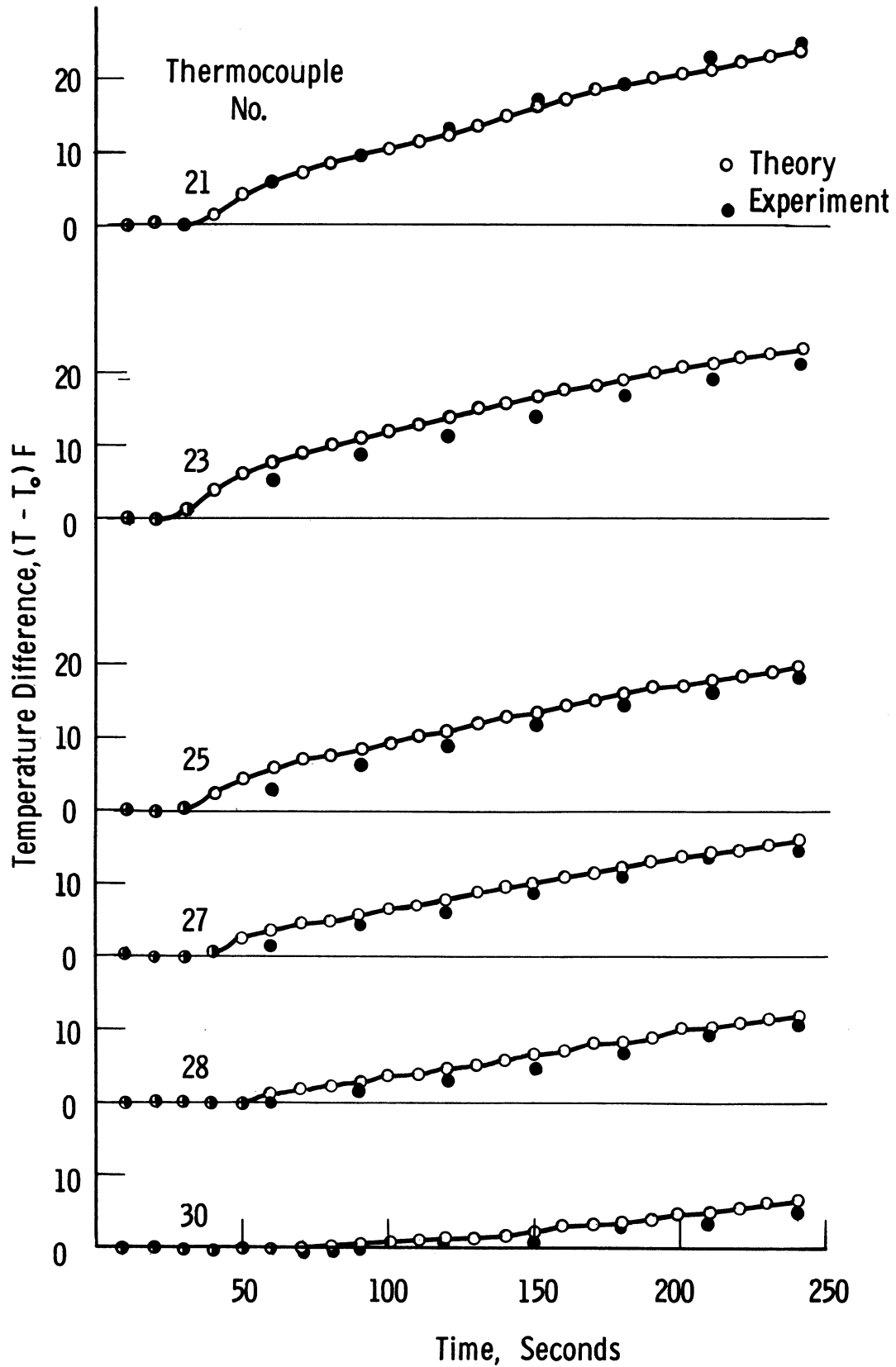


Fig. 37. Liquid temperature response in the cylindrical container, run 3. $(q/A)_w = 1000 \text{ Btu/hr ft}^2$, $T_0 = 73^\circ\text{F}$.

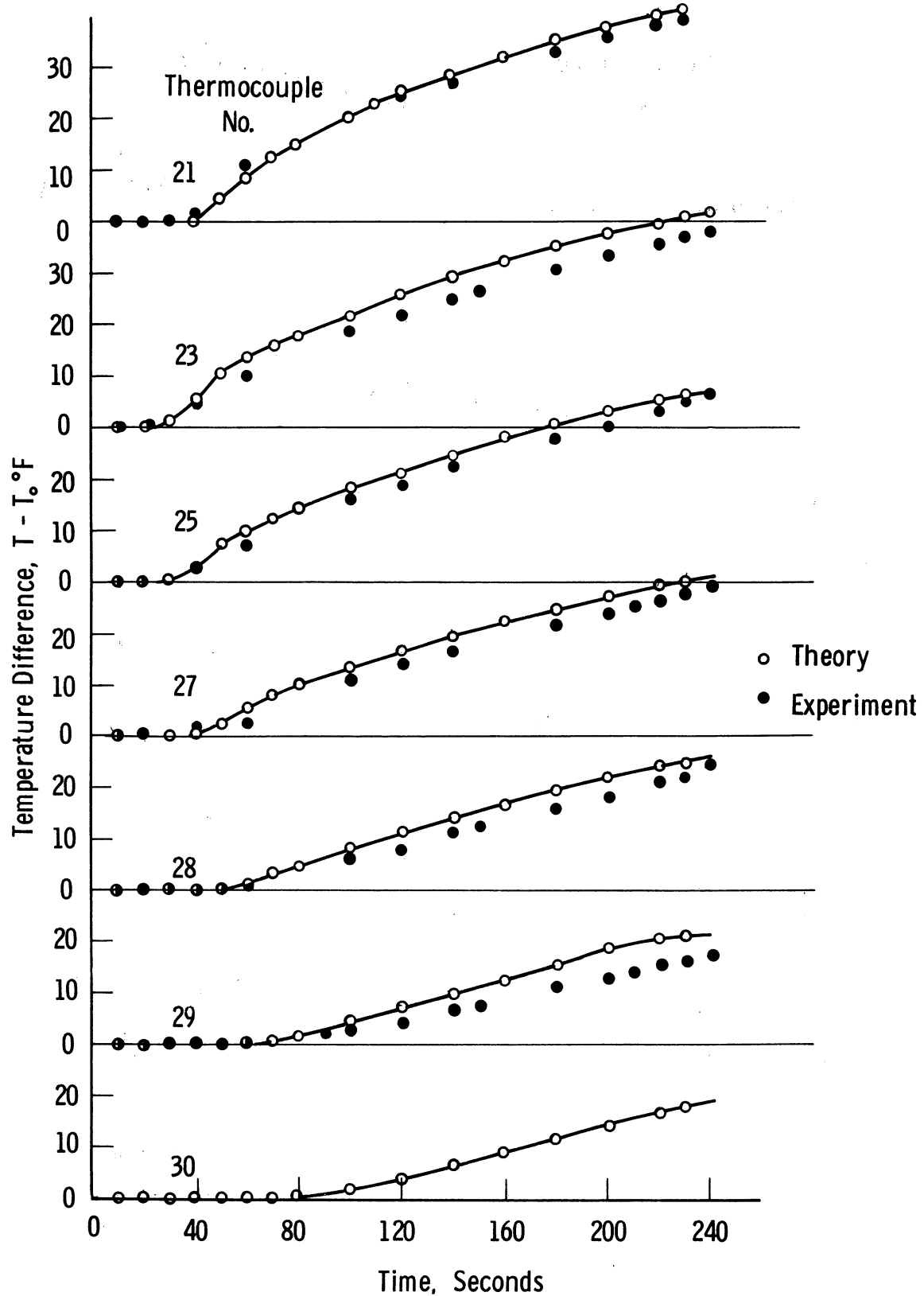


Fig. 38. Liquid temperature response in the cylindrical container, run 4. $(q/A)_w = 2000 \text{ Btu/hr ft}^2$, $T_0 = 80^\circ\text{F}$.

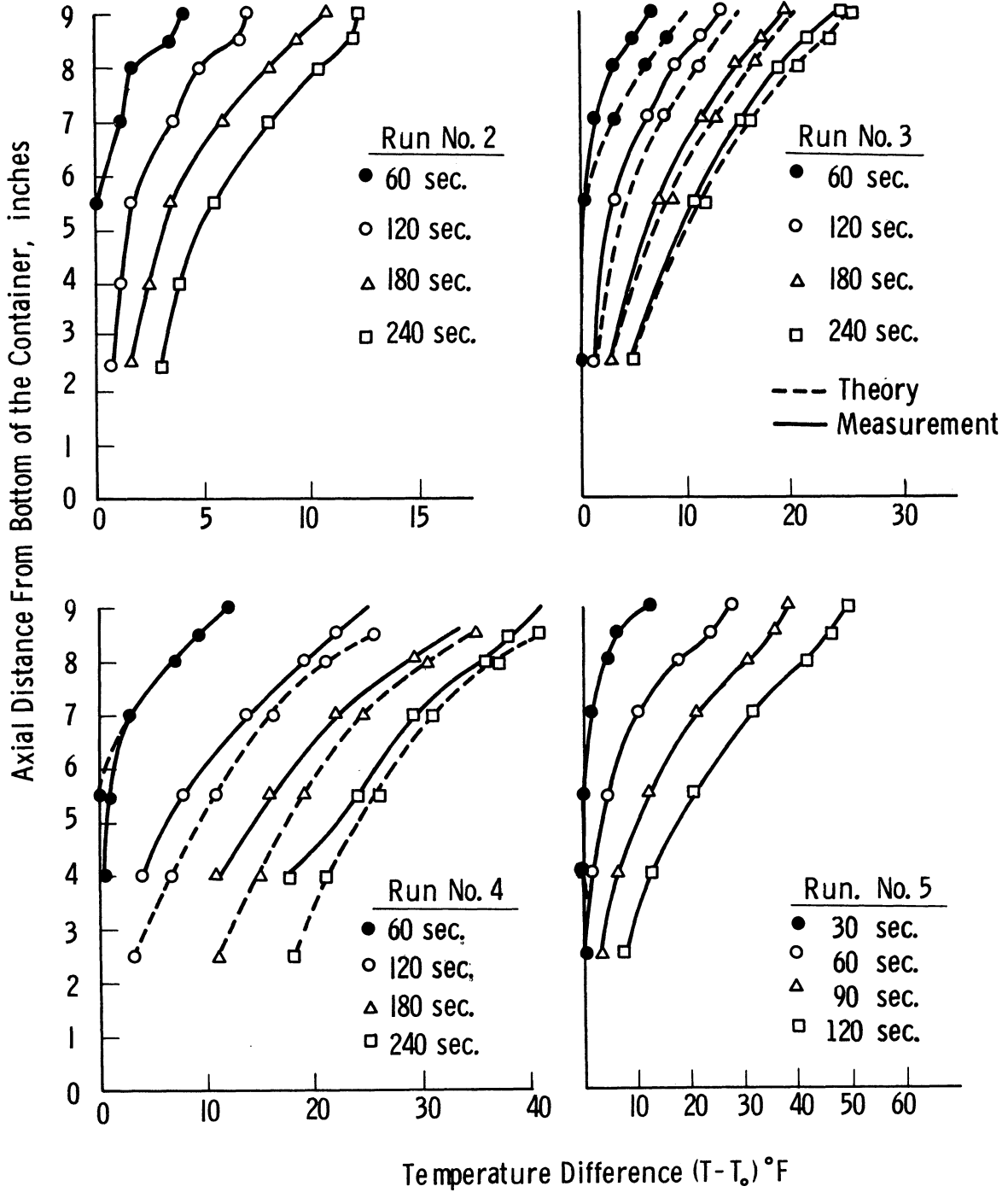


Fig. 39. Axial temperature distribution obtained for the cylindrical container.

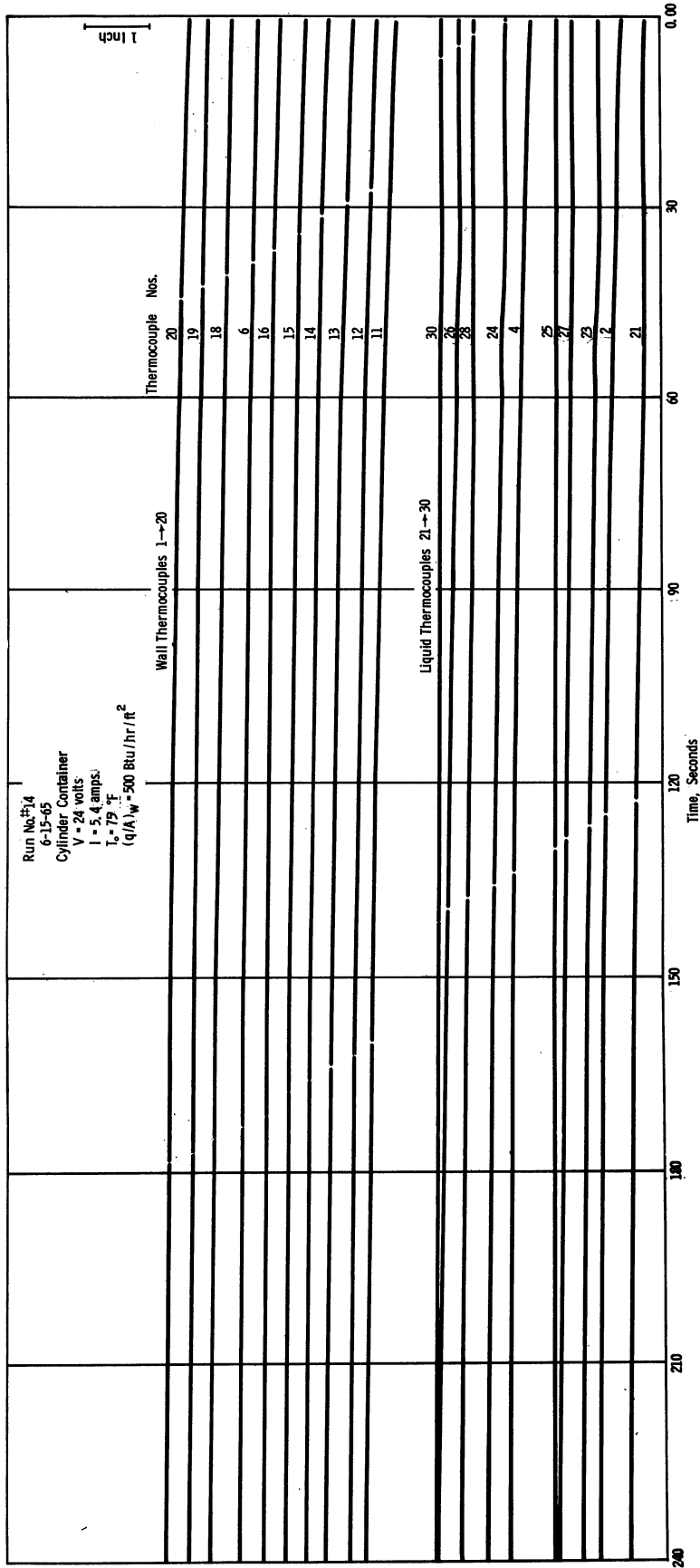


Fig. 40. Typical Visicorder output record. Heat flux = 500 Btu/hr ft².

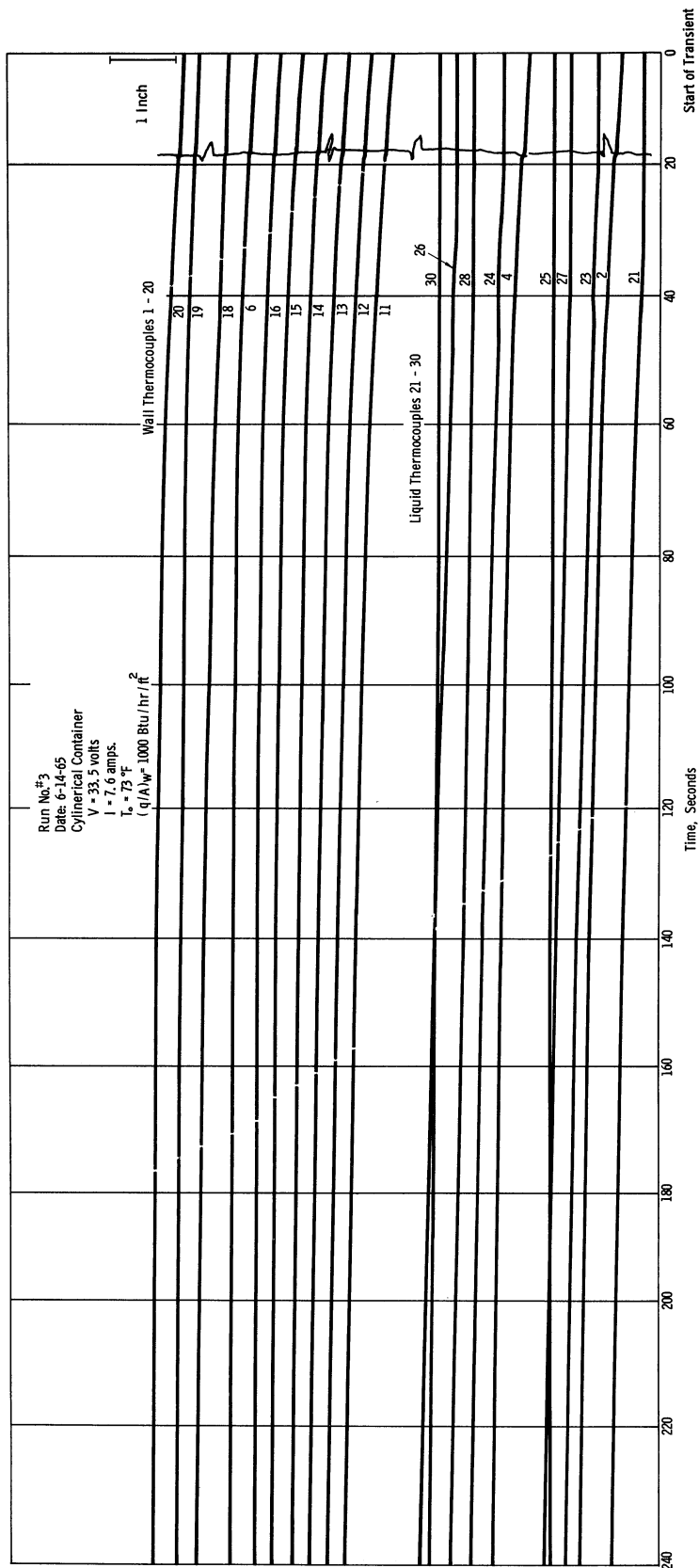


Fig. 41. Typical Visicorder output record. Heat flux = 1000 Btu/hr ft².

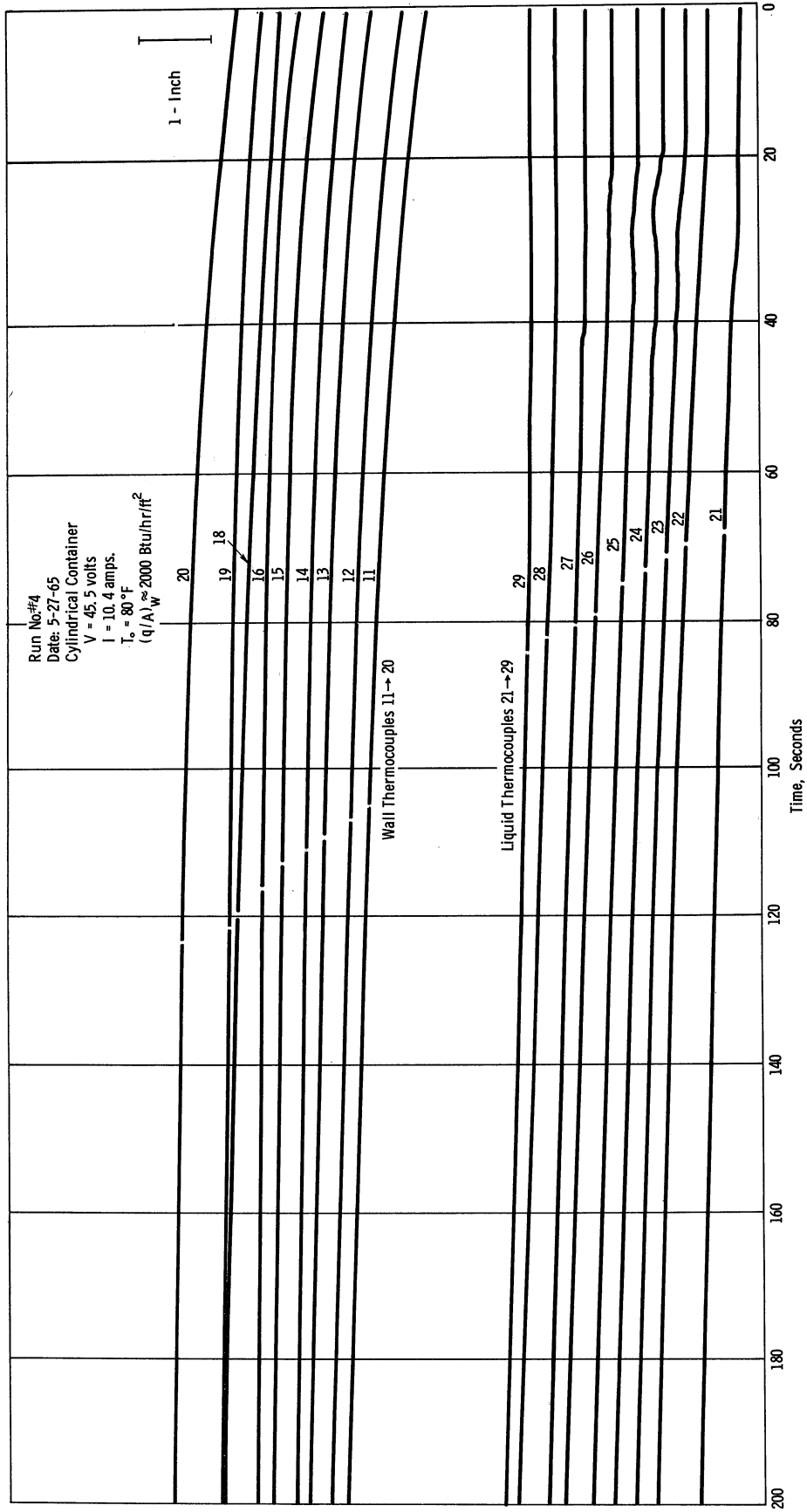


Fig. 42. Typical Visicorder output record. Heat flux = 2000 Btu/hr ft².

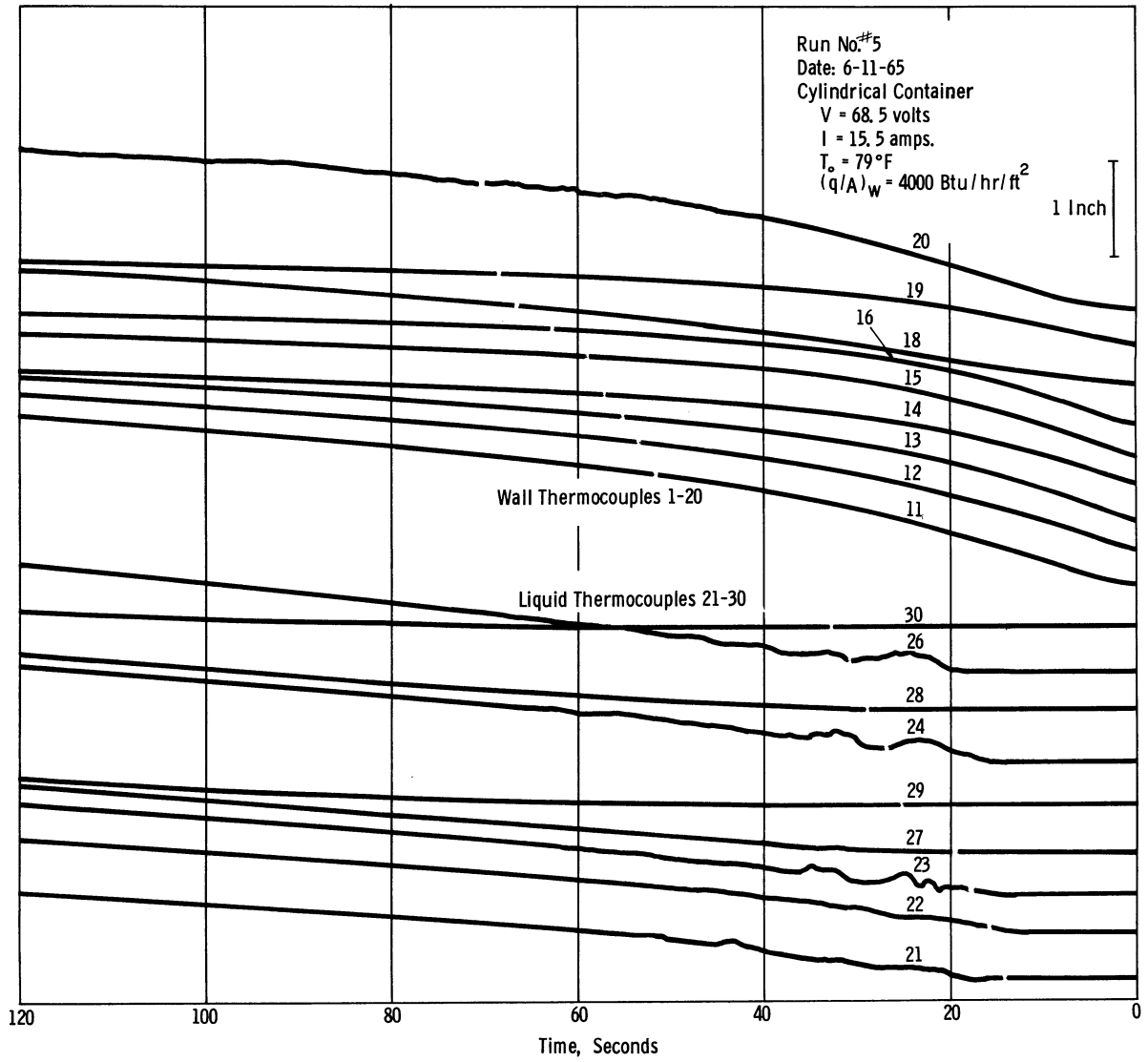


Fig. 43. Typical Visicorder output record. Heat flux = 4000 Btu/hr ft^2 .

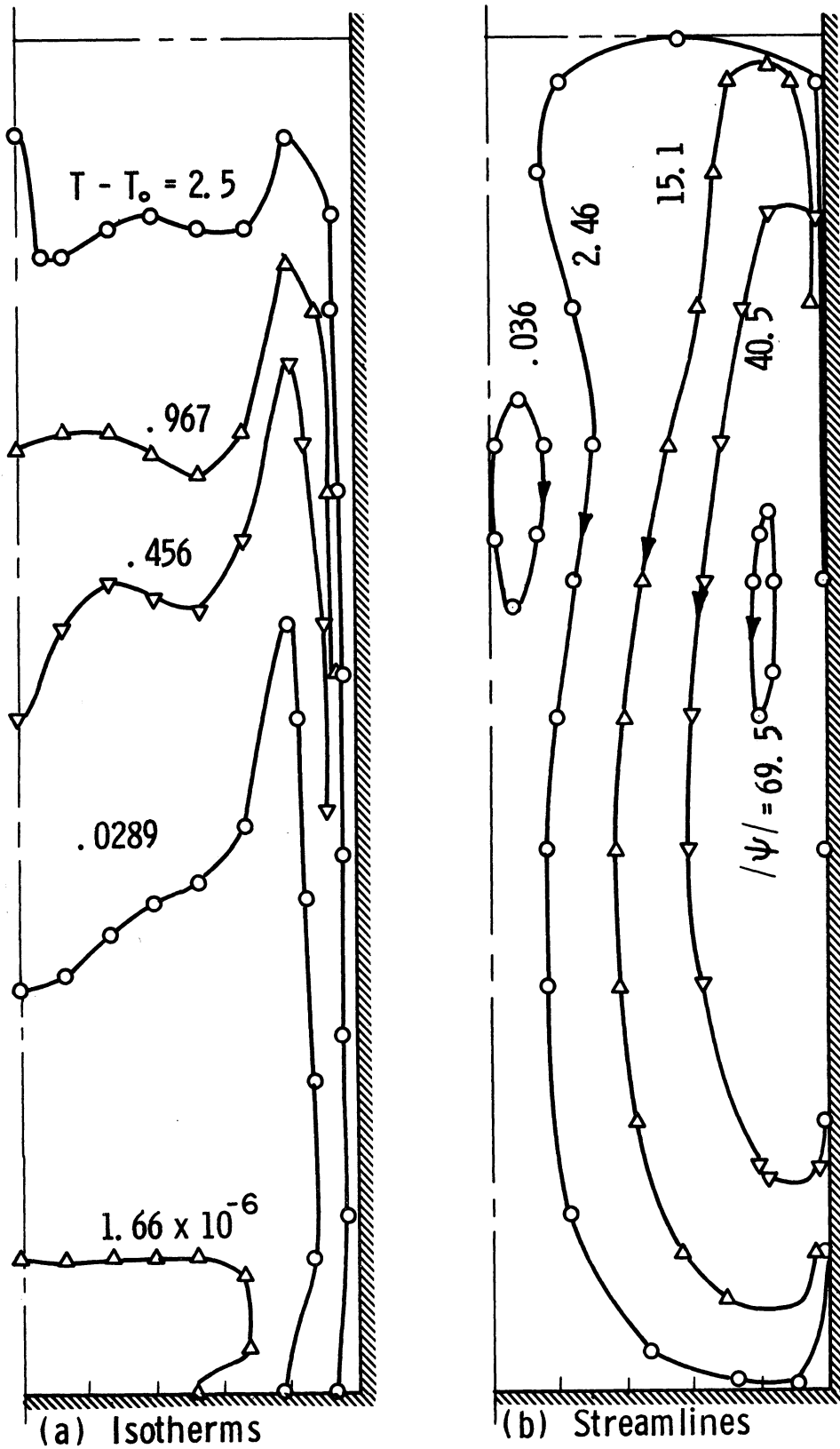


Fig. 44. Isotherms and streamlines in the cylindrical container, run 2. $(q/A)_w = 500 \text{ Btu/hr ft}^2$, time = 60 sec.

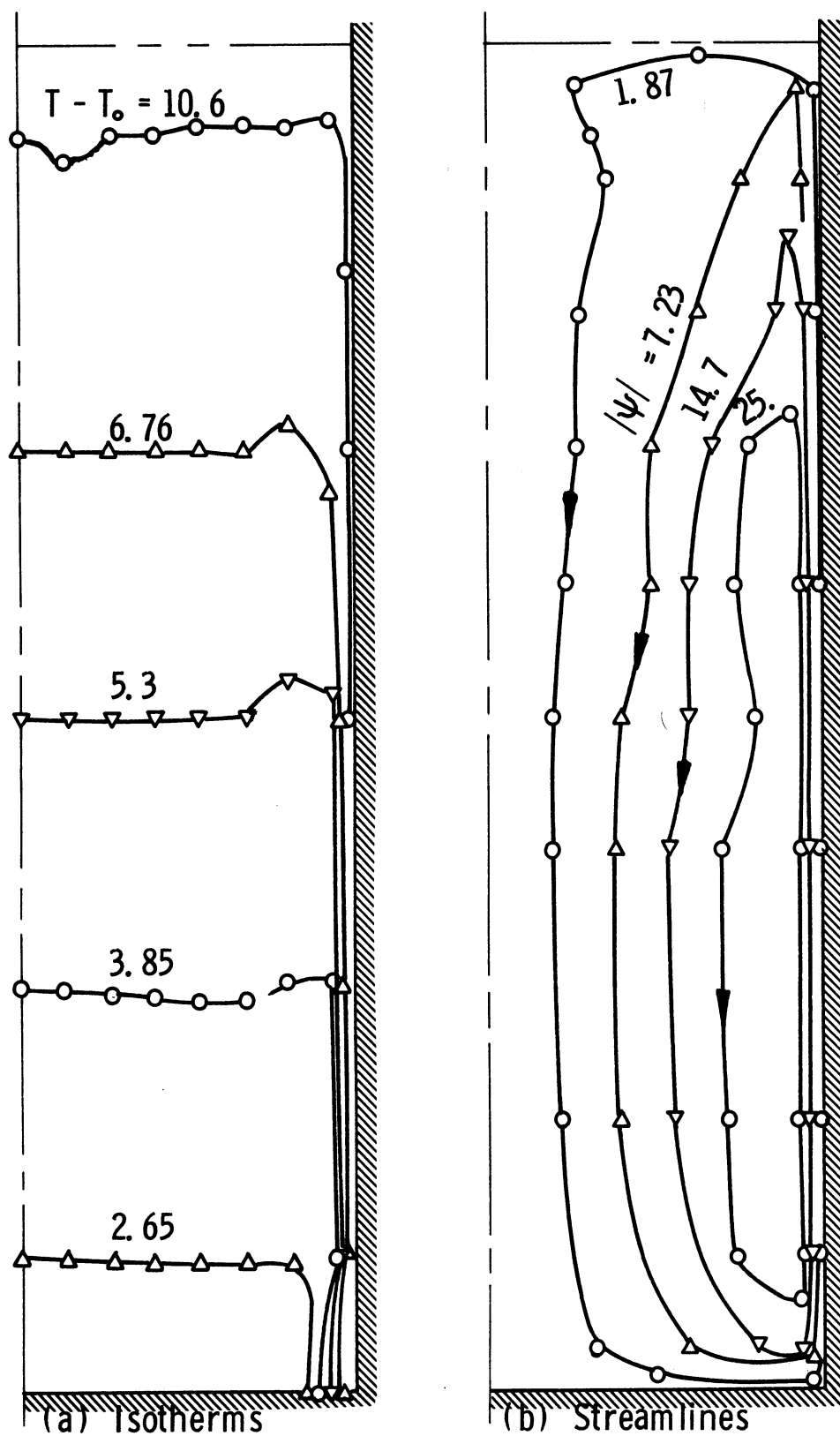


Fig. 45. Isotherms and streamlines in the cylindrical container, run 2. $(q/A)_w = 500 \text{ Btu/hr ft}^2$, time = 180 sec.

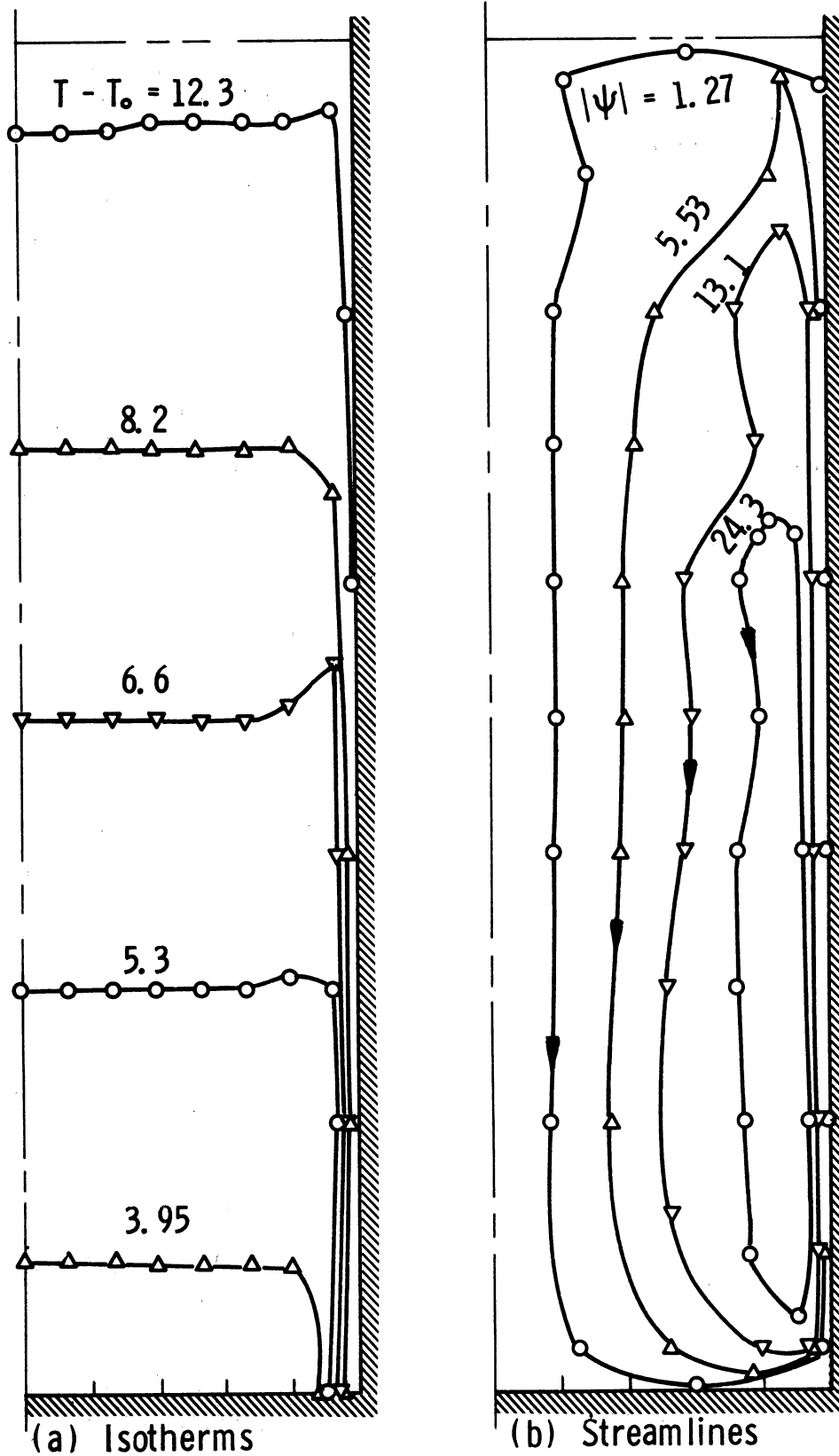


Fig. 46. Isotherms and streamlines in the cylindrical container, run 2. $(q/A)_w = 500 \text{ Btu/hr ft}^2$, time = 215 sec.

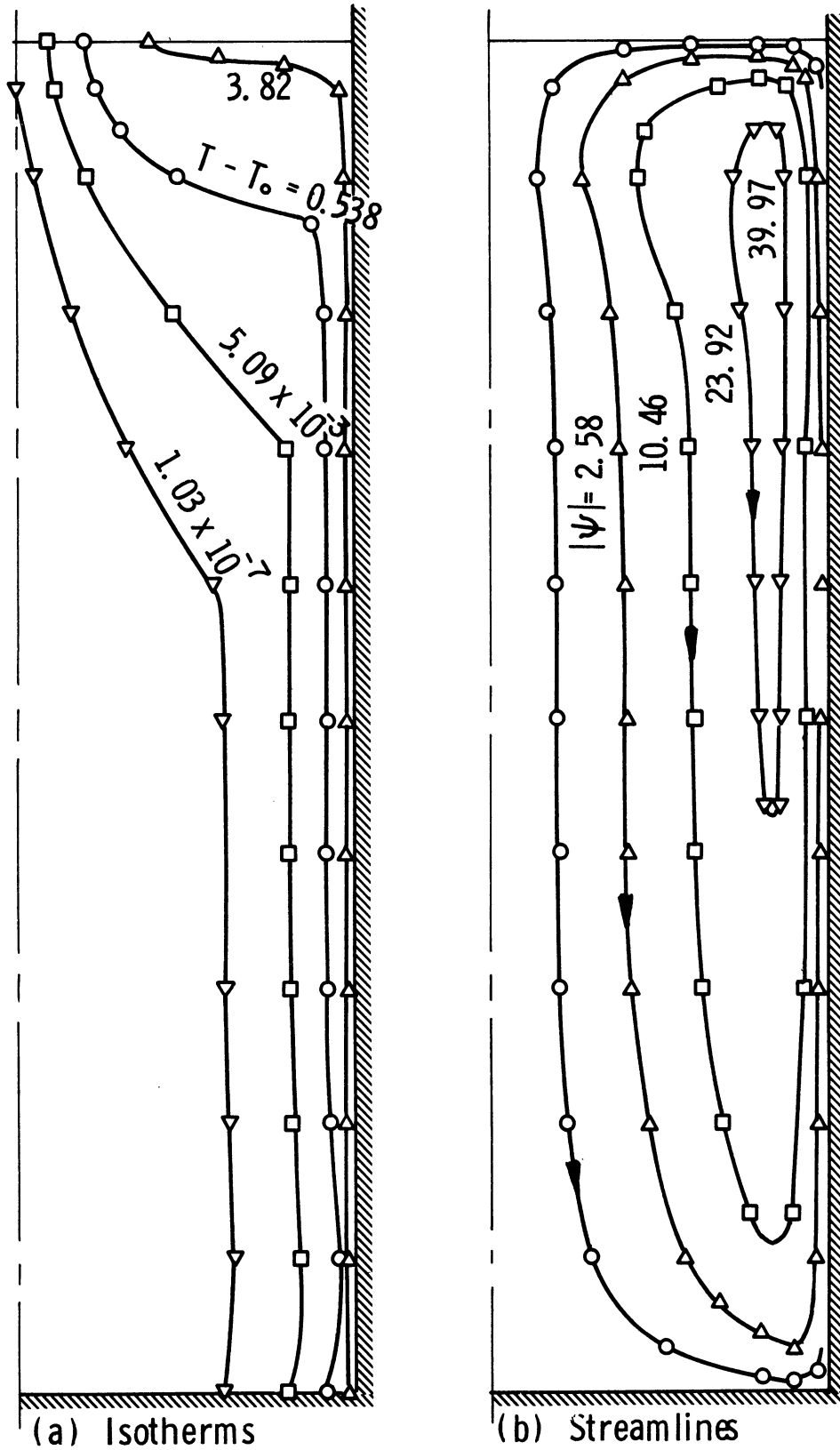


Fig. 47. Isotherms and streamlines in the cylindrical container, run 3. $(q/A)_w = 1000 \text{ Btu/hr ft}^2$, time = 30 sec.

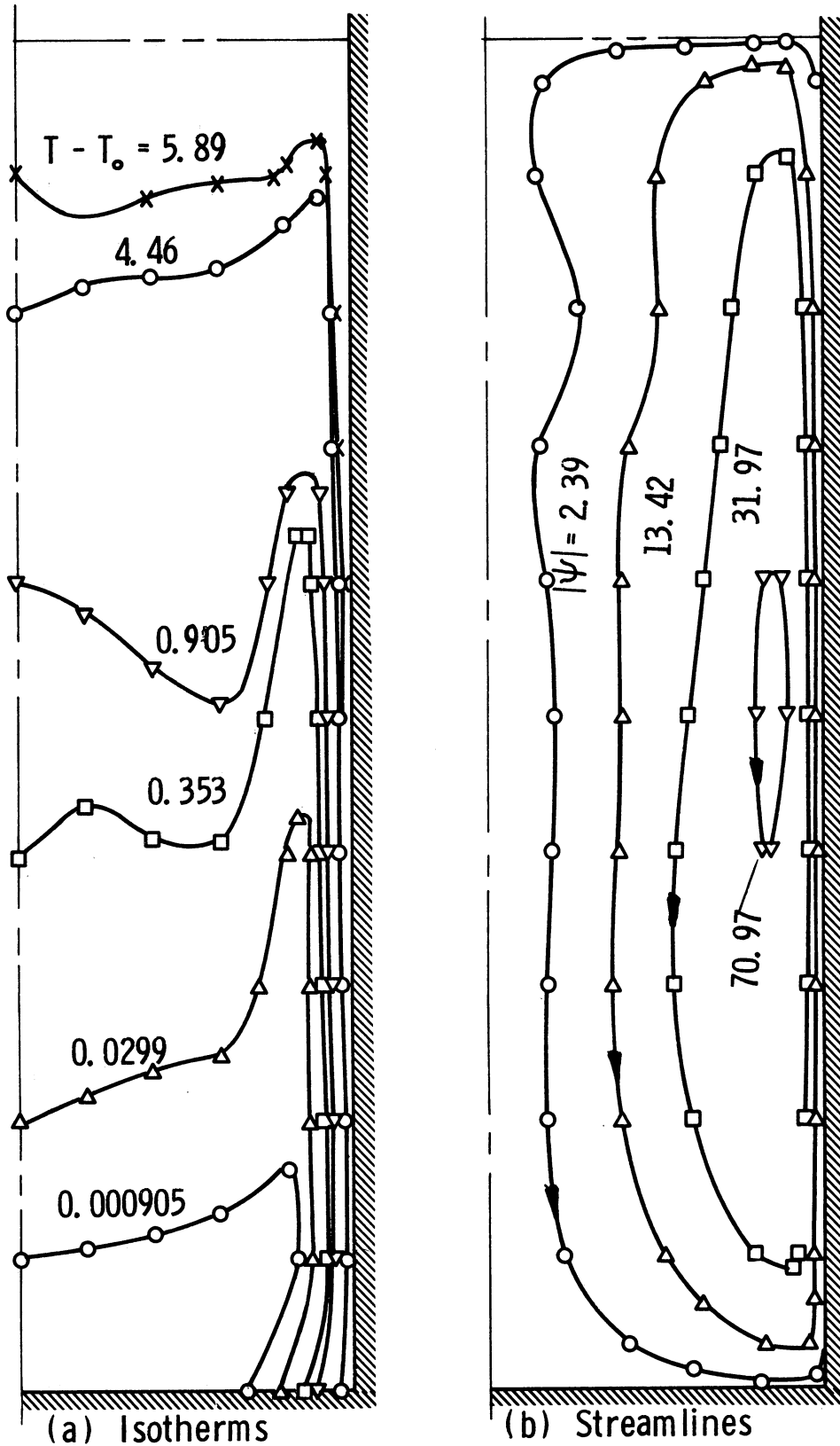


Fig. 48. Isotherms and streamlines in the cylindrical container, run 3. $(q/A)_w = 1000 \text{ Btu/hr ft}^2$, time = 60 sec.

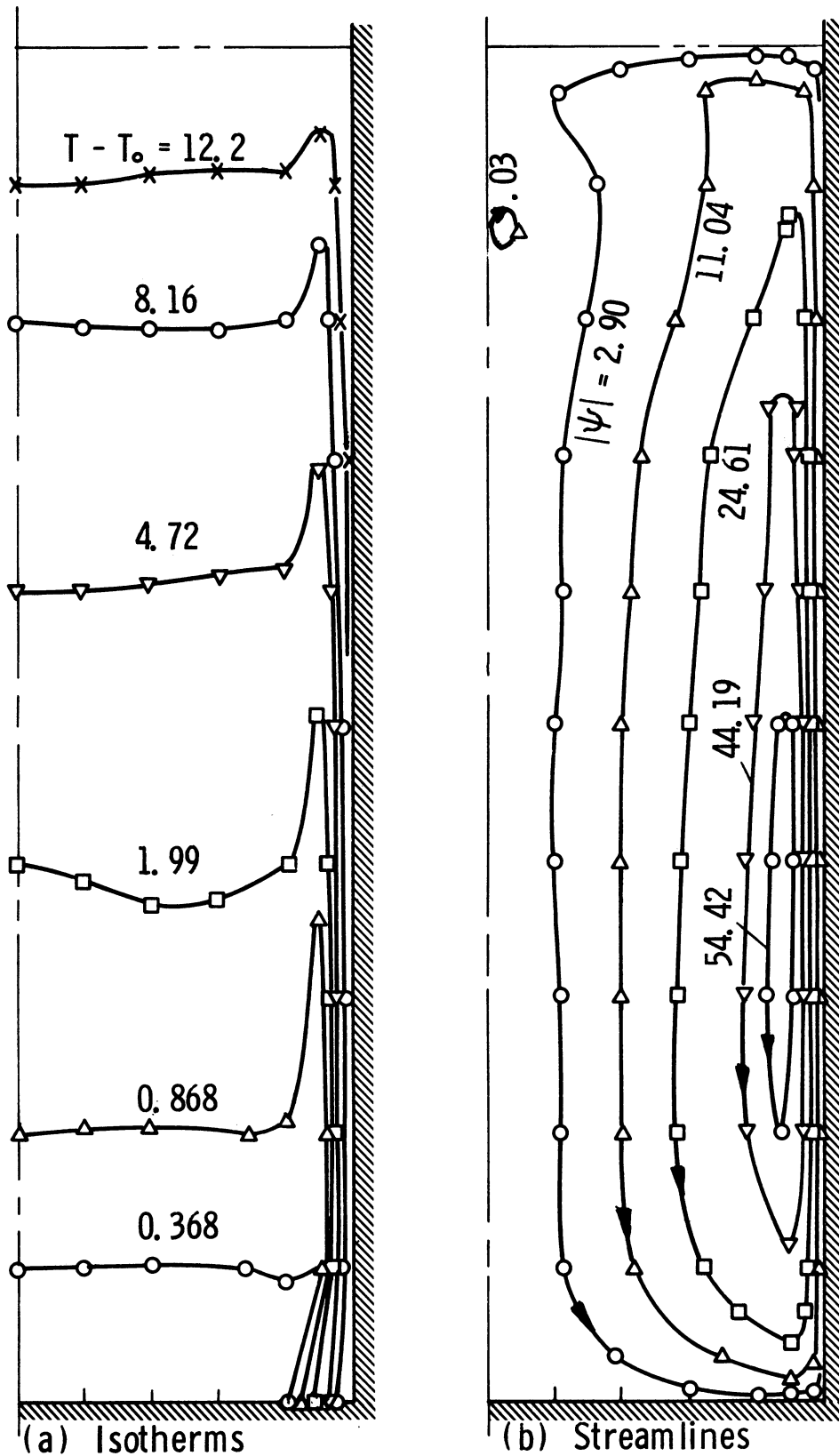


Fig. 49. Isotherms and streamlines in the cylindrical container, run 3. $(q/A)_w = 1000 \text{ Btu/hr ft}^2$, time = 120 sec.

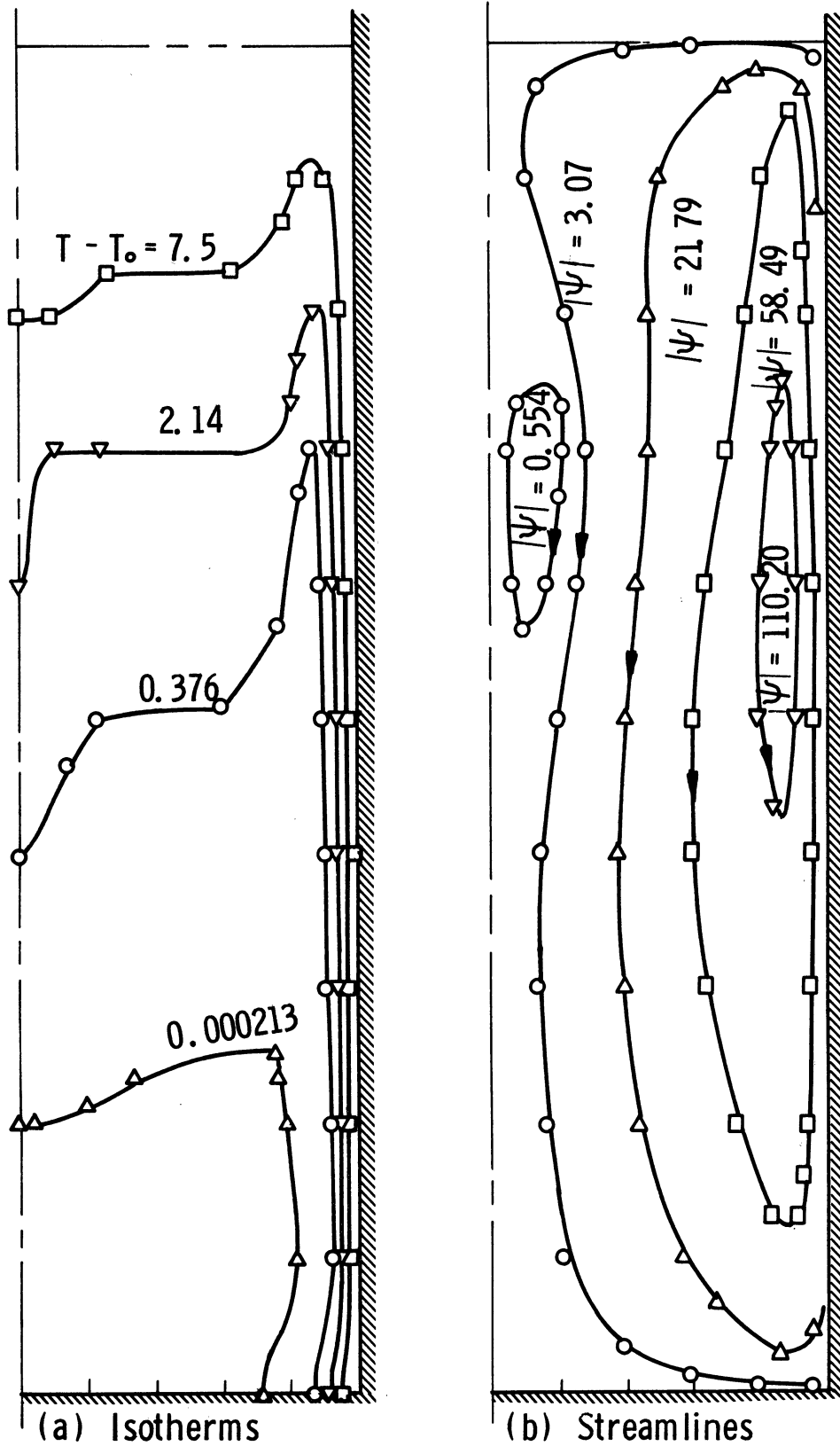


Fig. 50. Isotherms and streamlines in the cylindrical container, run 4. $(q/A)_w = 2000 \text{ Btu/hr ft}^2$, time = 60 sec.

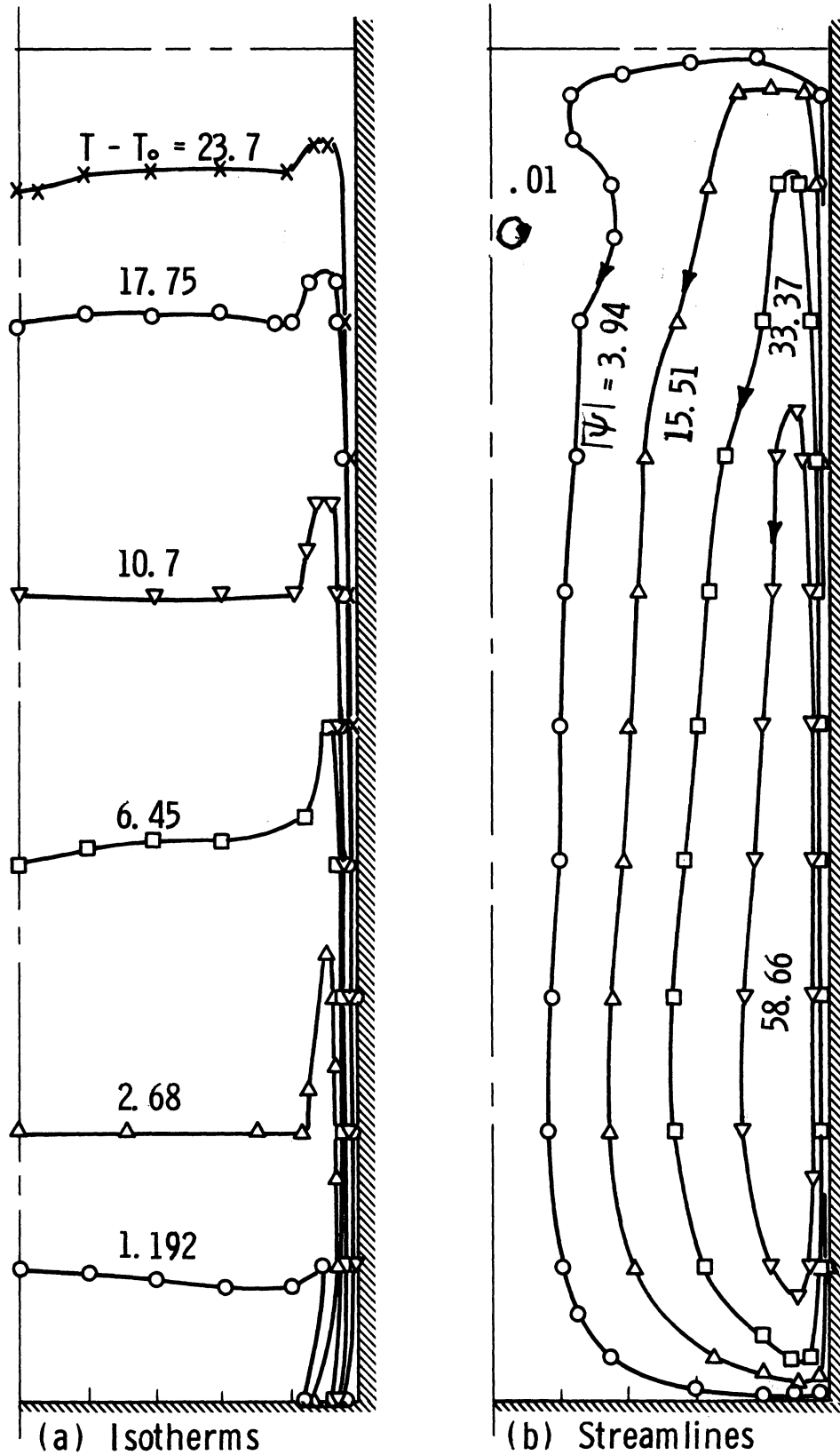


Fig. 51. Isotherms and streamlines in the cylindrical container, run 4. $(q/A)_w = 2000 \text{ Btu/hr ft}^2$, time = 120 sec.

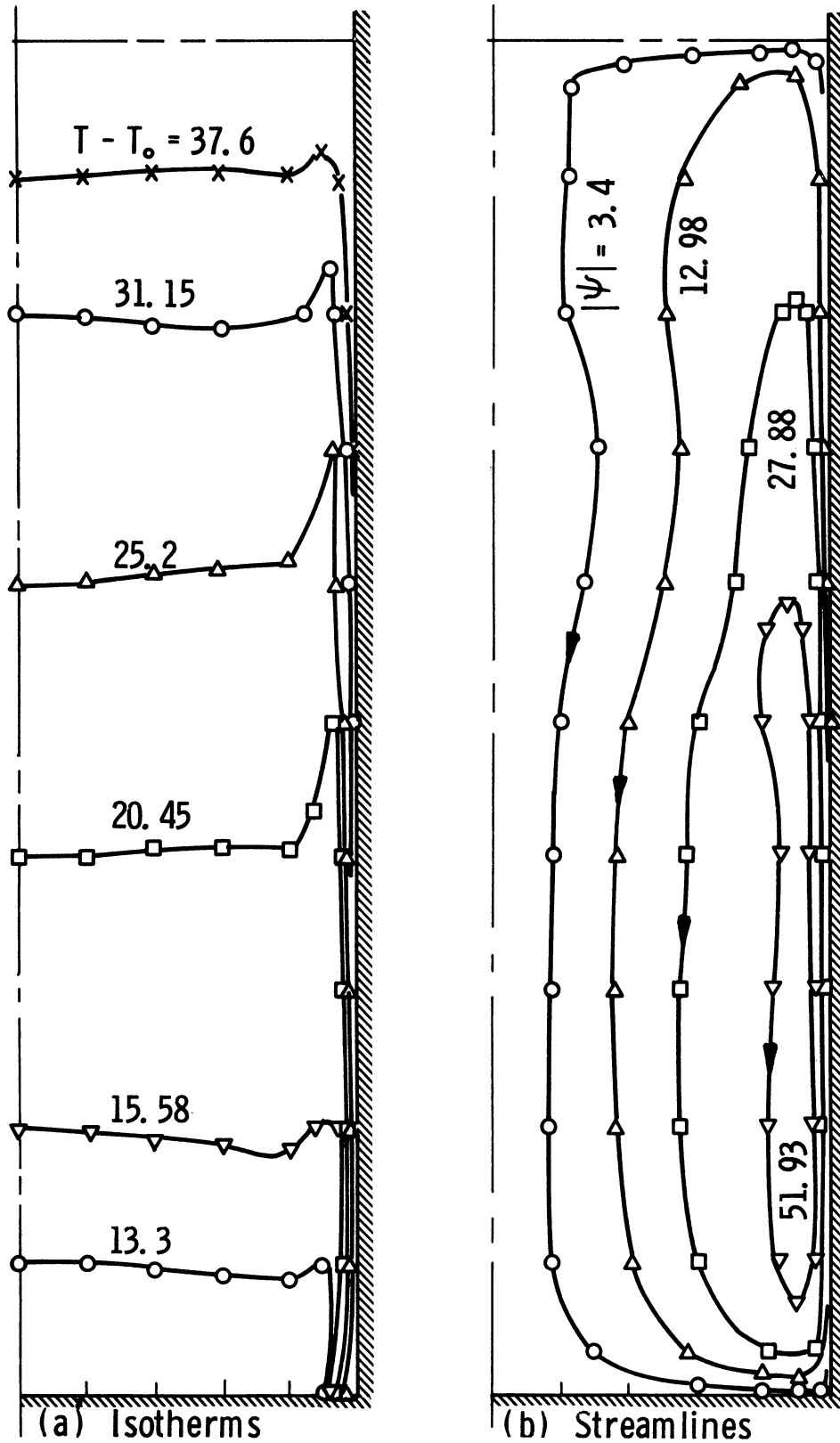


Fig. 52. Isotherms and streamlines in the cylindrical container, run 4. $(q/A)_w = 2000 \text{ Btu/hr ft}^2$, time = 230 sec.

vicinity and simultaneously moves downward as the stratified layer grows. Another vortex is observed at the centerline near the liquid surface, which breaks away when a certain size is reached and a new one begins to form.

The analytical results agree favorably with the measured values, Figs. 36 to 39. The results for run number 2 are less favorable than those of runs 3 and 4. The analytical results are 1 to 2°F higher than the measured temperature for run number 3 and it is 1 to 4°F higher for run number 4. However, these represent a difference of not more than 10% relative to the measured values at 240 sec. These differences are attributed to heat losses from the container bottom and top, variation in fluid properties and effects of three-dimensional flow. It is believed that the latter factor has more influence than the others. Apart from that the analytical solution adequately determines the time level at which transition takes place. Actually the agreement between the calculated and the measured time lag i.e., the time elapsed between the starting of the heating and the starting of the transients, is very satisfactory as shown in Figs. 36, 37 and 38. Also it is evident that the predicted and the measured surface temperature and axial temperature gradients are in good agreement. Fortunately, these latter two factors control the rate of heat and mass transfer across the interface, and accordingly the pressure variation in the vapor space.

The properties of the water used in the calculation were evaluated at the initial temperatures. These are given in Table II.

TABLE II
PROPERTIES OF WATER FOR THE CONDITIONS
OF RUNS 2, 3 AND 4

Run No.	Heat Flux, Btu/hr, ft ²	Initial Temp., °F	Thermal Diffusivity, α , ft ² /hr	Prandtl No.	Kinematic Viscosity, ν , ft ² /sec	Compress. Factor, β , R°
2	500	76	5.636×10^{-3}	6.26	9.8×10^{-6}	1.38×10^{-4}
3	1000	73	5.60×10^{-3}	6.50	1.10×10^{-5}	1.28×10^{-4}
4	2000	80	5.66×10^{-3}	5.84	9.2×10^{-6}	1.51×10^{-4}

8.5 EFFECT OF GRID SIZE

The use of finite-differences requires the determination of appropriate grid sizes ΔX , ΔY and ΔR such that the discretization errors become small. A possible resolution of this question can be obtained by observing the behavior of the solution as the grid sizes become smaller. This procedure was followed in solving the rectangular cavity problem, i.e., Poots problem. Calculations were carried out using 11x11, 21x21 and 31x31 grids. The results of the 11x11 grid showed large deviation from those given by Poots, Fig. 18. While those obtained using 21x21 and 31x31 grids showed essentially the same kind of favorable agreement with Poots results, Fig. 17. Accordingly it was concluded that since a 21x21 grid yielded good agreement with the analytical solution, a

31x31 will be sufficient for the present purpose. This point was substantiated further by carrying calculations using a 51x31 grid for the case of run number 1. These results are compared with those obtained utilizing 31x31 grid in Table III, which reveals that the difference is not appreciable.

TABLE III
EFFECT OF GRID SIZE ON THE COMPUTED RESULTS
FOR RUN NO. 1, RECTANGULAR CONTAINER

Time, sec	Grid	Calculated $(T-T_0)$ corresponding to location of thermocouple			
		11	9	5	4
25	31x31	1.87	1.75	1.49	.16
	51x31	1.54	1.525	1.43	.267
30	31x31	5.47	5.30	4.7	1.23
	51x31	4.83	4.77	4.33	0.98
35	31x31	12.65	12.23	8.6	0.75
	51x31	11.80	11.50	7.48	0.52

When the wall heat flux is specified instead of specifying the wall temperature, the boundary condition is approximated by Equation (5.49). In such a case, the calculated wall temperature will be affected by the grid size ΔY or ΔR employed in the solution, which in turn will affect the temperature and velocity distributions. Figure 53 shows the dimensionless wall temperature at location $X=0.6$ obtained using 11x11, 16x16 and 21x21 grids plotted against dimensionless time

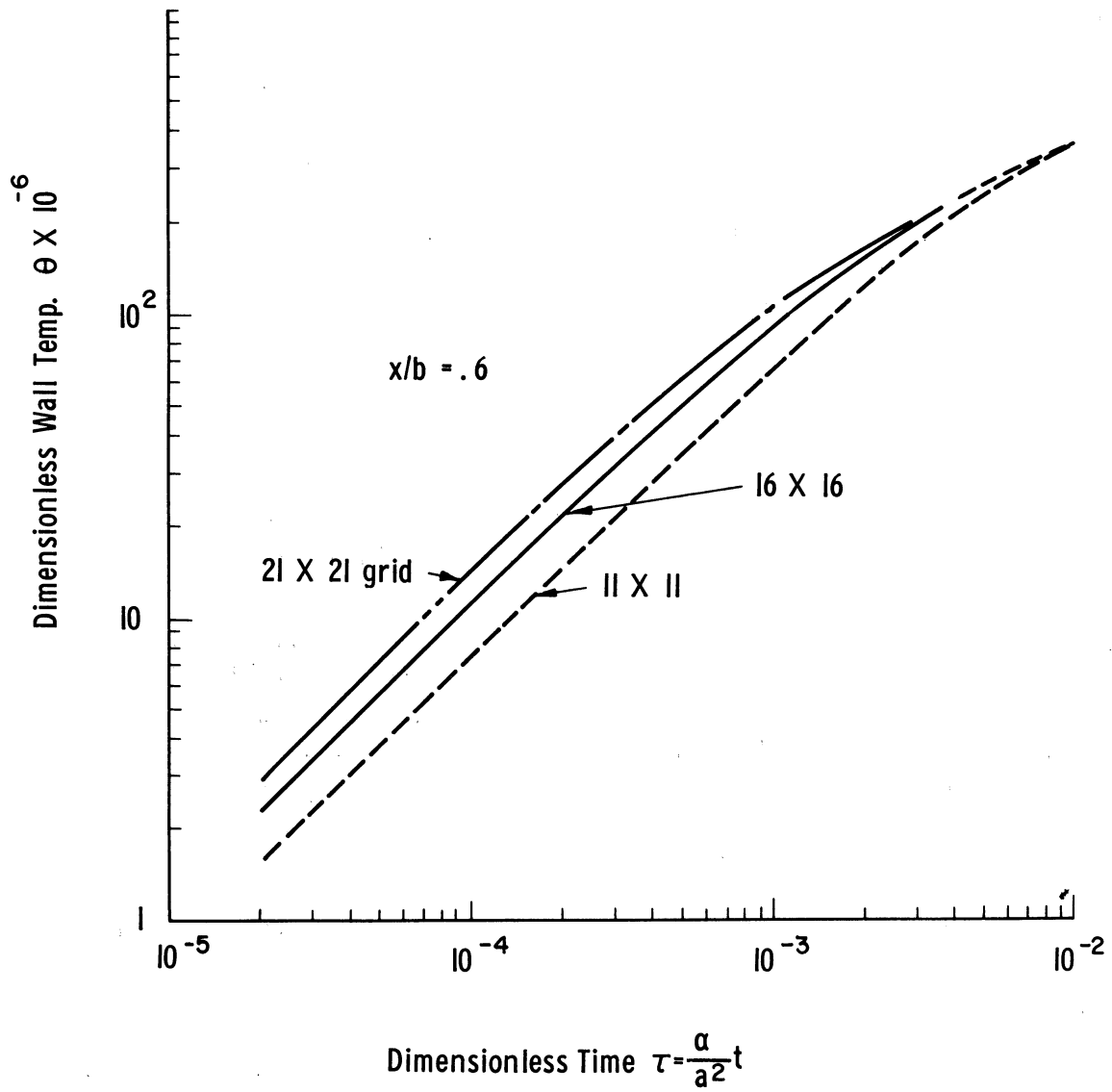


Fig. 53. Effect of the grid size on the calculated wall temperature.

τ , corresponding to the case of constant wall heat flux of 10 Btu/hr ft² with fluid surface kept at the initial temperature. The fluid properties employed are those given in Table I. These results show that the deviation is greatest for small times. The difference decreases with time and is practically negligible for dimensionless time of 0.003. This behavior is due to the fact that at larger time levels the magnitude of the truncation error becomes smaller and will approach zero near the steady state.

There is always the question of whether a realistic velocity distribution near the boundary is predicted by the finite-difference solutions. Such solutions should give a velocity distribution which has the following character: The velocity component parallel to the wall is small near the solid boundary. It increases in magnitude with increasing distance from the wall, reaches a maximum, decreases again and changes direction as it approaches the centerline of the container. The nature of the finite-difference solution depends upon the magnitudes of the boundary layer thickness and the grid size used in the calculations. If the boundary layer thickness is large compared to the grid size, the solution obtained will exhibit the above described character. This will be the case for low Grashof numbers or large values of time. The latter case is shown in Fig. 54, in which the calculated velocity changes from its value at the wall in the above described manner. On the other hand, if the boundary layer thickness is small compared to the grid size, the results will show that the

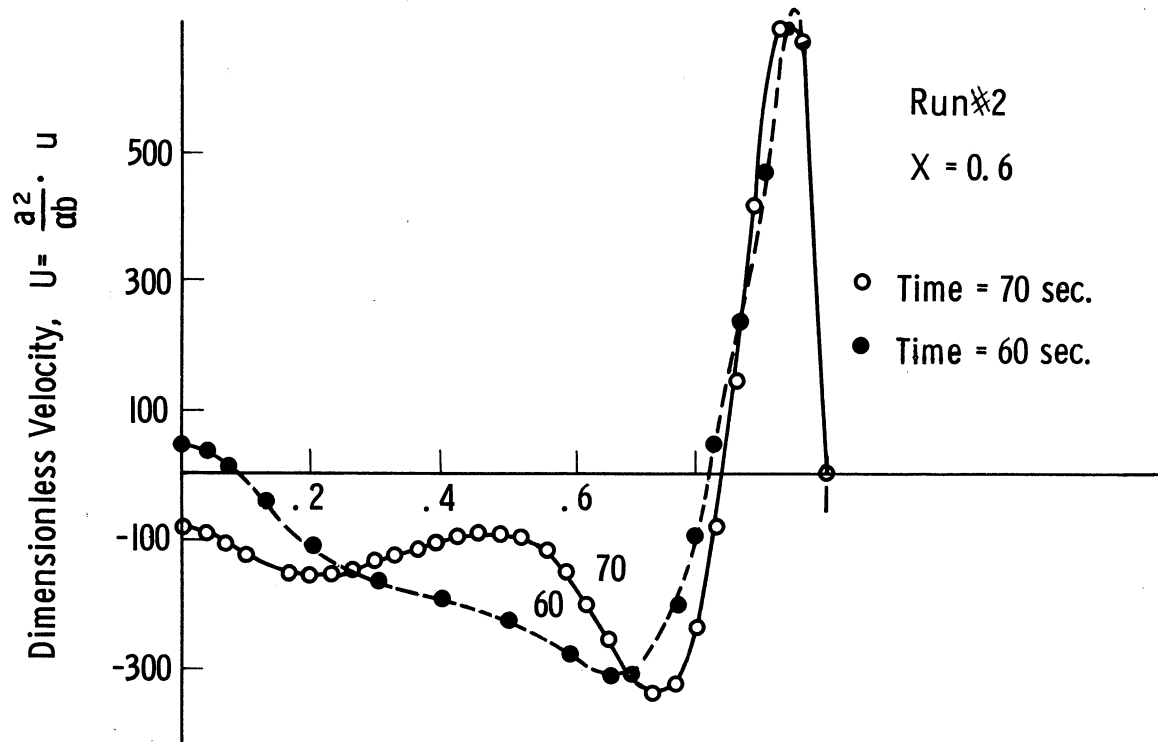


Fig. 54. Calculated velocity distribution at high values of time in the cylindrical container, run 2. $(q/A)_w = 500$ Btu/hr ft².

velocity in the boundary layer is maximum at the nodal points subsequent to the boundary. This will take place for high Grashof numbers and/or low values of time. The latter situation is shown in Fig. 55.

Although the continuity equation has been satisfied by introducing the stream function, a mass balance for the case of an incompressible fluid of the net rate of the fluid flow across any section of the liquid container i.e., $\int_0^1 U dY$ for rectangular containers and $\int_0^1 \bar{U} R dR$ for the cylindrical containers, will provide a means of checking the calculated velocity distribution and also give an indication to the propriety of the grid size used. The value of the above mentioned integral should be equal to zero. However, due to numerical errors this integral assumes finite-value. It was observed that this value approaches zero as the grid size is made smaller. When the above integration was carried at the section $X=0.5$ using the trapezoidal rule, the net flow rate across that section was less than 0.8% of the total upward flow rate at that section for run number 2 at time level 215 sec.

8.6 SUMMARY OF THE RESULTS

In the previous chapters a numerical method for solving the non-linear partial differential equations describing the two-dimensional transient laminar natural convection in closed rectangular and cylindrical containers was presented. The method has been utilized to study

$$C \int_0^1 U \cdot 2\pi R dR \Rightarrow \int_0^1 u(2\pi r) dr$$

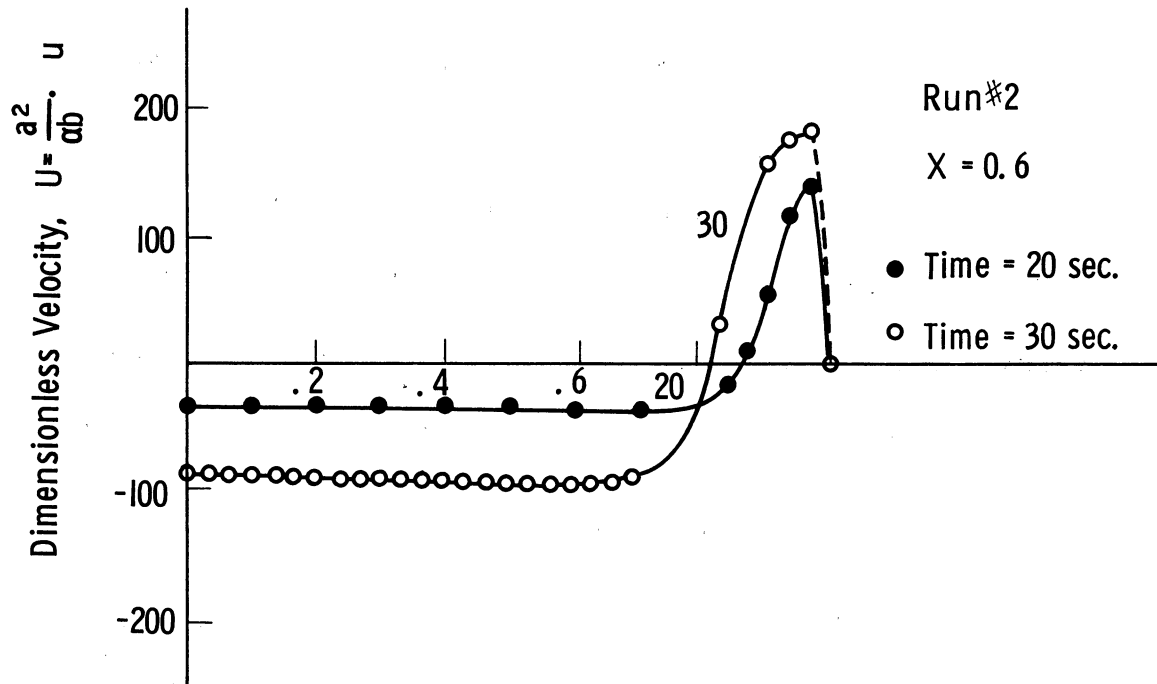


Fig. 55. Calculated velocity distribution at low values of time in the cylindrical container, run 2. $(q/A)_w = 500 \text{ Btu/hr ft}^2$.

the thermal stratification of fluids contained in vessels subjected to wall heating. Calculations are presented for different boundary conditions as well as for different heat flux levels. Also the effect of the gravity level on the stratification process was examined. The following principal results and conclusions can be made.

1. The formation of a thermally stratified layer at the liquid surface is caused by either side wall heating or by heat transfer across the interface or by both. The first case is demonstrated by calculations and measurements reported above for two-dimensional rectangular and cylindrical containers with adiabatic fluid surface. In the absence of wall heating, a stable, motionless, stratified fluid layer will be formed due to conduction.

The thermal transients within the liquid will be higher for both side wall and interfacial heating, because convection currents, caused by side wall heating, will increase the rate of energy transfer from both the wall and the liquid surface to the stratified layer. Also a higher fluid temperatures rise results from higher heat flux. In the absence of any side or bottom heating, the fluid temperature at any time will be proportional to the surface temperature. Although this latter case may not be realized in practice, it may approximate that of a well insulated vessel in a zero gravity field at small time levels after introducing the transient. The calculations also revealed that for a given geometry, fluid and heat flux, the surface temperature will rise at a lower rate at reduced gravity conditions than at standard

gravity levels.

2. The flow development and the downward movement of the stratified layer front are of the same nature for both the rectangular and the cylindrical containers.

3. The experimental measurements are in good agreement with the theoretical results. Satisfactory agreement with the theoretical results obtained by Poots for the rectangular cavity is obtained. Such an agreement indicates the validity of the model used in the calculation and the usefulness of the method of solution. Furthermore the flow pattern obtained agrees with that experimentally reported by others.

4. The method of solution presented here is applicable to any two-dimensional geometry. Four various finite-difference formulations are presented. The stability requirements for each of these methods were determined. Verification of the validity of the results of the stability analysis was obtained by actual calculations. Calculations have been carried for a wide range of Grashof numbers, from 10^7 to 5×10^9 . No signs of instability were encountered during the calculations.

5. The results of the mathematical experimentation show that the application of the von Neumann method of stability analysis to partial differential equations of the form,

$$\frac{\partial f}{\partial t} = a_0 \frac{\partial^2 f}{\partial x^2} + a_1 \frac{\partial f}{\partial x}$$

may lead to erroneous conclusions. A different method to examine the stability conditions of such equations is presented. The application

of this method to finite-difference formulations, for which known stability criteria exist, leads to the same criteria.

8.7 RECOMMENDATIONS FOR FUTURE WORK

The method of solution developed here has been utilized to study the natural convection in partially filled liquid containers with and without simultaneous pressurization of the container. The investigation of the heat and mass transfer in both the liquid and the vapor phases, which takes into account the interfacial energy and mass transport, offers a challenging area for future studies. The calculation of the pressure-time history in such cases is another possibility. The study of the mass and heat transfer interactions during the pressurized discharge, taking into consideration the various processes that take place inside the container is another important problem. A computer program has been written to study the velocity-time history during the discharge process although it is not involved here. This program is capable of examining the nature of the decay of the transients after the discharge process is stopped.

Apart from application to natural convection in closed containers, the method of solution can be utilized for the study of natural and forced convection flows for any two-dimensional geometry.

The extension of the method for solving three-dimensional fluid flow problems represents an interesting line of study. If such extension

becomes possible, it should be anticipated that the machine time required for handling such problems will be large. However, this would represent the only present possibility of solving three-dimensional laminar flow problems with exactness. Furthermore, the rapid developments in digital computing machines and methods of solution will make it possible to analyze systems, which may seem to be formidable by the present methods.

APPENDIX I

METHOD OF SOLUTION OF A SYSTEM OF LINEAR ALGEBRAIC
EQUATIONS HAVING A THREE DIAGONAL MATRIX

The iterative method employed for solving the stream function-vorticity equation require the solution of a system of algebraic equations having a tridiagonal matrix. The algorithm given below for the solution of such systems is derived from the Gaussian elimination method. This procedure was first used by Bruce, Peaceman and Rachford (9). The method may be summarized as follows. For a system of equations,

$$B_0 P_0 + C_0 P_1 = D_0$$

$$A_j P_{j-1} + B_j P_j + C_j P_{j+1} = D_j \quad 1 \leq j \leq n-1$$

$$A_n P_{n-1} + B_n P_n = D_n$$

Let

$$w_0 = B_0$$

$$w_j = B_j - A_j b_{j-1} \quad 1 \leq j \leq n$$

$$b_j = \frac{C_j}{w_j} \quad 0 \leq j \leq n-1$$

and

$$g_0 = \frac{D_0}{w_0}$$

$$g_j = (D_j - A_j g_{j-1}) / w_j \quad 1 \leq j \leq n$$

The solution is

$$P_n = g_n$$

$$P_j = g_j - b_j P_{j+1} \quad 0 \leq j \leq n-1$$

APPENDIX II

THE STABILITY ANALYSIS OF FORMULATION (ii) USING VON NEUMANN METHOD

For simplicity the following one-dimensional equation will be considered

$$\frac{\partial \theta}{\partial t} + U \frac{\partial \theta}{\partial x} = \frac{\partial^2 \theta}{\partial x^2} \quad (\text{A.1})$$

The finite difference approximation of the above equation, according to that of formulation (ii) will be

$$\frac{\theta_i^{n+1} - \theta_i^n}{\Delta t} + U \frac{\theta_{i+1}^n - \theta_{i-1}^n}{2\Delta x} = \frac{\theta_{i+1}^n - 2\theta_i^n + \theta_{i-1}^n}{(\Delta x)^2} \quad (\text{A.2})$$

The general term of the Fourier series expansion corresponding to the above one-dimensional equation can be written in the form,

$$\mu^{(n)} e^{ikx}$$

The substitution of this general term in Equation (A.1) gives the following relationship between $\mu^{(n+1)}$ and $\mu^{(n)}$;

$$\mu^{(n+1)} = \mu^{(n)} \left[1 - \frac{2\Delta t}{(\Delta x)^2} (1 - \cos k\Delta x) + i \frac{u\Delta t}{\Delta x} \sin k\Delta x \right] \quad (\text{A.3})$$

The amplification factor $\gamma^{(n)}$ (see Section 6.3) is given by

$$\gamma^{(n)} = 1 - \frac{2\Delta t}{(\Delta x)^2} (1 - \cos k\Delta x) + i \frac{u\Delta t}{\Delta x} \sin k\Delta x \quad (\text{A.4})$$

The absolute magnitude of this factor is obtained from

$$|\gamma^{(n)}|^2 = \left[1 - \frac{2\Delta t}{(\Delta x)^2} (1 - \cos k\Delta x) \right]^2 + \left(\frac{u\Delta t}{\Delta x} \right)^2 \sin^2 k\Delta x \quad (\text{A.5})$$

In order to obtain the maximum value of the absolute magnitude of $\gamma^{(n)}$, the right hand side of Equation (A.5) is differentiated with respect to $(k\Delta x)$ to obtain,

$$\frac{4 \Delta t}{(\Delta x)^2} \left[1 - \frac{2\Delta t}{(\Delta x)^2} (1 - \cos k\Delta x) \right] \sin k\Delta x - 2 \left(\frac{u\Delta t}{\Delta x} \right)^2 \sin k\Delta x \cos k\Delta x = 0$$

from which it is clear that $\gamma^{(n)}$ is maximum or minimum if;

$$(1) \quad \sin k_1 \Delta x = 0 \text{ i.e., } \cos k_1 \Delta x = \pm 1 \quad (A.6)$$

or

$$(2) \quad \frac{2\Delta t}{(\Delta x)^2} \left[1 - \frac{2\Delta t}{(\Delta x)^2} (1 - \cos k\Delta x) \right] - \left(\frac{u\Delta t}{\Delta x} \right)^2 \cos k\Delta x = 0 \quad (A.7)$$

The first of these conditions makes $|\lambda_1|$ does not exceed unity provided that

$$\Delta t \leq \frac{2}{(\Delta x)^2} \quad (A.8)$$

From the second condition (A.7), the following is obtained

$$1 - \frac{2\Delta t}{(\Delta x)^2} (1 - \cos k\Delta x) = \left[\frac{\left(\frac{u\Delta t}{\Delta x} \right)^2}{\left(\frac{2\Delta t}{(\Delta x)^2} \right)} \right] \cos k\Delta x \quad (A.9)$$

and

$$\cos k\Delta x = \left[1 - 2\Delta t / (\Delta x)^2 \right] / \left[\frac{u^2 \Delta t}{2} - \frac{2\Delta t}{(\Delta x)^2} \right] \quad (A.10)$$

Substituting Equation (A.9) in (A.5) we get,

$$\begin{aligned} |\gamma|^2 &= \left[\frac{\left(\frac{u\Delta t}{\Delta x} \right)^4}{\left(\frac{2\Delta t}{(\Delta x)^2} \right)^2} \right] \cos^2 k\Delta x + \left(\frac{u\Delta t}{\Delta x} \right)^2 \sin^2 k\Delta x \\ &= \left(\frac{u\Delta t}{\Delta x} \right)^2 \left[1 + \left[\frac{\left(\frac{u\Delta x}{2} \right)^2}{2} - 1 \right] \cos^2 k\Delta x \right] \end{aligned} \quad (A.11)$$

From Equation (A.11), the following conclusions can be made:

(i) If $U \leq \frac{2}{\Delta x}$, $|\gamma| \leq 1$ and inequality (A.8) is sufficient for

the stability of the difference Equation (A.2).

(ii) If $|U| > \frac{2}{\Delta x}$, then let $(\frac{u\Delta x}{2})^2 = 1 + a$ and $\frac{2\Delta t}{(\Delta x)^2} = \epsilon$

therefore

$$\cos k\Delta x = \frac{1-\epsilon}{a\epsilon}$$

and

$$|\gamma|^2 = \left(\frac{1+a}{a}\right) (a\epsilon^2 + (1-\epsilon)^2) \quad (\text{A.12})$$

Before proceeding to find the values of ϵ that makes Equation (A.2) stable, the following observations is made.

(1) For $\epsilon = 1$, i.e., $\Delta t = \frac{\Delta x^2}{2}$; $|\gamma| = (1+a) > 1.0$

These results indicate that if $|U| > \frac{2}{\Delta x}$ inequality (A.8) is not sufficient for the stability because in this case $|\gamma| > 1$.

(2) For $\epsilon = 0$, i.e., $\Delta t = 0$; $|\gamma| = \left(\frac{1+a}{a}\right)^{1/2} > 1.0$

This means that taking Δt very small does not lead to a stable solution.

In order to establish the value of ϵ which makes Equation (A.2) stable, the value of ϵ which makes $|\gamma|^2$ minimum is obtained. Differentiating Equation (A.12) with respect to ϵ the following is obtained

$$\frac{d(|\gamma|^2)}{d\epsilon} = 2 \left(\frac{1+a}{a}\right) [(1+a)\epsilon - 1] \quad (\text{A.13})$$

$$\frac{d^2(|\gamma|^2)}{d\epsilon^2} = 2 \frac{(1+a)^2}{a} > 0 \quad (\text{A.14})$$

Since the second derivative of $(|\gamma|^2)$ with respect to ϵ is positive, the value of ϵ which makes $|\gamma|^2$ minimum is obtained by equating the left hand side of Equation (A.13) to zero. This value of ϵ as well as the value of the corresponding amplification factor are given by

$$|\gamma| = 1$$

$$\epsilon = 1/(1+a)$$

From which Δt will be given by:

$$\Delta t = \frac{2}{U^2} < \frac{\Delta x^2}{2} \quad (\text{A.15})$$

Accordingly there is a unique value of Δt , given by Equation (A.15) which makes this finite-difference formulation stable. Values of Δt which differ from that given by Equation (A.15) lead to instability of the results. For problems with constant coefficients, Equation (A.15) can be satisfied at all nodal points. It also would be satisfied if U is not a function of location. If U assumes different values at different nodal points, Equation (A.15) cannot be satisfied and the method becomes unconditionally unstable if $|U| > \frac{2}{\Delta x}$.

APPENDIX III

THE COMPUTER PROGRAM FOR THE CYLINDER

The computer program used for the cylindrical container with specified time dependent wall temperature is given below. The wall temperature is specified at 7 axial locations $X=0, .208, .375, .542, .708, .875$ and 1.0 . The corresponding temperatures are denoted $T_0, T_1, T_2, T_3, T_4, T_5$ and T_6 respectively. The values of the temperature of each location at consecutive time levels were punched on data cards. These time levels were taken 60, 30 and 20 sec. apart for runs 2, 3 and 4 respectively. Linear interpolation in both space and time directions is used to determine the required values of the temperature at any location and time level.

The program is written in MAD language. The symbols, U, V, T, W and K are the same as in the text. The meaning of the principal symbols which are not defined in the program are given below:

$$DX = \Delta X$$

$$DR = \Delta R$$

$$DT = \Delta \tau$$

M = Number of divisions in the X-direction

N = " " " " " R-direction

G = Acceleration due to gravity, g

NEW = Kinematic viscosity ν

ALPHA = Thermal diffusivity α

BETA = Coefficient of thermal expansion β

PR = Prandtl number

SF = Stream function

ST = The value of the stream function at the previous iteration.

TO = Value of T at the previous time step

WO = " " W " " " " "

TIME = Dimensionless time

TAU = Time in seconds

X_1, X_2, \dots, X_6 correspond to the location of T1, T2, ..., T6.

MAD (01 MAY 1965 VERSION) PROGRAM LISTING ...

```

DIMENSION U(16CC,DIM), V(16CC,DIM), T(16CC,DIM), SF(16CC,DIM),
1 W(16CC,DIM), TO(16CC,DIM), MO(16CC,DIM), ST(16CC,DIM), EI(51),
2 EJ(51), F(51), DI(51), DRI(51), DRII(51)
3 J=DR2(50), DR22(50), DR3(50), DR33(50), DR4(50), DR44(50), R1(50),
4 R2(50), R3(50), R33(50), R4(50), R5(50), A1(50), A2(50), A3(50),
5 B1(51), C2(51), DI(51), CI(16CC,DIM), C3(16CC,DIM),
6 TO(40), T1(40), T2(40), T3(40), T4(40), T5(40), T6(40)
VECTOR VALUES DIM=2, I, O
INTEGER I, J, M, N, NT, NE, NE1, NE2, NE3, NR, NC, H, P, J1, J2, I1, I4, NP, Z
EXECUTE FTAP.
EXECUTE FTAP.
READ AND PRINT DATA
DIM(2)=N+1
EXECUTE ZERO.
1 ..T(M+1, N+1), W(1, 1), ..U(M+1, N+1), V(1, 1), ..V(M+1, N+1), T(1, 1),
2 SF(1, 1), ..SF(M+1, N+1), NE1, NT, TIME, TAU, COUNT
I1=N/2+1
Y=6OVERB
CX=1.7M
CR=1.0/N
DX2=DX*DX
DR2=DR*DR
DYY=2.0*DR2
DXR=CX2/DR2
CRX=CR2/DX2
A1=CRX*Y
A2=DXR/Y
B0=2.*(1+DXR/Y)
B0=2.*(1+DRX*Y)
B0=2.0*PR*Y/DX2+2.0*PR/DR2
CR6=DR2/2.0
CONST=A*A*360/ALPHA
CONST1=Y*PR*G*BEITA*(A.P.3)/NEW/NEW
CONST2=1.0/CONST
CONST3=1.0/CONST1
PRINT RESULTS CONST, CONST2, CONST1, CONST3
EJ(1)=0
THROUGH CG, FER J=2, I, J, G, N+1
A1(J)=DR2*DR2*(J-1)*(J-1)
A2(J)=CX2*DR2*(J-1)*(J-1)/Y/Y
A3(J)=DX2/Y/Y/(J-1)/DR2/2.
C2(J)=1.+1./(2.*(J-1))
D1(J)=B-J-C2(J)*EJ(J-1)
EJ(J)=(1.-1./(2.*(J-1)))/D1(J)
R33(J)=PR*N*N/(J-1)/2.
R1(J)=12*(J-1)*DR2
R2(J)=12*(J-1)*DR*DX
R4(J)=Y*Y*M*M/(J-1)/(J-1)/DR/DR/2
CR11(J)=N*N*(1.-0.5/(J-1))
DR22(J)=N*N*(1.-0.5/(J-1))
CR33(J)=N*N*PR*(1.-0.-1.5/(J-1))
CR44(J)=N*N*PR*(1.-0.-1.5/(J-1))

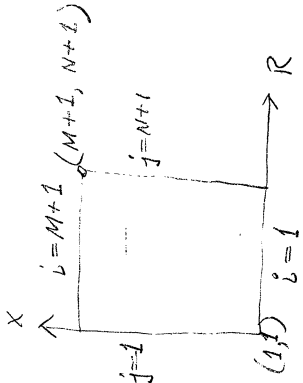
```

START

```

*001
*001
*001
*001
*001
*001
*002
*003
*004
*005
*006
*007
*007
*007
*008
*009
*010
*011
*012
*013
*014
*015
*016
*017
*018
*019
*020
*021
*022
*023
*024
*025
*026
*027
*028
*029
*030
*031
*032
*033
*034
*035
*036
*037
*038
*039
*040
*041
*042
*043
*044
*045

```



```

EI(I)=0
THROUGH VV, FOR I=2,1,I.G.M
VV EI(I)=1./(BI-EI(I-1)) *046
*047
*048
*049
*050
*051
*052
*053
*054
*055
*055
*055
*056
*057
*058
*059
*060
*061
*062
*063
*064
*065
*066
*067
*068
*069
*070
*071
*072
*073
*074
*075
*076
*077
*078
*079
*080
*081
*082
*083
*084
*085
*086
*087
*088
*089
*090
*091
*092
*093
*094
*095
*096
*097
*098
*099
*100
EI(I)=0
THROUGH VV, FOR I=2,1,I.G.M
VV EI(I)=1./(BI-EI(I-1))
READ FORMAT TEMP, T0(0)...T0(P), T1(0)...T1(P), T2(0)...T2(P),
1 T3(0)...T3(P), T4(0)...T4(P), T5(0)...T5(P), T6(0)...T6(P)
PRINT RESULTS T0(0)...T0(P), T1(0)...T1(P), T2(0)...T2(P),
1 T3(0)...T3(P), T4(0)...T4(P), T5(0)...T5(P), T6(0)...T6(P)
WHENEVER CODE .E. 1
READ FORMAT INPUT ,A,ADVERB,PR,QHALL,NI,TIME,
1 T(I,1)...T(M+1,N+1),SF(I,1)...SF(M+1,N+1)
THROUGH JJJ, FOR I=2,1,I.G.M
THROUGH JJJ, FOR J=2,1,J.G.M
JJJ W(I,J)=((SF(I+1,J)-2 *SF(I,J)+SF(I-1,J))*Y+Y/DX2-(SF(I,J+1)-
1 SF(I,J-1))/DR2/(J-1.0)/2+(SF(I,J+1)-2.0*SF(I,J)+SF(I,J-1))/
2 DR2)/DR2/(J-1.0)/(J-1.0)
CODE=2
TRANSFER TO ML
END OF CONDITIONAL
NT=NT+1
SMAX=0
THROUGH CCD, FOR I=2,1,I.G.M+1
THROUGH CCD, FOR J=1,1,J.G.M
S=80+.ABS. U(I,J)/DX+.ABS. V(I,J)/DR
WHENEVER SMAX .L. S, SMAX=S
WHENEVER (SMAX*DT) .G. 0.8, DT=0.80/SMAX
DTO=DT
NPL=IAU/TAU
NP=NPL
WHENEVER N2 .E. 1, TRANSFER TO CONT
WHENEVER NPL .E. NP, TRANSFER TO CONT
WHENEVER ((NP+1-NPL)*TAU/CONST/REQ) .L. DT
DT=(NP+1-NPL)*TAU/CONST/REQ
CRIT=2
END OF CONDITIONAL
DX1=DT/DX
THROUGH CD, FOR J=2,1, J.G.M+1
DR1(J)=DR1(J)*DT
DR2(J)=DR2(J)*DT
DR3(J)=DR3(J)*DT
R3(J)=R3(J)*DT
DR4(J)=DR4(J)*DT
DX3=M*M*Y*Y*CT
CR3=N*N*DT
DR4=N*DT
DR5=4.*DR3
CR1=2.*DR3
CX5=2.*DX3
DX7=DX3*PR
CR7=CR3*PR
C1=1.0-DX5-DR5
C2=1.0-DX5-DR1
C3=1.0-2.0*DX7-2.0*DR7
CS=2*Q*DT/DR+Q*DT
TIME=TIME+FREQ*DT
TAU=TIME * CONST
Z1=TAU/TAU2
Z=Z1
THROUGH STEPI, FOR I=1,1,I.G.M+1
X=(I-1.0)*DX
WHENEVER X.LE.X1

```

```

T(I,N+1)=(TO(Z)*(X1-X)+T1(Z)*X)*(Z+1-C-Z1)/X1+
1 (TO(Z+1)*(X1-X)+T1(Z+1)*X)*(Z1-Z)/X1
UR WHENEVER X.G. X1 .AND. X.LE. X2
T(I,N+1)=(T1(Z)*(X2-X)+T2(Z)*(X-X1))*(Z+1.0-Z1)/(X2-X1)+
1 (T1(Z+1)*(X2-X)+T2(Z+1)*(X-X1))*(Z1-Z)/(X2-X1)
OR WHENEVER X.G. X2 .AND. X .LE. X3
T(I,N+1)=(T2(Z)*(X3-X)+T3(Z)*(X-X2))*(Z+1.0-Z1)/(X3-X2)
1 +(T2(Z+1)*(X3-X)+T3(Z+1)*(X-X2))*(Z1-Z)/(X3-X2)
GR WHENEVER X.G. X3 .AND. X.LE. X4
T(I,N+1)=(T3(Z)*(X4-X)+T4(Z)*(X-X3))*(Z+1.0-Z1)/(X4-X3)+
1 (T3(Z+1)*(X4-X)+T4(Z+1)*(X-X3))*(Z1-Z)/(X4-X3)
OR WHENEVER X.G. X4 .AND. X .LE. X5
T(I,N+1)=(T4(Z)*(X5-X)+T5(Z)*(X-X4))*(Z+1.0-Z1)/(X5-X4)+
1 (T4(Z+1)*(X5-X)+T5(Z+1)*(X-X4))*(Z1-Z)/(X5-X4)
OTHERWISE
T(I,N+1)=(T5(Z)*(1.0-X)+T6(Z)*(X-X5))*(Z+1.0-Z1)/(1.0-X5)+
1 (T5(Z+1)*(1.0-X)+T6(Z+1)*(X-X5))*(Z1-Z)/(1.0-X5)
END OF CONDITIONAL
STEP 1
T(I,N+1)=T(I,N+1)*CUNST1
THROUGH BBB, FOR I=2,1,I.G.M+1
THROUGH BA ,FOR J=1,1,J.G. N+1
W0(I,J)=W(I,J)
T0(I,J)=T(I,J)
C1(I,J)=U(I,J)*DX1
C3(I,J)=V(I,J)*DR4
COUNT=COUNT+1
THROUGH BA, FOR I=1,1,I.G.M+1
THROUGH BA ,FOR J=1,1,J.G. N+1
W0(I,J)=W(I,J)
T0(I,J)=T(I,J)
THROUGH BB, FOR J=2,1,J.G.N
WHENEVER V(M+1,J) .GE. 0
D=(TO(M+1,J-1)-TO(M+1,J))*C3(M+1,J)
OTHERWISE
D=(TO(M+1,J)-TO(M+1,J+1))*C3(M+1,J)
END OF CONDITIONAL
BB
1 +TO(M+1,J)=TO(M+1,J)*C2+TO(M,J)*DX5+TO(M+1,J-1)*DR1(J)
T(M+1,1)=TO(M+1,1)*DR2(J)+D
T(M+1,1)=TO(M+1,1)*C1+TO(M,1)*DX5+TO(M+1,2)*DR5
T(1,1)=TO(1,1)*C1+TO(1,2)*DX5+TO(2,1)*DR5
THROUGH PD, FOR I=2,1,I.G.M
WHENEVER U(I,1) .G. 0
C=(TO(I-1,1)-TO(I,1))*C1(I,1)
OTHERWISE
C=(TO(I,1)-TO(I+1,1))*C1(I,1)
END OF CONDITIONAL
DD
T(1,1)=TO(I,1)*C1+TO(1,2)*DR5+(TO(I+1,1)+TO(I-1,1))*DX3 +C
THROUGH EE, FOR J=2,1,J.G.N
T(1,J)=TO(1,J)*C2+TO(2,J)*DX5+TO(1,J-1)*DR1(J)
1 +TO(1,J+1)*DR2(J)
THROUGH FF, FOR J=2,1,J.G.N
THROUGH FF, FOR I=2,1,I.G.M
WHENEVER U(I,J) .G. C
C=(TO(I-1,J)-TO(I,J))*C1(I,J)
OTHERWISE
C=(TO(I,J)-TO(I+1,J))*C1(I,J)
END OF CONDITIONAL
WHENEVER V(I,J) .G. C
D=(TO(I,J-1)-TO(I,J))*C3(I,J)
OTHERWISE
D=(TO(I,J)-TO(I+1,J))*C3(I,J)
END OF CONDITIONAL
151 C1
152 C2
153 C1
154 C1
155 C1
156 C1
157 C1
158 C1
159 C1
160 C1
161 C1
162 C1
163 C1
164 C1
165 C1
166 C1
167 C1
168 C1
169 C1
170 C1
171 C1
172 C1
173 C1
174 C1
175 C1
176 C1
177 C1
178 C1
179 C1
180 C1
181 C1
182 C1
183 C1
184 C1
185 C1
186 C1
187 C1
188 C1
189 C1
190 C1
191 C1
192 C1
193 C1
194 C1
195 C1
196 C1
197 C1
198 C1
199 C1
200 C1
201 C1
202 C1
203 C1
204 C1
205 C1
206 C1
207 C1
208 C1
209 C1
210 C1
211 C1
212 C1
213 C1
214 C1
215 C1
216 C1
217 C1
218 C1
219 C1
220 C1
221 C1
222 C1
223 C1
224 C1
225 C1
226 C1
227 C1
228 C1
229 C1
230 C1
231 C1
232 C1
233 C1
234 C1
235 C1
236 C1
237 C1
238 C1
239 C1
240 C1
241 C1
242 C1
243 C1
244 C1
245 C1
246 C1
247 C1
248 C1
249 C1
250 C1
251 C1
252 C1
253 C1
254 C1
255 C1
256 C1
257 C1
258 C1
259 C1
260 C1
261 C1
262 C1
263 C1
264 C1
265 C1
266 C1
267 C1
268 C1
269 C1
270 C1
271 C1
272 C1
273 C1
274 C1
275 C1
276 C1
277 C1
278 C1
279 C1
280 C1
281 C1
282 C1
283 C1
284 C1
285 C1
286 C1
287 C1
288 C1
289 C1
290 C1
291 C1
292 C1
293 C1
294 C1
295 C1
296 C1
297 C1
298 C1
299 C1
300 C1
301 C1
302 C1
303 C1
304 C1
305 C1
306 C1
307 C1
308 C1
309 C1
310 C1
311 C1
312 C1
313 C1
314 C1
315 C1
316 C1
317 C1
318 C1
319 C1
320 C1
321 C1
322 C1
323 C1
324 C1
325 C1
326 C1
327 C1
328 C1
329 C1
330 C1
331 C1
332 C1
333 C1
334 C1
335 C1
336 C1
337 C1
338 C1
339 C1
340 C1
341 C1
342 C1
343 C1
344 C1
345 C1
346 C1
347 C1
348 C1
349 C1
350 C1
351 C1
352 C1
353 C1
354 C1
355 C1
356 C1
357 C1
358 C1
359 C1
360 C1
361 C1
362 C1
363 C1
364 C1
365 C1
366 C1
367 C1
368 C1
369 C1
370 C1
371 C1
372 C1
373 C1
374 C1
375 C1
376 C1
377 C1
378 C1
379 C1
380 C1
381 C1
382 C1
383 C1
384 C1
385 C1
386 C1
387 C1
388 C1
389 C1
390 C1
391 C1
392 C1
393 C1
394 C1
395 C1
396 C1
397 C1
398 C1
399 C1
400 C1
401 C1
402 C1
403 C1
404 C1
405 C1
406 C1
407 C1
408 C1
409 C1
410 C1
411 C1
412 C1
413 C1
414 C1
415 C1
416 C1
417 C1
418 C1
419 C1
420 C1
421 C1
422 C1
423 C1
424 C1
425 C1
426 C1
427 C1
428 C1
429 C1
430 C1
431 C1
432 C1
433 C1
434 C1
435 C1
436 C1
437 C1
438 C1
439 C1
440 C1
441 C1
442 C1
443 C1
444 C1
445 C1
446 C1
447 C1
448 C1
449 C1
450 C1
451 C1
452 C1
453 C1
454 C1
455 C1
456 C1
457 C1
458 C1
459 C1
460 C1
461 C1
462 C1
463 C1
464 C1
465 C1
466 C1
467 C1
468 C1
469 C1
470 C1
471 C1
472 C1
473 C1
474 C1
475 C1
476 C1
477 C1
478 C1
479 C1
480 C1
481 C1
482 C1
483 C1
484 C1
485 C1
486 C1
487 C1
488 C1
489 C1
490 C1
491 C1
492 C1
493 C1
494 C1
495 C1
496 C1
497 C1
498 C1
499 C1
500 C1
501 C1
502 C1
503 C1
504 C1
505 C1
506 C1
507 C1
508 C1
509 C1
510 C1
511 C1
512 C1
513 C1
514 C1
515 C1
516 C1
517 C1
518 C1
519 C1
520 C1
521 C1
522 C1
523 C1
524 C1
525 C1
526 C1
527 C1
528 C1
529 C1
530 C1
531 C1
532 C1
533 C1
534 C1
535 C1
536 C1
537 C1
538 C1
539 C1
540 C1
541 C1
542 C1
543 C1
544 C1
545 C1
546 C1
547 C1
548 C1
549 C1
550 C1
551 C1
552 C1
553 C1
554 C1
555 C1
556 C1
557 C1
558 C1
559 C1
560 C1
561 C1
562 C1
563 C1
564 C1
565 C1
566 C1
567 C1
568 C1
569 C1
570 C1
571 C1
572 C1
573 C1
574 C1
575 C1
576 C1
577 C1
578 C1
579 C1
580 C1
581 C1
582 C1
583 C1
584 C1
585 C1
586 C1
587 C1
588 C1
589 C1
590 C1
591 C1
592 C1
593 C1
594 C1
595 C1
596 C1
597 C1
598 C1
599 C1
600 C1
601 C1
602 C1
603 C1
604 C1
605 C1
606 C1
607 C1
608 C1
609 C1
610 C1
611 C1
612 C1
613 C1
614 C1
615 C1
616 C1
617 C1
618 C1
619 C1
620 C1
621 C1
622 C1
623 C1
624 C1
625 C1
626 C1
627 C1
628 C1
629 C1
630 C1
631 C1
632 C1
633 C1
634 C1
635 C1
636 C1
637 C1
638 C1
639 C1
640 C1
641 C1
642 C1
643 C1
644 C1
645 C1
646 C1
647 C1
648 C1
649 C1
650 C1
651 C1
652 C1
653 C1
654 C1
655 C1
656 C1
657 C1
658 C1
659 C1
660 C1
661 C1
662 C1
663 C1
664 C1
665 C1
666 C1
667 C1
668 C1
669 C1
670 C1
671 C1
672 C1
673 C1
674 C1
675 C1
676 C1
677 C1
678 C1
679 C1
680 C1
681 C1
682 C1
683 C1
684 C1
685 C1
686 C1
687 C1
688 C1
689 C1
690 C1
691 C1
692 C1
693 C1
694 C1
695 C1
696 C1
697 C1
698 C1
699 C1
700 C1
701 C1
702 C1
703 C1
704 C1
705 C1
706 C1
707 C1
708 C1
709 C1
710 C1
711 C1
712 C1
713 C1
714 C1
715 C1
716 C1
717 C1
718 C1
719 C1
720 C1
721 C1
722 C1
723 C1
724 C1
725 C1
726 C1
727 C1
728 C1
729 C1
730 C1
731 C1
732 C1
733 C1
734 C1
735 C1
736 C1
737 C1
738 C1
739 C1
740 C1
741 C1
742 C1
743 C1
744 C1
745 C1
746 C1
747 C1
748 C1
749 C1
750 C1
751 C1
752 C1
753 C1
754 C1
755 C1
756 C1
757 C1
758 C1
759 C1
760 C1
761 C1
762 C1
763 C1
764 C1
765 C1
766 C1
767 C1
768 C1
769 C1
770 C1
771 C1
772 C1
773 C1
774 C1
775 C1
776 C1
777 C1
778 C1
779 C1
780 C1
781 C1
782 C1
783 C1
784 C1
785 C1
786 C1
787 C1
788 C1
789 C1
790 C1
791 C1
792 C1
793 C1
794 C1
795 C1
796 C1
797 C1
798 C1
799 C1
800 C1
801 C1
802 C1
803 C1
804 C1
805 C1
806 C1
807 C1
808 C1
809 C1
810 C1
811 C1
812 C1
813 C1
814 C1
815 C1
816 C1
817 C1
818 C1
819 C1
820 C1
821 C1
822 C1
823 C1
824 C1
825 C1
826 C1
827 C1
828 C1
829 C1
830 C1
831 C1
832 C1
833 C1
834 C1
835 C1
836 C1
837 C1
838 C1
839 C1
840 C1
841 C1
842 C1
843 C1
844 C1
845 C1
846 C1
847 C1
848 C1
849 C1
850 C1
851 C1
852 C1
853 C1
854 C1
855 C1
856 C1
857 C1
858 C1
859 C1
860 C1
861 C1
862 C1
863 C1
864 C1
865 C1
866 C1
867 C1
868 C1
869 C1
870 C1
871 C1
872 C1
873 C1
874 C1
875 C1
876 C1
877 C1
878 C1
879 C1
880 C1
881 C1
882 C1
883 C1
884 C1
885 C1
886 C1
887 C1
888 C1
889 C1
890 C1
891 C1
892 C1
893 C1
894 C1
895 C1
896 C1
897 C1
898 C1
899 C1
900 C1
901 C1
902 C1
903 C1
904 C1
905 C1
906 C1
907 C1
908 C1
909 C1
910 C1
911 C1
912 C1
913 C1
914 C1
915 C1
916 C1
917 C1
918 C1
919 C1
920 C1
921 C1
922 C1
923 C1
924 C1
925 C1
926 C1
927 C1
928 C1
929 C1
930 C1
931 C1
932 C1
933 C1
934 C1
935 C1
936 C1
937 C1
938 C1
939 C1
940 C1
941 C1
942 C1
943 C1
944 C1
945 C1
946 C1
947 C1
948 C1
949 C1
950 C1
951 C1
952 C1
953 C1
954 C1
955 C1
956 C1
957 C1
958 C1
959 C1
960 C1
961 C1
962 C1
963 C1
964 C1
965 C1
966 C1
967 C1
968 C1
969 C1
970 C1
971 C1
972 C1
973 C1
974 C1
975 C1
976 C1
977 C1
978 C1
979 C1
980 C1
981 C1
982 C1
983 C1
984 C1
985 C1
986 C1
987 C1
988 C1
989 C1
990 C1
991 C1
992 C1
993 C1
994 C1
995 C1
996 C1
997 C1
998 C1
999 C1
1000 C1

```

```

FF      T(I,J)= TO(I,J)*C2+(TO(I+1,J)+TG(I-1,J))*DX3+      *153      02
1      TO(I,J-1)*DR1(J)+TO(I,J+1)*DR2(J)+C+D      *154
      THROUGH GGG, FOR I=2,1, I.G.M
      THROUGH GGG, FOR J=2,1, J.G.N
FI=R3(J)*(T(I,J+1)-T(I,J-1))      *155      02
      WHENEVER U(I,J) .G. 0      *156      02
C=(WG(I-1,J)-WO(I,J))*C1(I,J)      *157      02
      OTHERWISE      *158      02
      *159      02
C=(WG(I,J)-WO(I+1,J))*C1(I,J)      *160      02
      END OF CONDITIONAL      *161      02
      WHENEVER V(I,J) .G. 0      *162      02
D=(WO(I,J-1)-WO(I,J))*C3(I,J)      *163      02
      OTHERWISE      *164      02
      *165      02
D=(WO(I,J)-WO(I+1,J))*C3(I,J)      *166      02
      END OF CONDITIONAL      *167      02
GGG      W(I,J)=WO(I,J)*C3+(WO(I+1,J)+WO(I-1,J))*DX7+C+D +
1      WC(I,J-1)*DR3(J)+WO(I,J+1)*DK4(J)+FI      *168
      NEI=0      *169
      WHENEVER NEI .G. NE , TRANSFER TO PRINT      *170
      I=1      *171
      I=I+1      *172
      F(I)=0      *173
      THROUGH LM, FOR J=2,1, J.G.N      *174
DI(J)=(SF(I+1,J)+SF(I-1,J))*A1-W(I,J)*A1(J)      *175      01
      F(J)=(DI(J)+F(J-1)*C2(J))/D1(J)      *176      01
      THROUGH LN, FOR J=1,1, J.G.N-1      *177
      H=N+1-J      *178
      SF(I,H)=EJ(H)*SF(I,H+1)+F(H)      *179
      ST(I,H)=SF(I,H)      *180
      WHENEVER I.L.M, TRANSFER TO II      *181
      J=1      *182
      J=J+1      *183
      THROUGH MM, FOR I=2,1, I.G.M      *184
DI(I)=(SF(I,J+1)+SF(I,J-1))*A2-W(I,J)*A2(J)-(SF(I,J+1)-SF(I,J
1 -1))*A3(J)      *185
      F(I)=(DI(I)+F(I-1))*EI(I)      *186
      THROUGH NN, FOR I=1,1, I.G.M-1      *187
      H=N+1-I      *188
      SF(H,J)=EI(H)*SF(H+1,J)+F(H)      *189
      WHENEVER J.L.N, TRANSFER TO HH      *190
      WHENEVER NT .E. 1 .AND. NEI .E. 1, TRANSFER TO JJ      *191
      RMAX=0      *192
      THROUGH AAA, FOR I=2, NR, I.G.M      *193
      THROUGH AAA, FOR J=2, NR, J.G.N      *194
R3=ABS.((SF(I,J)-ST(I,J))/(ST(I,J)+I.CE-20))      *195
      WHENEVER RMAX .L. R3 , RMAX=R3      *196
      THROUGH LL, FOR I=2,1, I.G.M      *197
      THROUGH LL, FOR J=2,1, J.G.N      *198
      ST(I,J)=SF(I,J)      *199
      WHENEVER RMAX .G. EPSLGN , TRANSFER TO JJ      *200
      THROUGH BEE, FOR I=2,1, I.G.M      *201
      W(I,N+1)=(-SF(I,N-1)+8.C*SFI(N))/DYY      *202
      THROUGH CEE , FOR J=2,1, J.G.N      *203
      W(I,J)=(-SF(3,J)+8.0*SFI(2,J))*R4(J)      *204
      WHENEVER COUNT .L. FREQ, TRANSFER TO BEGIN      *205
      THROUGH BE , FOR I=2,1, I.G.M      *206
      U(I,N)=2.0*(3.0*SFI(N)-6.0*SFI(N-1)+SF(I,N-2))/RI(N)      *207
      U(I,1)=SF(I,2)/DR6      *208
      U(I,2)=2.0*(6.0*SFI(3)-3.0*SFI(2)-SF(I,4))/RI(2)      *209

```



```

      THROUGH BF, FOR J=2,1,J.G.N
      V(2,J)=2.0*(SF(4,J)-6.C*SF(3,J)+3.0*SF(2,J))/R2(J)
      V(M,J)=2.0*(6.C*SF(M-1,J)-3.C*SF(M,J)-SF(M-2,J))/R2(J)
      V(M+1,J)=2.0*(8*SF(M,J)-SF(M-1,J))/R2(J)
      THROUGH BBETA, FOR I=2,1,I.G.M
      THROUGH BBETA, FOR J=3,1,J.G.N-1
      U(I,J)=(SF(I,J-2)-8*SF(I,J-1)+8*SF(I,J+1))-SF(I,J+2))/R1(J)
      THROUGH BETA, FOR I=3,1,I.G.M-1
      THROUGH BETA, FOR J=2,1,J.G.N
      V(I,J)=(SF(I+2,J)-8*SF(I+1,J)+8*SF(I-1,J)-SF(I-2,J))/R2(J)
      N2=0
      WHENEVER NT.L.N1,TRANSFER TO PRINT
      WHENEVER NT .E.NMAX
      PUNCH FORMAT CDATA,A,ADVERB,PR,QWALL,NT,TIME,
      1 T(1,1),..T(M+1,N+1),SF(1,1),..SF(M+1,N+1)
      TRANSFER TO PRINT
      END OF CONDITIONAL
      WHENEVER CRIT .L. 2,TRANSFER TO BACK
      CRIT=0
      CT=DT0
      N2=1
      UR=U(I1,I)*R1(I)/2.0
      THROUGH DAL, FOR J=2,1,J.G.N+1
      UR=(UR+U(I1,J)*R1(J))/12.0
      WHENEVER NT .L. NC,TRANSFER TO NEXT
      R1=0
      THROUGH YZ, FOR I=2,1,I.G.M
      THROUGH YZ, FOR J=2,1,J.G.N+1
      R2=-ABS.(T(I,J)-T(I,J))/TU(I,J)
      WHENEVER R1 .L. R2, RI=R2
      PRINT RESULTS NT,TIME,U(I,1),..U(M+1,N+1),V(1,1),..V(M+1,N+1)
      1 T(1,1),..T(M+1,N+1),SF(1,1),..SF(M+1,N+1),RMAX,NEI,RI,
      2 UR,TAU,DT
      WHENEVER NEI .G. NE, TRANSFER TO END
      WHENEVER NT .E. NMAX, TRANSFER TO END
      WHENEVER NT .L. NMAX,TRANSFER TO BACK
      CONTINUE
      TRANSFER TO START
      VECTOR VALUES INPUT=#3F12.4,F12.2,I15, F15.8/(5E16.8)**$
      VECTOR VALUES CDATA=#3F12.4,F12.2,I15, F15.8/(5E16.8)**$
      VECTOR VALUES TEMP=#(10F8.2)**$
      END OF PROGRAM
  
```

```

*21C
*211 01
*212 01
*213 01
*214
*215 01
*216 02
*217
*218 01
*219 02
*220
*221
*222
*223 01
*224
*225 01
*226 01
*227
*228
*229
*230
*231
*232 01
*233
*234
*235
*236 01
*237 02
*238 02
*239
*240
*241
*242
*243
*244
*245
*246
*247
*248
  
```

THE FOLLOWING NAMES HAVE OCCURRED ONLY ONCE IN THIS PROGRAM.
 COMPILATION WILL CONTINUE.

```

ALPHA *025
EPSLON *200
K *024
N1 *221
NC *233
QS *093
TAU2 *096
  
```

APPENDIX IV

TYPICAL PRINTED COMPUTER OUTPUT

The computed values of the dimensionless temperature and stream function for run number 2 at time level 60 sec. are given in the following pages.

T(1,1)....T(31,31)

4.986519E-05	1.875870E-06	1.483765E-06	1.668992E-06	1.854089E-06	2.035122E-06	2.227993E-06	2.457666E-06
2.807596E-06	3.779240E-06	8.679883E-06	3.876686E-05	2.246500E-04	1.329615E-03	7.583625E-03	4.115459E-02
2.115950E-01	1.027921E 00	4.706631E 00	2.026227E 01	8.181097E 01	3.090257E 02	1.089354E 03	3.5755376E 03
1.090306E 04	3.084119E 04	8.084106E 04	1.963176E 05	4.416436E 05	9.142385E 05	1.726356E 06	
5.073709E-04	9.376217E-04	5.936854E-04	6.474779E-04	6.923155E-04	7.314368E-04	7.707614E-04	8.155870E-04
8.699919E-04	9.372056E-04	1.020082E-03	1.121449E-03	1.244655E-03	1.396459E-03	1.603136E-03	1.990950E-03
3.154955E-03	7.731065E-03	2.665002E-02	1.023398E-01	3.888749E-01	1.409942E 00	4.841561E 00	1.587742E 01
5.186491E 01	1.955916E 02	1.150565E 03	1.148111E 04	1.436132E 05	6.242463E 05	1.693156E 06	
2.219295E-02	2.317021E-02	2.477688E-02	2.599852E-02	2.665495E-02	2.694893E-02	2.714259E-02	2.742905E-02
2.792172E-02	2.867887E-02	2.972654E-02	3.107003E-02	3.249385E-02	3.455150E-02	3.654932E-02	3.854252E-02
4.041999E-02	4.255022E-02	4.746299E-02	6.538655E-02	1.308663E-01	3.542988E-01	1.107792E 00	4.007297E 00
1.937378E 01	1.357911E 02	1.231331E 03	1.232056E 04	1.138308E 05	5.823801E 05	1.659957E 06	
3.911761E-01	3.934808E-01	4.097628E-01	4.159375E-01	4.111130E-01	4.000334E-01	3.875142E-01	3.766015E-01
3.687197E-01	3.642824E-01	3.631728E-01	3.649900E-01	3.691053E-01	3.745844E-01	3.800249E-01	3.834055E-01
3.822851E-01	3.754494E-01	3.692467E-01	3.973350E-01	5.763411E-01	1.260356E 00	3.537248E 00	1.150041E 01
4.706382E 01	2.659759E 02	1.928488E 03	1.537437E 04	1.147249E 05	5.804031E 05	1.626758E 06	
3.949616E 00	4.036788E 00	4.107155E 00	4.048404E 00	3.873720E 00	3.644043E 00	3.411524E 00	3.204943E 00
3.034758E 00	2.901198E 00	2.799901E 00	2.724681E 00	2.668355E 00	2.622398E 00	2.575963E 00	2.514800E 00
2.421323E 00	2.279421E 00	2.093326E 00	1.942583E 00	2.122891E 00	3.498456E 00	8.518221E 00	2.538394E 01
9.246991E 01	4.487325E 02	2.782015E 03	1.894511E 04	1.224343E 05	5.877104E 05	1.593559E 06	
2.862429E 01	2.920265E 01	2.910990E 01	2.795733E 01	2.599425E 01	2.373706E 01	2.157115E 01	1.968090E 01
1.811180E 01	1.684022E 01	1.581712E 01	1.498808E 01	1.429916E 01	1.369526E 01	1.311510E 01	1.248554E 01
1.171959E 01	1.072910E 01	9.476485E 00	8.113177E 00	7.290682E 00	8.834214E 00	1.747642E 01	4.742934E 01
1.580972E 02	6.831323E 02	3.752693E 03	2.273269E 04	1.321015E 05	5.971881E 05	1.560360E 06	
1.591673E 02	1.600162E 02	1.566870E 02	1.470834E 02	1.333578E 02	1.186813E 02	1.051457E 02	9.359733E 01
8.411500E 01	7.644131E 01	7.022683E 01	6.513235E 01	6.085374E 01	5.711138E 01	5.362550E 01	5.008950E 01
4.615597E 01	4.146701E 01	3.579220E 01	2.937185E 01	2.357593E 01	2.205425E 01	3.326196E 01	7.967660E 01
2.460666E 02	9.699611E 02	4.821326E 03	2.659977E 04	1.420766E 05	6.059106E 05	1.527161E 06	
6.892518E 02	6.883233E 02	6.638028E 02	6.108951E 02	5.420241E 02	4.720292E 02	4.095807E 02	3.574921E 02
3.153613E 02	2.815819E 02	2.543657E 02	2.321222E 02	2.135191E 02	1.974153E 02	1.827505E 02	1.684346E 02
1.532797E 02	1.360635E 02	1.158885E 02	9.303888E 01	7.039588E 01	5.526555E 01	6.237986E 01	1.252746E 02
3.575883E 02	1.306383E 03	5.964570E 03	3.045207E 04	1.517136E 05	6.138644E 05	1.515701E 06	
2.382173E 03	2.365781E 03	2.253084E 03	2.039077E 03	1.776918E 03	1.521033E 03	1.299339E 03	1.118317E 03
9.740867E 02	8.596356E 02	7.680852E 02	6.936945E 02	6.318818E 02	5.788965E 02	5.314012E 02	4.860813E 02
4.393883E 02	3.876593E 02	3.280337E 02	2.605898E 02	1.914752E 02	1.356806E 02	1.192325E 02	1.906863E 02
4.948953E 02	1.689328E 03	7.175074E 03	3.428310E 04	1.609604E 05	6.215869E 05	1.511107E 06	
6.632483E 03	6.561933E 03	6.189009E 03	5.525337E 03	4.747567E 03	4.014504E 03	3.396311E 03	2.901331E 03
2.512198E 03	2.206110E 03	1.962717E 03	1.765891E 03	1.603201E 03	1.464722E 03	1.341740E 03	1.225611E 03
1.106984E 03	9.760663E 02	8.249359E 02	6.527816E 02	4.729545E 02	3.169747E 02	2.323304E 02	2.888476E 02
6.634728E 02	2.121680E 03	8.455840E 03	3.811264E 04	1.698755E 05	6.291898E 05	1.506512E 06	

1.507050E 04	1.485364E 04	1.391096E 04	1.228957E 04	1.045645E 04	8.783257E 03	7.407506E 03	6.325361E 03
5.484177E 03	4.826930E 03	4.306466E 03	3.886955E 03	3.541519E 03	3.248814E 03	2.989744E 03	2.744493E 03
2.491632E 03	2.206875E 03	1.870835E 03	1.480520E 03	1.065307E 03	6.923451E 02	4.510989E 02	4.426195E 02
8.735463E 02	2.609825E 03	9.815120E 03	4.196610E 04	1.785239E 05	6.366716E 05	1.501918E 06	
2.845147E 04	2.797354E 04	2.606511E 04	2.286134E 04	1.935831E 04	1.625311E 04	1.375651E 04	1.182265E 04
1.033372E 04	9.177261E 03	8.265854E 03	7.534675E 03	6.935715E 03	6.430594E 03	5.983036E 03	5.553055E 03
5.093243E 04	4.550990E 03	3.882279E 03	3.079712E 03	2.207068E 03	1.406504E 03	8.505167E 02	6.871319E 02
1.142343E 03	3.166643E 03	1.127090E 04	4.588673E 04	1.870144E 05	6.441383E 05	1.497323E 06	
4.597481E 04	4.513432E 04	4.191690E 04	3.661146E 04	3.099386E 04	2.615765E 04	2.235598E 04	1.945688E 04
1.724787E 04	1.554558E 04	1.421444E 04	1.315765E 04	1.230315E 04	1.159019E 04	1.056635E 04	1.032582E 04
9.603731E 03	8.682167E 03	7.469612E 03	5.949884E 03	4.252678E 03	2.668096E 03	1.532329E 03	1.068915E 03
1.494689E 03	3.812502E 03	1.285017E 04	4.992711E 04	1.954519E 05	6.515141E 05	1.489283E 06	
6.576712E 04	6.453924E 04	5.985735E 04	5.221910E 04	4.436404E 04	3.779731E 04	3.276418E 04	2.900489E 04
2.619193E 04	2.406396E 04	2.243615E 04	2.117914E 04	2.019498E 04	1.939448E 04	1.867556E 04	1.790464E 04
1.690755E 04	1.548302E 04	1.345486E 04	1.078637E 04	7.711191E 03	4.776637E 03	2.631073E 03	1.643201E 03
1.961629E 03	4.574082E 03	1.458466E 04	5.413452E 04	2.038992E 05	6.587184E 05	1.480094E 06	
8.597026E 04	8.443524E 04	7.838039E 04	6.851335E 04	5.861375E 04	5.057920E 04	4.460504E 04	4.027913E 04
3.715066E 04	3.487937E 04	3.323242E 04	3.204910E 04	3.120450E 04	3.057363E 04	2.995538E 04	2.924431E 04
2.801194E 04	2.596113E 04	2.280262E 04	1.846581E 04	1.329481E 04	8.194217E 03	4.354438E 03	2.479723E 03
2.580231E 03	5.485148E 03	1.651212E 04	5.855718E 04	2.124132E 05	6.657476E 05	1.470905E 06	
1.053935E 05	1.037331E 05	9.663115E 04	8.491296E 04	7.337764E 04	6.429744E 04	5.780422E 04	5.332862E 04
5.029438E 04	4.828072E 04	4.700457E 04	4.627475E 04	4.594092E 04	4.583854E 04	4.572920E 04	4.525221E 04
4.391761E 04	4.117371E 04	3.656836E 04	2.999220E 04	2.194342E 04	1.368671E 04	7.117163E 03	3.707162E 03
3.399991E 03	6.590170E 03	1.868123E 04	6.325463E 04	2.210733E 05	6.726876E 05	1.461717E 06	
1.236074E 05	1.220508E 05	1.144078E 05	1.013958E 05	8.874820E 04	7.911898E 04	7.259426E 04	6.845365E 04
6.598991E 04	6.468891E 04	6.421125E 04	6.433272E 04	6.490270E 04	6.571412E 04	6.645049E 04	6.658502E 04
6.538064E 04	6.200342E 04	5.576594E 04	4.647006E 04	3.476468E 04	2.235734E 04	1.181684E 04	5.675373E 03
4.511068E 03	7.952025E 03	2.116105E 04	6.831549E 04	2.300258E 05	6.800810E 05	1.452528E 06	
1.407058E 05	1.395207E 05	1.319635E 05	1.183190E 05	1.051344E 05	9.548232E 04	8.944270E 04	8.614841E 04
8.474131E 04	8.459037E 04	8.528572E 04	8.658937E 04	8.835503E 04	9.039971E 04	9.234262E 04	9.347776E 04
9.276722E 04	8.901013E 04	8.118360E 04	6.890424E 04	5.290836E 04	3.535897E 04	1.965760E 04	9.3558043E 03
6.177363E 03	9.683365E 03	2.409333E 04	7.401893E 04	2.400002E 05	6.902092E 05	1.450139E 06	
1.572220E 05	1.566526E 05	1.498789E 05	1.363126E 05	1.231959E 05	1.140610E 05	1.090267E 05	1.070733E 05
1.071594E 05	1.085019E 05	1.106050E 05	1.132320E 05	1.163127E 05	1.197542E 05	1.231835E 05	1.257363E 05
1.260304E 05	1.223941E 05	1.133242E 05	9.809713E 04	7.741763E 04	5.387650E 04	3.178205E 04	1.600241E 04
9.480711E 03	1.216272E 04	2.786273E 04	8.178581E 04	2.556355E 05	7.046463E 05	1.450139E 06	
1.743010E 05	1.745153E 05	1.692635E 05	1.564048E 05	1.439526E 05	1.358764E 05	1.323202E 05	1.321057E 05
1.339898E 05	1.370065E 05	1.405222E 05	1.444084E 05	1.486549E 05	1.534117E 05	1.584445E 05	1.628078E 05
1.647519E 05	1.620061E 05	1.523842E 05	1.346020E 05	1.091592E 05	7.899571E 04	4.944220E 04	2.688254E 04
1.594711E 04	1.763135E 04	3.578658E 04	9.581002E 04	2.781325E 05	7.233091E 05	1.450139E 06	

1.960514E 05	1.950731E 05	1.811142E 05	1.693788E 05	1.627723E 05	1.608909E 05	1.624999E 05
1.602036E 05	1.708422E 05	1.803919E 05	1.853477E 05	1.909969E 05	1.974582E 05	2.038820E 05
2.081848E 05	2.073541E 05	1.982569E 05	1.488832E 05	1.118249E 05	7.397056E 04	4.351341E 04
2.720542E 04	2.771211E 04	4.955327E 04	3.076567E 05	7.455454E 05	1.450139E 06	
2.224882E 05	2.234217E 05	2.227119E 05	2.051448E 05	1.990178E 05	1.977490E 05	2.003030E 05
2.51895E 05	2.110263E 05	2.167122E 05	2.267564E 05	2.397027E 05	2.397027E 05	2.480669E 05
2.553217E 05	2.576120E 05	2.505436E 05	1.973794E 05	1.536529E 05	1.069618E 05	6.761688E 04
4.511175E 04	4.439123E 04	7.093760E 04	3.435002E 05	7.700374E 05	1.450139E 06	
2.897178E 05	2.878614E 05	2.812820E 05	2.625082E 05	2.546744E 05	2.501575E 05	2.500054E 05
2.536555E 05	2.593216E 05	2.651179E 05	2.740361E 05	2.786383E 05	2.853901E 05	2.948618E 05
3.031740E 05	3.117323E 05	3.085984E 05	2.956335E 05	2.062523E 05	1.505869E 05	1.012597E 05
7.133124E 04	6.896417E 04	1.004290E 05	3.833938E 05	7.952311E 05	1.457122E 06	
4.036721E 05	4.072011E 05	3.996036E 05	3.617075E 05	3.418103E 05	3.270831E 05	3.191660E 05
3.174354E 05	3.197260E 05	3.235080E 05	3.293501E 05	3.317497E 05	3.363654E 05	3.451698E 05
3.575670E 05	3.688828E 05	3.716215E 05	3.248199E 05	2.720149E 05	2.079165E 05	1.472008E 05
1.073526E 05	1.016343E 05	1.362116E 05	4.236215E 05	8.189514E 05	1.466311E 06	
4.749168E 05	4.898458E 05	4.940904E 05	4.655584E 05	4.437519E 05	4.292560E 05	4.099384E 05
4.013592E 05	3.973885E 05	3.961159E 05	3.953168E 05	3.949992E 05	3.963958E 05	4.024750E 05
4.146016E 05	4.294954E 05	4.390690E 05	4.056934E 05	3.534317E 05	2.828500E 05	2.093541E 05
1.547355E 05	1.396860E 05	1.739743E 05	4.605157E 05	8.400243E 05	1.475500E 06	
5.158178E 05	5.435169E 05	5.616964E 05	5.632546E 05	5.381967E 05	5.223323E 05	5.083249E 05
4.971737E 05	4.887899E 05	4.825052E 05	4.734486E 05	4.704116E 05	4.695422E 05	4.728254E 05
4.822664E 05	4.973925E 05	5.115896E 05	4.963237E 05	4.501711E 05	3.77832E 05	2.925004E 05
2.181325E 05	1.835450E 05	2.104529E 05	4.953794E 05	8.625980E 05	1.484689E 06	
5.422944E 05	5.833049E 05	6.144250E 05	6.259194E 05	6.191393E 05	6.098072E 05	5.999453E 05
5.905280E 05	5.819236E 05	5.742179E 05	5.619283E 05	5.581908E 05	5.572899E 05	5.605438E 05
5.688376E 05	5.812548E 05	5.938831E 05	5.896072E 05	5.929599E 05	4.859020E 05	3.960815E 05
3.050281E 05	2.456980E 05	2.557571E 05	5.421277E 05	8.993045E 05	1.493878E 06	
5.608294E 05	6.157024E 05	6.582603E 05	6.879590E 05	6.894087E 05	6.871648E 05	6.829288E 05
6.776971E 05	6.721345E 05	6.667941E 05	6.592560E 05	6.586130E 05	6.611120E 05	6.671295E 05
6.761362E 05	6.861532E 05	6.935947E 05	6.796882E 05	6.457928E 05	5.869242E 05	5.036979E 05
4.126932E 05	3.450897E 05	3.482264E 05	6.290178E 05	9.643302E 05	1.496175E 06	
5.743159E 05	6.435741E 05	6.960414E 05	7.436130E 05	7.537659E 05	7.595269E 05	7.625134E 05
7.633387E 05	7.644016E 05	7.650140E 05	7.664342E 05	7.741168E 05	7.808912E 05	7.891723E 05
7.977917E 05	8.047383E 05	8.070330E 05	7.812202E 05	7.444349E 05	6.889482E 05	6.193333E 05
5.497269E 05	5.062883E 05	5.272632E 05	6.119356E 05	1.062493E 06	1.496175E 06	
5.841376E 05	6.684116E 05	7.306984E 05	7.700079E 05	8.166646E 05	8.321426E 05	8.447924E 05
8.556335E 05	8.654311E 05	8.748001E 05	8.42358E 05	9.045461E 05	9.154770E 05	9.264034E 05
9.303635E 05	9.438470E 05	9.468045E 05	9.295878E 05	9.058023E 05	8.725989E 05	8.352569E 05
8.3045261E 05	7.9655331E 05	8.240500E 05	1.007572E 06	1.199265E 06	1.496175E 06	
5.908568E 05	6.881739E 05	7.596279E 05	8.083279E 05	8.763502E 05	9.035257E 05	9.283060E 05
9.514969E 05	9.736319E 05	9.950915E 05	1.016164E 06	1.037073E 06	1.079050E 06	1.100296E 06
1.121710E 06	1.143170E 06	1.164499E 06	1.185297E 06	1.224579E 06	1.242786E 06	1.260171E 06
1.277083E 06	1.294096E 06	1.312116E 06	1.332723E 06	1.359268E 06	1.401157E 06	1.496175E 06

0.000000 00	-1.073639E-01	-4.322173E-01	-9.819464E-01	-1.768151E 00	-2.803028E 00	-4.095677E 00	-5.655888E 00
-7.485658E 00	-9.588963E 00	-1.196778E 01	-1.462318E 01	-1.755515E 01	-2.076211E 01	-2.423995E 01	-2.798045E 01
-3.196859E 01	-3.617811E 01	-4.056469E 01	-4.505578E 01	-4.953673E 01	-5.383311E 01	-5.768938E 01	-6.074124E 01
-6.247331E 01	-6.214696E 01	-5.868495E 01	-5.055530E 01	-3.601561E 01	-1.539112E 01	.000000E 00	
.000000E 00	-9.504202E-02	-3.864332E-01	-8.884793E-01	-1.622288E 00	-2.609129E 00	-3.865936E 00	-5.404406E 00
-7.232088E 00	-9.353760E 00	-1.177241E 01	-1.448972E 01	-1.750614E 01	-2.443007E 01	-2.832761E 01	-2.832761E 01
-3.250027E 01	-3.692374E 01	-4.155524E 01	-4.631898E 01	-5.109089E 01	-5.567681E 01	-5.979003E 01	-6.302577E 01
-6.482330E 01	-6.439834E 01	-6.063434E 01	-5.198438E 01	-3.677309E 01	-1.556343E 01	.000000E 00	
.000000E 00	-7.703011E-02	-3.189969E-01	-7.489431E-01	-1.399635E 00	-2.303244E 00	-3.484923E 00	-4.961877E 00
-6.745108E 00	-8.841458E 00	-1.125509E 01	-1.398837E 01	-1.704234E 01	-2.041695E 01	-2.411089E 01	-2.812080E 01
-3.243878E 01	-3.704712E 01	-4.190837E 01	-4.694916E 01	-5.203800E 01	-5.695946E 01	-6.138973E 01	-6.487516E 01
-6.680283E 01	-6.634051E 01	-6.233410E 01	-5.322879E 01	-3.741812E 01	-1.569499E 01	.000000E 00	
.000000E 00	-5.550521E-02	-2.379676E-01	-5.799086E-01	-1.126590E 00	-1.921703E 00	-2.999001E 00	-4.381372E 00
-6.083247E 00	-8.113131E 00	-1.047653E 01	-1.317555E 01	-1.621182E 01	-1.958664E 01	-2.330212E 01	-2.736130E 01
-3.176620E 01	-3.651173E 01	-4.157302E 01	-4.688457E 01	-5.231158E 01	-5.761728E 01	-6.243429E 01	-6.624877E 01
-6.838485E 01	-6.795753E 01	-6.377711E 01	-5.428549E 01	-3.795059E 01	-1.578749E 01	.000000E 00	
.000000E 00	-3.279129E-02	-1.519430E-01	-3.991188E-01	-8.317111E-01	-1.504545E 00	-2.459517E 00	-3.724597E 00
-5.318845E 00	-7.245782E 00	-9.516041E 00	-1.212950E 01	-1.508735E 01	-1.839254E 01	-2.205232E 01	-2.608005E 01
-3.049398E 01	-3.530999E 01	-4.052495E 01	-4.608896E 01	-5.186798E 01	-5.760346E 01	-6.287992E 01	-6.711167E 01
-6.954529E 01	-6.923458E 01	-6.495479E 01	-5.515023E 01	-3.836834E 01	-1.584021E 01	.000000E 00	
.000000E 00	-1.084518E-02	-6.816265E-02	-2.215614E-01	-5.393303E-01	-1.086347E 00	-1.911589E 00	-3.046872E 00
-4.510399E 00	-6.310844E 00	-8.450797E 00	-1.092983E 01	-1.374787E 01	-1.690943E 01	-2.042849E 01	-2.433256E 01
-2.868274E 01	-3.346500E 01	-3.876848E 01	-4.454892E 01	-5.068015E 01	-5.688344E 01	-6.268978E 01	-6.743089E 01
-7.025934E 01	-7.015438E 01	-6.585462E 01	-5.581247E 01	-3.866088E 01	-1.584254E 01	.000000E 00	
.000000E 00	8.856537E-03	7.928124E-03	-5.850277E-02	-2.677949E-01	-6.933708E-01	-1.389866E 00	-2.391350E 00
-3.715353E 00	-5.367801E 00	-7.347426E 00	-9.649926E 00	-1.227276E 01	-1.522141E 01	-1.851717E 01	-2.220431E 01
-2.635197E 01	-3.104440E 01	-3.635356E 01	-4.229234E 01	-4.875276E 01	-5.544202E 01	-6.183640E 01	-6.717504E 01
-7.049890E 01	-7.069393E 01	-6.645545E 01	-5.624885E 01	-3.880096E 01	-1.576978E 01	.000000E 00	
.000000E 00	2.517119E-02	7.223197E-02	8.177031E-02	-3.038069E-02	-3.444229E-01	-9.191398E-01	-1.789316E 00
-2.970211E 00	-4.463468E 00	-6.262618E 00	-8.358287E 00	-1.074419E 01	-1.342532E 01	-1.642893E 01	-1.981567E 01
-2.368484E 01	-2.816452E 01	-3.337910E 01	-3.939139E 01	-4.612538E 01	-5.328539E 01	-6.029730E 01	-6.630090E 01
-7.020760E 01	-7.078539E 01	-6.667085E 01	-5.634341E 01	-3.865122E 01	-1.555415E 01	.000000E 00	
.000000E 00	3.704575E-02	1.210544E-01	1.921548E-01	1.621975E-01	-5.387284E-02	-5.177177E-01	-1.263919E 00
-2.304672E 00	-3.636657E 00	-5.247667E 00	-7.122645E 00	-9.250257E 00	-1.163232E 01	-1.429776E 01	-1.731896E 01
-2.082244E 01	-2.498170E 01	-2.998123E 01	-3.594756E 01	-4.285422E 01	-5.041988E 01	-5.803115E 01	-6.472785E 01
-6.927519E 01	-7.029423E 01	-6.634250E 01	-5.593741E 01	-3.811568E 01	-1.517037E 01	.000000E 00	
.000000E 00	4.246978E-02	1.476759E-01	2.606702E-01	2.936162E-01	1.584685E-01	-2.084919E-01	-8.419624E-01
-1.751619E 00	-2.929591E 00	-4.358045E 00	-6.016357E 00	-7.887040E 00	-9.965120E 00	-1.227406E 01	-1.488802E 01
-1.795135E 01	-2.167859E 01	-2.631856E 01	-3.207530E 01	-3.899321E 01	-4.682967E 01	-5.495331E 01	-6.231447E 01
-6.752383E 01	-6.903899E 01	-6.531194E 01	-5.492099E 01	-3.714777E 01	-1.461904E 01	.000000E 00	
.000000E 00	3.476204E-02	1.280319E-01	2.425512E-01	3.042997E-01	2.253162E-01	-6.201093E-02	-5.953124E-01
-1.384741E 00	-2.619754E 00	-3.678120E 00	-5.134131E 00	-6.764233E 00	-8.553854E 00	-1.051275E 01	-1.270250E 01
-1.526318E 01	-1.845231E 01	-2.256544E 01	-2.789498E 01	-3.459454E 01	-4.247748E 01	-5.093416E 01	-5.885346E 01
-6.470606E 01	-6.676354E 01	-6.336631E 01	-5.316098E 01	-3.570232E 01	-1.390562E 01	.000000E 00	

.000000E 00	2.442193E-03	1.549431E-02	3.620634E-02	3.538334E-02	-4.531918E-02	-2.755616E-01	-7.106498E-01
-1.374863E 00	-2.262398E 00	-3.349452E 00	-4.606874E 00	-6.006502E 00	-7.524650E 00	-9.151835E 00	-1.092228E 01
-1.295795E 01	-1.550436E 01	-1.891853E 01	-2.358290E 01	-2.975129E 01	-3.736179E 01	-4.586797E 01	-5.414987E 01
-6.057288E 01	-6.323509E 01	-6.034208E 01	-5.059818E 01	-3.380972E 01	-1.307844E 01	.000000E 00	
.000000E 00	-5.748087E-02	-1.878197E-01	-3.409055E-01	-4.948224E-01	-6.697265E-01	-9.171371E-01	-1.295434E 00
-1.845588E 00	-2.579661E 00	-3.484938E 00	-4.555767E 00	-5.702966E 00	-6.957043E 00	-8.272629E 00	-9.649944E 00
-1.116506E 01	-1.303072E 01	-1.561575E 01	-1.937476E 01	-2.468532E 01	-3.163399E 01	-3.980916E 01	-4.816481E 01
-5.503416E 01	-5.837393E 01	-5.623577E 01	-4.731893E 01	-3.159433E 01	-1.220803E 01	.000000E 00	
.000000E 00	-1.177400E-01	-3.914148E-01	-7.246807E-01	-1.056464E 00	-1.377895E 00	-1.719571E 00	-2.127410E 00
-2.640462E 00	-3.278299E 00	-4.039650E 00	-4.908523E 00	-5.861119E 00	-6.869359E 00	-7.902379E 00	-8.937181E 00
-1.000021E 01	-1.124025E 01	-1.298588E 01	-1.571448E 01	-1.990442E 01	-2.581001E 01	-3.322217E 01	-4.27594E 01
-4.839067E 01	-5.245605E 01	-5.134043E 01	-4.361710E 01	-2.928042E 01	-1.138130E 01	.000000E 00	
.000000E 00	-1.643321E-01	-5.513747E-01	-1.040987E 00	-1.550608E 00	-2.148640E 00	-2.841750E 00	-3.655074E 00
-3.614965E 00	-4.238297E 00	-4.928741E 00	-5.677961E 00	-6.468535E 00	-7.276162E 00	-8.071974E 00	-8.830852E 00
-9.558072E 00	-1.034463E 01	-1.143921E 01	-1.326368E 01	-1.631680E 01	-2.097894E 01	-2.726554E 01	-3.458475E 01
-4.158627E 01	-4.623051E 01	-4.622580E 01	-3.987863E 01	-2.704989E 01	-1.061768E 01	.000000E 00	
.000000E 00	-1.936781E-01	-6.541570E-01	-1.257547E 00	-1.915845E 00	-2.584059E 00	-3.248142E 00	-3.910945E 00
-4.581005E 00	-5.265122E 00	-5.964370E 00	-6.672558E 00	-7.376162E 00	-8.055504E 00	-8.688731E 00	-9.262486E 00
-9.794840E 00	-1.037258E 01	-1.119093E 01	-1.256715E 01	-1.489807E 01	-1.855086E 01	-2.366534E 01	-2.990653E 01
-3.624178E 01	-4.087794E 01	-4.153854E 01	-3.628654E 01	-2.478855E 01	-9.763186E 00	.000000E 00	
.000000E 00	-2.025107E-01	-6.870145E-01	-1.339659E 00	-2.077372E 00	-2.851978E 00	-3.637160E 00	-4.420025E 00
-5.194259E 00	-5.955464E 00	-6.697970E 00	-7.412958E 00	-8.088250E 00	-8.710866E 00	-9.274231E 00	-9.791527E 00
-1.031454E 01	-1.095338E 01	-1.188734E 01	-1.335563E 01	-1.562017E 01	-1.889507E 01	-2.323438E 01	-2.836949E 01
-3.349420E 01	-3.713743E 01	-3.732273E 01	-3.230727E 01	-2.183624E 01	-8.474019E 00	.000000E 00	
.000000E 00	-1.851095E-01	-6.309525E-01	-1.241224E 00	-1.946876E 00	-2.703811E 00	-3.483559E 00	-4.266886E 00
-5.039682E 00	-5.790206E 00	-6.507574E 00	-7.181832E 00	-7.806579E 00	-8.383507E 00	-8.930384E 00	-9.489527E 00
-1.013562E 01	-1.097966E 01	-1.216506E 01	-1.385493E 01	-1.619406E 01	-1.925583E 01	-2.295114E 01	-2.691536E 01
-3.040094E 01	-3.225371E 01	-3.110959E 01	-2.600542E 01	-1.705929E 01	-6.435986E 00	.000000E 00	
.000000E 00	-1.260052E-01	-4.267170E-01	-8.396734E-01	-1.322556E 00	-1.847819E 00	-2.396064E 00	-2.952378E 00
-3.504431E 00	-4.041649E 00	-4.535365E 00	-5.040027E 00	-5.495506E 00	-5.930365E 00	-6.365672E 00	-6.838530E 00
-7.404100E 00	-8.134367E 00	-9.111385E 00	-1.041228E 01	-1.208329E 01	-1.410135E 01	-1.632585E 01	-1.845230E 01
-1.999344E 01	-2.032740E 01	-1.885608E 01	-1.525399E 01	-9.754415E 00	-3.628252E 00	.000000E 00	
.000000E 00	.000000E 00	.000000E 00	.000000E 00	.000000E 00	.000000E 00	.000000E 00	.000000E 00
.000000E 00	.000000E 00	.000000E 00	.000000E 00	.000000E 00	.000000E 00	.000000E 00	.000000E 00
.000000E 00	.000000E 00	.000000E 00	.000000E 00	.000000E 00	.000000E 00	.000000E 00	.000000E 00
.000000E 00	.000000E 00	.000000E 00	.000000E 00	.000000E 00	.000000E 00	.000000E 00	.000000E 00

UR = 1.923796

R1(0) = 1.884517E-37,

WEI = 1,

RMAX = 1.190172E-03,

DT = 1.788753E-C5

TAU = 60.000000,

REFERENCES

1. Anderson, B. H. and M. J. Kolar, "Experimental Investigation of the Behavior of a Confined Fluid Subjected to Nonuniform Source and Wall Heating," NASA TN D-2079, November 1963.
2. Arnett, R. W. and Millhiser, D. R. "Theoretical Model for Predicting Thermal Stratification and Self Pressurization of a Fluid Container," Proc. Conf. on Prop. tank Press. and Strat., MSFC, Huntsville, AIA., Jan. 1965.
3. Bailey, T. E. and R. F. Fearn, "Analytical and Experimental Determination of Liquid Hydrogen Temperature Stratification," Advances in Cryogenic Engineering, Vol. 9, 1964, p. 254.
4. Bailey, T. E., R. Vanderkoppel, G. Skartvedt and T. Jefferson, "Cryogenic Propellant Stratification Analysis and Test Data Correlation," AIAA Journal, Vol. 1, No. 7, July 1963, p. 1657.
5. Bailey, T. E. and others, "Analytical and Experimental Determination of Liquid Hydrogen Temperature Stratification," Final Report, Contract NAS 8-5046, Martin Company, Denver, Colorado, April 1963, Contractor to Marshall Space Flight Center.
6. H. Z. Barakat and John A. Clark "On the Solution of the Diffusion by Numerical Methods," ASME paper, 64-H-131.
7. Barnett, D. O., T. W. Wimstead and L. S. McReynolds, "An Investigation of LH₂ Stratification in a Large Cylindrical Tank of Saturn Configuration," Paper U-12, 1964 Cryogenic Engineering Conference, Philadelphia, August 1964.
8. Batchelor, Quart. Applied Math. 12-1954, pp. 209-203.
9. Bruce, Peaceman, Rachford and Rice "Calculations of Unsteady-state Gas Flow through Porous Media." Petroleum Transactions, AIME, Vol. 198, 1953.
10. Clark, J. A. "A Review of Pressurization, Stratification and Interfacial Phenomena," Vol. 10, International Advances in Cryogenic Engineering, Paper S-1, p. 259-284, Plenum Press, 1965.

REFERENCES (Continued)

11. Clark, J. A. and H. Z. Barakat, "Transient, Laminar, Free-Convection Heat and Mass Transfer in Closed, Partially Filled, Liquid Containers," Technical Report No. 1, Heat Transfer Laboratory, University of Michigan, Ann Arbor, Contract NAS 8-825, Marshall Space Flight Center, January 1964. (Report completed in July 1963 and advanced copies submitted to NASA for approval).
12. J. A. Clark, G. J. Van Wylen and S. K. Fenster "Transient Phenomena associated with the Pressurized Discharge of a Cryogenic Liquid from a Closed Container," Advances in Cryogenic Engineering, Vol. 5, pp. 467-480.
13. Coxe, E. F. and J. W. Taton, "Analysis of the Pressurizing Gas Requirements for an Evaporated Propellant Pressurization System," Advances in Cryogenic Engineering, Vol. 7, 1962, p. 234.
14. A. N. Curren and C. F. Zalabak "Effect of Closed End Coolant Passages on Natural Convection Water Cooling of Gas Turbine Blades," NACA RM E55J 18-a.
15. Dufort, E. C. and Frankl, S. P., "Stability Conditions in the Numerical Treatment of Parabolic Differential Equations," Math. Tables Aids Comput., 7, pp. 135-152, 1953.
16. Dusinberre, "A Note on the 'Implicit' Method for Finite-Difference Heat Transfer Calculations," ASME Trans., J. Heat Transfer, Series C. Feb. 1961, pp. 94-95.
17. R. Eichhorn, "Flow Visualization and Velocity Measurement in Natural Convection with Tellurium Die Method," ASME Trans., J. Heat Transfer, Vol. 83, Series C. pp. 379-381.
18. Eulitz, W. R., "Practical Consequences of Liquid Propellants SLOsh Characteristics Derived by Nomographic Methods," Marshall Space Flight Center Memo MTP-P and VE-P-63-7, October 22, 1963.
19. S. K. Fenster, G. J. Van Wylen and J. A. Clark, "Transient Phenomena Associated with the Pressurization of Liquid Nitrogen Boiling at Constant Heat Flux," Advances in Cryogenic Engineering, Vol. 5, pp. 226-234.
20. G. Forsythe and W. Wasow, "Finite-Difference Methods for Partial-Differential Equations." John Wiley and Sons, 1964.

REFERENCES (Continued)

21. Fromm, J. "A Method for Computing Nonsteady, Incompressible, Viscous Fluid Flows," Los Alamos Sci. Lab., Sept. 1963.
22. B. Gebhart, "Natural Convection Transients," ASME Transactions, J. Heat Transfer, Series C, 85, pp. 184-185. See also J. Heat Transfer, 85, pp. 10 and 83, p. 61.
23. F. G. Hammitt, "Heat and Mass Transfer in Closed, Vertical, Cylindrical Vessels with Internal Heat Sources for Homogeneous Reactors," Ph.D. Thesis, University of Michigan, Dec. 1957.
24. Harper, E. Y., S. E. Hurd and J. O. Donaldson, "A Study of Liquid Stratification in a Cylindrical Container," Lockheed Missiles and Space Co., Report 803973, March 1964.
25. Harper, E. Y., J. H. Chin, S. E. Hurd, A. N. Levy and H. M. Satterlee, "Analytical and Experimental Study of Liquid Orientation and Stratification in Standard and Reduced Gravity Fields," Preliminary Report, Lockheed Missiles and Space Co., June 1964. Contract NAS 8-11525, Marshall Space Flight Center, "Theoretical and Experimental Studies of Zero-g Heat Transfer Modes."
26. J. P. Hartnett, W. E. Welch and F. W. Larson, "Free Convection Heat Transfer to Water and Mercury in an Enclosed Cylindrical Tube," Nuclear Engineering and Science Conference, Preprint 27, Session XX, Chicago, March 17-21, 1958.
27. J. P. Hartnett and W. E. Welch, "Experimental Studies of Free Convection Heat Transfer in a Vertical Tube with Uniform Heat Flux," Trans. ASME Vol. 79, 1957, p. 1551.
28. J. D. Hellums, "Finite-Difference Computation of Natural Convection Flow," Ph.D. Thesis, University of Michigan, Sept. 1960.
29. F. Herzberg, "Effective Density of Boiling Liquid Oxygen," Advances in Cryogenic Engineering, Vol. 5.
30. Karplus, W. J., "An Electric Circuit Theory Approach to Finite-Difference Stability," Trans. AIEE, 77, 1, 1958.
31. Landau and Lifshitz, "Fluid Mechanics," Adison-Wesly, 1959.

REFERENCES (Continued)

32. F. W. Larsen and J. P. Hartnett, "Effect of Aspect Ratio and Tube Orientation on Free Convection Heat Transfer to Water and Mercury in Enclosed Circular Tubes," ASME Trans., J. Heat Transfer, Vol. 83, Series C, pp. 87-93.
33. Lax, P. D. and Richtmeyer, R. D., "Survey of the Stability of Linear Finite-Difference Equations," Comm. Pure Appl. Math., 9, 1956, pp. 267-293.
34. A. F. Leitzke, "Theoretical and Experimental Investigation of Heat Transfer by Natural Convection Between Parallel Plates," NACA Report 1223, 1955.
35. S. Levy, "Integral Methods in Natural Convection Flow," ASME Paper No. 55-APM-22.
36. M. J. Lighthill, "Theoretical Consideration on Free Convection in Tubes," Quart. J. Mech. and App. Math., Vol. 6, 1953, pp. 398-439.
37. Liu, C. K., "Sloshing and Pressure-Decay in Pressurized Cryogenic Tanks of Launch Vehicles," Marshall Space Flight Center Memo, MTP-P and VE-P-61-23, December 18, 1961.
38. B. W. Martin, "Free Convection in an Open Thermosyphen with Special Reference to Turbulent Flow," Proc. Roy. Soc., Series A, Vol. 230, 1955, pp. 502-530.
39. Neff, B. D. "Investigation of Stratification Reduction Techniques." Proceedings of the Conference on Propellant Tank Pressurization and Stratification, MSFC, Huntsville, Ala., Jan. 1965.
40. Nein, M. E. and R. R. Head, "Experiences with Pressurized Discharge of Liquid Oxygen from Large Flight Vehicle Propellant Tanks," Advances in Cryogenic Engineering, Vol. 7, 1962, p. 244.
41. Nein, M. E. and J. F. Thompson, "Experimental and Analytical Studies of Pressurization Systems for Cryogenic Propellants," Propulsion Division, NASA, Marshall Space Flight Center, Huntsville, Ala., July 1964.
42. O'Brien, G. G., Hyman M., and Kaplan S., "A Study of the Numerical Solution of Partial-Differential Equations," J. Math. Phys., 29, 1951, pp. 223-251.

REFERENCES (Continued)

43. Ordin, P. M., S. Weiss and H. Christenson, "Pressure-Temperature Histories of Liquid Hydrogen under Pressurization and Venting Conditions," Advances in Cryogenic Engineering, Vol. 5, 1960, p. 481.
44. S. Ostrach, "An Analysis of Laminar Free Convection Flow and Heat Transfer about a Flat Plate Parallel to the Direction of the Generating Body Force," NACA Report 11-1953.
45. S. Ostrach, "Laminar Natural Convection Flow and Heat Transfer to Fluids with and without Heat Sources with Constant Wall Temperature," NACA Tn-2863, Dec. 1952.
46. S. Ostrach, "Combined Natural and Forced Convection Laminar Flow and Heat Transfer to Fluids with and without Heat Sources in Channels with Linearly Varying Wall Temperature," NACA Tn 3141 April 1954.
47. S. Ostrach and P. R. Thronton, "On the Stagnation of Natural Convection Flows in Closed End Tubes," ASME Paper No. 57-SA-2.
48. G. A. Ostromov, "Free Convection under the Conditions of the Internal Problem," NACA Tn 1407.
49. Platt, G. K., M. E. Nein, J. L. Vaniman and C. C. Wood, "Feed System Problems Associated with Cryogenic Propellant Engines," Paper 687A, SAE-ASME, National Aeronautical Meeting and Production Engineering Forum, April 1963.
50. E. Pohlhausen, Zamm1, 115 (1921).
51. G. Poots, "Heat Transfer by Laminar Free Convection in Enclosed Plane Gas Layers," Quart. J. Mech. and Appl. Math., Vol. XX, Pt. 3, 1958, pp. 257-273.
52. R. D. Richtmyer, "Difference Methods for Initial Value Problem," Interscience Publication, 1957.
53. Robbins, J. H. and A. C. Rogers, "An Analysis on Predicting Thermal Stratification in Liquid Hydrogen," Manuscript submitted to AIAA, April 1964.

REFERENCES (Continued)

54. A. G. Romnov, "Study of Heat Exchange in a Dead End Channel under Free Convection Conditions," *Izvestiya Akademii Nau, USSR. Otdeleni Tekhnisheskikh*, No. 6, 1956, pp. 63-76.
55. Ruder, J. M., "Stratification in a Pressurized Container with Sidewall Heating," *AIAA Journal*, Vol. 2, No. 1, January 1964, p. 135.
56. R. S. Schechter, "Natural Convection Heat Transfer in Regions of Maximum Fluid Density," *AICHE Paper No. 57-HT-25*.
57. E. Schmidt and W. Bachmann, *Forsch Ing-Wes.* 1, 391 (1930).
58. Schwind, R. G. and G. C. Vliet, "Observations and Interpretations of Natural Convection and Stratification in Vessels," *Proceeding, 1964 Heat Transfer and Fluid Mechanics Institute, Stanford University Press*.
59. Scott, L. E., R. F. Robins, D. B. Mann and B. W. Birmingham, "Temperature Stratification in a Nonventing Helium Dewar," *Journal of Research, NBS*, Vol. 64C, No. 1, 1960, p. 19.
60. Segel, M., "Experimental Studies of Stratification Phenomena and Pressurization for Liquid Hydrogen," *Paper U-11, 1964, Cryogenic Engineering Conference, Philadelphia, August 1964*.
61. R. Seigel, "Transient Free Convection from a Vertical Flat Plate," *ASME Paper No. 57-SA-8*.
62. R. Seigel and R. H. Norris, "Test of Free Convection in a Partially Enclosed Spaces between Two Heated Vertical Plates," *ASME Paper No. 56-SA-5*.
63. R. G. S. Skipper, I. S. C. Holt and O. A. Saunders, "Natural Convection in Viscous Oil," *International Development in Heat Transfer, Part 5*, pp. 1003-1009.
64. Smith, W. "Natural Convection in a Rectangular Cavity," *Ph.D. Thesis, University of Michigan, 1964*.
65. E. M. Sparrow and J. L. Gregg, "The Variable Fluid Property," *ASME Paper No. 57-A-46*.

REFERENCES (Continued)

66. E. M. Sparrow, J. L. Gregg, "Similar Solutions for Free Convection from a Nonisothermal Vertical Plate," ASME Paper No. 57-SA-3.
67. E. M. Sparrow and S. J. Kauffmann, "Visual Study of Free Convection in a Narrow Vertical Enclosure," NACA RM E55 L 14-a, Feb. 1956.
68. Swim, R. T., "Temperature Distribution in Liquid and Vapor Phases of Helium in Cylindrical Dewars," Advances in Cryogenic Engineering, Vol. 5, 1960, p. 498.
69. Tatom, J. W., W. H. Brown, L. H. Knight and E. F. Coxe, "Analysis of Thermal Stratification of Liquid Hydrogen in Rocket Propellant Tanks," Advances in Cryogenic Engineering, Vol. 9, 1964, p. 265.
70. Tellep, D. M. and E. Y. Harper, "Approximate Analysis of Propellant Stratification," AIAA Journal, Vol. 1, No. 8, Aug. 1963.
71. J. Todd, "Survey of Numerical Analysis," McGraw-Hill, 1962, Chapter 11.
72. G. J. Van Wylen, S. K. Fenster, H. Merte, Jr. and W. A. Warren, "Pressurized Discharge of Liquid Nitrogen from an Uninsulated Tank," Proceedings of the 1958 Cryogenic Engineering Conference, 1959.
73. Vliet, G. C. and Brogan, J. J., "Investigation on the Effects of Baffles on Natural Convection Flow and on Stratification," Proceedings of the Conference on Propellant Tank Pressurization and Stratification, MSFC, Huntsville, Ala., Jan. 1965.
74. Wilkes, J. O., "The Finite-Difference Computation of Natural Convection in an Enclosed Rectangular Cavity," Ph.D. Thesis, University of Michigan, August 1963.
75. Wu, J. C., "On the Finite-Difference Solution of Laminar Boundary Layer Problems," Proceedings of the 1961 Heat Transfer and Fluid Mechanics Institute, Stanford Univ., Press, R. Binder Editor, p. 55.
76. S. L. Zeiberg and W. K. Mueller, "Transient Laminar Combined Free and Forced Convection in a Duct," ASME Trans., J. Heat Transfer Vol. 84, Series C, pp. 141-148.

REFERENCES (Concluded)

77. "A Compendium of the Properties of Materials at Low Temperature Phase I and II," R. B. Stewart and V. J. Johnson, Editors.
78. Petrovsky, I. G., "Lectures on Partial Differential Equations," Interscience Publication, N. Y. 1954.
79. J. H. Chin, et al., "Analytical and Experimental Study of Liquid Orientation and Stratification in Standard and Reduced Gravity Fields," Report No. 2-05-64-1, July 1964, Lockheed Missile and Space Company, NASA Contract NAS 8-11525.

UNIVERSITY OF MICHIGAN



3 9015 02229 0079